PAP 355

DRAFT TUBE SURGE RESEARCH

FOREWORD

In November 1966 a meeting was called by the Chief Engineer of the Bureau to discuss problems which might arise by increasing the specific speed for the Grand Coulee Third Powerplant turbines above normal Bureau practice. This meeting led to several others in which the problems of draft tube surging and mechanical vibrations were considered. The conclusion of the series of meetings was that mechanical vibrations presented no particular concerns. However, the problem of draft tube surging was not resolved.

To attack the surge problem a two-phase research program was initiated. The first phase consisted of meetings with a Board of Consultants to review and aid in the establishment of research goals. The second phase of the program was to conduct model and analytic investigations to:

a. Study the fundamental hydrodynamics

b. Determine the variables controlling the surge

c. Study mechanisms to control surging

d. Determine characteristic parameters to be used in correlating model and prototype data

The Board of Consultants was convened in February 1968. It consisted of Dr. J. W. Daily, Dr. Hunter Rouse, and Mr. Ray Quick. After presentations of the Bureau's concerns, library studies of surging, and analysis of model and prototype data, the Board concurred with the second phase research program.

The reports and papers in this compilation are the direct result of the draft tube research program. The first three purposes of the program have been rather thoroughly investigated. Although the basic correlating parameters in part d of the program have been established, some discrepancies still exist between the model and prototype characteristics. The causes of these discrepancies are presently being investigated.

HENRY T. FALVEY
Dr - Ing.

REC-OCE-69-5

EXPERIMENTAL STUDY AND ANALYSIS OF DRAFT TUBE SURGING

Dr. J. J. Cassidy
Division of Research
Office of Chief Engineer
Bureau of Reclamation

October 1969

REC-OCE-69-5
Report No. HYD-591

EXPERIMENTAL STUDY AND ANALYSIS OF DRAFT-TUBE SURGING

by

Dr. J. J. Cassidy

October 1969

HYDRAULICS BRANCH
DIVISION OF RESEARCH

UNITED STATES DEPARTMENT OF THE INTERIOR * BUREAU OF RECLAMATION
Office of Chief Engineer . Denver, Colorado

ACKNOWLEDGEMENTS

This study was conducted while the writer (Professor of Civil Engineering, University of Missouri, Columbia, Missouri) was a Ford Foundation Engineer Resident with the Hydraulics Branch, Division of Research. Design of experimental equipment was performed primarily by Dr. H. T. Falvey. Mr. U. J. Palde collected a portion of the data while Mr. W. M. Batts performed the photography. Turbine performance data and advice relative to hydraulic machinery were furnished by Mr. C. G. Bates and Mr. G. H. Johnson, Hydraulic Machinery Branch, Division of Design. The manuscript was reviewed critically by Dr. H. T. Falvey. Head, Hydraulics Research Section. The entire project was under the direction of Mr. H. M. Martin, Hydraulics Branch Chief.

CONTENTS

Figures

ABSTRACT

Draft-tube surge experiments were conducted with models of draft tubes, using air as the fluid. The occurrence, frequency, and amplitude of surges were correlated with flow and draft-tube geometry variables. Studies show that surges arise when angular momentum reaches a critical value relative to linear momentum. Surge frequency and peak-to-peak pressures are independent of viscous effects for Reynolds numbers above 80,000, and are correlated with a dimensionless momentum parameter for a particular draft-tube shape. A criterion is given for predicting the surging threshold. Results of the study are applied to analysis of draft-tube surging in the Fontenelle and Hoover replacement turbines.

DESCRIPTORS—/ *draft tubes/ *turbines/ *hydroelectric plants/ hydraulic machinery/ fluid mechanics/ dimensional analysis/ *surges/ air/ unsteady flow/ pressure/ laboratory tests/ model tests/ fluid flow/ non-uniform flow
IDENTIFIERS—/ fluid dynamics/ hydraulic resonance

Where approximate or nominal English units are used to express a value or range of values, the converted metric units in parentheses are also approximate or nominal. Where precise English units are used, the converted metric units are expressed as equally significant values. A table of conversion factors—BRITISH TO METRIC UNITS OF MEASUREMENT—is provided at the end of this report.

NOMENCLATURE

Unless otherwise noted, all dimensions are in the foot-pound-second (meter-kilogram-second) system.

A = area

B = height of wicket gates

D = diameter of draft-tube throat

D_R = runner diameter at midpoint of wicket gates

H = net head across turbine

H_B = atmospheric pressure head minus vapor pressure head

H_S = static draft head on turbine (negative for turbines set above tailwater)

L = length of draft tube

P = power

ΔP = peak-to-peak value of pressure surge

Q = discharge

R = Reynolds number = WD/ν

V = velocity

$W = Q/A$ = average axial velocity

f = frequency

f_n = natural frequency

g = acceleration due to gravity

n = rotation speed (rev/sec)

r = coordinate in radial direction

u = velocity component in radial direction

v = velocity component in peripheral direction

w = velocity component in axial direction

z = coordinate in axial direction

Ω = rate of flow of angular momentum

γ = specific weight

$\phi = \dfrac{\pi Dn}{60\sqrt{2gH}}$ = peripheral speed coefficient; also, a function

α = angle between a radial line and velocity vector

θ = coordinate angle in cylindrical coordinate system

ν = kinematic viscosity of fluid

π = 3.1416

ρ = fluid density

$\sigma = (H_B - H_S)/H$ = turbine cavitation number

ω = angular velocity (rad/sec)

PURPOSE

The analysis and experimental investigation were conducted in order to gain an understanding of draft-tube surging and to correlate occurrence, frequency, and amplitude of draft-tube surges with flow and geometric variables involved in turbine and draft-tube flow.

CONCLUSIONS

1. Draft-tube surges are a stable unsteady form of flow arising when the rate of flow of angular momentum reaches a critical value relative to the rate of flow of linear momentum. The dimensionless momentum parameter $\Omega D/\rho Q^2$ has a critical value above which surging exists.

2. Frequency and peak-to-peak values of draft-tube pressure surges are independent of viscous effects for Reynolds numbers above approximately 80,000. Prototype Reynolds numbers greatly exceed 80,000.

3. Dimensionless parameters for peak-to-peak pressures and frequency of draft-tube surging can be correlated with a dimensionless momentum parameter for a particular draft-tube geometry.

APPLICATIONS

The results of this study can be applied to the analysis of flow through turbine draft tubes, or conceivably, to flow through pump intakes. The surge frequency and amplitude predicted by similitude yield reasonable prototype values. If the analysis for turbines is fully developed, designers could conceivably predict in advance operational conditions at which surging would occur for a particular unit. However, it would be highly desirable to correlate the results of this study with the frequency, amplitude, and threshold of surging observed in a carefully planned prototype observation, one in which discharge, head, gate, plant sigma, and turbine geometry as well as surge characteristics are observed or known.

INTRODUCTION

Draft-tube surges have been observed in hydroelectric plants using Francis-type turbines apparently since the time these units first went into operation.[1] Effects of surges have been observed as power swings or general noise and vibration. In most cases powerplant operators rapidly learn where the "rough" areas of operation are and avoid operation in those regions. In some cases vertical vanes are spaced around the periphery of the draft-tube entrances in an attempt to modify or eliminate the swirl in the flow and thus reduce the severity of, or eliminate, surging. Air is also frequently admitted below the runner to "smooth out" operation.

The phenomenon of surging is known to be due to rotation of flow passing through the draft tube. Pictures of the helical vortex thus generated have been taken by Wigle[2] and Hosoi[3] to mention only two. However, very little in the way of quantitative information, useful to the engineer, is currently available beyond the equation proposed by Rheingans[1] for the expected frequency of the surge:

$$f = \frac{n}{3.6}$$

f is the surge frequency in cycles per second and n is the turbine rotational speed in revolutions per second.

Purely axial flow through a straight tube is stable once the transition to a fully turbulent flow takes place. If some rotation is superimposed on this flow, however, the flow pattern makes a drastic change from that of the purely axial flow.[4] The axial velocity decreases on the centerline and increases near the wall. The peripheral component of velocity also increases near the wall. Figure (1) shows a typical velocity distribution in axial and axial-with-rotation flows. If the discharge is kept constant and the rotational velocity of the flow is increased, a radical change in flow pattern occurs. A reversal in flow takes place at the tube axis and a stagnation point is developed on the centerline. On the centerline, flow is toward the stagnation point from both the upstream and downstream directions. The development of reversed flow along the axis of the tube has been referred to as vortex breakdown.[6]

Basic investigation of this vortex breakdown first occurred not as a result of interest on the part of turbine users or manufacturers, but rather as the result

[1] Rheingans, W. J., "Power Swings in Hydroelectric Power Plants," Trans. ASME, Vol. 62, 1940.
[2] Wigle, D. A., et al, "Hydraulic Model Studies for Turbines at Grand Coulee Powerplant," U.S. Bureau of Reclamation, Hydraulic Laboratory Report, HYD-198, Denver, Colorado, 1946.
[3] Hosoi, Y., "Experimental Investigations of Pressure Surge in Draft Tubes of Francis Water Turbines," Hitachi Review, V. 14, No. 12, 1965.
[4] Kreith, F. and O. K. Sonju, "The Decay of a Turbulent Swirl in a Pipe," JOURNAL OF FLUID MECHANICS, Vol. 22, Part 2, 1965.
[6] Benjamin, T. B., "Theory of the Vortex Breakdown Phenomenon," JOURNAL OF FLUID MECHANICS, Vol. 14, 1962.

of observations made by people interested in acoustics[5] and the "breakdown" observed on the vortices forming above delta wings on high-speed modern airplanes.[6]

The analytical study by Benjamin[6] indicated that the "breakdown" was actually a transition from one stable regime of flow to another. He showed that prior to the breakdown an axisymmetric standing wave could not exist in the flow while the breakdown produced a flow which could support such a wave. Benjamin used the well-understood hydraulic jump as an analogy to what occurred in the vortex breakdown.

Quantitative information on the occurrence of vortex breakdown was apparently first obtained by Squire[7] in an analytical study. According to Squire's theory, breakdown occurred when the maximum swirl angle (the angle whose tangent is v/w - See Figure 1) was 52° or greater.

Harvey[8] in an experimental study using air flowing through a straight tube measured a maximum swirl angle of 51° using smoke injected in the flow just upstream from the breakdown.

If, after breakdown has occurred, the rotational velocity of the fluid is further increased, the flow downstream from the point of transition forms a precessing helical vortex. It is the precession of this vortex which produces the pressure surge. This aspect of the phenomenon, which is the most important to the engineer, has received very little basic investigation.

Chanaud[9] studied both the steady and unsteady part of the transition. He found that the Strouhal number fD/W (D is tube diameter and W is the average axial velocity) of the precessing vortex depended upon the tube length to diameter ratio L/D and the axial Reynolds number of the flow. Unfortunately, Chanaud's data regarding rotation are in error because he assumed that the flow moving through a revolving tube was set into rigid body motion equivalent to that of the pipe. However, qualitatively his results are of considerable interest. He found that the transition to helical-spiral (surging) flow took place more readily at larger Reynolds numbers. For Reynolds numbers below 250 unsteady flow could not be produced in the tube regardless of the degree of rotation imparted to the fluid.

Quantitative information regarding both the onset of surging and the characteristics of frequency and amplitude of the resultant surge would be of considerable value to the engineer concerned with design and selection of hydraulic machinery. This study was designed to produce both qualitative information on the nature of surges in contemporary turbine draft tubes, and to obtain quantitative information on occurrence and characteristics of surge frequency and amplitude.

EQUIPMENT

For the sake of convenience, it was decided to conduct the experiments with air as the fluid medium. The apparatus is shown in photographs in Figure 2 and schematically in Figure 3. Because a study involving a model of the Fontenelle draft tube and spiral case had been previously conducted, many of the details of the experimental apparatus were actually scale models of corresponding Fontennelle components[10].

Because the phenomena is quite complex at best, it was highly desirable, at least for this initial study, to simplify the geometry as much as possible. Hence, no turbine runner was to be installed in the draft tube. Rotation was introduced as the flow passed through inclined vanes in the radial approach to the draft tube. Radial inclination of these vanes was readily adjusted by a control extending outside the stilling chamber. With this control the angle between the gates and a radial line could be set at any value between 0° and 52.5°. At 0° the gates are fully open and no rotation is imparted to the flow.

Discharge was controlled by the motor-driven cone valve at the entrance to the stilling chamber and computed from the differential pressure across the orifice in the supply line. The supply line leading from the fan to the stilling chamber had a 9.952-inch inside diameter and the orifice diameter was 4.801 inches. Pressure differential across the orifice was measured using a calibrated 2.5 psig Statham pressure cell.

Piezometers (1/16 inch in diameter) were installed in the draft tubes for the measurement of peak-to-peak pressures of the surges. A 2.5 psig Statham pressure cell was used as a transducer for the pressure surges. After amplification, the signal from the pressure cell was displayed on an oscilloscope equipped with a variable

[5] Chenaud, R. C., "Experiments Concerning the Vortex Whistle," JOURNAL OF THE ACOUSTICAL SOCIETY OF AMERICA, Vol. 35, No. 7, 1963.
[7] Squire, H. B., "Analysis of the Vortex Breakdown Phenomenon, Part I," Aero, Dept., Imperial College, Rep. No. 102, 1960.
[8] Harvey, J. K., "Some Observations of the Vortex Breakdown Phenomenon," JOURNAL OF FLUID MECHANICS, Vol. 14, 1962.
[9] Chenaud, R. C., "Observations of Oscillatory Motion in Certain Swirling Flows," JOURNAL OF FLUID MECHANICS, Vol. 21, 1965.
[10] Falvey, H. T., "Hydraulic Model Studies of the Fontenelle Powerplant Draft Tube and Tailrace," Report No. Hyd-571, U.S. Bureau of Reclamation, Denver, Colorado, August 1967.

persistence screen. With the variable persistence feature it was possible to retain as many traces as desired and then store the result as a permanent image. When stored, the resultant image was static and could be scrutinized for frequency and peak-to-peak value.

Taps were also mounted on the draft tubes so that velocity measurements could be made using a hot-film anemometer. The signal from the anemometer could also be displayed on the oscilloscope. Calibration of the hot-film was accomplished by placing the probe in an air jet, the velocity of which had been measured using a stagnation tube and a differential manometer.

ANALYSIS

In order to be able to utilize the results of this study in an actual hydraulic-turbine application, it was necessary to generalize the results in a basic fashion. Complete analytical solution to the problem of draft-tube surging would naturally provide the necessary generalization. However, such a solution seems as yet to be unattainable. An experimental study was therefore indicated.

When faced with the need to generalize experimental results, dimensional analysis can be very useful if the phenomenon is at least partially understood.

In this case, the assumption was made that the frequency of the surge is a function of only the fluid density ρ, the fluid viscosity ν, the draft tube diameter D and Length L, the discharge Q, and the rate of flow of angular momentum Ω. Thus,

$$f = \phi\ (\rho, \nu, D, L, Q, \Omega) \tag{2}$$

Application of standard techniques of dimensional analysis to Equation (2) produces

$$\frac{fD^3}{Q} = \phi_1\left(\frac{\Omega D}{\rho Q^2}, \frac{L}{D}, \frac{Q}{D\nu}\right) \tag{3}$$

as one possible set of dimensionless parameters. The frequency parameter is actually a form of Strouhal number written in terms of discharge rather than mean velocity. The first parameter on the right of Equation (3) is a dimensionless ratio of angular-momentum flux to linear-momentum flux. If the discharge is held constant and angular-momentum flux is increased for a particular tube the magnitude of the momentum parameter is increased. The last parameter on the right of Equation (3) is simply the Reynolds number and will be represented as $R = WD/\nu$ throughout the remainder of this report.

The peak-to-peak value ΔP of the pressure produced at a particular point by the surge can be assumed to be a function of the same variables as the frequency. Thus,

$$\Delta P = \phi_2\ (\rho, \nu, D, L, Q, \Omega) \tag{4}$$

or in one possible combination of dimensionless terms

$$\frac{\Delta P D^3}{\Omega} = \phi_3\ (\frac{\Omega D}{\rho Q^2}, \frac{L}{D}, R) \tag{5}$$

Two things should be noted at this point. First, the role of draft-tube shape cannot be incorporated in this type of analysis and data plotted according to Equations (3) and (5) will produce different results for each tube shape tested. Second, the parameter $\Omega D/\rho Q^2$ is obviously a gross parameter quite in contrast to the local swirl angle $\tan^{-1}\frac{V}{W}$ as used by previous analysts and experimenters. Because of its gross feature, this momentum parameter is easily utilized, but in utilizing it, the assumption must be made that regardless of the manner in which angular momentum is introduced into the flow the resulting flow pattern will be the same as long as $\Omega D/\rho Q^2$ is constant.

With the exception of Ω all variables in Equations (3) and (5) could be measured directly with the experimental equipment. The flux of angular momentum was computed from the geometry of the inlet to the draft tube as follows:

From the gate diagram (see Figure 20)

$$Q = \int V_o \cos\alpha\ dA = \int_o^{2\pi} V_o Br \cos\alpha\ d\theta$$

where B is the height of the wicket gates.

Also,

$$\Omega = \rho \int V_o \cos\alpha\ (rV_o \sin\alpha) dA = \int_o^{2\pi} \rho V_o^2 Br^2 \cos\alpha \sin\alpha\ d\theta$$

Assuming that V_o, B, and r are constant with respect to θ

$$Q = V_o \cos\alpha\ 2\pi rB$$

$$\Omega = \rho V_o^2 \cos\alpha \sin\alpha\ 2\pi r^2 B$$

Thus,

$$\frac{\Omega D}{\rho Q^2} = \frac{D \tan\alpha}{2\pi B} \tag{6}$$

Hence, the momentum parameter is a function of only the gate opening, draft-tube inlet diameter, and height of gates.

EXPERIMENTAL PROCEDURE

A. THE ONSET OF SURGING

A qualitative and quantitative description of the transition from steady uniformly-swirling flow to unsteady surging flow was obtained by two separate experimental methods. At average velocities below 5 fps (1.64 m/s) smoke was injected on the centerline of the tube at the upstream cover. The gate angle--and thus $\Omega D/\rho Q^2$ --at which the transition took place was recorded. Because the longitudinal location of the transition point moved upstream as $\Omega D/\rho Q^2$ was increased, two critical values of the momentum parameter were recorded: (1) When the transition occurred just within the tube exit; and (2) when surging occurred throughout the tube.

A hot-film anemometer was used to detect transition to surging at high average flow velocities. A cylindrical hot-film probe was positioned at the centerline near the tube exit. Flow was established with no rotation. Then $\Omega D/\rho Q^2$ was gradually increased (by closing the wicket gates). The value of $\Omega D/\rho Q^2$ at which a reversal in velocity was noted at the centerline was recorded as the critical value. At these large velocities, transition appeared to progress rapidly upstream. Two critical values were not observed since flow seemed to become unsteady throughout the entire tube almost simultaneously.

B. FREQUENCY AND AMPLITUDE OF SURGING

Two separate measurements were made of surge frequency. Using the previously described pressure cell to detect pressure surging and cylindrical hot-film probe to detect velocity near the piezometer, traces of velocity and pressure were displayed simultaneously on the dual-beam oscilloscope. Figure (9) is a picture of two traces thus made. Approximately 50 traces of both velocity and pressure were retained for the photograph in Figure (9) through use of the persistence feature of the oscilloscope screen.

Peak-to-peak pressures were obtained by measuring the peak-to-peak voltage of the oscilloscope display and relating this to the calibrated output of the pressure cell and its associated amplifier.

Experimental procedure was the same for each tube. A particular gate angle was set with maximum obtainable discharge (approximately 10 ft^3/sec-- 0.283 m^3/sec). The discharge was then successively decreased in small increments by closing the cone valve. Frequency and peak-to-peak pressures were measured and recorded for each discharge.

C. TUBES STUDIED

Straight tubes studied included two different diameters--6.13 inches (15.56 cm), 3.44 inches (8.76 cm)--with lengths giving rise to L/D ratios ranging from 1.63 to 7.20. In addition, a model of the Fontenelle draft tube with a throat diameter of 6.13 inches (15.26 cm) and a straight cone having the same expansion ratio, throat diameter, and centerline length as the draft tube were also studied. All tubes were formed from transparent plexiglass in order to facilitate flow visualization. The draft tube can be seen in Figure (2) and the remaining tubes studied are shown in Figure (7).

D. FLOW VISUALIZATION

Smoke was chosen as the most desirable agent for obtaining flow visualization for this particular study. After some experimentation, pipe tobacco proved to produce the least objectionable of the varieties of smoke which were dense enough to provide good visualization. The smoke generator developed for this study is shown schematically in Figure (4).

DISCUSSION OF RESULTS

A. INFLUENCE OF VISCOSITY

Figures 10, 11, and 12 show dimensionless frequency and pressure plotted against Reynolds number for straight pipes and the Fontenelle draft tube. The frequency and pressure parameters are both seen to be essentially constant for Reynolds numbers beyond 80,000. Since a prototype hydraulic turbine would have a Reynolds number well above this (for Fontenelle design conditions R = 18,600,000) viscosity does not seem to be an important variable in surging of hydraulic turbines.

B. NATURE OF THE ONSET OF SURGING

As pointed out in the introduction, most investigators have utilized the magnitude of the swirl angle as the predictor of the onset of vortex breakdown. In each case observed here the breakdown began at the center of the pipe. Invariably the maximum swirl angle is found at some distance away from the centerline. In fact Harvey[8] found it to occur quite near the

boundary. Thus, it would seem that it is not the swirl angle itself which is important, but rather the combined rotational and axial gross characteristics.

The maximum swirl angle, like the onset of surging itself, is more likely a dependent quantity governed by the particular combination of angular-momentum flux, discharge, and draft-tube diameter. However, this assumes that regardless of how angular momemtum is introduced into the draft tube only one unique flow pattern will develop for each value of $\Omega D/\rho Q^2$ In this study, angular momentum was introduced in only one manner--the wicket gates--and, hence, that assumption was not verified or disproved. However, sharp-edged and bell-mouth entrances were used on the 0.286-foot-diameter tube. Equal-length tubes were found to have the same dimensionless frequency and pressure characteristics regardless of entrance condition.

The onset of surging took place in an interesting chain of events. Figure (5a) shows the flow pattern during steady rotating flow. As the wicket gates were closed, increasing the angular-momentum flux in the tube, a zone of reverse flow eventually formed in the jet downstream from the tube. Further increase in $\Omega D/\rho Q^2$ served to move the zone of reversed flow into the tube and upstream along the centerline. Figure (5b) shows the more or less spherical pattern marking the stagnation point which occurs at the upstream end of the reversed-flow zone. Downstream from the spherical pattern the helical-spiral vortex can be seen in Figure (5b). Further closure of the wicket gates moved the centerline stagnation point to the upstream limit of the tube and produced a helical-spiral vortex throughout the length of the tube as shown in Figure (6a). Diffusion of the smoke by turbulence made it impossible to visualize the flow pattern near the downstream end once surging was established throughout the tube.

Two critical values of $\Omega D/\rho Q^2$ were recorded for each tube, one for the value at which reversal occurred at the downstream end of the tube and one corresponding to fully developed surging throughout the tube. For the case of the jet (L/D = 0) there was only one critical value. The spiral vortex observed for the jet is shown in Figure 6(b) while Figure (7b) shows the spiral vortex for fully developed surging in the Fontenelle model draft tube. In the curved draft tube the onset of surging was first observed near the elbow and although smoke patterns never revealed a spiral vortex downstream from the elbow, measurements there did reveal that pressure surging did occur throughout. The critical values of $\Omega D/\rho Q^2$ are shown in Figure (8) along with values obtained by Gore and Ranz[11] and Harvey[8]. For these comparative values it was necessary to assume an axial-velocity distribution in order to compute $\Omega D/\rho Q^2$ since both investigations used swirl angle as the critical parameter. Figure (8) indicates that longer tube lengths produce greater stability against surging.

Figure 8 also indicates that the bend in the draft tube does not influence the breakdown threshold. The divergent cone tested (see Figure 7) had the same expansion rate and same centerline length as the draft tube, but was not bent or deformed. Using centerline length and entrance diameter the L/D ratio of the draft tube and the cone were both 4.77. Expansion of the tube appears to make the flow only slightly less stable against breakdown. The effect of expansion appears reasonable because the local value of $\Omega D/\rho Q^2$ increases as D increases while Ω,p, and Q must remain constant.

Smoke visualization of the helical vortex showed a much more distinct, well defined spiral for both the draft tube and the cone than for the straight tubes (see Figure 7). However, the vortex could not pass through the draft tube bend and was always broken up and diffused at the bend.

C. FREQUENCY AND PRESSURE CHARACTERISTICS

Dimensionless characteristics of pressure and frequency are shown respectively in Figures 13 and 14 in composite for all tubes tested. The values shown were all computed from runs made at Reynolds numbers well beyond 80,000 and therefore do not reflect viscous effects. All experimental points are at values of $\Omega D/\rho Q^2$ above the critical because the pressure-surge signal was difficult to filter out of turbulent noise at low surge amplitudes.

As can be seen, both amplitude and frequency of the surge become smaller as the pipe is made longer, all other variables being held constant. Although pressure variation along the tube was not recorded, it was

[11] Gore, R. W., and W. E. Ranz, "Backflows in Rotating Fluids Moving Axially Through Expanding Cross-Sections," AIChE JOURNAL, January 1964.

observed that the frequency of the surge was constant all along the tube. However the peak-to-peak value of the pressure surge varied along the length of the tube being greatest near the exit of the tube and lowest at the inlet end.

When surging occurred within the exit tube, a pressure fluctuation of equal frequency was observed upstream from the wicket gates inside the stilling chamber. In most cases the amplitude of this upstream pressure fluctuation was at least a factor of five smaller than that observed at the draft tube throat. However, when the surge frequency was near the natural frequency of the system, the amplitude of the pressure fluctuation within the box increased significantly. Natural frequencies of the system (stilling chamber and exit tube) were determined by two different methods. The first method, suggested by Rayleigh, involved observing the frequency of the fluctuations produced by blowing compressed air across the exit opening of the draft tube.[12] In the second method, a loud speaker was driven at successively different frequencies and the pressure response of the system was observed.

The following table shows the natural frequencies of the system as they were determined experimentally. The natural frequencies were substantially different from the frequency of the surge for nearly all recorded measurements. Therefore, it is improbable that the natural frequency had any effect upon the measured surge amplitude or frequency.

TUBE DESCRIPTION		NATURAL FREQUENCY OF SYSTEM
D (ft.)	L/D	f_n (cps)
0.511	3.26	230
0.511	1.63	230
0.511	0	8
0.286	7.20	250

Using the hot-film anemometer to monitor velocity near the tube wall provided a verification that the pressure surge was indeed produced by the precessing helical vortex. Figure 9 shows that the velocity near the piezometer and the pressure signal have the same frequency. (This is an important feature because it clearly shows the connection between the pressure surge and the vortex.)

APPLICATION TO HYDRAULIC TURBINES

The experimental results of this study can be used to investigate the surging potential of hydraulic turbines. Since the parameter $\Omega D/\rho Q^2$ indicates the probability of surging as well as the resulting frequency and pressure-fluctuation amplitude, analysis of a turbine must be directed toward the determination of this parameter.

A. ANALYSIS

In flow through a hydraulic-turbine runner, angular momentum is imparted to the flow as it passes through the wicket gates. As the flow then passes through the turbine runner an exchange of angular momentum is made between the flow and the runner resulting in a net torque on the runner. The torque is equal to the change in the rate of flow of angular momentum produced as the flow passes from the inlet to the outlet of the runner. Figure 15 is a simplified schematic diagram for flow through a runner. The equation for the torque on the runner is

$$T = \Omega_1 - \Omega_2 \tag{7}$$

where $\Omega_1 - \Omega_2$ is the rate of change of angular momentum occurring between points 1 and 2, respectively, the entrance to and exit from the runner. Power delivered by the runner is equal to torque multiplied by ω the angular velocity of the runner. Thus,

$$\frac{P}{\omega} = \Omega_1 - \Omega_2 \tag{8}$$

Multiplication of both sides of Equation (8) by $D/\rho Q^2$ and subsequent rearrangement yields

$$\frac{\Omega_2 D}{\rho Q^2} = \frac{\Omega_1 D}{\rho Q^2} - \frac{PD}{\rho \omega Q^2} \tag{9}$$

[12] Rayleigh, Lord, "Theory of Sound," Dover Press, 1963.

which by incorporation of Equation (6) can be written as

$$\frac{\Omega_2 D}{\rho Q^2} = \frac{D \tan \alpha_1}{2\pi B} \cdot \frac{PD}{\rho \omega Q^2} \qquad (10)$$

The left side of Equation (10) is the momentum parameter of Equations (3) and (5) for the draft tube. On the right side of Equation (10) the first term is the momentum parameter for the flow entering the runner and can be determined if the inlet geometry of the turbine is known. The second term can be determined if the performance characteristics of the turbine are known.

Equation (10) can be used to determine the operating conditions under which the momentum parameter $\Omega_2 D/\rho Q^2$ for the draft tube exceeds the critical value as given in Figure 8. If load and discharge on the turbine are such that flow leaves the runner with no swirl then Ω_2 will be zero, as will $\Omega_2 D/\rho Q^2$, and no surging could occur. The sketch in Figure (20) shows the velocity diagram for flow from the discharge side of a runner blade. The absolute velocity V_2 is determined by the two components: the runner velocity $r_2\omega$ and V_r the velocity of the water relative to the blade. The runner velocity $r_2\omega$ is constant on a speed-regulated unit. However, any change in Q produces a change in V_r. If Q is decreased V_r decreases and V_2 develops a peripheral component in the direction of turbine rotation. If Q is increased, V_r increases and V_2 develops a peripheral component in the direction opposite to turbine rotation. The change in V_r can be caused by either a change in gate opening or a change in head. If swirl occurs in the direction of the runner, Ω_2 in Equation (10), and hence $\Omega_2 D/\rho Q^2$ as well, will be positive. For swirl in the direction opposite to the runner, the sign of $\Omega_2 D/\rho Q^2$ will be negative. Surging is independent of swirl direction and, thus, it is the absolute value of $\Omega_2 D/\rho Q^2$ which is of importance.

Equation (10) was used to analyze model-performance data for the Fontenelle and Hoover-replacement runners. Figure (16) shows the $\Omega D/\rho Q^2$ and efficiency characteristics for the Fontenelle model as a function of standard unit parameters. For operation within the $\Omega D/\rho Q^2 = 0.4$ contour surging should not be expected. However, operation outside of that contour should produce surging. Note that the region of maximum efficiency lies within the smooth operation region, but that rough operation could conceivably occur at a discharge only slightly larger than that realized at maximum efficiency (assuming constant head). Contours of large $\Omega D/\rho Q^2$ will indicate regions of relatively high frequency and pressure-fluctuation amplitude.

Upward and to the left of the dashed line in Figure (16) the flow in the draft tube whirls in the same direction as the runner while below and to the right of the line the whirl is opposite to the runner. Power swings observed on the Fontenelle prototype are plotted on Figure (16) in megawatts. Because the interaction between turbine and power system is not known, little can be said about the power swings except that they are in general agreement with predicted regions of surging.

Analysis of the Hoover model data produced the plot of characteristics shown in Figure (17). Again a region of surge-free operation is predicted. The manufacturer of the Hoover model did not provide as large a range of performance data as was available for the Fontenelle model. However, the water leaving the wicket gates does not necessarily leave tangent to the gate. Experience with the Hoover data showed that the method used in determining $\Omega_1 D/\rho Q^2$ for use in Equation (9) needs further investigation. Using D tan $\alpha_1/2\pi B$ may produce an $\Omega_2 D/\rho Q^2$ which is incorrect.

B. EFFECT OF TAILWATER

In prototype plants it has been noted that increasing tailwater depth generally results in stronger pressure surges while decreasing the depth seems to alleviate the surging. In the air model such a phenomenon could not be observed because an increase in pressure at the outlet end would simply increase the pressure throughout the system and decrease the discharge for a given gate opening. This, according to the results of this study summarized in Figures (13) and (14), would not change $\Omega D/\rho Q^2$ and would, hence, not change the frequency or pressure parameter.

One must conclude, therefore, that the tailwater effect is a condition involving two-phase flow. If the tailwater depth is reduced the pressure in the draft tube is reduced and water vapor may be created and fill the core or air may be drawn in through existing aeration devices and then may replace the core of the vortex in the draft tube. At high tailwater cavitation may be eliminated and because of increased draft-tube pressure air may not be drawn into the draft tube. Under these conditions the core will fill with water and the surge is dynamically similar to the air model observed in this study. Air injection is known to alleviate surging which agrees with the above reasoning.[12] The air or vapor-filled core has been observed by many investigators.[2, 3, 12] With the vortex core filled with air or vapor the mass of fluid oscillating in the draft tube is reduced and thus one would expect the pressure amplitudes to be reduced even though the surge frequency may possibly remain the same.

Figure (18) shows a dimensionless plot of surge frequency parameter versus $\Omega D/\rho Q^2$ for various values of σ for the Hoover model (σ is the cavitation number for the turbine).

Figure (19) shows a corresponding plot of the pressure parameter. The plots indicate that both frequency and pressure decrease as σ is decreased. At $\sigma = 0.30$ the frequency parameters and pressure parameters are in reasonable agreement with those of this study for corresponding values of $\Omega D/\rho Q^2$.

MODEL-PROTOTYPE SIMILITUDE

Equations (3) and (5) express functionally the relationships of interest in applying the experimental results of this study to a prototype turbine draft tube.

$$\frac{fD^3}{Q} = \phi_1\left(\frac{\Omega D}{\rho Q^2}, \frac{L}{D}, R\right) \qquad (3)$$

$$\frac{\Delta P D^3}{\Omega} = \phi_2\left(\frac{\Omega D}{\rho Q^2}, \frac{L}{D}, R\right) \qquad (5)$$

Using subscripts of M and P to represent model and prototype, respectively, the conditions of dynamic and geometric similitude are

$$\left(\frac{\Omega D}{\rho Q^2}\right)_M = \left(\frac{\Omega D}{\rho Q^2}\right)_P \qquad \left(\frac{L}{D}\right)_M = \frac{L}{D}\Big)_P \qquad (11)$$

For viscous similarity all that is required is that the Reynolds number of the prototype be at least equal to 80,000.

If the similitude relationships of Equations (11) are satisfied it follows from Equations (3) and (5) that

$$\left(\frac{fD^3}{Q}\right)_M = \left(\frac{fD^3}{Q}\right)_P \qquad \left(\frac{\Delta P D^3}{\Omega}\right)_M = \left(\frac{\Delta P D^3}{\Omega}\right)_P \qquad (12)$$

Thus, the prototype surge amplitude will be

$$\Delta P_p = \Delta P_M \left(\frac{D_M}{D_P}\right)^3 \left(\frac{\Omega_P}{\Omega_M}\right) \qquad (13)$$

Using the first of the similitude relations in Equation (11)

$$\Delta P_p = \left(\frac{\Delta P D^3}{\Omega}\right)_M \left(\frac{\Omega D}{\rho Q^2}\right)_M \left(\frac{\rho Q^2}{D^4}\right)_P \qquad (14)$$

similarly, the prototype surge frequency will be

$$f_P = f_m \left(\frac{D_m}{D_p}\right)^3 \frac{Q_p}{Q_m} \qquad (15)$$

If information on the model is known in terms of $\Omega D/\rho Q^2$ Equations (14) and (15) can be used to determine frequency and magnitude of pressure surging for the prototype. Predicted pressure may, however, be altered by plant σ and by possible resonance in the system.

(Example)

For Fontenelle turbine and draft tube

$D_p = 10.00'$ (3.048 m), $\rho_p = 1.94$ slugs/ft^3 (1.0 gm/cm^3)

Picking a point on Figure (16) where $\Omega D/\rho Q^2 = 1.00$,

$Q/D_R^2\sqrt{H} = 1.75$ and $\pi D_R n/60\sqrt{2gH} = 0.80$

Then, because D_{R_p}=7.416' (2.2606 m) and np=150 rpm, H_P = 83' (25.2 m) and Q_P = 880 cfs (24.9 m^3/sec).

From Figures (13) and (14) we obtain $\left(\frac{fD^3}{Q}\right)_M = 0.88$ and $\left(\frac{\Delta PD^3}{\Omega}\right)_M = 4.5$

Thus,

$$f_P = \left(\frac{fD^3}{Q}\right)_M \left(\frac{Q}{D^3}\right)_P = 0.88 \left(\frac{880}{1000}\right) = 0.78 \text{ cps}$$

$$\Delta P_P = \left(\frac{\Delta PD^3}{\Omega}\right)_M \left(\frac{\Omega D}{PQ^2}\right)_M \left(\frac{\rho Q^2}{D^4}\right)_P$$

$$= 4.5\ (1.00)\ \frac{1.94\ (880)^2}{(10)^4} = 695 \text{ psf} = 11.1 \text{ ft (3.38 m) water}$$

The rotational speed for Fontenelle is 150 rpm, Rheingans Equation (1) predicts a frequency of 0.63 cps. Thus, the predicted results above appear reasonable.

FIGURE 1
REPORT HYD-591

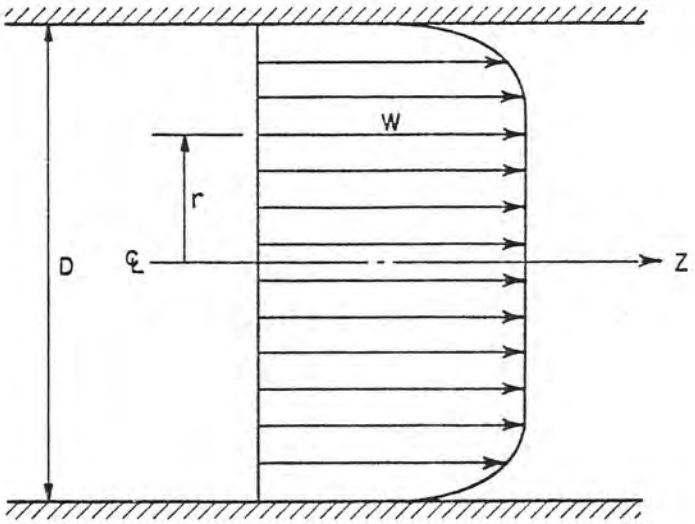

(a) PURELY AXIAL TURBULENT FLOW

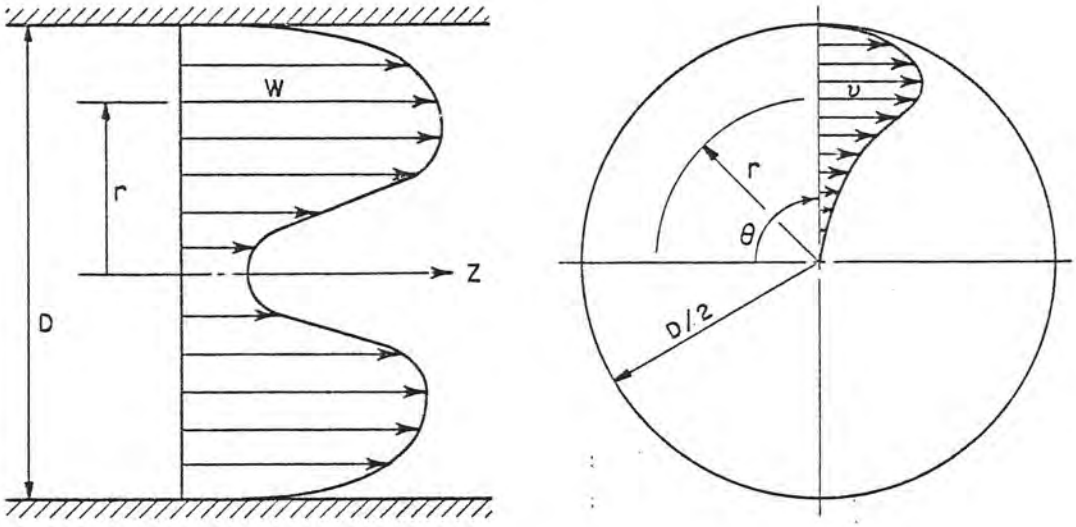

(b) AXIAL FLOW WITH ROTATION

EFFECT OF ROTATION ON FLOW PATTERN

739

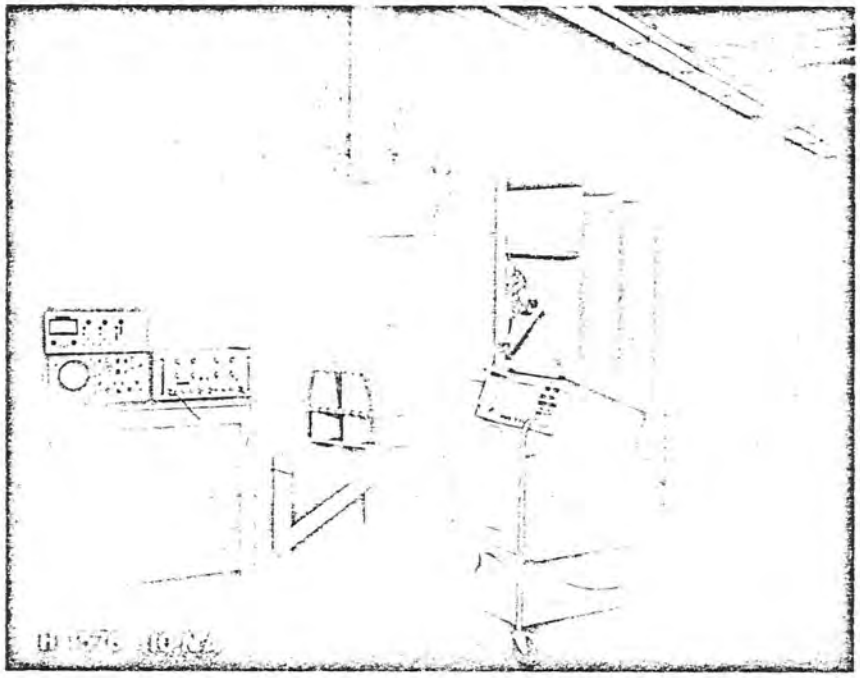

A. Overall view from downstream end. Photo PX-D-64111.

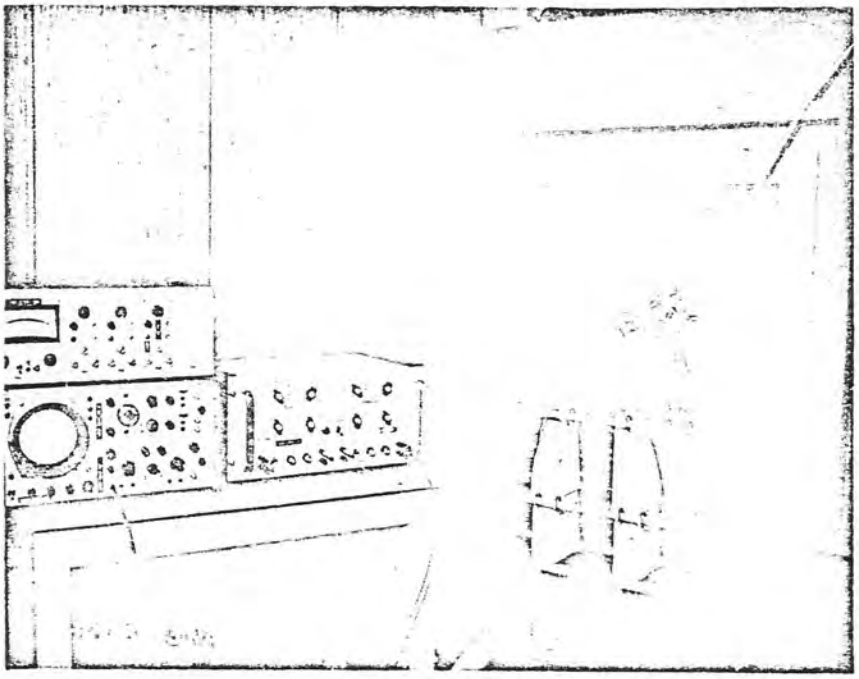

B. View of outlet with model of Fontenelle draft tube mounted. Photo PX-D-64112.

DRAFT–TUBE SURGE STUDY
Experimental Apparatus

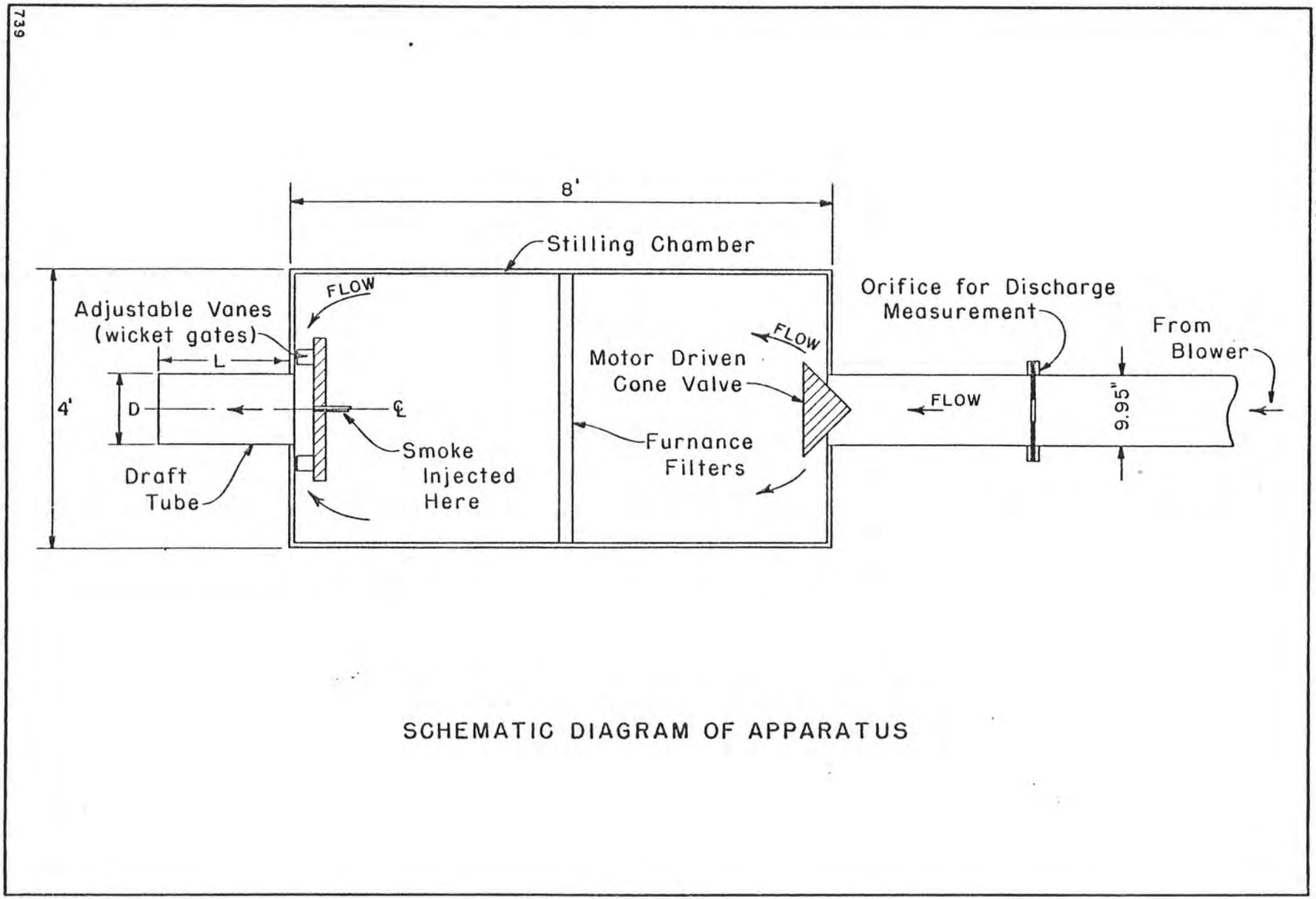

SCHEMATIC DIAGRAM OF APPARATUS

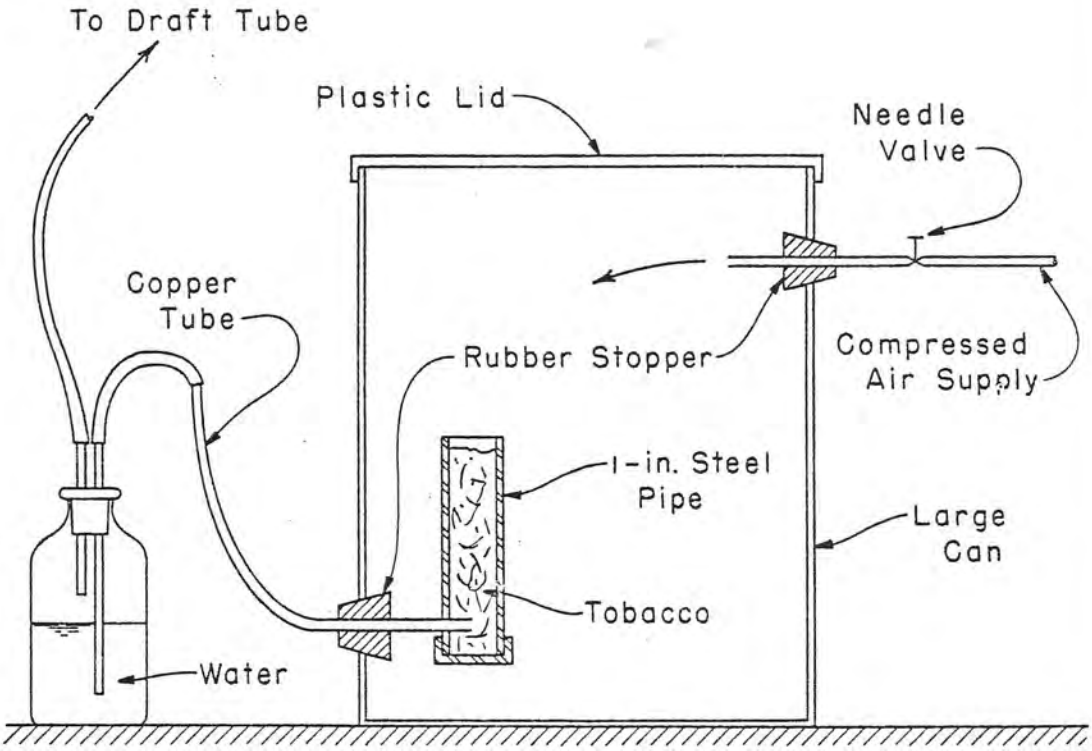

SMOKE GENERATOR

739

Figure 5
Report HYD-591

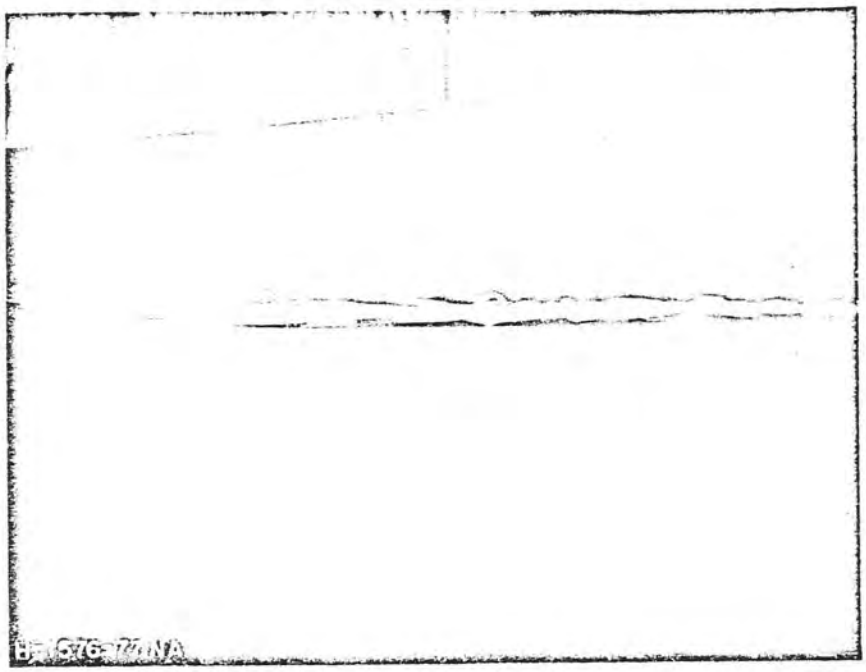

A. Steady uniformly swirling flow
D = 3.44 in. (8.76 cm), $\frac{L}{D}$ = 7.20, $\frac{\Omega D}{\rho Q^2}$ = 0.100

Photo PX-D-64109.

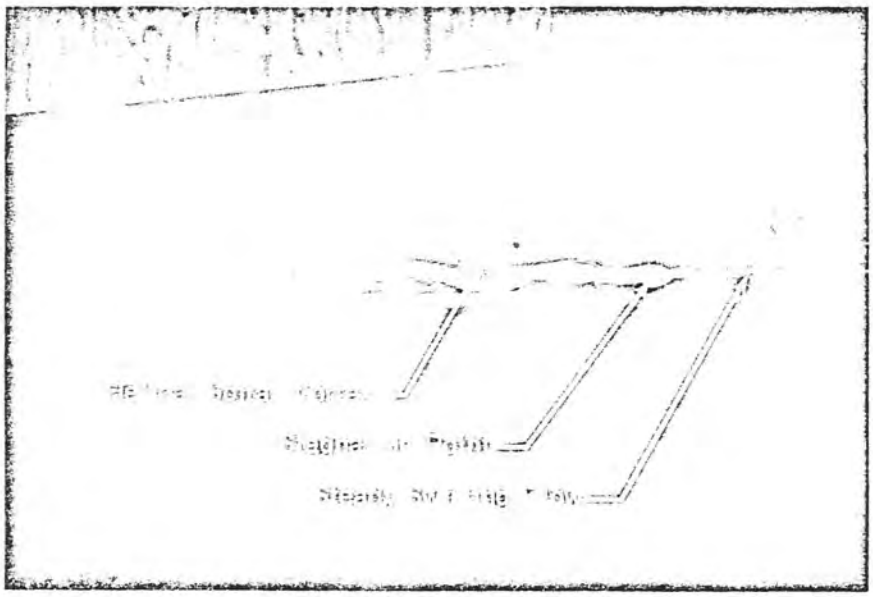

B. Reversal and surging

D = 3.144 in. (8.76 cm), $\frac{L}{D}$ = 7.20 $\frac{\Omega D}{\rho Q^2}$ = 0.280

Photo PX-D-64110.

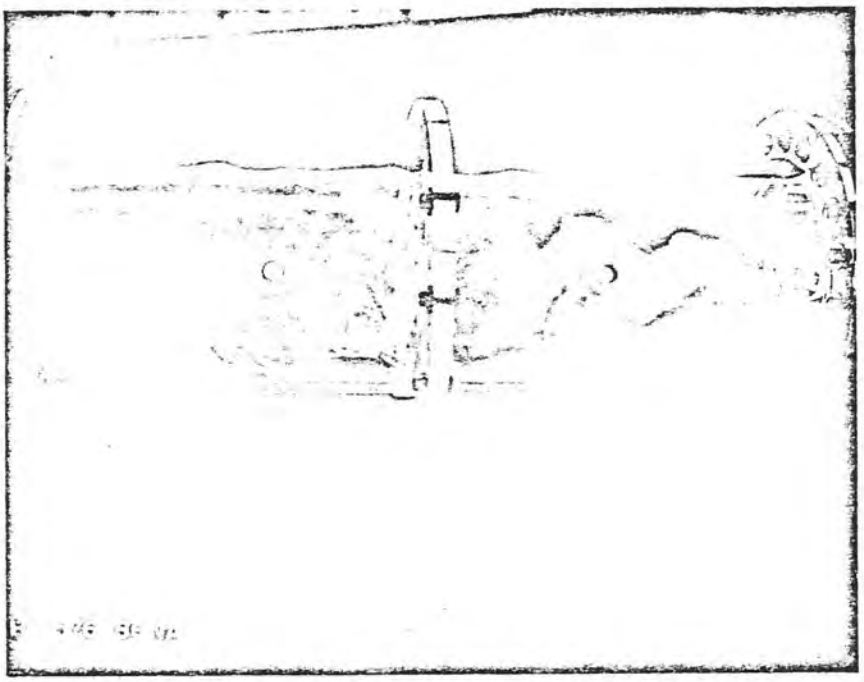

A. Fully established surging

D = 6.13 in. (15.56 cm), $\frac{L}{D}$ = 3.26, $\frac{\Omega D}{\rho Q^2}$ = 0.354

Photo PX-D-64107

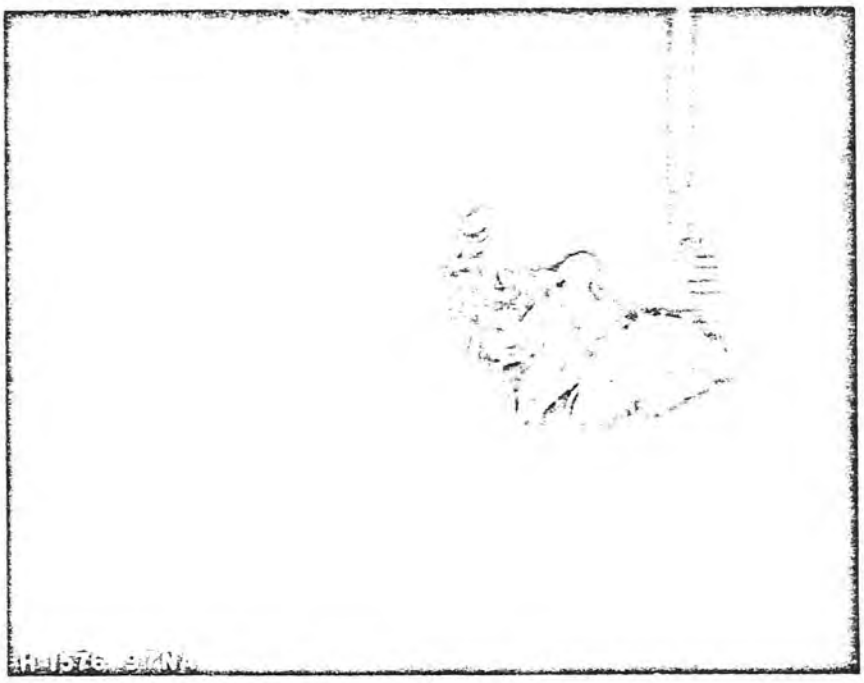

B. Surging in an open jet

D = 6.13 in. (15.56 cm), $\frac{L}{D}$ = 0.0, $\frac{\Omega D}{\rho Q^2}$ = 0.300

Photo PX-D-64108.

DRAFT-TUBE SURGE STUDY
Photographs of Flow Patterns

Figure 7
Report HYD-591

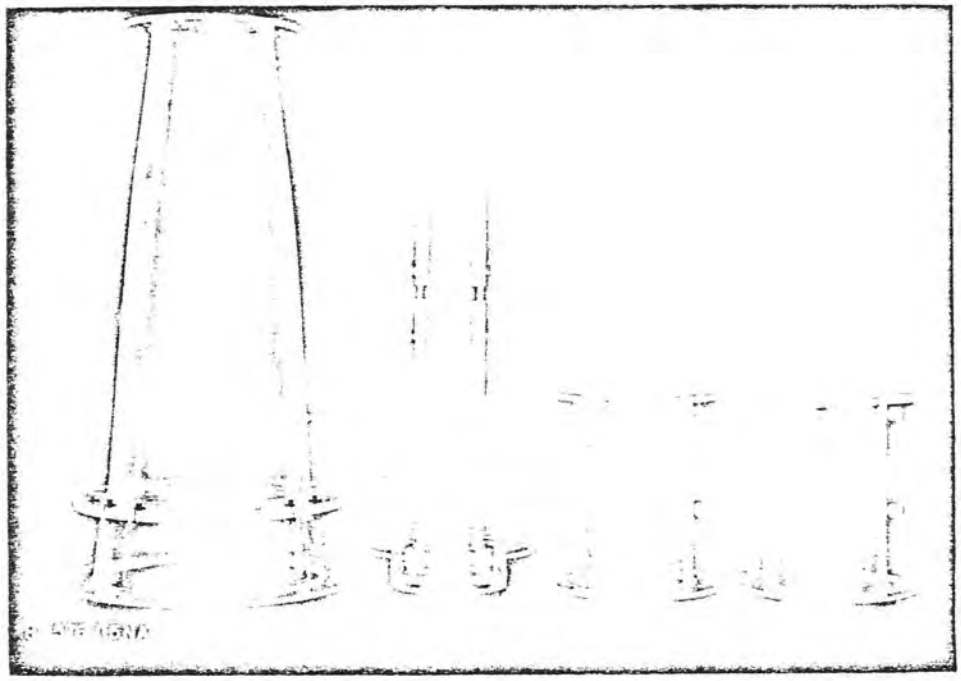

A. Draft tubes that were tested. Photo PX-D-64105.

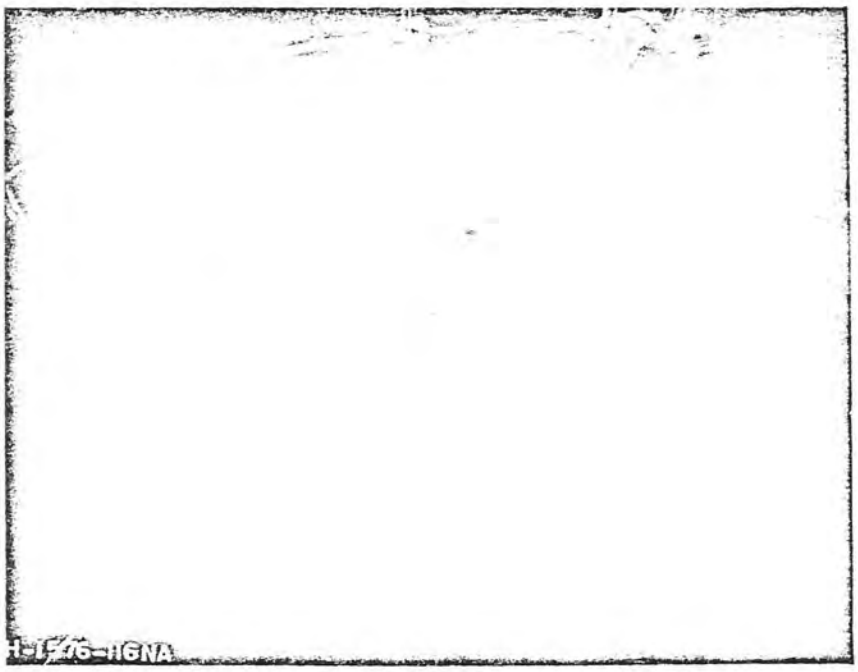

B. Fully established surging in the model of the Fontenelle Draft Tube.

D = 6.13 in. (15.56 cm), $\frac{L}{D} = 4.77$, $\frac{\Omega D}{\rho Q^2} = 0.400$

Photo PX-D-64106.

DRAFT-TUBE SURGE STUDY
Draft Tubes and Flow Patterns

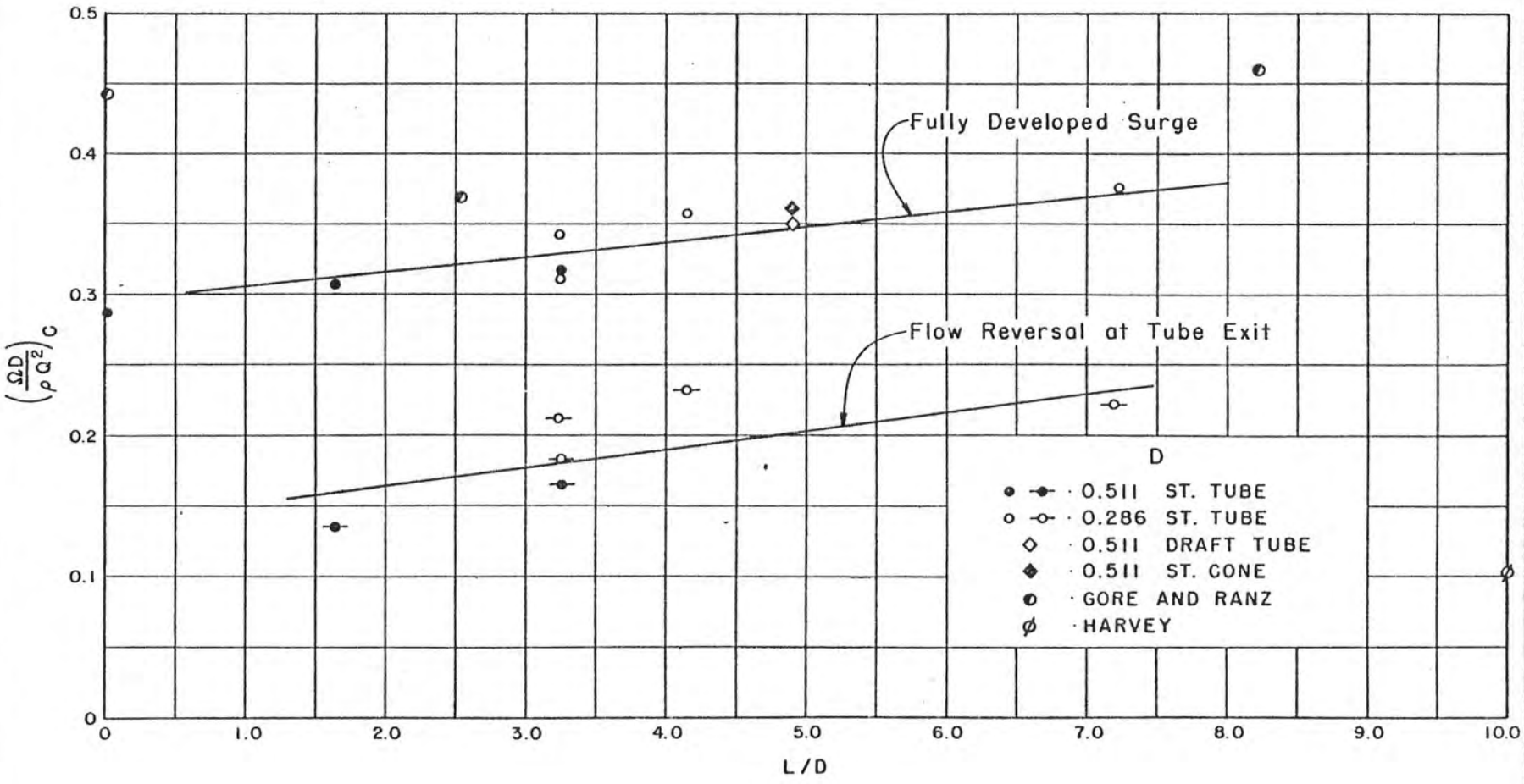

CRITICAL VALUES OF $\Omega D/\rho Q^2$

FIGURE 8
REPORT HYD-591

Figure 9
Report HYD-591

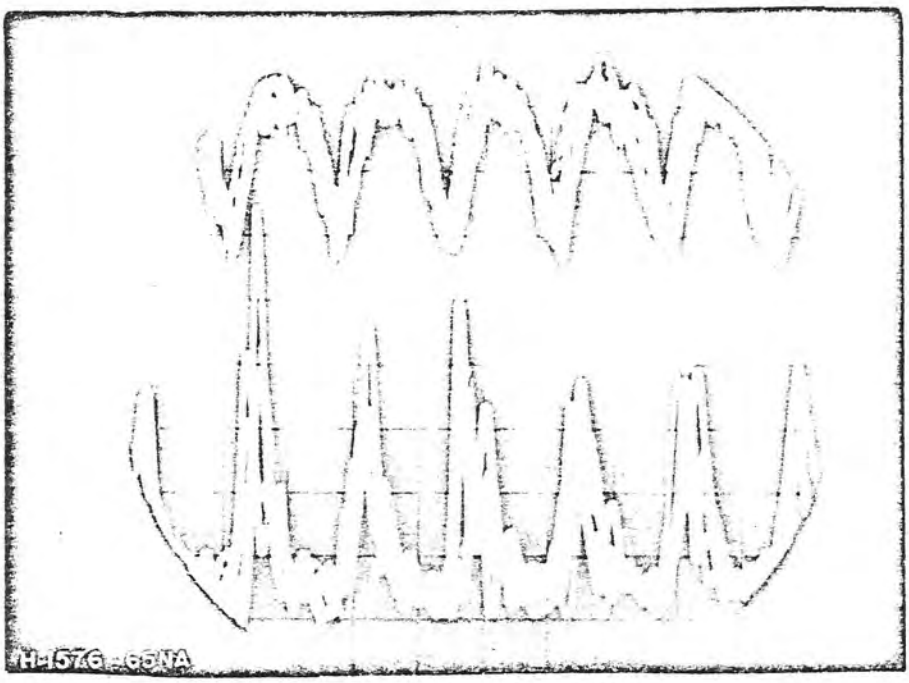

Velocity (upper) and pressure (lower) traces photographed on the oscilloscope

D = 6.13 in. (15.56 cm), $\frac{L}{D}$ = 1.63, $\frac{\Omega D}{\rho Q^2}$ = 1.000

Photo PX-D-64104.

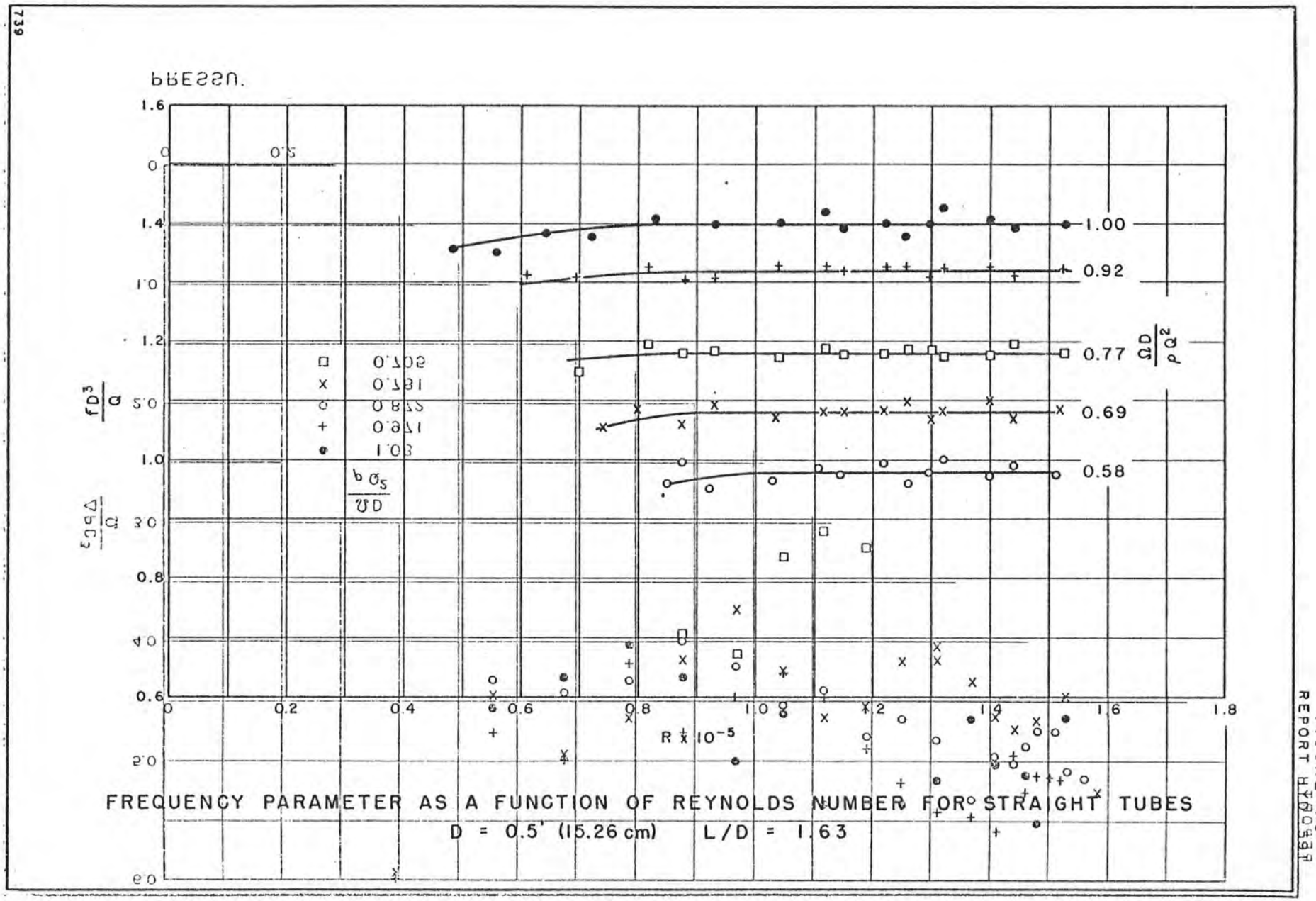

FREQUENCY PARAMETER AS A FUNCTION OF REYNOLDS NUMBER FOR STRAIGHT TUBES

D = 0.5' (15.26 cm) L/D = 1.63

FIGURE 10

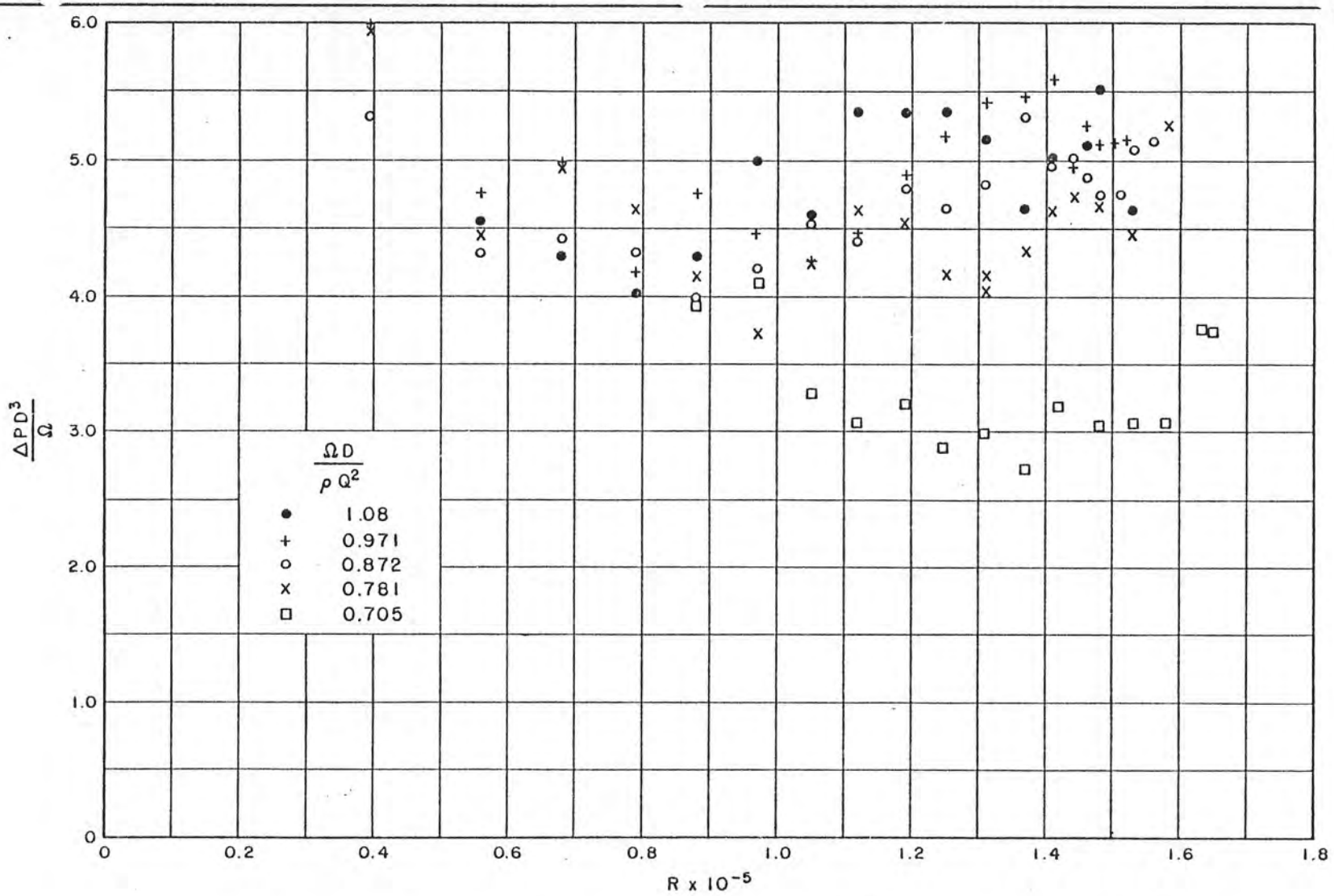

PRESSURE PARAMETER AS A FUNCTION OF REYNOLDS NUMBER, STRAIGHT TUBE
D = 0.5' (15.26 cm) L/D = 4.771

FIGURE 11
REPORT HYD-591

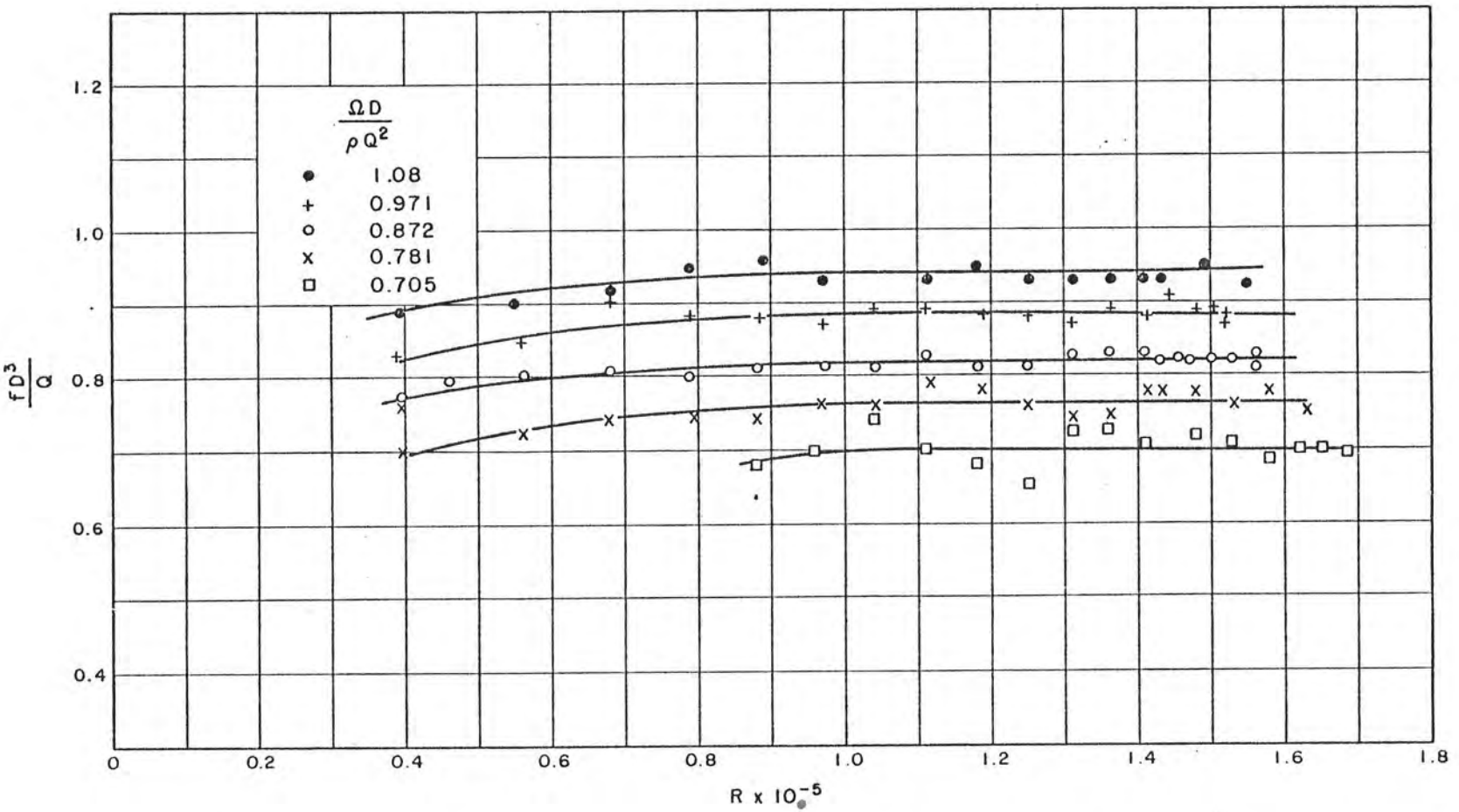

FIGURE 12
REPORT HYD-591

FREQUENCY PARAMETER AS A FUNCTION OF REYNOLDS NUMBER FOR THE FONTENELLE DRAFT TUBE
D = 0.5' (15.26 cm) L/D = 4.77

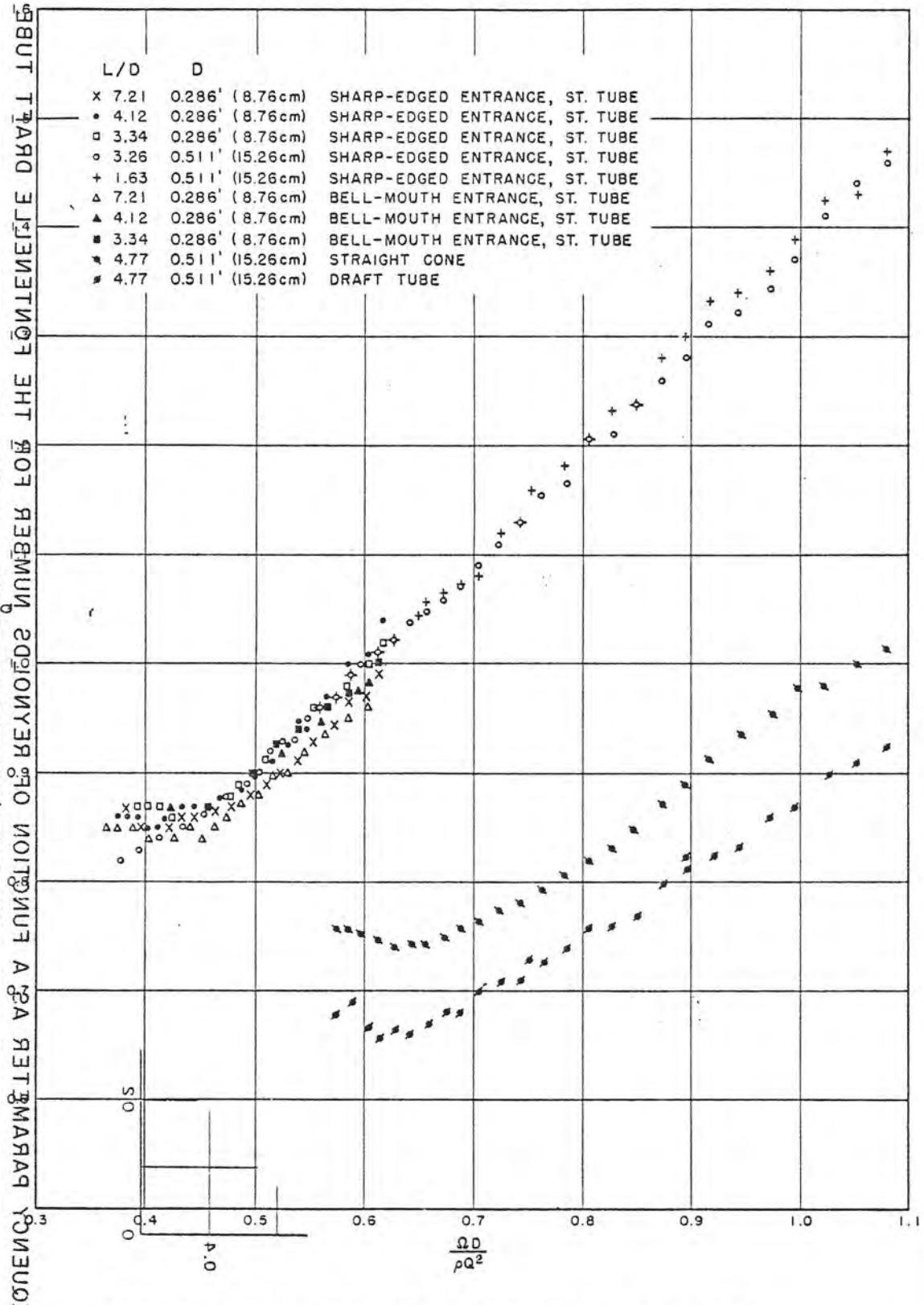

FREQUENCY PARAMETER FOR ALL TUBES AS A FUNCTION OF THE MOMENTUM PARAMETER

FIGURE 14
REPORT HYD-591

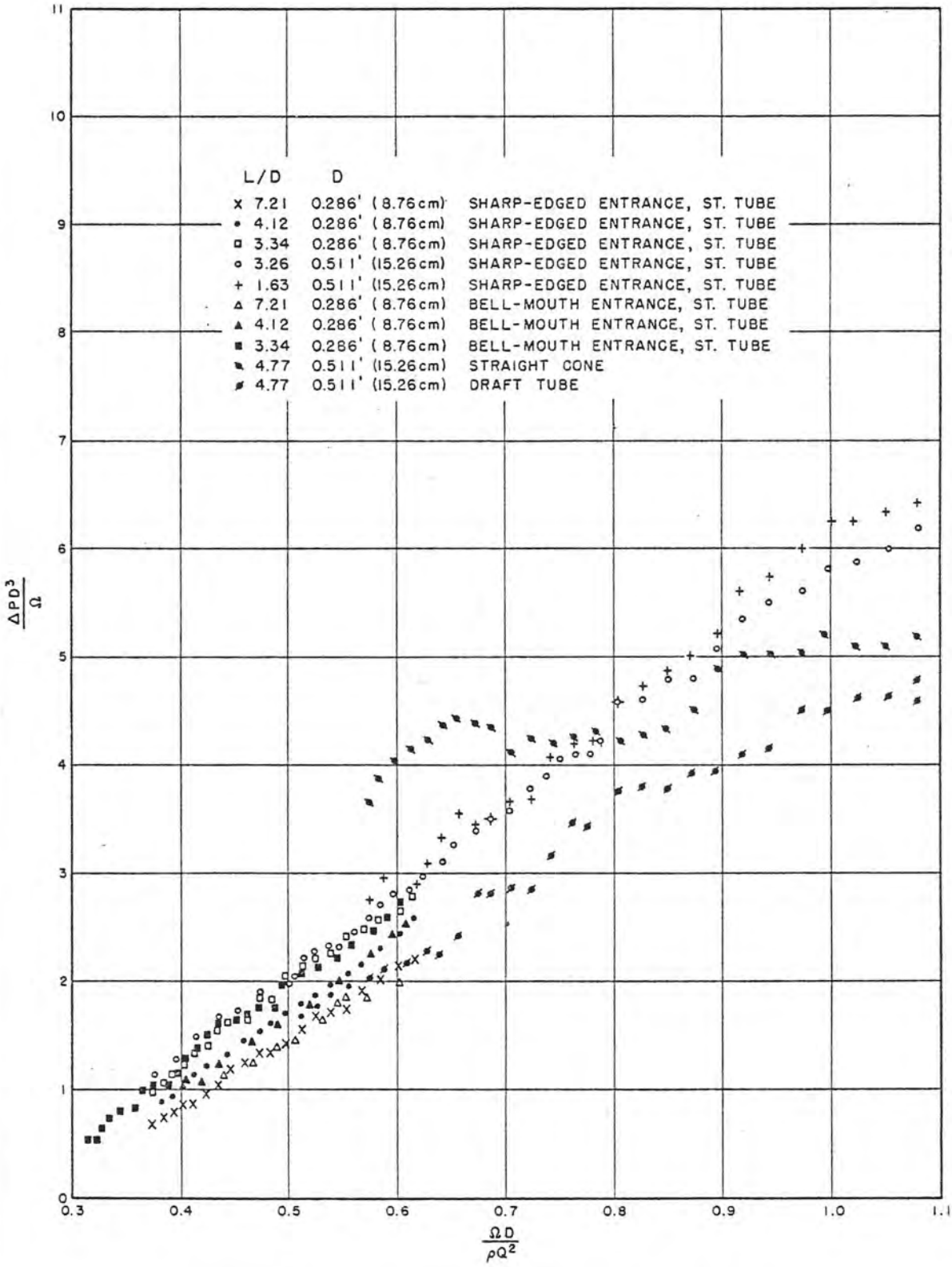

PRESSURE PARAMETER FOR ALL TUBES AS A FUNCTION OF MOMENTUM PARAMETER

739

FIGURE 15
REPORT HYD-591

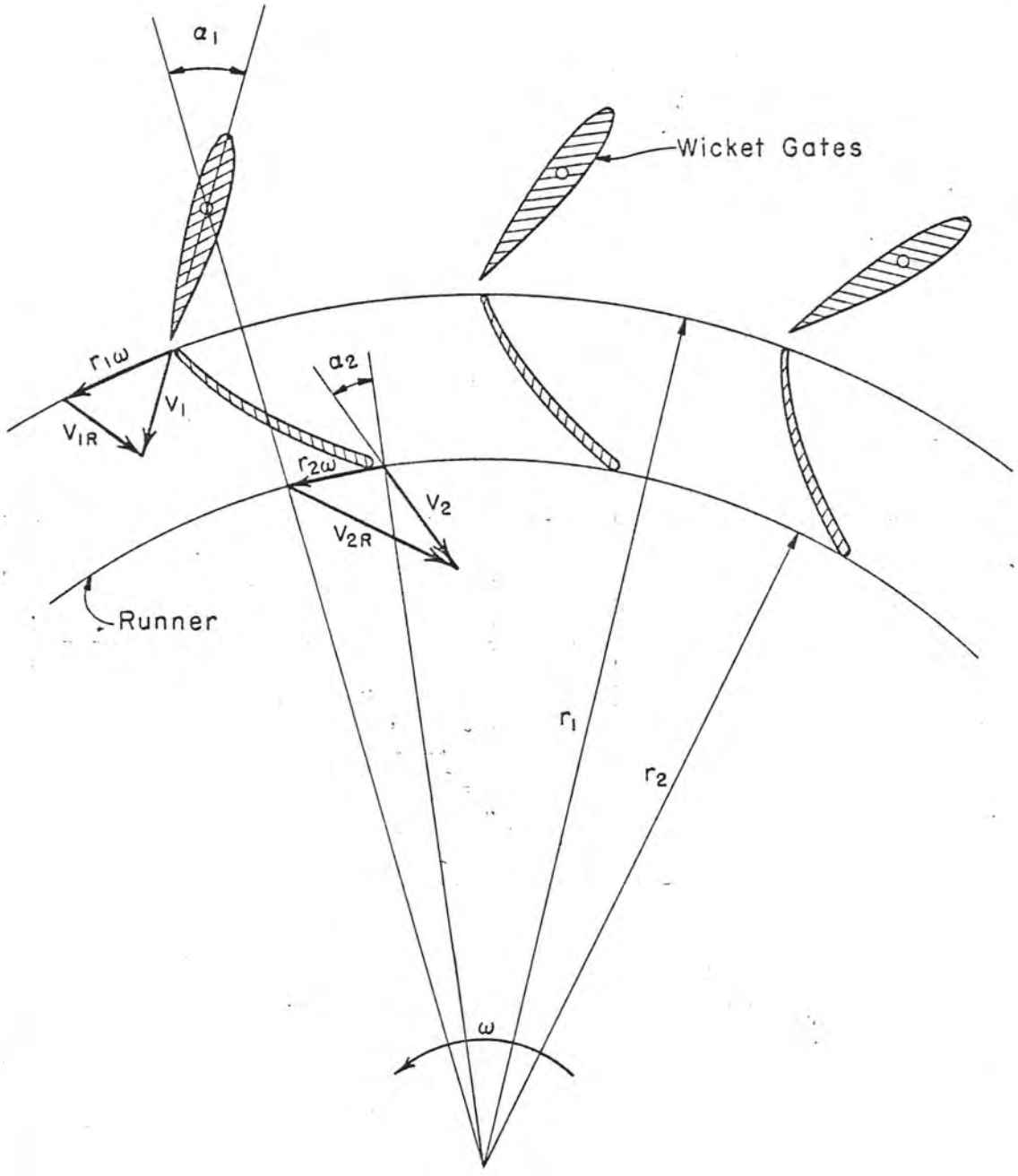

VELOCITY DIAGRAMS FOR A TURBINE RUNNER

739

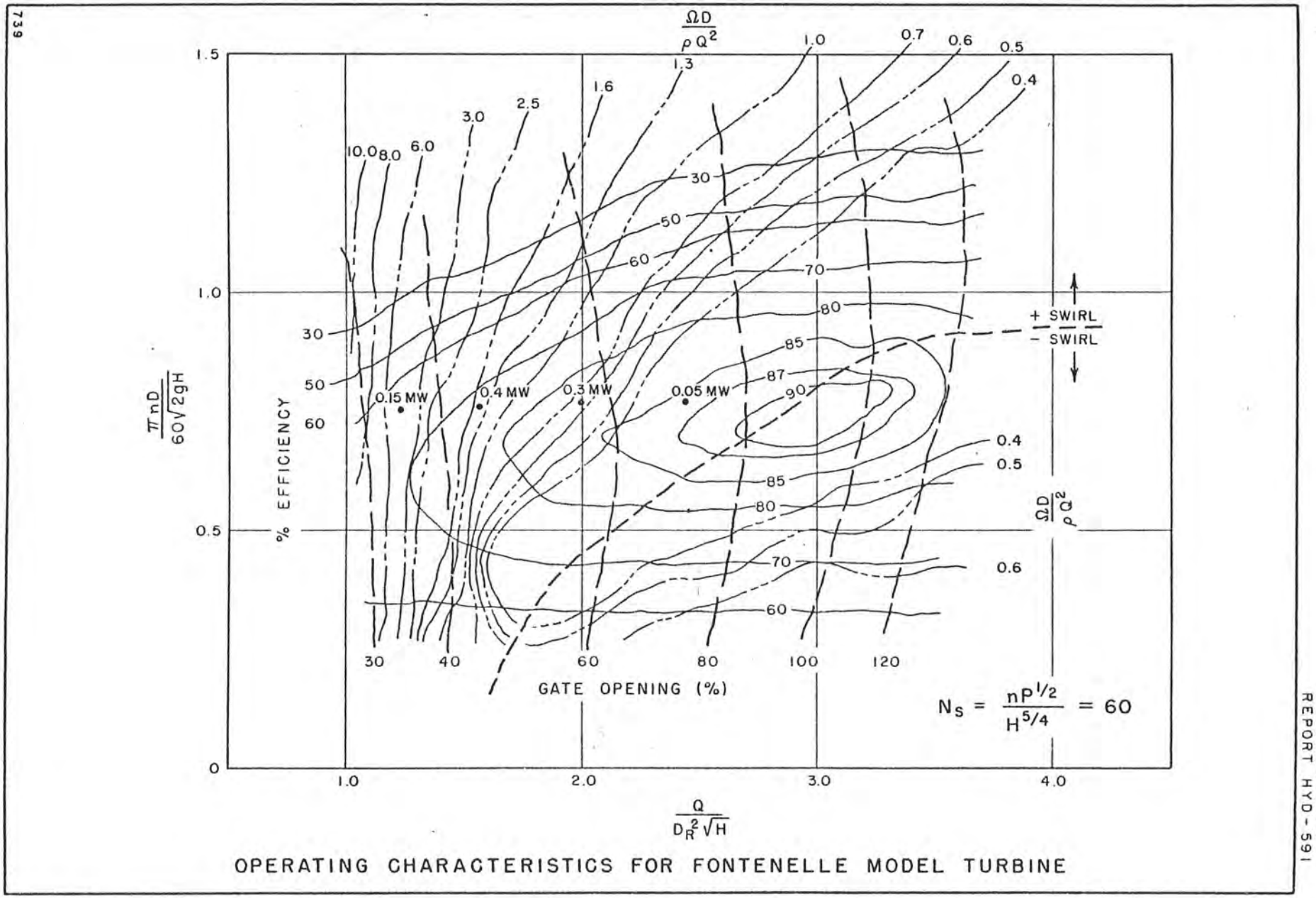

OPERATING CHARACTERISTICS FOR FONTENELLE MODEL TURBINE

FIGURE 16
REPORT HYD-591

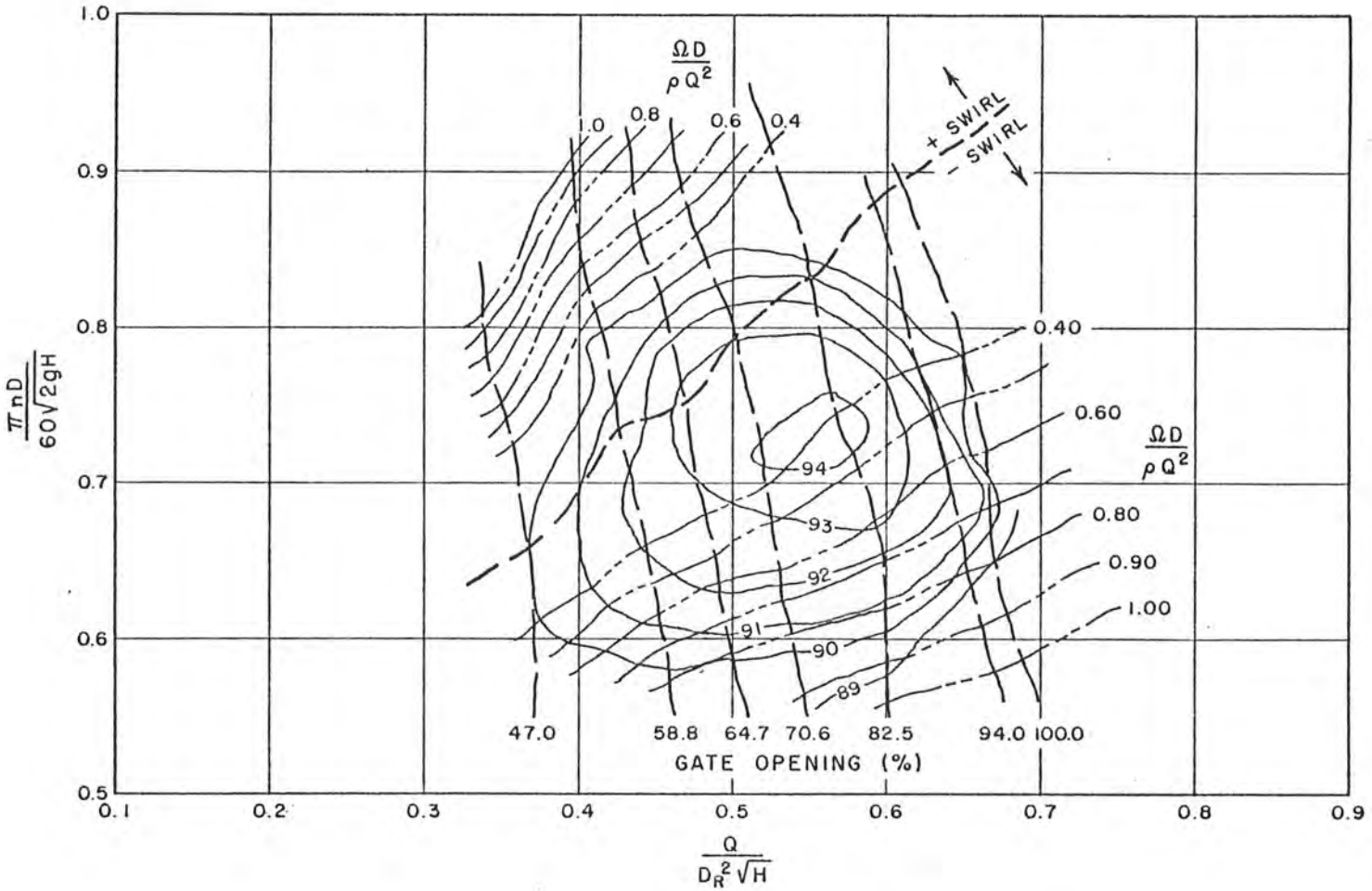

EFFICIENCY HILL - HOOVER REPLACEMENT RUNNER - MODEL DATA

$$N_S = \frac{n P^{1/2}}{H^{5/4}} = 28$$

FIGURE 17
REPORT HYD-591

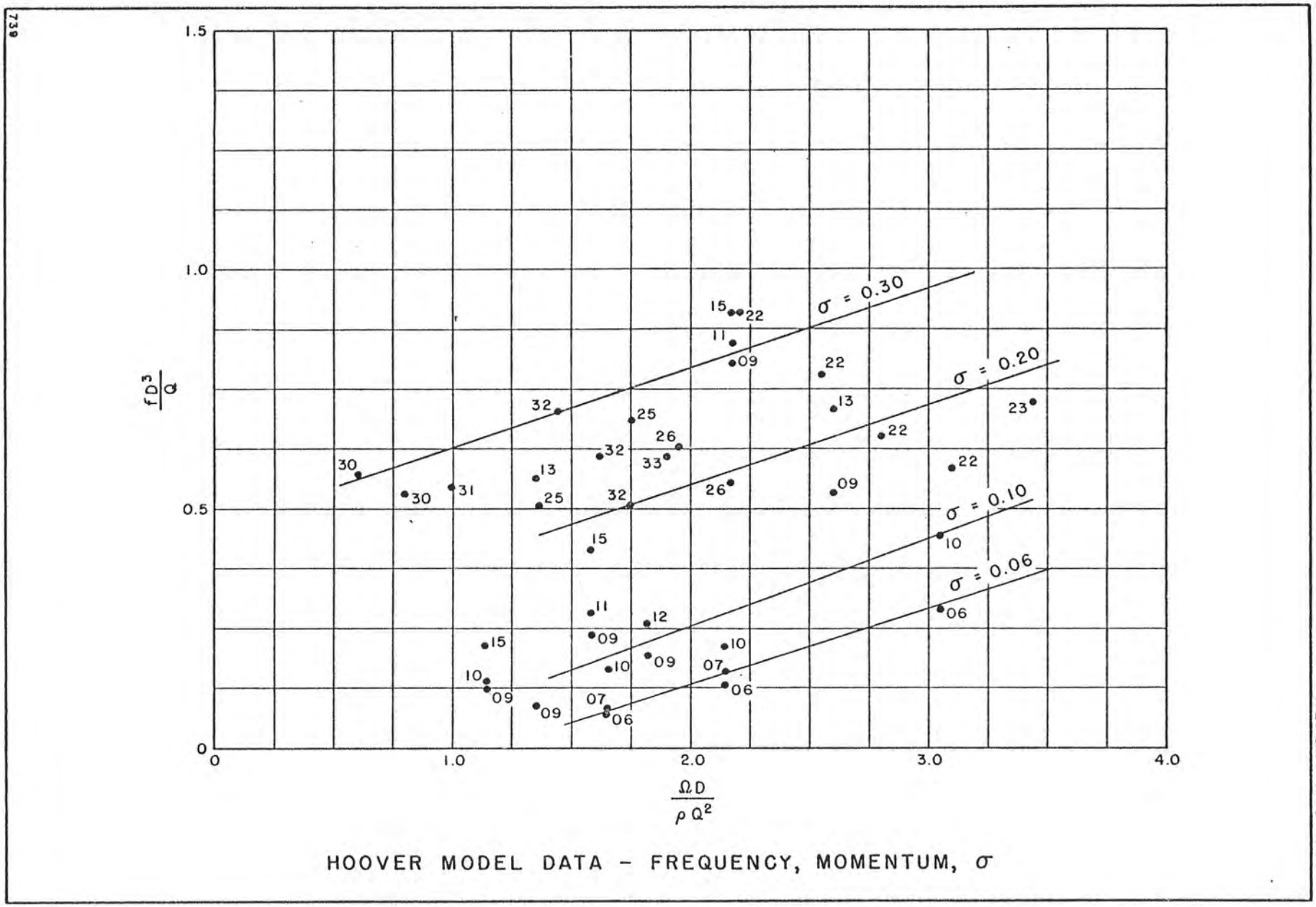

HOOVER MODEL DATA – FREQUENCY, MOMENTUM, σ

FIGURE 18
REPORT HYD-591

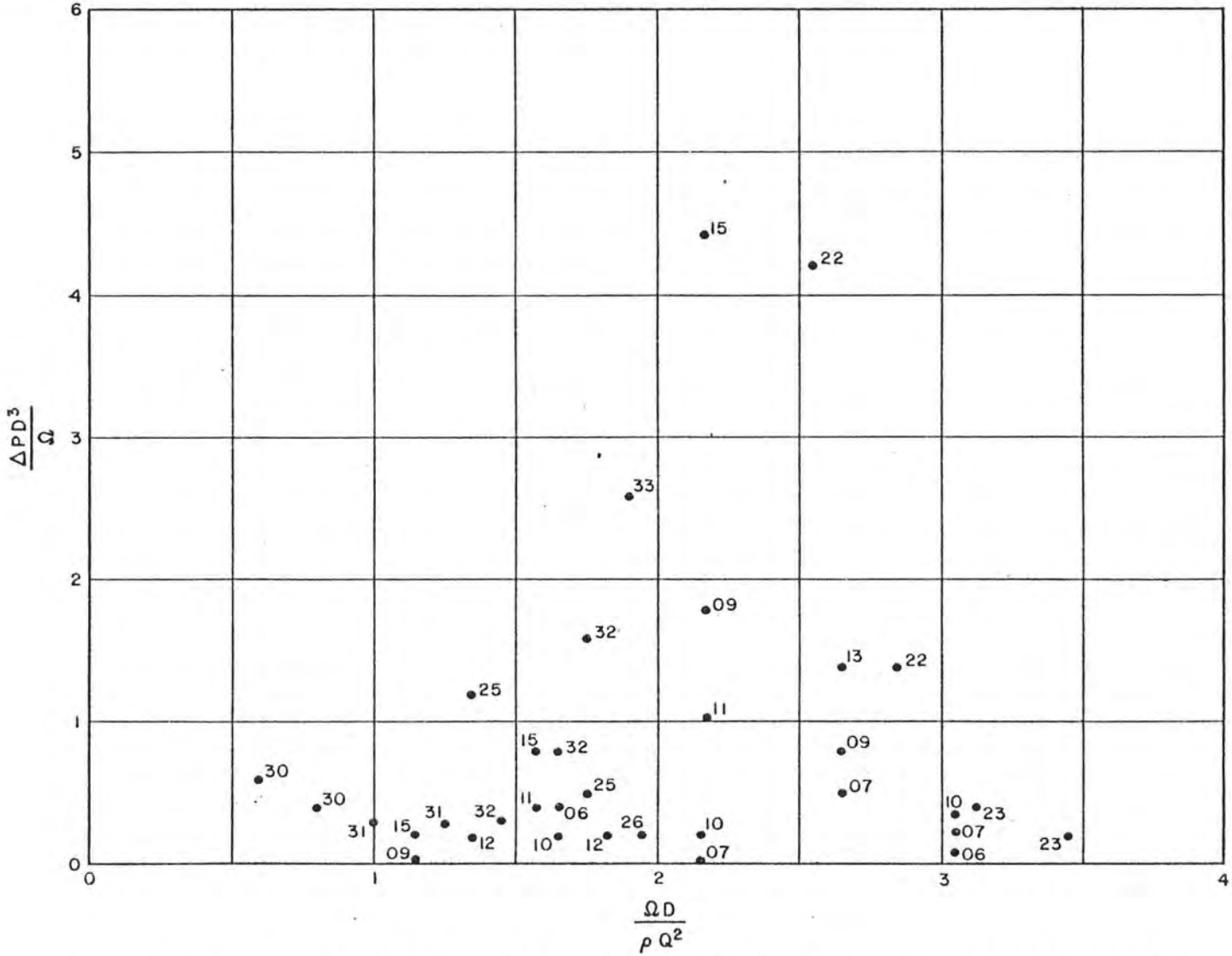

HOOVER REPLACEMENT RUNNER MODEL DATA, PRESSURE PARAMETER VERSUS MOMENTUM PARAMETER FOR VARIOUS VALUES OF σ

FIGURE 19
REPORT HYD-591

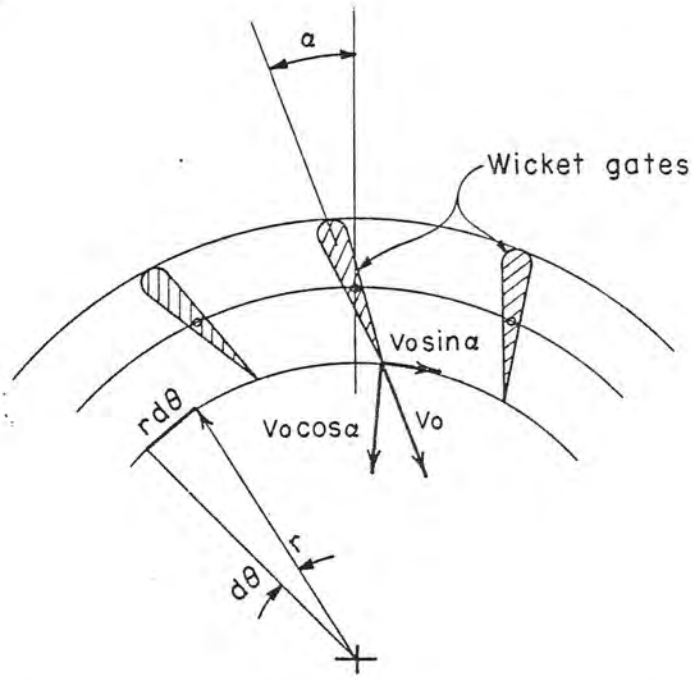

a. FLOW LEAVING WICKET GATES

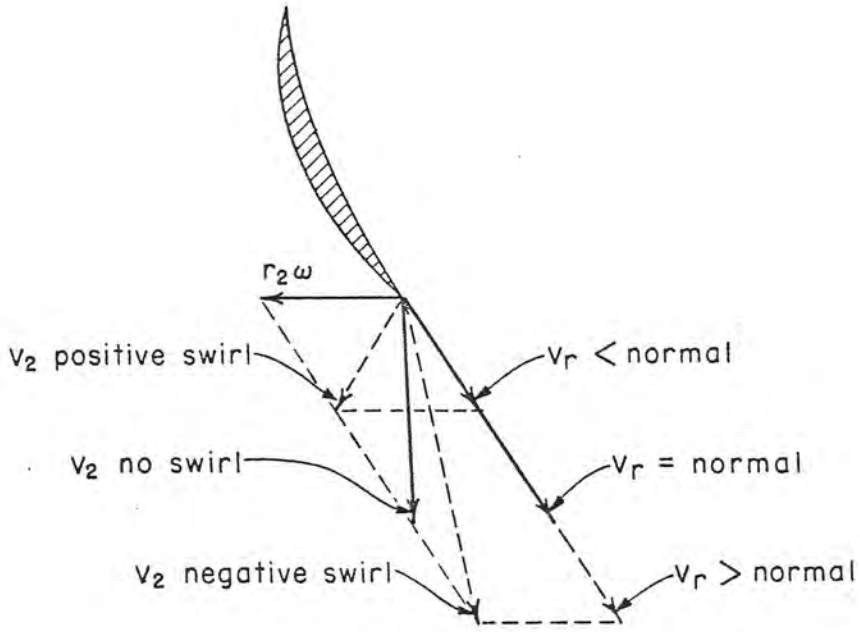

b. FLOW AT EXIT FROM TURBINE RUNNER

FLOW THROUGH A TURBINE

739

7-1750
(2-67)
Bureau of Reclamation

CONVERSION FACTORS--BRITISH TO METRIC UNITS OF MEASUREMENT

The following conversion factors adopted by the Bureau of Reclamation are those published by the American Society for Testing and Materials (ASTM Metric Practice Guide, January 1964) except that additional factors (*) commonly used in the Bureau have been added. Further discussion of definitions of quantities and units is given on pages 10-11 of the ASTM Metric Practice Guide.

The metric units and conversion factors adopted by the ASTM are based on the "International System of Units" (designated SI for Systeme International d'Unites), fixed by the International Committee for Weights and Measures; this system is also known as the Giorgi or MKSA (meter-kilogram (mass)-second-ampere) system. This system has been adopted by the International Organization for Standardization in ISO Recommendation R-31.

The metric technical unit of force is the kilogram-force; this is the force which, when applied to a body having a mass of 1 kg, gives it an acceleration of 9.80665 m/sec/sec, the standard acceleration of free fall toward the earth's center for sea level at 45 deg latitude. The metric unit of force in SI units is the newton (N), which is defined as that force which, when applied to a body having a mass of 1 kg, gives it an acceleration of 1 m/sec/sec. These units must be distinguished from the (inconstant) local weight of a body having a mass of 1 kg; that is, the weight of a body is that force with which a body is attracted to the earth and is equal to the mass of a body multiplied by the acceleration due to gravity. However, because it is general practice to use "pound" rather than the technically correct term "pound-force," the term "kilogram" (or derived mass unit) has been used in this guide instead of "kilogram-force" in expressing the conversion factors for forces. The newton unit of force will find increasing use, and is essential in SI units.

Table I

QUANTITIES AND UNITS OF SPACE

Multiply	By	To obtain
LENGTH		
Mil	25.4 (exactly)	Micron
Inches	25.4 (exactly)	Millimeters
	2.54 (exactly)*	Centimeters
Feet	30.48 (exactly)	Centimeters
	0.3048 (exactly)*	Meters
	0.0003048 (exactly)*	Kilometers
Yards	0.9144 (exactly)	Meters
Miles (statute)	1,609.344 (exactly)*	Meters
	1.609344 (exactly)	Kilometers
AREA		
Square inches	6.4516 (exactly)	Square centimeters
Square feet	929.03*	Square centimeters
	0.092903	Square meters
Square yards	0.836127	Square meters
Acres	0.40469*	Hectares
	4,046.9*	Square meters
	0.0040469*	Square kilometers
Square miles	2.58999	Square kilometers
VOLUME		
Cubic inches	16.3871	Cubic centimeters
Cubic feet	0.0283168	Cubic meters
Cubic yards	0.764555	Cubic meters
CAPACITY		
Fluid ounces (U.S.)	29.5737	Cubic centimeters
	29.5729	Milliliters
Liquid pints (U.S.)	0.473179	Cubic decimeters
	0.473166	Liters
Quarts (U.S.)	946.358*	Cubic centimeters
	0.946331*	Liters
Gallons (U.S.)	3,785.43*	Cubic centimeters
	3.78543	Cubic decimeters
	3.78533	Liters
	0.00378543*	Cubic meters
Gallons (U.K.)	4.54609	Cubic decimeters
	4.54596	Liters
Cubic feet	28.3160	Liters
Cubic yards	764.55*	Liters
Acre-feet	1,233.5*	Cubic meters
	1,233,500*	Liters

Table II

QUANTITIES AND UNITS OF MECHANICS

Multiply	By	To obtain
MASS		
Grains (1/7,000 lb)	64.79891 (exactly)	Milligrams
Troy ounces (480 grains)	31.1035	Grams
Ounces (avdp)	28.3495	Grams
Pounds (avdp)	0.45359237 (exactly)	Kilograms
Short tons (2,000 lb)	907.185	Kilograms
	0.907185	Metric tons
Long tons (2,240 lb)	1,016.05	Kilograms
FORCE/AREA		
Pounds per square inch	0.070307	Kilograms per square centimeter
	0.689476	Newtons per square centimeter
Pounds per square foot	4.88243	Kilograms per square meter
	47.8803	Newtons per square meter
MASS/VOLUME (DENSITY)		
Ounces per cubic inch	1.72999	Grams per cubic centimeter
Pounds per cubic foot	16.0185	Kilograms per cubic meter
	0.0160185	Grams per cubic centimeter
Tons (long) per cubic yard	1.32894	Grams per cubic centimeter
MASS/CAPACITY		
Ounces per gallon (U.S.)	7.4893	Grams per liter
Ounces per gallon (U.K.)	6.2362	Grams per liter
Pounds per gallon (U.S.)	119.829	Grams per liter
Pounds per gallon (U.K.)	99.779	Grams per liter
BENDING MOMENT OR TORQUE		
Inch-pounds	0.011521	Meter-kilograms
	1.12985×10^6	Centimeter-dynes
Foot-pounds	0.138255	Meter-kilograms
	1.35582×10^7	Centimeter-dynes
Foot-pounds per inch	5.4431	Centimeter-kilograms per centimeter
Ounce-inches	72.008	Gram-centimeters
VELOCITY		
Feet per second	30.48 (exactly)	Centimeters per second
	0.3048 (exactly)*	Meters per second
Feet per year	0.965873×10^{-6}*	Centimeters per second
Miles per hour	1.609344 (exactly)	Kilometers per hour
	0.44704 (exactly)	Meters per second
ACCELERATION*		
Feet per second^2	0.3048*	Meters per second^2
FLOW		
Cubic feet per second (second-feet)	0.028317*	Cubic meters per second
Cubic feet per minute	0.4719	Liters per second
Gallons (U.S.) per minute	0.06309	Liters per second
FORCE*		
Pounds	0.453592*	Kilograms
	4.4482*	Newtons
	4.4482×10^{-5}*	Dynes

Multiply	By	To obtain
WORK AND ENERGY*		
British thermal units (Btu)	0.252*	Kilogram calories
	1,055.06	Joules
Btu per pound	2.326 (exactly)	Joules per gram
Foot-pounds	1.35582*	Joules
POWER		
Horsepower	745.700	Watts
Btu per hour	0.293071	Watts
Foot-pounds per second	1.35582	Watts
HEAT TRANSFER		
Btu in./hr ft^2 deg F (k, thermal conductivity)	1.442	Milliwatts/cm deg C
	0.1240	Kg cal/hr m deg C
Btu ft/hr ft^2 deg F	1.4880*	Kg cal m/hr m^2 deg C
Btu/hr ft^2 deg F (C, thermal conductance)	0.568	Milliwatts/cm^2 deg C
	4.882	Kg cal/hr m^2 deg C
Deg F hr ft^2/Btu (R, thermal resistance)	1.761	Deg C cm^2/milliwatt
Btu/lb deg F (c, heat capacity)	4.1868	J/g deg C
Btu/lb deg F	1.000*	Cal/gram deg C
Ft^2/hr (thermal diffusivity)	0.2581	Cm^2/sec
	0.09290*	M^2/hr
WATER VAPOR TRANSMISSION		
Grains/hr ft^2 (water vapor transmission)	16.7	Grams/24 hr m^2
Perms (permeance)	0.659	Metric perms
Perm-inches (permeability)	1.67	Metric perm-centimeters

Table III

OTHER QUANTITIES AND UNITS

Multiply	By	To obtain
Cubic feet per square foot per day (seepage)	304.8*	Liters per square meter per day
Pound-seconds per square foot (viscosity)	4.8824*	Kilogram second per square meter
Square feet per second (viscosity)	0.092903*	Square meters per second
Fahrenheit degrees (change)*	5/9 exactly	Celsius or Kelvin degrees (change)*
Volts per mil	0.03937	Kilovolts per millimeter
Lumens per square foot (foot-candles)	10.764	Lumens per square meter
Ohm-circular mils per foot	0.001662	Ohm-square millimeters per meter
Millicuries per cubic foot	35.3147*	Millicuries per cubic meter
Milliamps per square foot	10.7639*	Milliamps per square meter
Gallons per square yard	4.527219*	Liters per square meter
Pounds per inch	0.17858*	Kilograms per centimeter

GPO 855 - 412

ABSTRACT

Draft-tube surge experiments were conducted with models of draft tubes, using air as the fluid. The occurrence, frequency, and amplitude of surges were correlated with flow and draft-tube geometry variables. Studies show that surges arise when angular momentum reaches a critical value relative to linear momentum. Surge frequency and peak-to-peak pressures are independent of viscous effects for Reynolds numbers above 80,000, and are correlated with a dimensionless momentum parameter for a particular draft-tube shape. A criterion is given for predicting the surging threshold. Results of the study are applied to analysis of draft-tube surging in the Fontenelle and Hoover replacement turbines.

ABSTRACT

Draft-tube surge experiments were conducted with models of draft tubes, using air as the fluid. The occurrence, frequency, and amplitude of surges were correlated with flow and draft-tube geometry variables. Studies show that surges arise when angular momentum reaches a critical value relative to linear momentum. Surge frequency and peak-to-peak pressures are independent of viscous effects for Reynolds numbers above 80,000, and are correlated with a dimensionless momentum parameter for a particular draft-tube shape. A criterion is given for predicting the surging threshold. Results of the study are applied to analysis of draft-tube surging in the Fontenelle and Hoover replacement turbines.

ABSTRACT

Draft-tube surge experiments were conducted with models of draft tubes, using air as the fluid. The occurrence, frequency, and amplitude of surges were correlated with flow and draft-tube geometry variables. Studies show that surges arise when angular momentum reaches a critical value relative to linear momentum. Surge frequency and peak-to-peak pressures are independent of viscous effects for Reynolds numbers above 80,000, and are correlated with a dimensionless momentum parameter for a particular draft-tube shape. A criterion is given for predicting the surging threshold. Results of the study are applied to analysis of draft-tube surging in the Fontenelle and Hoover replacement turbines.

ABSTRACT

Draft-tube surge experiments were conducted with models of draft tubes, using air as the fluid. The occurrence, frequency, and amplitude of surges were correlated with flow and draft-tube geometry variables. Studies show that surges arise when angular momentum reaches a critical value relative to linear momentum. Surge frequency and peak-to-peak pressures are independent of viscous effects for Reynolds numbers above 80,000, and are correlated with a dimensionless momentum parameter for a particular draft-tube shape. A criterion is given for predicting the surging threshold. Results of the study are applied to analysis of draft-tube surging in the Fontenelle and Hoover replacement turbines.

Hyd-591
Cassidy, J. J.
EXPERIMENTAL STUDY AND ANALYSIS OF DRAFT-TUBE SURGING
Bur Reclam Lab Rep Hyd-591, Hydraul Br, May 1969. Bureau of Reclamation, Denver, 9 p, 20 fig, 3 tab, 13 ref

DESCRIPTORS--/ *draft tubes/ *turbines/ *hydroelectric plants/ hydraulic machinery/ fluid mechanics/ dimensional analysis/ *surges/ air/ unsteady flow/ pressure/ laboratory tests/ model tests/ fluid flow/ non-uniform flow
IDENTIFIERS--/ fluid dynamics/ hydraulic resonance

Hyd-591
Cassidy, J. J.
EXPERIMENTAL STUDY AND ANALYSIS OF DRAFT-TUBE SURGING
Bur Reclam Lab Rep Hyd-591, Hydraul Br, May 1969. Bureau of Reclamation, Denver, 9 p, 20 fig, 3 tab, 13 ref

DESCRIPTORS--/ *draft tubes/ *turbines/ *hydroelectric plants/ hydraulic machinery/ fluid mechanics/ dimensional analysis/ *surges/ air/ unsteady flow/ pressure/ laboratory tests/ model tests/ fluid flow/ non-uniform flow
IDENTIFIERS--/ fluid dynamics/ hydraulic resonance

Hyd-591
Cassidy, J. J.
EXPERIMENTAL STUDY AND ANALYSIS OF DRAFT-TUBE SURGING
Bur Reclam Lab Rep Hyd-591, Hydraul Br, May 1969. Bureau of Reclamation, Denver, 9 p, 20 fig, 3 tab, 13 ref

DESCRIPTORS--/ *draft tubes/ *turbines/ *hydroelectric plants/ hydraulic machinery/ fluid mechanics/ dimensional analysis/ *surges/ air/ unsteady flow/ pressure/ laboratory tests/ model tests/ fluid flow/ non-uniform flow
IDENTIFIERS--/ fluid dynamics/ hydraulic resonance

Hyd-591
Cassidy, J. J.
EXPERIMENTAL STUDY AND ANALYSIS OF DRAFT-TUBE SURGING
Bur Reclam Lab Rep Hyd-591, Hydraul Br, May 1969. Bureau of Reclamation, Denver, 9 p, 20 fig, 3 tab, 13 ref

DESCRIPTORS--/ *draft tubes/ *turbines/ *hydroelectric plants/ hydraulic machinery/ fluid mechanics/ dimensional analysis/ *surges/ air/ unsteady flow/ pressure/ laboratory tests/ model tests/ fluid flow/ non-uniform flow
IDENTIFIERS--/ fluid dynamics/ hydraulic resonance

HENRY T. FALVEY,
Dr - Ing.

Symposium Stockholm 1970

Transactions Part 1

International Association for Hydraulic Research
Section for Hydraulic Machinery. Equipment and Cavitation

Association Internationale de Recherches Hydrauliques
Section Machines Hydrauliques. Equipements et Cavitation

Svenska Centralkommittén för Internationella Ingenjörskongresser
c/o Vattenfall, S-162 87 Vällingby, Sweden

SYMPOSIUM 1970
STOCKHOLM

FREQUENCY AND AMPLITUDE OF PRESSURE SURGES GENERATED BY SWIRLING FLOW

H. T. Falvey, Head, Hydraulic Research Section, U. S. Bureau of Reclamation, Denver, Colorado, USA

J. J. Cassidy, Professor of Civil Engineering, University of Missouri, Columbia, Missouri, USA

SYNOPSIS

This paper reports on the investigation of swirling flow through tubes. Frequencies and amplitudes of pressure surges produced by the swirling flow were measured and found to be essentially independent of viscous effects for Reynolds numbers larger than 1×10^5. Dimensionless frequency and pressure parameters as well as the onset of surging were correlated with the parameter $\Omega D/\rho Q^2$ where Ω and Q are respectively the fluxes of angular momentum and volume through the tube, D is the tube diameter and ρ is the fluid density. Relative length and shape of the tube were also found to be important.

The results of the study were used to analyze a particular draft tube for potential surging. Using performance data obtained from the model of the turbine and draft tube, a region of surge-free operation was outlined on the efficiency hill for the unit. Comparison was made between measured power swings and the predicted pressure fluctuations in the draft tube.

RÉSUMÉ

Cette communication a trait à une recherche sur un courant tourbillonnaire passant dans des tubes. Les fréquences et les amplitudes des surpressions créees par le courant tourbillonnaire ont été mesurées et trouvées essentiellement independantes des effets de viscosité pour des nombres de Reynolds supérieurs à 1×10^5. Des paramètres sans dimension liés à la frequence et à la pression et l'établissement de la surpressions ont été relie's au paramètre $\Omega D/\rho Q^2$ où Ω et Q sont respectivement les flux du moment angulaire et du volume dans le tube, D le diamètre du tube et ρ la densité du fluide. On a trouvé que la longueur relative et la forme du tube sont egalement importantes.

On a utilisé les résultats de cette étude pour analyser l'établissement de la surpressions dans une conduite d'ecoulement particulière. En utilisant les donnees de fonctionnement obtenues a partier d'un modele de turbine et de conduite d'ecoulement, on a trouvé un domaine de marche sans surpressions sur le diagramme de rendement de l'unité. On a comparé les résultats des mesures des amplitudes de puissance et ceux des calculs des fluctuations de pression dans la conduite d'ecoulement.

INTRODUCTION

Draft-tube surging has been recognized as a problem in the operation of hydro-power plants for several decades [1]. History shows that the attack on draft-tube surging has been one of alleviation rather than prevention. New units are placed in operation and if objectionable surging occurs within the operating range various types of remedial action are attempted or, if possible, operation is not permitted in the critical range. However, because of automation of the generating systems, plants are frequently required to operate over a wide range of turbine gate openings. Remedial measures including air admission to the draft tube or the placement of fins in the draft-tube throat are only occasionally successful. If it were possible to predict the possibility of surging prior to installation and operation of a unit, considerable advantage could be realized.

It appears to be generally accepted that draft-tube surging arises as a result of rotation remaining in the water as it leaves the turbine runner and enters the draft tube [2]. Moreover, the phenomenon is complicated by many factors including vaporization of the water, geometry of the turbine and draft tube, and the dynamic characteristics of the penstock and electrical network. Swirling flow has been investigated analytically and experimentally by several people in the field of fluid mechanics [3,4,5,6]. These studies have shown that when a fluid flows in a swirling fashion (axial flow with superimposed rotation) the resulting flow pattern depends upon the relative amount of rotation in the fluid. If the flux of angular momentum entering the tube is sufficiently large as compared to the flux of linear momentum, a reversal in flow direction occurs along the centerline of the tube [3]. For large Reynolds numbers the flow becomes unsteady forming a helical vortex with the reversed flow occurring along the spiral core of the vortex [7]. This phenomenon is known as "vortex breakdown" in the fluid mechanics literature and as draft-tube surging in the hydraulic-machinery literature [8].

This paper describes a study initiated in order to investigate the characteristics of swirling flow in tubes and to correlate these characteristics with the occurrence and nature of draft-tube surging.

THE BASIC STUDY

Because of the excessive number of variables which could be involved it was not only desirable but necessary to simplify the experimental model as much as possible. Air was used as the working fluid in order to eliminate the possible effects of a two-phase flow. No turbine runner was installed in order to simplify geometry. Instead the air entered the tube (Figure 1) radially through wicket-gate type vanes. It was possible to accurately determine the amount of swirl imparted to the flow as it entered the tube. The angle between the vanes and a radial line could be set at any angle between 0° and 82°. At 0° the vanes were

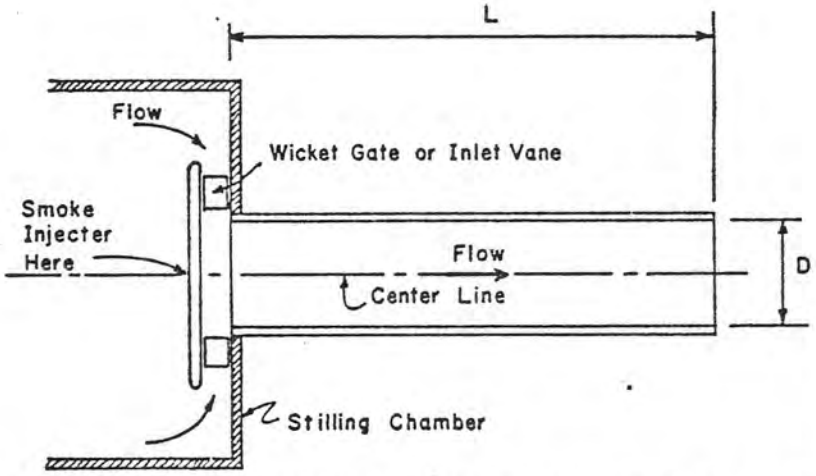

FIGURE 1 EXPERIMENTAL APPARATUS SHOWING STRAIGHT TUBE

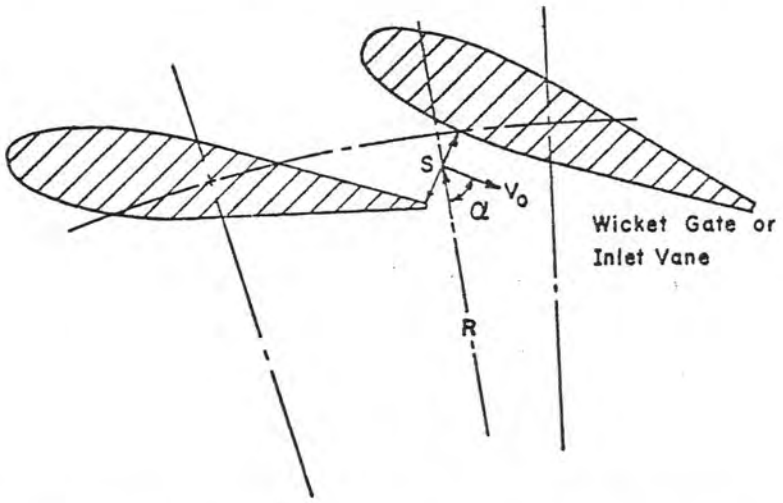

FIGURE 2 DEFINITION SKETCH OF INLET FLOW TO TUBE OR RUNNER

radial and no rotation was applied to the flow (Figure 2). Overall configuration of the apparatus is shown in Figure 1 and is described in more detail by Cassidy [7]. Clear plastic was used in construction to facilitate flow visualization with smoke. Pressures at points on the tube wall were measured using pressure cells and a root-mean-square meter. Frequencies of the unsteady pressure were determined using an oscilloscope with a retentive screen.

Flow through three types of tubes was studied:

1) circular tubes of uniform diameter; 2) a model of a draft tube used in Fontenelle Dam; 3) an expanding cone having the same length-to-area relationship as the draft tube.

ANALYSIS

It was assumed that, for a particular draft-tube shape, the root-mean-square amplitude ΔP and frequency f of the unsteady pressure surge are both functions of the fluid density ρ and viscosity ν, draft-tube diameter D and length L, discharge Q, and flux of angular momentum Ω. Standard techniques of dimensional analysis yield the following functional relationships

$$\frac{D^4 \Delta P}{\rho Q^2} = \phi_1\left(\frac{\Omega D}{\rho Q^2}, \frac{L}{D}, \mathcal{R}\right) \qquad (1)$$

$$\frac{f D^3}{Q} = \phi_2\left(\frac{\Omega D}{\rho Q^2}, \frac{L}{D}, \mathcal{R}\right) \qquad (2)$$

where $\mathcal{R}$ is the Reynolds number $4Q/\pi D\nu$.

The angular momentum flux Ω entering the tube was computed as (see Figure 2)

$$\Omega = \rho Q R V_0 \sin\alpha \qquad (3)$$

in which $Q = SBNV_0$. The variables S, α, V_0, and R are defined in Figure (2); N is the number of vanes around the inlet; and B is the dimension of the vanes perpendicular to the plane of Figure 2. The momentum parameter contained in Equations (1) and (2) is then computed as

$$\frac{\Omega D}{\rho Q^2} = \frac{DR \sin\alpha}{BNS} \qquad (4)$$

and is seen to be a function of geometry only for the particular inlet conditions of this study. In all experiments the momentum parameter $\Omega D/\rho Q^2$ was calculated according to Equation (4).

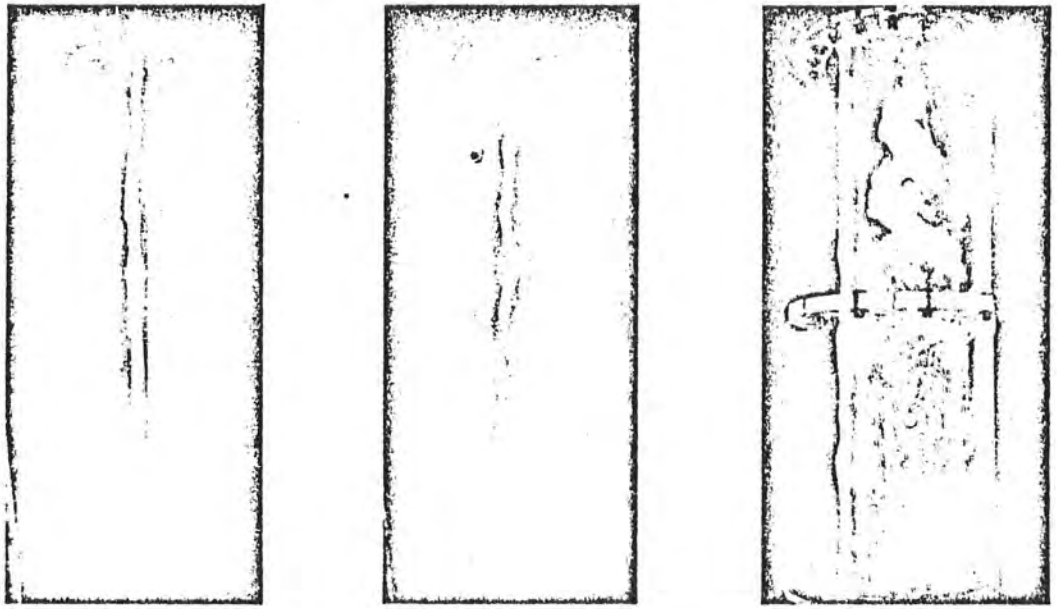

a.) Steady Swirling Flow, no surging, D=3.46 inches, L/D=7.15, $\Omega D/\rho Q^2$=0.150

b.) Stagnation Point at the Centerline With Surging downstream D=3.46 inches, L/D=7.15, $\Omega D/\rho Q^2$=0.330

c.) Fully Developed Surging, $\Omega D/\rho Q^2$=0.454, D=6.13 inches, L/D=3.26.

Figure 3. SWIRLING FLOW IN STRAIGHT TUBES

RESULTS

Flow patterns at low velocities were readily made visible with smoke. With the inlet vanes in the radial position no rotation was imparted to the fluid and streamlines in the test section were essentially straight and parrallel to the tube centerline. With the vanes inclined slightly from the radial position (discharge held constant) streamlines in the test section became steady spirals. That condition is shown in Figure 3a. Further closure of the vanes eventually produced vortex breakdown. Figure 3b shows the stagnation point occurring near the right quarter point of the tube with a helical vortex occurring downstream from the stagnation point. Still further closure of the vanes moved the stagnation point to the upstream limit of the tube. Figure 3c shows the helical vortex filling the tube. A comparison of this helical vortex pattern with those observed below a turbine runner [2,8] establishes the similarity.

Although flow patterns could be observed only at low velocities (below 5 feet per second) unsteady pressures could be measured only at higher velocities. To insure that similar flow patterns occurred at these higher velocities, a hot-wire anemometer was used to measure air velocities near the tube wall and at the tube centerline. These measurements showed that surging began at the same gate setting (same $\Omega D/\rho Q^2$) regardless of discharge.

In the experiments pressure amplitudes and frequencies occurring after surging commenced were measured near the open end of the straight tubes, upstream from the elbow of the draft tube, and near the entrance of the straight cone. The onset of surging (vortex breakdown) was correlated with the value of $\Omega D/\rho Q^2$. It was also found to be a function of L/D and shape. For the elbow draft-tube and the straight cone the critical value of $\Omega D/\rho Q^2$ was 0.4. Above this value surging occurred.

The dimensionless frequency and pressure parameters of Equations (1) and (2), calculated from the experimental measurements, are shown in Figures (4) and (5). These parameters were found to be independent of viscous effects for Reynolds numbers greater than 1×10^5 and the results for smaller Reynolds numbers are not shown here.

In order to obtain reproducible results, it was necessary to measure the root-mean-square values of the pressure fluctuations and it is these values which were used in the preparation of Figure 4. Straight tubes are seen to have pressure characteristics which are strongly influenced by relative length. The pressure characteristics of the elbow draft-tube and straight cone are striking since the pressure parameters exhibit a maximum value as $\Omega D/\rho Q^2$ is made larger.

Frequencies of the unsteady pressure were quite regular and, thus, relatively easy to measure. The regularity indicates that the helical vortex precesses about the tube centerline at a reasonably regular rate. Figure (5) shows that the divergent tubes significantly reduce the frequency of surging. However, the bend in the draft tube has an insignificant effect upon frequency.

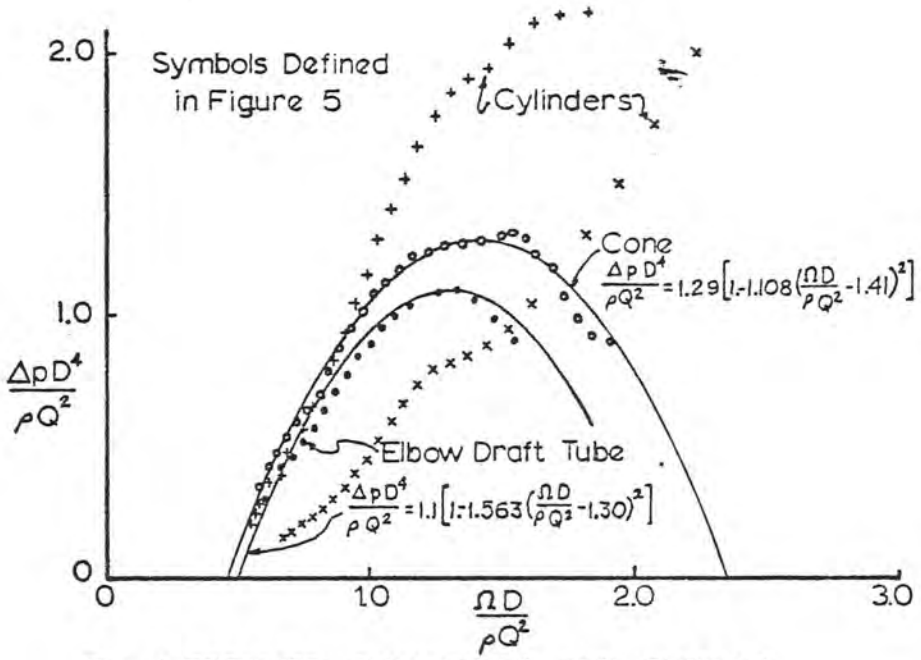

Fig. 4-PRESSURE PARAMETERS FOR SURGING

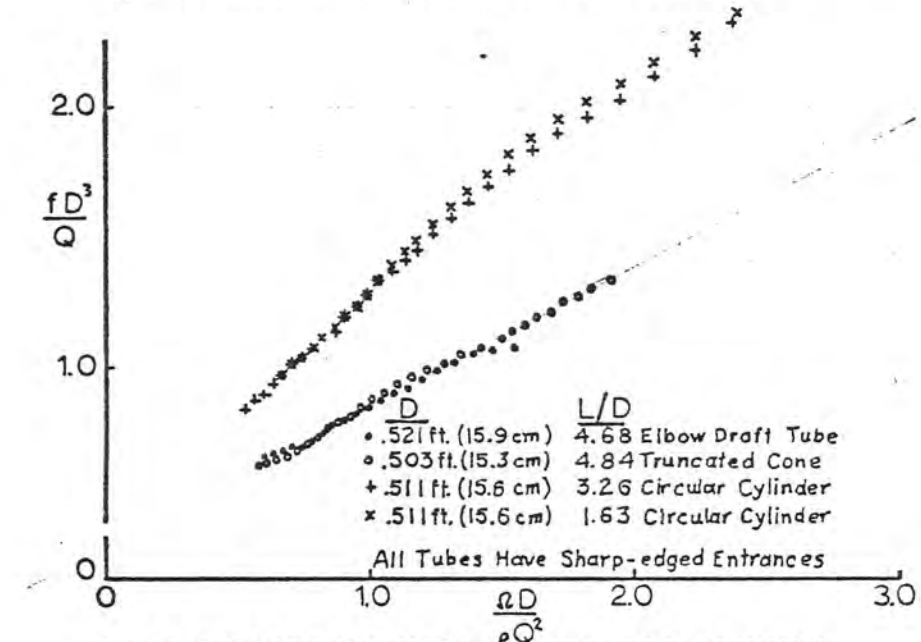

Fig. 5-FREQUENCY PARAMETERS FOR SURGING

E 1

ANALYSIS OF DRAFT-TUBE SURGING IN A TURBINE

Occurrence and severity of draft-tube surging in a given hydraulic turbine and associated draft tube can be predicted using the experimental results of this study. To do this it is necessary to be able to compute the parameter $\Omega D/\rho Q^2$ of the flow as it leaves the turbine runner and enters the draft tube.

Analysis of Turbine

Horsepower P imparted to the turbine runner by water flowing through it is given by the classic expression

$$P = \frac{2\pi n}{60}(\Omega_1 - \Omega_2)/550 \qquad (5)$$

where n is the rotational speed of the turbine in revolutions per minute, and $(\Omega_1 - \Omega_2)$ is the rate of change in angular momentum occurring in the flow as it passes through the runner. Subscripts 1 and 2 refer to the entrance and exit sides of the runner respectively. Multiplying both sides of Equation (5) by $550\ D/n\rho Q^2$ and using Equation (4) yields

$$\frac{\Omega_2 D}{\rho Q^2} = \frac{DR\sin\alpha}{8NS} - \frac{550}{2\sqrt{2g}}\frac{P_{11}}{\rho Q_{11}^2 \phi}\frac{D}{D_2} \qquad (6)$$

where ϕ, P_{11}, Q_{11}, and D_2 are respectively the specific speed, power, discharge and runner diameter and are defined in Figure 6 and $\Omega_2 D/\rho Q^2$ is the momentum parameter associated with the flow leaving the turbine runner and entering the draft tube. The first term on the right of Equation (6) is the momentum parameter associated with the flow leaving the wicket gates and entering the turbine and can be evaluated if the wicket-gate geometry is known. The second term on the right of Equation (6) can be evaluated if the performance characteristics and geometry of the turbine are known.

Specific Application

Equation (6) was used to analyze the hydraulic turbine at Fontenelle Dam [9]. The efficiency hill for the turbine, as determined from model tests, is shown in Figure 6. Any point on this efficiency hill yields a particular value of $\Omega_2 D/\rho Q^2$ and, thus, areas of potential surging--where $\Omega_2 D/\rho Q^2$ exceeds 0.4--can be determined. Figure 7 shows the regions in which surging can be expected and also shows a line representing operating conditions for which flow leaving the turbine and entering the draft tube has zero swirl. To the left of this line flow in the draft tube swirls opposite to the turbine rotation while to the right swirl is with the runner. The point of maximum efficiency falls on the line of zero swirl for this unit although this is not apparently true of all units.

Figure (4) predicts that for the elbow draft tube a maximum pressure amplitude occurs at $\Omega_2 D/\rho Q^2 = 1.30$. The line on which surging would produce this maximum pressure amplitude is also shown on Figure 7. A parabolic curve was fitted to the pressure data for the elbow draft tube. This parabolic expression (shown in Figure 4) was used in conjunction with Equation (6) to calculate relative values

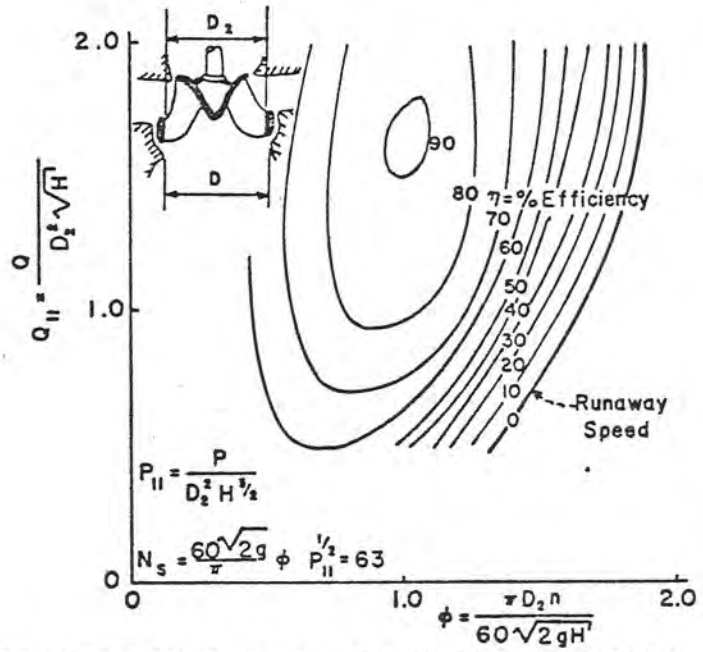

FIGURE 6 EFFICIENCY HILL FOR FONTENELLE TURBINE

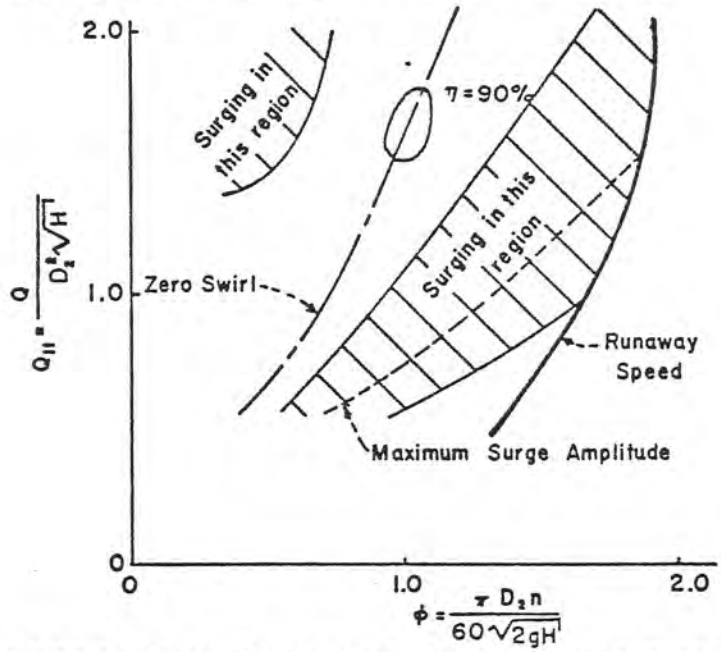

FIGURE 7 PREDICTED SURGING FOR FONTENELLE TURBINE

E 1

($\Delta P/\rho gH$ where H is net head on the unit) of pressure amplitudes for the Fontenelle unit. The results of this computation are shown on Figure 8 along with relative power swings actually measured at the plant. Excellent agreement is shown for the wicket gate opening at which maximum surging occurred. Numerical agreement of the % power swing and % pressure fluctuation was not expected because the dynamics of the mechanical and electrical system are necessarily involved in determining the power swing arising as a result of the pressure surging which is the driving force. The lack of agreement occurring at each side of Figure 8 may also be due to the use of Equation (4). Analysis of other units indicated that this expression may not give an entirely accurate estimate of the momentum parameter for all gate openings usually because the exact geometry of the wicket gate assembly is not accurately known.

CONCLUSIONS

A particular hydraulic turbine can be analyzed for possible surging within the desired range of operation by the method presented herein. Dimensionless frequencies and root-mean-square amplitudes of unsteady pressures measured herein are directly convertible to prototype conditions by similitude considerations. However, they can be expected to predict prototype conditions only for the "hard-core" vortex condition. For low-tailwater conditions, for which the vortex core becomes unwatered, a two-phase flow occurs and pressure surges are usually somewhat milder.

ACKNOWLEDGEMENTS

Mr. U. J. Palde of the Hydraulics Branch, U.S. Bureau of Reclamation, took much of the data and carefully refined the experimental methods and equipment used.

REFERENCES

1.) Rheingans, W.J., "Power Swings in Hydroelectric Power Plants," Transactions, American Society of Mechanical Engineers, Vol. 62, 1940.

2.) Hosoi, Y., "Experimental Investigations of Pressure Surge in Draft Tubes of Francis Water Turbines," Hitachi Review, Volume 14, Number 12, 1965.

3.) Harvey, J.K., "Some Observation of the Breakdown Phenomenon," Journal of Fluid Mechanics, Vol. 14, 1962.

4.) Chanaud, R.C., "Observations of Oscillatory Motion in Certain Swirling Flows," Journal of Fluid Mechanics, Vol. 21, 1965.

5.) Benjamin, T.B., "Theory of the Vortex Breakdown Phenomenon," Journal of Fluid Mechanics, Vol. 14, 1962.

6.) Squire, H.B., "Analysis of the Vortex Breakdown Phenomenon, Part I," Aero Department, Imperial College, Report Number 102, 1960.

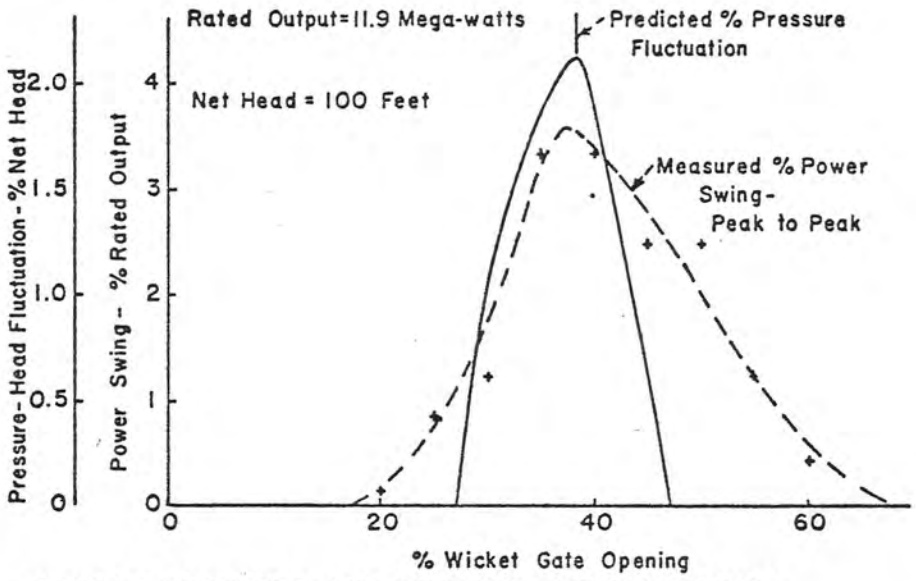

FIGURE 8 PREDICTED AND MEASURED SURGING EFFECTS

J. Fluid Mech. (1970), *vol.* 41, *part* 4, *pp.* 727–736
Printed in Great Britain

Observations of unsteady flow arising after vortex breakdown

By JOHN J. CASSIDY
University of Missouri, Columbia, Missouri
AND HENRY T. FALVEY
U.S. Bureau of Reclamation, Denver, Colorado

(Received 11 July 1969)

In rotating flow moving axially through a straight tube, a helical vortex will be generated if the angular momentum flux is sufficiently large relative to the flux of linear momentum. This paper describes an experimental study of the occurrence, frequency and peak-to-peak amplitude of the wall pressure generated by this vortex. The experimental results are displayed in dimensionless form in terms of a Reynolds number, a momentum parameter and tube geometry.

Introduction

In recent years considerable attention has been focused on the transformation in flow pattern which can occur in a swirling flow. A swirling flow is defined as one undergoing simultaneous axial and vortex motions. The vortex is said to be 'broken down' when reverse flow occurs along the axis. Squire (1960) studied this occurrence analytically and deduced that breakdown would occur when the local swirl angle ($\tan^{-1} v/w$) exceeds 52·5°. In the swirl ratio w and v are the local axial and transverse velocity components. Harvey (1962) obtained experimental results agreeing with Squire's analysis. Benjamin (1962, 1967) deduced that the breakdown was in actuality a transformation to a conjugate flow pattern capable of sustaining an axisymmetric standing wave. Fraenkel (1967) and Scheer (1968) have enlarged upon Benjamin's analysis.

As long as the Reynolds number is very low the flow appears to remain steady after the transition. However, as the Reynolds number is increased, the alternate flow pattern takes the form of a helical vortex precessing about the tube centreline. This unsteady state of flow has been witnessed in the breakdown of the vortex formed by flow over a delta-wing airplane and since much earlier times in the flow through turbine draft tubes. Batchelor (1967) refers to this phenomenon as 'bursting' of the vortex.

Chanaud (1965) studied both the steady and unsteady aspects of conjugate rotating flows experimentally and outlined, on a graph of swirl ratio *versus* Reynolds number, regions in which the particular patterns of flow would occur.

In this study observations and measurements were made on the unsteady vortex flow developing at high axial Reynolds numbers in straight tubes.

Apparatus

A schematic diagram of the experimental apparatus is shown in figure 1. The swirl vanes at the inlet to the test section could be rotated about axes parallel to the tube axis. Thus, rotating the vanes so as to increase the angle β between a vane and a radial line increased the flux of angular momentum entering the tube. Discharge was controlled independently of the swirl vanes with a motor-operated cone valve at the upstream end of the stilling chamber. Discharge was computed from differential pressure across a calibrated orifice in the upstream supply pipe.

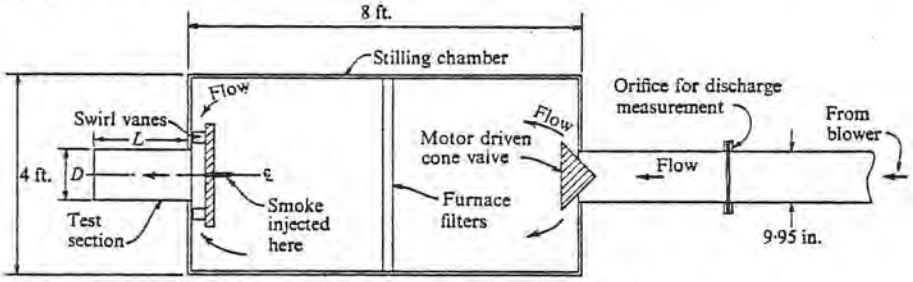

FIGURE 1. Schematic diagram of apparatus.

Discharge could be varied from 0 to approximately 0·4 cubic metres per second. The angle between the swirl vanes and a radial line could be varied continuously from 0° to 52·5°.

Transparent plexiglass tubes 15·24 and 8·73 cm in diameter were used as test sections. Tubes with length to diameter ratios of 1·63, 3·26, 4·77 and 7·40 were used.

Two methods of observation were incorporated in the investigation. Tobacco smoke could be injected on the axis at the upstream limit of the tube in order to make visual observation of the flow pattern in the tube possible at least for low velocities. For velocities at which turbulent diffusion rendered visualization with smoke impossible, measurements of wall pressure and velocity were made respectively by means of a calibrated pressure cell and a constant-temperature hot-film anemometer. Piezometers accommodating the pressure cell were drilled in the tube wall and mounts were provided for the anemometer in such a manner that the hot-film probe could be positioned anywhere on a diameter. Signals from the pressure cell and the anemometer were displayed on a two-channel oscilloscope equipped with a variable persistence screen. Any number of traces could be superimposed on the oscilloscope, stored, and displayed in a static mode for determination of frequency and peak-to-peak amplitude.

Observations

Observations of flow pattern using smoke

The apparatus used in this study was quite similar to that used by Harvey (1962) in his observations of the conditions under which vortex breakdown takes

place. Hence, the ma
in the two studies.

A flow rate throug
the tube centreline a
produce a greater flux
drastically. With onl
observed as shown ir
flux was increased, t
served to occur in the
angular momentum f
tube just as was obse

Figure 3, plate 1,
stream quarter point
steady and swirling.
developed an unstea
tube centreline in the

Further increase of
to the upstream lim
throughout the tube

Straight tubes of c
downstream from th
vortex. In no case co
the breakdown point
end.

Flow in a jet (tub
observed downstrean
in the jet served to m
helical vortex shown

At all these low vel
and would move ups
This sensitivity has

Obs

At velocities above
visualization of the fl
Reynolds numbers R
D is the tube diame
a cylindrical, constar
was established and t
momentum flux was g
flux the centreline-v
(the hot-film probe w
in flow, was assumed
the minimum centre

Once unsteady flo
within the tube coul

shown in figure 1. The
ed about axes parallel
se the angle β between
omentum entering the
l vanes with a motor-
amber. Discharge was
rifice in the upstream

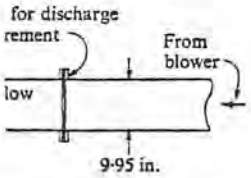

us.

ubic metres per second.
e va: continuously

eter were used as test
26, 4·77 and 7·40 were

nvestigation. Tobacco
of the tube in order to
ssible at least for low
red visualization with
elocity were made re-
constant-temperature
essure cell were drilled
emometer in such a
where on a diameter.
displayed on a two-
screen. Any number
red, and displayed in
)-peak amplitude.

e

hat used by Harvey
rtex breakdown takes

place. Hence, the manner of visual observation utilized was also quite similar in the two studies.

A flow rate through the tube was established and smoke was introduced on the tube centreline at the upstream limit. As the swirl vanes were adjusted to produce a greater flux of angular momentum, the flow pattern was seen to change drastically. With only a low angular-momentum flux, steady swirling flow was observed as shown in figure 2, plate 1. Eventually as the angular momentum flux was increased, the discharge being held constant, a flow reversal was observed to occur in the jet downstream from the tube exit. Further increase in the angular momentum flux forced the reversed-flow beginning upstream into the tube just as was observed by Harvey (1962).

Figure 3, plate 1, shows the point of breakdown at approximately the upstream quarter point of the tube. Upstream of the point of breakdown flow is steady and swirling. Downstream from the breakdown the flow is seen to have developed an unsteady helical vortex. The helical vortex precesses about the tube centreline in the same direction as the rotation imparted by the swirl vanes.

Further increase of the angular momentum flux moved the breakdown point to the upstream limit of the tube and produced a precessing helical vortex throughout the tube as is shown in figure 4, plate 1.

Straight tubes of constant diameter all produced similar flow patterns. Flow downstream from the breakdown point always produced a precessing helical vortex. In no case could the flow be forced to remain steady downstream from the breakdown point without decreasing the tube diameter at the downstream end.

Flow in a jet (tube length $L = 0$) was also observed. Breakdown was first observed downstream from the opening. Increasing the angular momentum flux in the jet served to move the breakdown point upstream producing the precessing helical vortex shown in figure 5, plate 2.

At all these low velocities the breakdown was quite sensitive to any disturbance and would move upstream rapidly if any type of probe were placed in the flow. This sensitivity has also been noted by previous investigators.

Observations of unsteady pressure and velocity

At velocities above approximately 6 feet per second turbulent diffusion made visualization of the flow pattern impossible. Observations of breakdown at axial Reynolds numbers WD/ν greater than 10,000 (W is the average axial velocity, D is the tube diameter and ν is the fluid viscosity) were made by positioning a cylindrical, constant-temperature, hot-film probe at the tube axis. A flow rate was established and the signal from the anemometer was observed as the angular momentum flux was gradually increased. With increase of the angular momentum flux the centreline-velocity decreased, reached a minimum, and then increased (the hot-film probe was not directionally sensitive). The breakdown, or reversal in flow, was assumed to have taken place at the swirl-gate setting which produced the minimum centreline-velocity.

Once unsteady flow occurred measurements of mean velocity or pressure within the tube could no longer be made because of the time-wise directional

change in local velocities produced by the precessing helical vortex. The frequency and peak-to-peak values of the wall pressure near the tube exit were observed by displaying the amplified pressure-cell signal on the oscilloscope. In order to verify that the unsteady pressure was indeed produced by a precessing helical vortex such as was observed with smoke at lower axial Reynolds numbers, the hot-film probe was positioned inside the tube near the piezometer at which the pressure was being observed. Signals from the hot-film anemometer and the pressure cell were displayed simultaneously on the oscilloscope. Figure 6, plate 2, shows the simultaneous traces obtained for one unsteady condition. The velocity and pressure are seen to have the same frequency. A slight phase difference existed because pressure and velocity were not measured at exactly the same point.

The sensitivity of the flow pattern to disturbances observed at low velocities did not seem to exist at the high velocities at which velocity and pressure measurements were made. Positioning the $\frac{1}{8}$ inch diameter hot-film probe entirely across the diameter of the tube did not cause a measurable difference in either the frequency or magnitude of the unsteady wall pressure. However, the frequency of the unsteady pressure was substantially increased when the exit was partially blocked with a flat plate.

Analysis of the results

Unsteady pressures

Vortex breakdown was correlated with flow variables in terms of the local swirl angle by Squire (1960) and Harvey (1962). Because the unsteady aspects of flow were of primary interest in this study the local swirl angle of the flow could not be used. Once the helical vortex existed throughout the tube, no quantitative measurements could be made within. Thus, it was necessary to develop a gross parameter descriptive of the relative rotational and axial characteristics of the flow for use in correlating the experimental results.

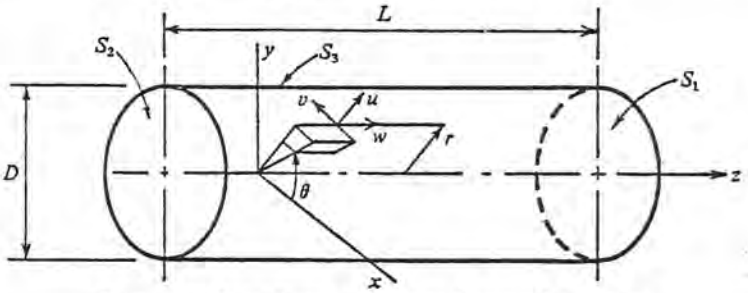

FIGURE 7. Co-ordinate system and control volume.

The desired parameters were formulated through consideration of the momentum equation (for a fluid of zero viscosity) for an axis oriented parallel to the mean flow (see figure 7).

$$r\rho\frac{\partial v}{\partial t}+r\rho\left(u\frac{\partial v}{\partial r}+\frac{1}{r}\frac{v\,\partial v}{\partial\theta}+rw\,\frac{\partial v}{\partial z}+\frac{uv}{r}\right)=-\frac{\partial p}{\partial\theta}. \qquad (1)$$

Integration of (1)
continuity equation,

$$\frac{d}{dt}\int_V r\rho v\,dV+\int_S$$

Choosing the contr
in figure 7 makes it p

$$\frac{d}{dt}\int_V r\rho v\,dV-$$

The second integra
Since this integral wa
symbol Ω and used a
from all variables tra

$$\left(\frac{\rho Q^2}{\Omega D}\right)\left(\frac{fD^3}{Q}\right)\frac{d}{d\bar{t}}\int_{\bar{V}}\bar{r}\bar{v}$$

where Q is the volum
The dimensionless
tube length L/D, wer
quency and pressure
Reynolds number, sh
pendent of viscosity
for a particular value

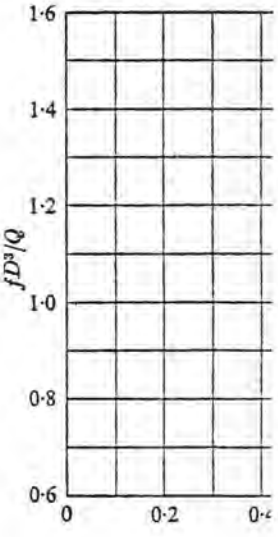

FIGURE 8. Frequency

In figure 9 values
which viscous effects
a similar plot for whi

ielical vortex. The fre-
ear the tube exit were
ial on the oscilloscope.
ed produced by a pre-
it lower axial Reynolds
ibe near the piezometer
ie hot-film anemometer
e oscilloscope. Figure 6,
nsteady condition. The
quency. A slight phase
ot measured at exactly

served at low velocities
. velocity and pressure
eter hot-film probe en-
neasurable difference in
pressure. However, the
ncreased when the exit

terms of the local swirl
he unsteady aspects of
l angle of the flow could
he tube, no quantitative
ssary to develop a gross
al characteristics of the

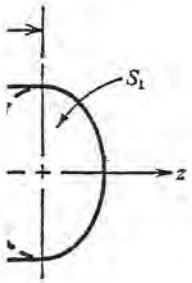

volume.

onsideration of the mo-
axis oriented parallel to

$$= -\frac{\partial p}{\partial \theta}. \qquad (1)$$

Integration of (1) over an arbitrary control volume, incorporation of the continuity equation, and use of Gauss's theorem yields

$$\frac{d}{dt}\int_V r\rho v\,dV + \int_S \rho rv\left(u\frac{\partial r}{\partial n} + vr\frac{\partial \theta}{\partial n} + w\frac{\partial z}{\partial n}\right)ds + \int_V \rho uv\,dV = -\int_V \frac{\partial p}{\partial \theta}dV. \qquad (2)$$

Choosing the control volume V as the tube of length L and diameter D shown in figure 7 makes it possible to modify (2) to

$$\frac{d}{dt}\int_V r\rho v\,dV - \int_{S_1} \rho rvw\,ds + \int_{S_2} \rho rvw\,ds + \int_V \frac{\rho urv}{r}dV = -\int_V \frac{\partial p}{\partial \theta}dV. \qquad (3)$$

The second integral in (3) is the flux of angular momentum into the tube. Since this integral was an independent variable in this study, it was given the symbol Ω and used as a reference quantity. Forming dimensionless quantities from all variables transforms (3) to

$$\left(\frac{\rho Q^2}{\Omega D}\right)\left(\frac{fD^3}{Q}\right)\frac{d}{d\bar{t}}\int_{\bar{V}} \bar{r}\bar{v}\,d\bar{V} - 1 + \left(\frac{\rho Q^2}{\Omega D}\right)\left\{\int_{\bar{S}_1} \bar{r}\bar{w}\bar{v}\,d\bar{s} + \int_{\bar{V}} \bar{u}\bar{v}\,d\bar{V}\right\} = -\left(\frac{P_0 D^3}{\Omega}\right)\int_{\bar{V}} \frac{\partial \bar{p}}{\partial \theta}d\bar{V},$$

where Q is the volume rate of flow and f is frequency.

The dimensionless parameters fD^3/Q, P_0D^3/Ω, $\Omega D/\rho Q^2$, along with the relative tube length L/D, were then utilized to correlate the experimental data on frequency and pressure. Figure 8, a plot of fD^3/Q *versus* the average-velocity Reynolds number, shows that frequency of the flow is indeed essentially independent of viscosity for large Reynolds numbers but tends to become constant for a particular value of $\Omega D/\rho Q^2$.

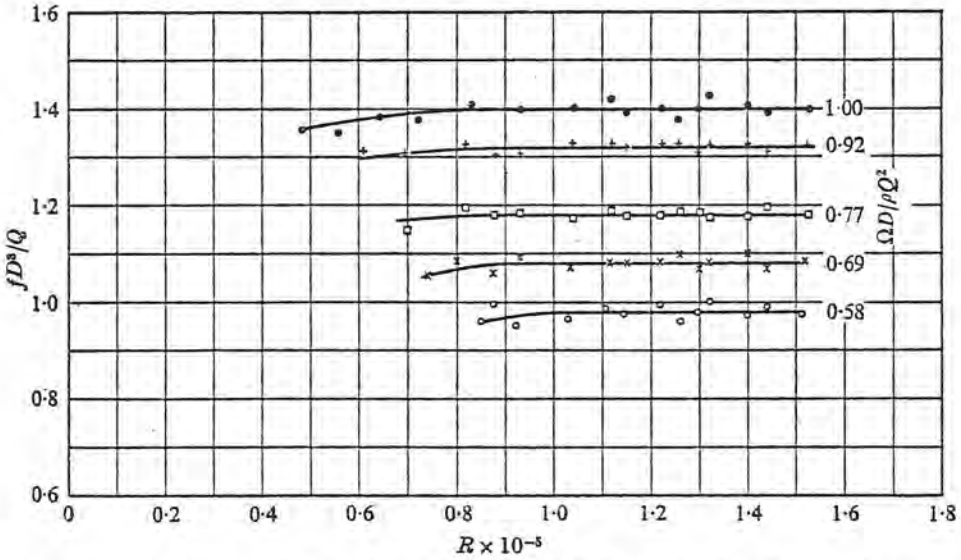

FIGURE 8. Frequency parameter as a function of Reynolds number for straight tubes.

In figure 9 values of fD^3/Q have been plotted against $\Omega D/\rho Q^2$ for the range in which viscous effects are not important as shown in figure 8. Figure 10 shows a similar plot for which the pressure parameter of (2) is the dependent variable.

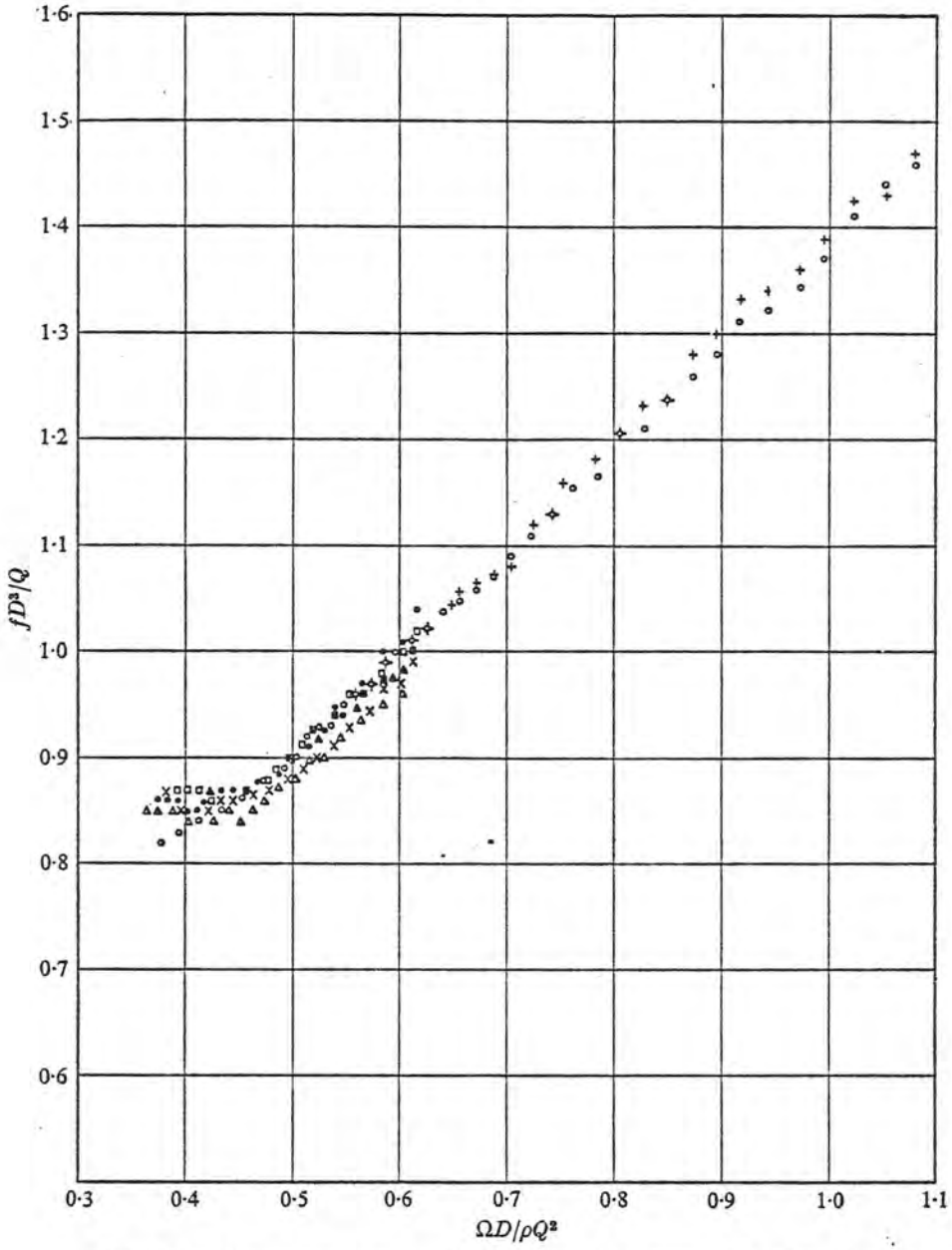

FIGURE 9. Frequency as a function of momentum parameter. Straight tube.

Symbol	L/D	D ft.	D cm	
×	7·21	0·286	8·76	Sharp-edged entrance
●	4·12	0·286	8·76	
□	3·34	0·286	8·76	
○	3·26	0·511	15·26	
+	1·63	0·511	15·26	
△	7·21	0·286	8·76	Bell-mouth entrance
▲	4·12	0·286	8·76	
■	3·34	0·286	8·76	

Dimensionless frequer
increasing $\Omega D/\rho Q^2$. B
the tube exit. Measu
points farther upstrea
any point on the tub
the upstream directio
chamber was noted.
with a frequency equa
amplitude that was a

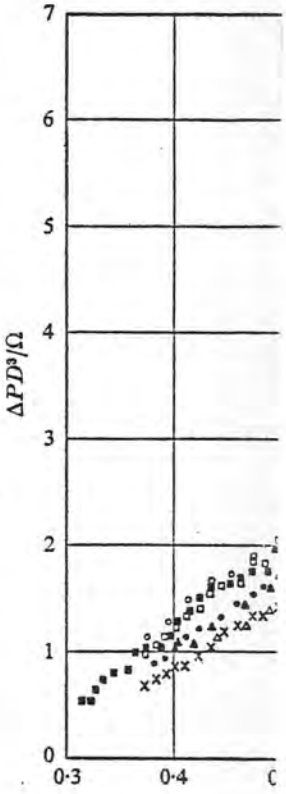

FIGURE 1

The unsteady wall
a solid cylinder inside
large transient forces

Figure 11 displays th
noted. Two values are
the helical vortex fille

Dimensionless frequencies and pressures are both seen to increase rapidly with increasing $\Omega D/\rho Q^2$. Both frequencies and amplitudes were measured quite near the tube exit. Measurements were made of frequency and pressures at other points farther upstream in the tube. Frequencies were found to be the same at any point on the tube wall but pressure amplitudes were found to decrease in the upstream direction. Communication of the unsteady pressures to the stilling chamber was noted. This unsteady pressure in the stilling chamber occurred with a frequency equal to that of the unsteady pressure in the tube, but with an amplitude that was always reduced by at least a factor of five.

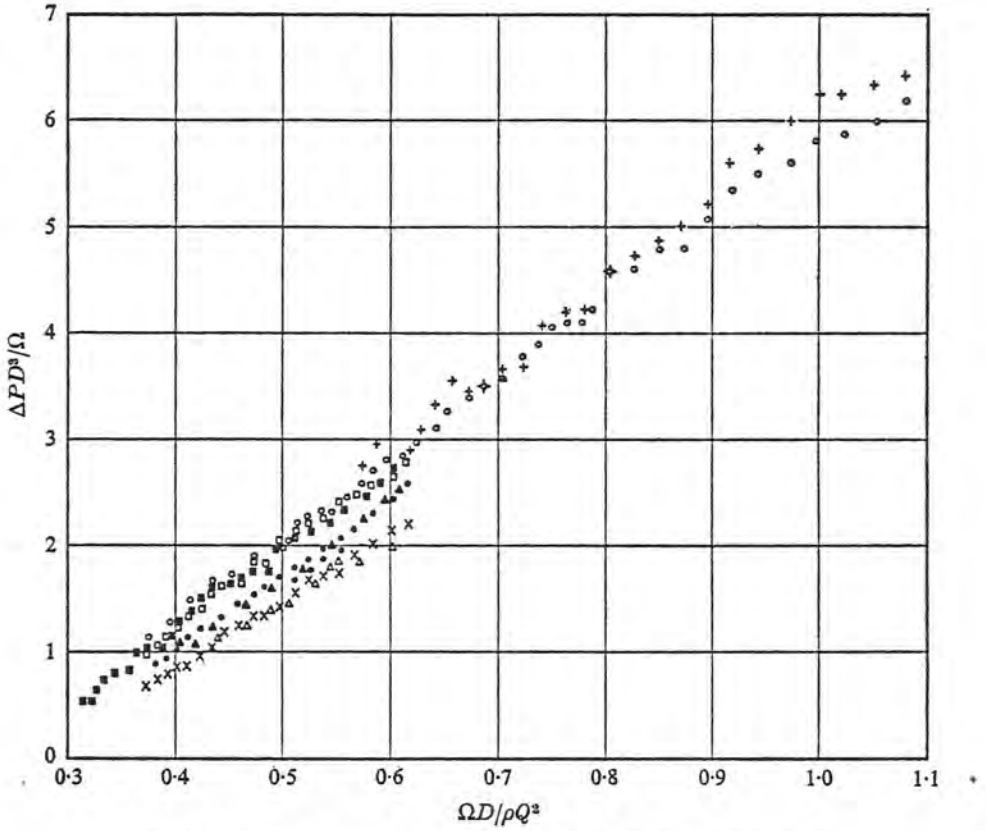

FIGURE 10. Pressure as a function of momentum parameter. Straight tube. Same symbols as figure 9.

The unsteady wall pressure was found to be completely eliminated by placing a solid cylinder inside the tube forming an annular flow passage. However, rather large transient forces were required to hold the cylinder centred.

Vortex breakdown

Figure 11 displays the critical values of $\Omega D/\rho Q^2$ at which vortex breakdown was noted. Two values are plotted for each tube. The lower points are those for which the helical vortex filled the tube. At high Reynolds numbers breakdown appeared

to take place simultaneously throughout the tube and no lower critical value of $\Omega D/\rho Q^2$ was noted.

Critical values of $\Omega D/\rho Q^2$ were computed from the results of Harvey (1962) and Gore & Ranz (1964). In order to make the computation it was necessary to assume that flow ahead of the breakdown rotated with rigid-body motion. Bearing this assumption in mind, agreement appears to be reasonable.

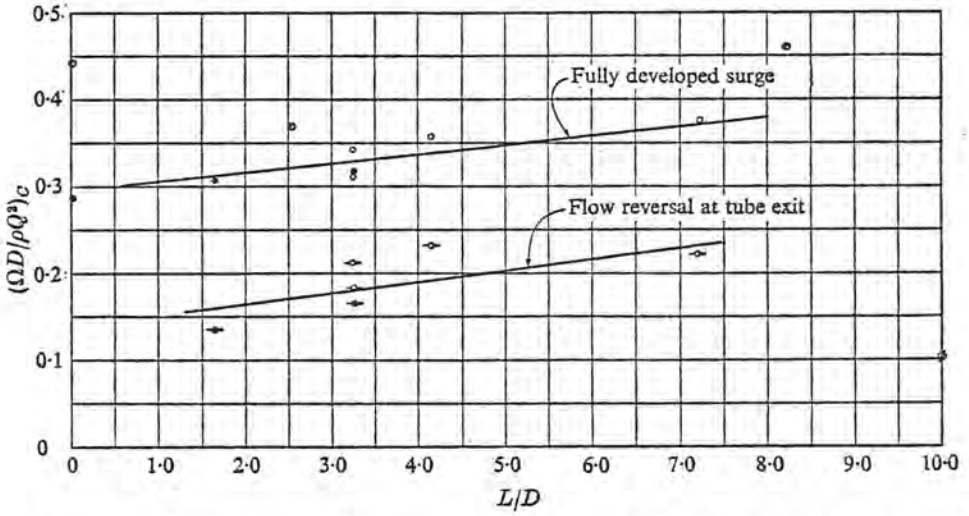

FIGURE 11. Critical values of the momentum parameter. Straight tube, D: ●, -●-, 0·511; ○, -○-, 0·286. ◐ Gore & Ranz; ⌀, Harvey.

Observations were made of vortex breakdown in flow through a tube in which the diameter was abruptly reduced from 15·24 cm to 8·73 cm. The downstream tube, 50·8 cm long and 8·73 cm in diameter, was bolted to the upstream section, 25·4 cm long and 15·24 cm in diameter as shown in figure 12. Three separate modes of breakdown were observed in this tube using smoke for visual observation of the flow pattern:

1. At $\Omega D/\rho Q^2 = 0{\cdot}189$ ($D = 15{\cdot}24$ cm) breakdown occurred in the larger tube but a reversion to swirling flow without a reversed-flow core occurred as the flow contracted to enter the 8·73 cm tube. No breakdown occurred in the smaller tube.

2. Between $\Omega D/\rho Q^2 = 0{\cdot}492$ and $0{\cdot}575$ ($D = 15{\cdot}24$ cm) steady reversed flow persisted along the axis of both tubes. Smoke patterns formed during this phase of flow were striking. Although rotation was in the same direction throughout both tubes, the upstream flow near the tube axis produced spiral patterns having a pitch opposite to those produced by the outer flow moving downstream.

3. At $\Omega D/\rho Q^2 = 0{\cdot}830$ ($D = 15{\cdot}24$ cm) reversed flow occurred in the larger tube. The flow reverted to steady swirling flow without reversal upon passing through the contraction, and breakdown occurred downstream in the smaller tube. Photographs of the resulting flow patterns are shown in figure 13, plate 3.

Careful observations were made of the flow patterns produced in both tubes as the angular momentum flux entering the tubes was steadily increased. The

l no lower critical value

results of Harvey (1962)
ntation it was necessary
with rigid-body motion.
o be reasonable.

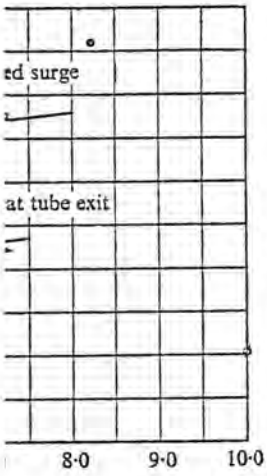

ight tube, D: ●, ⬬, 0·511;
rvey.

flow through a tube in
m to 8·73 cm. The down-
s bolted to the upstream
own in figure 12. Three
e using smoke for visual

curred in the larger tube
core occurred as the flow
urred in the smaller tube.
m) steady reversed flow
formed during this phase
me direction throughout
ed spiral patterns having
noving downstream.
r occurred in the larger
it reversal upon passing
wnstream in the smaller
own in figure 13, plate 3.
produced in both tubes
steadily increased. The

mathematical solution for swirling flow presented by Batchelor (1967) predicts that a reversal of axial velocity should occur near the boundary in contracting flow. However, at no time was any reversal noted except on the axis. In his solution, Batchelor assumed a uniform axial velocity and rigid-body rotation upstream. The measurements made here indicated that prior to breakdown the rotation was approximately rigid-body, but that the axial velocity is not nearly uniform. With rotation the axial velocity always appeared to be low along the tube centreline, and high near the boundaries. This difference between actual and assumed conditions is apparently of some importance.

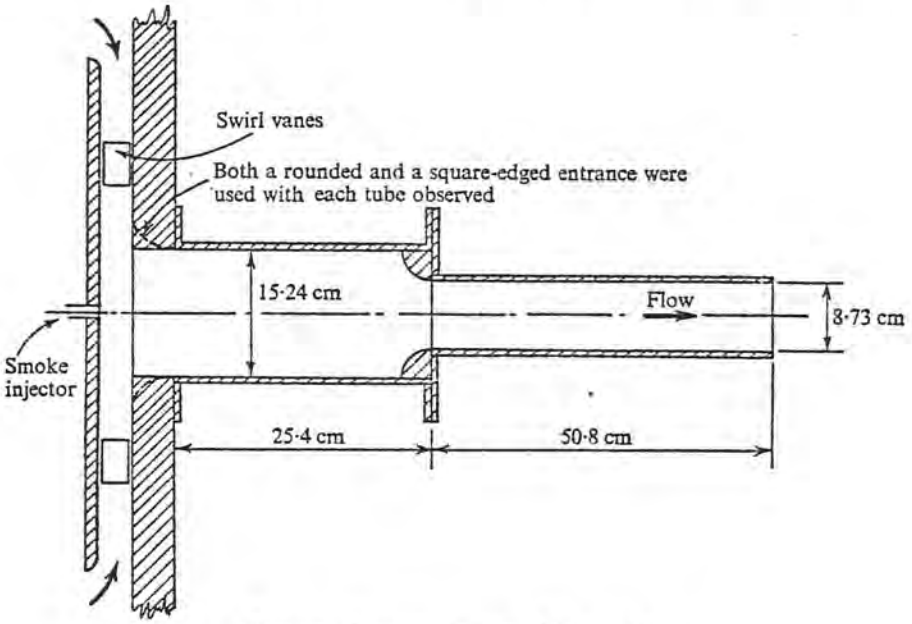

FIGURE 12. Arrangement of flow inlet.

Conclusions

1. The unsteady pressures are produced by a helical vortex precessing about the axis of the tube.

2. Frequency and amplitude of unsteady wall pressures produced after vortex breakdown are independent of viscous effects for high Reynolds numbers.

3. Breakdown and the frequency and amplitude of the unsteady wall pressure arising after breakdown can be correlated in dimensionless form with the gross momentum parameter $\Omega D/\rho Q^2$.

REFERENCES

BATCHELOR, G. K. 1967 *An Introduction to Fluid Dynamics*. Cambridge University Press.

BENJAMIN, T. B. 1962 Theory of the vortex breakdown phenomenon. *J. Fluid Mech.* **14**, 593.

BENJAMIN, T. B. 1967 Some developments in the theory of vortex breakdown. *J. Fluid Mech.* **28**, 65.

CHANAUD, R. C. 1965 Observations of oscillatory motion in certain swirling flows. *J. Fluid Mech.* **21**, 111.

FRAENKEL, L. E. 1967 On Benjamin's theory of conjugate vortex flows. *J. Fluid Mech.* **28**, 85.

GORE, R. W. & RANZ, W. E. 1964 Backflows in rotating fluids moving axially through expanding cross sections. *Am. Inst. Chem. Engrs J.* **10**, 83.

HARVEY, J. K. 1962 Some observations of the vortex breakdown phenomenon. *J. Fluid Mech.* **14**, 585.

SCHEER, A. F. 1968 On the nature of conjugate vortex flows. *J. Fluid Mech.* **33**, 625.

SQUIRE, H. B. 1960 Analysis of the vortex breakdown phenomenon, Part I. *Aero. Dept., Imp. Coll. Rep.* no. 102.

FIGURE 2. Steady s
Q = 0·005

FIGURE 3. Breakdown a
Q = 0·005

FIGURE 4. Helical
Q = 0·0167

y

nics. Cambridge University

iomenon. *J. Fluid Mech.* **14**,

vortex breakdown. *J. Fluid*

ertain swirling flows. *J. Fluid*

vortex flows. *J. Fluid Mech.*

uids moving axially through
33.
down phenomenon. *J. Fluid*

s. *J. Fluid Mech.* **33**, 625.
omenon, Part I. *Aero. Dept.*,

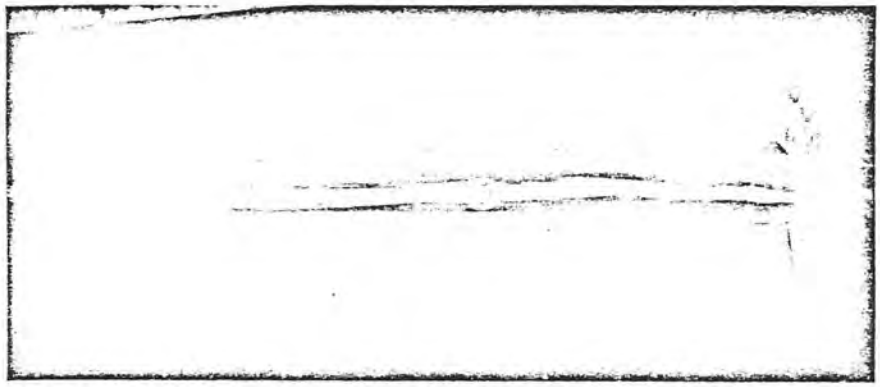

FIGURE 2. Steady swirling flow, $D = 8{\cdot}73$ cm, $L/D = 4{\cdot}77$, $\rho Q = 7{\cdot}1$ gm/sec, $Q = 0{\cdot}0055$ m³/sec, $\Omega = 0{\cdot}0447$ gm-m²/sec, $\Omega D/\rho Q^2 = 0{\cdot}10$.

FIGURE 3. Breakdown and helical vortex, $D = 8{\cdot}73$ cm, $L/D = 4{\cdot}77$, $\rho Q = 7{\cdot}1$ gm/sec, $Q = 0{\cdot}0055$ m³/sec, $\Omega = 0{\cdot}125$ gm-m²/sec, $\Omega D/\rho Q^2 = 0{\cdot}280$.

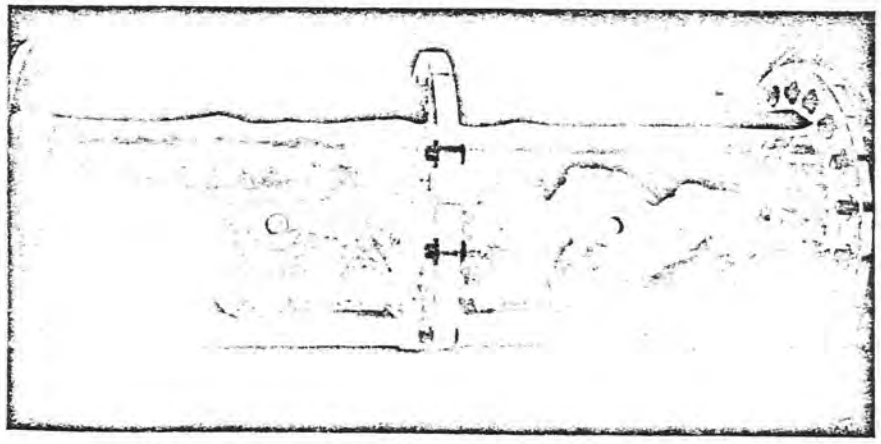

FIGURE 4. Helical vortex, $D = 15{\cdot}24$ cm, $L/D = 3{\cdot}26$, $\rho Q = 21{\cdot}7$ gm/sec, $Q = 0{\cdot}0167$ m³/sec, $\Omega = 0{\cdot}842$ gm-m²/sec, $\Omega D/\rho Q^2 = 0{\cdot}354$.

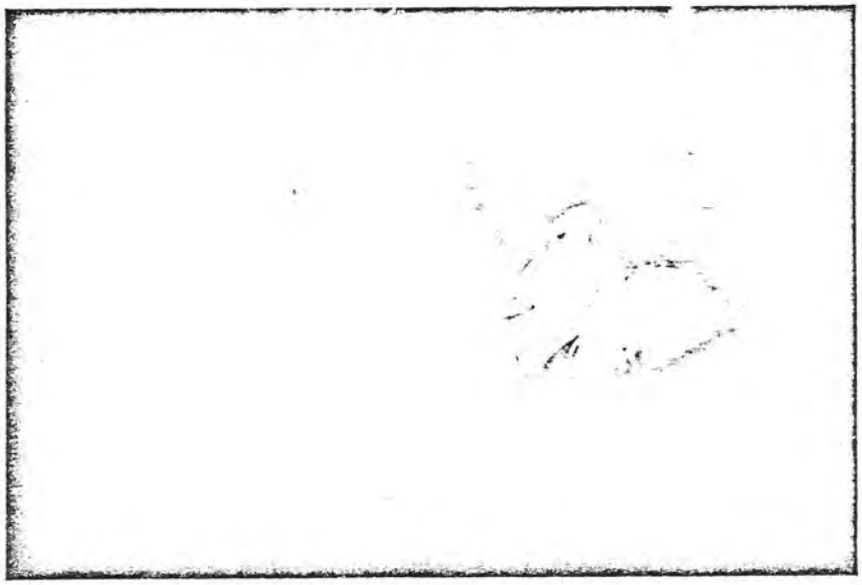

FIGURE 5. Flow in a swirling jet, $L/D = 0$, $\rho Q = 21{\cdot}7$ gm/sec, $Q = 0{\cdot}0167$ m³/sec, $\Omega = 0{\cdot}714$ gm-m²/sec, $\Omega D/\rho Q^2 = 0{\cdot}300$.

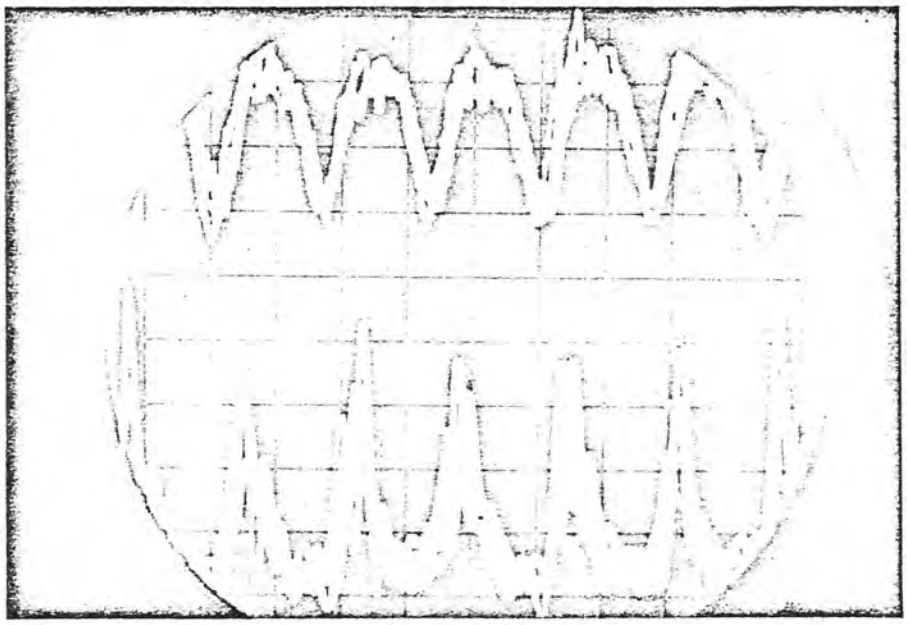

FIGURE 6. Oscilloscope traces of velocity (upper trace) and pressure.

FIGURE 13. Flow throu
flow in the small tube.
axis of the large tube

Q = 21·7 gm/sec,
$\lambda D/\rho Q^2$ = 0·300.

trace) and pressure.

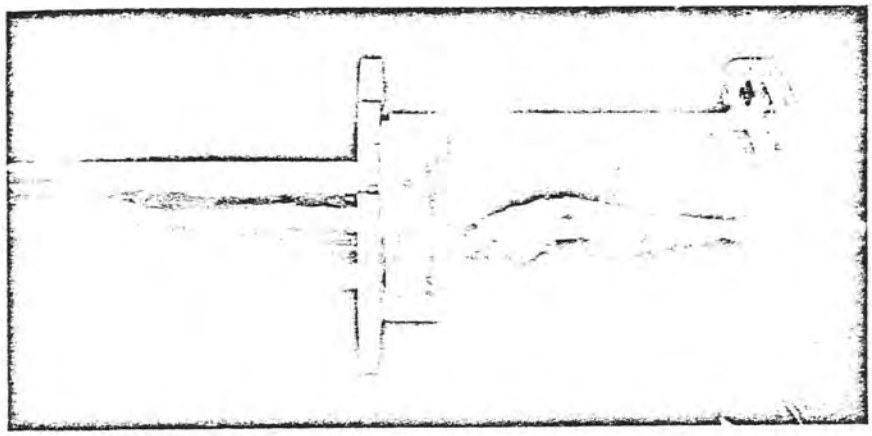

(*a*)

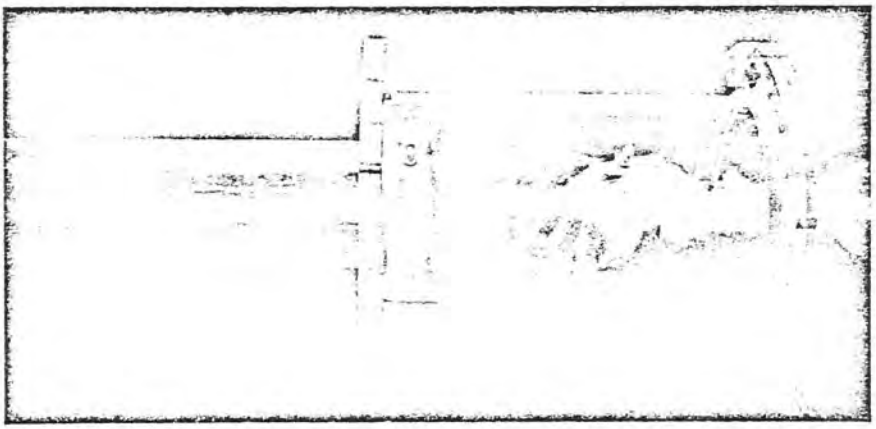

(*b*)

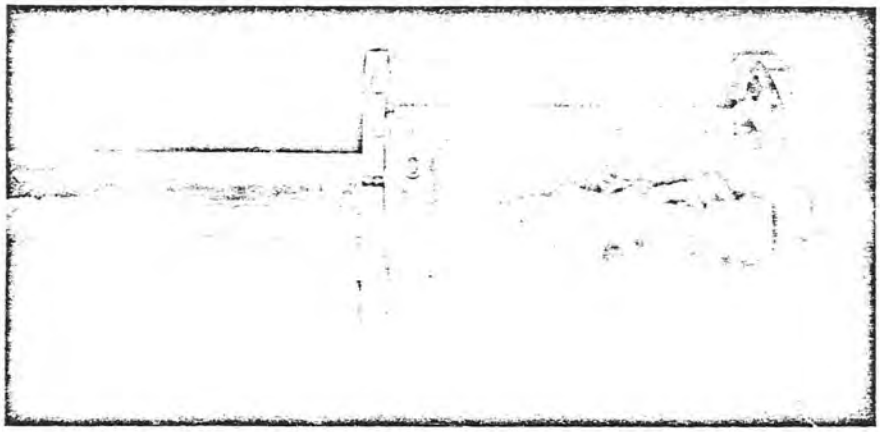

(*c*)

FIGURE 13. Flow through a contraction. (*a*) Breakdown in the large tube, steady swirling flow in the small tube. (*b*) Reversed flow throughout both tubes. (*c*) Reverse flow on the axis of the large tube with a second breakdown in the smaller tube.

REC-ERC-71-42

H. T. Falvey
Code 1532

DRAFT TUBE SURGES

A Review of Present Knowledge and an Annotated Bibliography

H. T. Falvey
Engineering and Research Center
Bureau of Reclamation

December 1971

MS-230 (8-70)
Bureau of Reclamation

TECHNICAL REPORT STANDARD TITLE PAGE

1. REPORT NO.	2. GOVERNMENT ACCESSION NO.	3. RECIPIENT'S CATALOG NO.
REC-ERC-71-42		

4. TITLE AND SUBTITLE	5. REPORT DATE
Draft Tube Surges—A Review of Present Knowledge and an Annotated Bibliography	Dec 71
	6. PERFORMING ORGANIZATION CODE
7. AUTHOR(S)	8. PERFORMING ORGANIZATION REPORT NO.
H. T. Falvey	REC-ERC-71-42
9. PERFORMING ORGANIZATION NAME AND ADDRESS	10. WORK UNIT NO.
Engineering and Research Center Bureau of Reclamation Denver, Colorado 80225	11. CONTRACT OR GRANT NO.
	13. TYPE OF REPORT AND PERIOD COVERED
12. SPONSORING AGENCY NAME AND ADDRESS	
Same	14. SPONSORING AGENCY CODE

15. SUPPLEMENTARY NOTES

16. ABSTRACT

A literature survey and a review of material related to draft tube surges is presented. The literature survey consists of an annotated bibliography of 68 articles published between 1910 and 1970. The review is restricted to three major areas: experiments with elementary models, experime ts with model and prototype turbines, and field expedients to reduce surging. Velocity distributions and surge frequencies are given special attention in the first two areas. Present knowledge is sufficient for predicting the order of magnitude of draft tube surge frequencies and relative surge amplitudes. Additional studies are needed to refine prediction methods and to extend their scope to include pumps and pump-turbines. Model testing at full prototype heads is apparently not required to investigate draft tube surging. Has 68 references.

17. KEY WORDS AND DOCUMENT ANALYSIS

a. *DESCRIPTORS*-- / *draft tubes/ * turbines/ *surges/ *hydroelectric powerplants/ hydraulic machinery/ fluid mechanics/ unsteady flow/ laboratory tests/ model tests/ fluid flow/ non-uniform flow/ vortices/ bibliographies/ annotations/ velocity distribution/ amplitude/ air admission/ frequency

b. *IDENTIFIERS*-- /hydrodynamic stability

c. *COSATI Field/Group* 13G

18. DISTRIBUTION STATEMENT	19. SECURITY CLASS (THIS REPORT)	21. NO. OF PAGES
Available from the National Technical Information Service, Operations Division, Springfield, Virginia 22151.	UNCLASSIFIED	25
	20. SECURITY CLASS (THIS PAGE)	22. PRICE
	UNCLASSIFIED	$3.00

REC-ERC-71-42

DRAFT TUBE SURGES

A Review of Present Knowledge and an Annotated Bibliography

by
H. T. Falvey

December 1971

Hydraulics Branch
Division of General Research
Engineering and Research Center
Denver, Colorado

UNITED STATES DEPARTMENT OF THE INTERIOR
Rogers C. B. Morton
Secretary

*

BUREAU OF RECLAMATION
Ellis L. Armstrong
Commissioner

CONTENTS

LIST OF FIGURES

APPLICATIONS

The results of this study are encouraging. Sufficient knowledge is presently available to permit the analytic prediction of draft tube surge frequencies and relative amplitudes knowing the wicket gate geometry and turbine characteristics. Additional studies are needed to refine existing surge prediction methods and to extend their scope to include pumps and pump-turbines. Testing models at the full prototype head does not appear to be necessary to investigate surge characteristics of a turbine. The quantities presented in the section "Field Expedients to Reduce Surging" represent observations of specific installations. The absolute value of these quantities will undoubtedly vary from installation to installation. However, the order of magnitude of the quantities can probably be used for estimations.

INTRODUCTION

Draft tube surge is the term applied to a hydrodynamic instability which forms in draft tubes containing swirling flow. The instability is present in almost every reaction-type installation when the unit is not operating near maximum efficiency. It has also been observed with Kaplan-type (propeller) runners.

Flow visulization studies with model turbines have shown that the instability or surging is intimately connected with the presence of a corkscrew or spiral-shaped vortex which rotates around the axis of the conduit, Figure 1. The surging exists with the vortex core filled with air, water, or water vapor. However, when the vortex core is filled with air or water vapor, the amplitude of the surges is reduced. A vortex core which forms coaxially with the conduit produces no surges. Apparently, the spiral vortex represents a flow configuration conducive to self-excited oscillations.

In hydroelectric plants, the surges are responsible for many undesirable operating characteristics which may occur individually or in combination. These undesirable characteristics are: noise, vibrations, variations in power output, vertical movement of the runner and shaft, and pressure pulsations in the penstock. The existence of so many different adverse characteristics of the draft tube surge, as well as inconsistencies in the character of the surge between apparently identical units, has led to much confusion in analyzing the problem.

This report presents a compilation and analysis of known facts and observations about the draft tube surges in an effort to explain some of the inconsistencies. In addition, an annotated bibliography is included to provide the reader with additional sources of information.

Figure 1. Spiral vortex in a cylindrical tube. Flow is from right to left.

In conducting the library study, any material pertaining to rotational flow in a conduit was gathered. Although the sources were often very remote from the field of hydraulic machinery, their inclusion in the bibliography adds insight into the nature of the problem.

EXPERIMENTAL OBSERVATIONS WITH SIMPLIFIED MODELS

General

In a normal Francis-type turbine installation, the analysis of the flow beneath the runner is made extremely complex by the effects of the bend in the draft tube, the conical diffuser section of the draft tube, and the velocity distribution imparted by the runner itself. Some authors have suggested that the flow distribution in the spiral case or distributor may also be a significant parameter. In view of the multitude of factors to be considered, investigations with simplified models is clearly indicated. With a simplified model, the effect of each factor can be investigated separately and its contribution to surging evaluated.

Tests of simplified models were made with either water or air flow in cylindrical, convergent, and divergent pipe sections. Swirl was imparted through rotation of upstream pipe sections, spiral chambers, vanes, and rotating perforated disks placed perpendicular to the

axis of the pipe. Axial, radial, and tangental velocity distributions were measured for conditions just preceding the transition into the spiral vortex, as well as for conditions with considerable swirl. In addition, frequency characteristics for various flow rates were observed.

Velocity Distribution

The velocity distribution in the conduits was found to depend upon both a characteristic Reynolds number and the amount of swirl in the flow. Six flow regimes with swirling flow in divergent conduits were identified (Harvey, So, Talbot), Figure 2.

A systematic study of the velocity distribution for each one of the flow regimes has not been conducted. However, some data have been published for certain specific cases. For instance, axial and tangential velocity distributions for Regimes 4 and 5 type flow have been measured. These measurements typically indicate a reduced axial velocity on the axis of the tube. The tangential velocity distribution with Regime 4 can be approximated with an equation of the type defining a viscous vortex,

$$V_t = \frac{AR}{r}\left(1 - e^{\frac{Br^2}{R^2}}\right) .$$

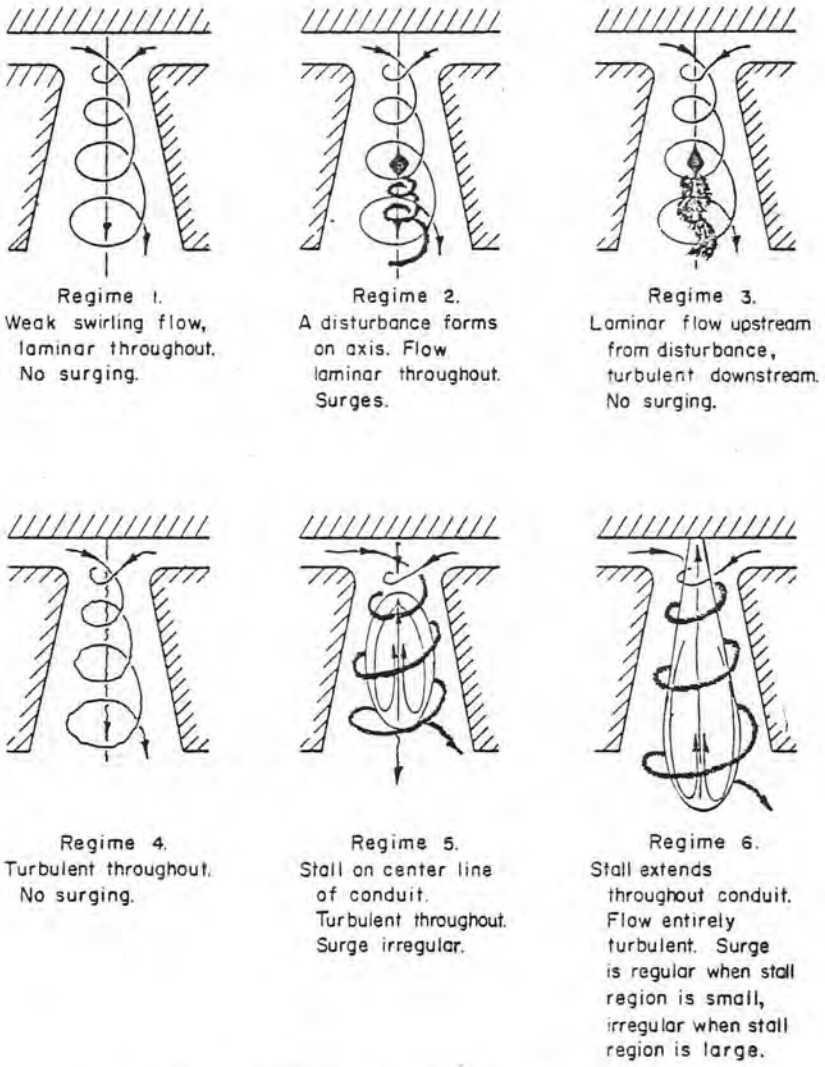

Regime 1. Weak swirling flow, laminar throughout. No surging.

Regime 2. A disturbance forms on axis. Flow laminar throughout. Surges.

Regime 3. Laminar flow upstream from disturbance, turbulent downstream. No surging.

Regime 4. Turbulent throughout. No surging.

Regime 5. Stall on center line of conduit. Turbulent throughout. Surge irregular.

Regime 6. Stall extends throughout conduit. Flow entirely turbulent. Surge is regular when stall region is small, irregular when stall region is large.

Figure 2. Flow regimes with swirling flow in divergent conduits.

Tests were also made with air in straight cylindrical conduits (Harvey). A series of vanes were used to induce spiral flow. The swirl angle upstream from the disturbance was measured directly with a stream of smoke. The author indicated that the flow was laminar upstream from the disturbance and turbulent downstream which is indicative of Regime 3 type flow. However, upstream flow conditions at which the tests were conducted give a Reynolds number of about 9×10^3 and thus indicate the inception of Regime 5 type flow. Tests have shown that moderate rotation or swirl has a dampening effect upon turbulence which could explain the laminar appearance of the flow even though it is in the turbulent range (i.e., Reynolds numbers greater than about 2×10^3). A viscous vortex equation could not be made to fit the swirl angle measurements exactly. This lack of fit is probably caused by a nonuniform axial velocity distribution across the cross section.

The rope-like vortex which precesses around the cell of reversed flow with Regime 5 or 6 type flows produces periodic variations in the velocity measurements. In general, the manner in which the various investigators analyzed these velocity fluctuations at a point to obtain a single mean velocity value was not indicated in their publications.

Surge Frequencies

The frequency of the oscillations was found to vary inversely as the diameter of the tube and inversely as the length of the tube. The amplitude of the fluctuation was lower with conically divergent tubes than with cylindrical tubes. In all the tests, the relationship between discharge and frequency was very linear for a given tube and inlet swirl condition. This concept has been used by at least one manufacturer in a flow-metering device.

Mathematical Description of the Swirling Flow

Many attempts have been made to describe the swirling flow in cylindrical and divergent tubes mathematically. Almost without exception, the basic assumptions restrict the classes of solutions to rotationally symmetric flow. This means that any disturbances which are predicted will be symmetrical and will appear on the axis of the conduit. Prediction of a spiral-shaped vortex is automatically eliminated by the basic assumptions. In general, it is not possible to make the necessary assumptions about the flow, a *priori*, which permits a description of the spiral vortex. However, it is possible to obtain analytic descriptions of the spiraling flow empirically.

In one empirical method, an interpretation or explanation of the pressure fluctuations is made on rational grounds. Then an equation, containing constants to be determined experimentally, is written to describe the phenomenon. For instance, it has been assumed that the vibrations are produced by pertubations of the velocity and density of the fluid in the tube (Michelson, Vonnegut). This assumption leads to an expression for the frequency of the form

$$f = \frac{A\,V_S}{\pi D}\left[1 - p_2/p_1\right]^{1/2} \qquad (1)$$

The approach leads to the conclusion that high speed and motion in more than one dimension are necessary for the generation of the surge (Michelson). Although the explanation seems plausible, velocity measurements in air and water have shown that surging can exist even though the flow is everywhere definitely subsonic.

Another method for obtaining an empirical equation for the surging flow is to write the governing differential equations in dimensionless form. This results in a set of dimensionless parameters which can be used to correlate the experimental data. The approach leads to equations of the form

$$\frac{f D^3}{Q} = \frac{A\Omega D}{\rho Q^2} + B \qquad (2)$$

where A and B are empirically determined constants (Cassidy, Falvey). This method implies that gross flow parameters are sufficient to describe the surge phenomenon with swirling flow. In general, good correlations have been obtained with this approach even when using such widely different density fluids as air and water.

Instead of studying fully surging flow, some investigators have tried to define the conditions at which a disturbance will form with swirling flow. These attempts have led to the conclusion that the disturbance is a finite transition between two states of flow (Benjamin).

Analytic studies indicate that the disturbance will occur when the ratio of the rotational velocity component to the axial component is greater than about 1.0 (Squire). The critical breakdown point can also be described by the empirical expression mentioned above. Expressed in terms of the gross parameters, the disturbance will occur in a straight pipe when

$$\frac{\Omega D}{\rho Q_2} = 0.008 \frac{L}{D} + 0.17 \ . \qquad (3)$$

The empirical methods mentioned above could be eliminated if the upstream and downstream boundary conditions could be accurately described. One attempt was made to approximate these conditions through an iterative procedure using the simplified equations of motion (Gore, Ranz). Through this procedure a flow field was obtained which has some of the important features of the observed flow.

OBSERVATIONS WITH MODEL AND PROTOTYPE TURBINES

General

Often the use of hydraulic models to predict prototype performance is questioned. In some cases, these doubts are justified, especially when the flow phenomena under study have not been carefully defined. Some of the authors conducted model-prototype comparisons and indicate areas in which model tests can be beneficial.

For instance, it has been demonstrated that with turbulent vortices neither the velocity distribution nor the circulation are functions of viscosity if the flow is turbulent and fully developed (Hoffman and Joubert). Thus, one would expect flow patterns, velocity distributions, and pressure fluctuations in the model and prototype to be related through an Euler number relationship. These considerations have been verified in experiments which showed close agreement between the size of the vortex core underneath model and prototype runners, as well as damage areas to be expected from cavitation (Girand).

Attempts to correlate penstock frequencies and amplitudes have, on the other hand, been rather unsuccessful. The reason for these discrepancies is apparent if the entire power generating system is considered as a vibrating system having several degrees of freedom with each capable of resonance being driven by some forcing function. The forcing function which drives the system is created by pressure fluctuations in the draft tube. The frequency and amplitude of these fluctuations can be obtained from a hydraulic model study. The degrees of freedom or parts of the system which could resonate include the penstock, other generators connected to the same penstock, the surge tank, the turbine generator unit and connecting shafts, the regulating system, and the electrical power network. Obviously, this multitude of factors cannot be accurately simulated in the hydraulic model. Therefore, correlation of amplitudes and frequencies in the penstock between model and prototype measurements would be fortuitous. However, this does not imply that data from the model study cannot be used to predict prototype penstock pressure fluctuations. Existing analytical methods based on impedance concepts have proven highly successful in predicting penstock frequency and amplitudes created by periodic pressure or discharge fluctations (Streeter, Zolotov).

A model can thus be expected to accurately represent velocity distributions, forcing frequencies, and amplitudes in the prototype draft tube. The appearance of cavitation and areas which can be expected to sustain cavitation damage can also be predicted on the basis of model experiments. The model data can then be used in a mathematical description of the system to determine power swings and penstock pressure fluctuations in the prototype.

The scaling laws to convert model frequencies and amplitudes to prototype values are

$$f_p = f_m \, (D_m/D_p) \, (H_p/H_m)^{1/2} \qquad (4)$$

for frequency, and

$$\Delta p_p = H_p \, (\Delta p_m/H_m) \qquad (5)$$

for amplitude.

Velocity Distributions

The type of flow observed during periods of large pressure surges is described by most experimenters as being typical of Regime 5 or 6 type flow, Figure 2. Without surging, a Regime 4 type flow is observed in the model. These regimes are modified to some extent by the pressure in the draft tube. For high tailwater levels, the vortex core remains solid. With lower tailwater levels, the pressure in the center of the vortex core decreases until at some critical value of tailwater the pressure in the vortex core reaches the vapor pressure of the water and a hollow vortex core results. If air is admitted to the draft tube, a hollow core can be achieved at pressures greater than the vapor pressure of water.

A distinction was made between hollow and solid vortex cores. The hollow vortex was called "soft" and the solid vortex "hard" (Vuskovic and Velensek). This terminology was developed during observations of

pressure fluctuations in the draft tube. With a solid core the intensity of the pulsations was severe. By admitting air or dropping the tailwater level to form water vapor in the vortex core, the intensity of the pulsations decreased or softened. The use of this terminology is unfortunate. Recent tests have revealed that air admission or decreasing the tailwater level can make the intensity of the pulsations increase in some cases (Ulith).

The velocity distribution in the throat of the draft tube is a function of the runner speed, distributor proportions, discharge, and the shape of the runner blades. Until recently, velocity distributions were obtained from simplified theories involving runner speed (i.e., assuming ru = constant) or from model tests. With the advent of the computer, better methods for computing the three-dimensional velocity distribution have been developed (Jansen). These have reduced the need for a comprehensive model test program. With the mathematical model, various parameters can be examined and a final design developed. The final design can then be verified by a model study. These methods, although a tremendous improvement over previous computational methods, still are inadequate since the effect of velocity distributions produced in the draft tube are not considered.

Experiments with models thus seem to be the only reliable method of determining velocity distributions in the draft tube. Some velocity distributions for typical units have been measured with a vapor-filled vortex core and with a solid vortex core (Dziallas, Yamazaki). In both cases, a positive, nonzero value of peripheral velocity was measured over the entire cross section. These results are clearly incorrect since the peripheral velocity must be zero somewhere in the cross section. For flow which rotates both clockwise and counterclockwise in the cross section, there must be an odd number of points on the diameter of the section having zero peripheral velocity. However, the experiments of one investigator are particularly noteworthy (Mollenkopf). Through the use of a hot film probe, he was able to obtain velocity measurements in the draft tube which represent essentially a "snapshot" of the instantaneous distribution. The circumferential velocity distribution computed from Mollenkopf's work differs significiantly from the distribution of a potential vortex in a cylinder, Figure 3.

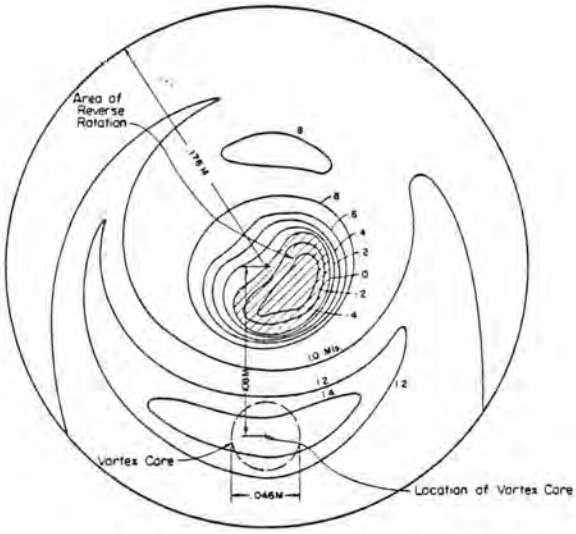

Derived from Mollenkopf (67), Figures 14 and 15, Plane IIZ
Rotational Speed of Vortex around tube about 1.8 rev/sec.

a. Measured distribution.

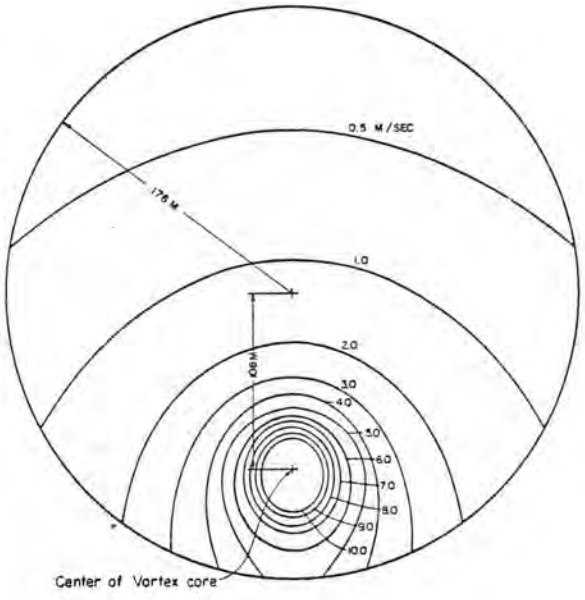

Vortex Strength K = .217 M^2/sec.
Rotational Speed of Vortex around Tube = 1.8 rev./sec.

b. Theoretical distribution resulting from irrotational flow around a vortex.

Figure 3. Circumferential velocity distribution in a conduit.

Surge Frequencies

The earliest prediction of the surge frequencies was in 1940 (Rheingans). The well known relationship is

$$f = \frac{n/60}{3.6} \qquad (6)$$

This equation is based on observations of existing plants and represents the surge frequency when the greatest pressure fluctuations occur. Other investigators have argued that the constant in the denominator should be something closer to 4.0. However, the exact magnitude of the constant is somewhat immaterial since the equation is empirical with no firm theoretical basis.

The next major attempt to develop a mathematical model for predicting the surge frequency utilized the concept of a rotational vortex moving in an irrotational vortex field (Hosoi). The equation which was developed had the form of the Rheingans equation. It was

$$f = 1/2\ (V_a/R)^2(N/60)$$

Model tests indicated Va/R varied between 0.7 and 0.8. Unfortunately, velocity distribution studies have not substantiated the velocity field assumptions made in this method.

The most recent attempts to predict the surge frequency utilize gross flow parameters (Falvey, Cassidy, 1970). For a given draft tube size, the surge frequency is given by

$$f = \frac{Q}{D^3}\left(0.54\,\frac{\Omega D}{\rho Q^2} + 0.31\right) \qquad (7)$$

The parameter $(\Omega D/\rho Q^2)$ can be computed for a particular turbine from the following expression

$$\frac{\Omega D}{\rho Q^2} = \frac{DR \sin \alpha}{BNS} - \frac{550\, p_{11}\, D}{2\sqrt{2g\rho}\, Q_{11}^2\, \phi\, D_2} \qquad (8)$$

The first term on the right of the equal sign is a function of the wicket gate geometry. The second term represents the turbine runner characteristics. The dimensionless ratio thus takes both the wicket gate geometry and the turbine runner characteristics into account when predicting the surge frequency. The effect of draft tube geometry on the constants in Equation 7 has not been established.

FIELD EXPEDIENTS TO REDUCE SURGING

Air Admission

The most frequently mentioned means to reduce the amplitude of the surging is the admission of air into the runner or draft tube. With low tailwater levels, the pressure below the runner is less than atmospheric. In this case, suitable venting is all that is required to supply air to the vortex. On the other hand high tailwater levels require the use of an air compressor to force the air into the draft tube. Since the most severe pulsations can occur with the high tailwater levels, provision for the admission of air may be costly.

Both the location and the manner of air injection are important. For instance, air admitted to the inlet side of a turbine runner eliminated pressure pulsations for all gate openings less than 72 percent of optimum gage (Konig, Whippen). Normally, however, air is admitted to the lower side of the runner. Many air admission schemes have been used. They include air admission through extensions of the turbine shaft, through pipes or especially formed streamlined shapes, oriented across the draft tube, and behind the runner band (Dziallas), Figure 4. For axial flow runners the most effective location for air injection is through holes in the runner cone (Isaev). Recent studies indicate the most effective aeration location with high specific speed Francis-type runners is injection of compressed air into the annular chamber between the wicket gates and the runner (Ulith). Other injection locations have been used successfully. Even injection from the draft tube wall or from behind the runner band can reduce the surge amplitude. The migration of the air to the vortex core in these cases is due to recirculation of water in the draft tube.

The quantities of air needed to reduce surging are normally expressed in terms of the ratio of the volumetric airflow at standard temperature and pressure to the turbine discharge at full load point with rated head. Using this definition, the air quantities needed for maximum surge attenuation with injection through the runner cone in low specific speed units are in the range 1 to 2 percent. Whereas, with air injection into the space between the wicket gates and the runner only 0.05 to 0.10 percent air is needed with high specific speed units (Ulith).

The location at which the air is admitted has a significant effect on the efficiency of the unit. For instance, admission of air either upstream from the runner or through deflecting surfaces of the head cover result in loss of efficiency. Air admission between the runner and the wicket gates may result in slight increases in efficiency. Whereas, air admission through the runner cone has, in some cases, led to a 0.5 to 1.0 percent increase in efficiency (Isaev). In these cases, the gain in efficiency with air admission through the cone may be attributed to improved flow conditions in the draft tube as a result of air filling the reversed flow region.

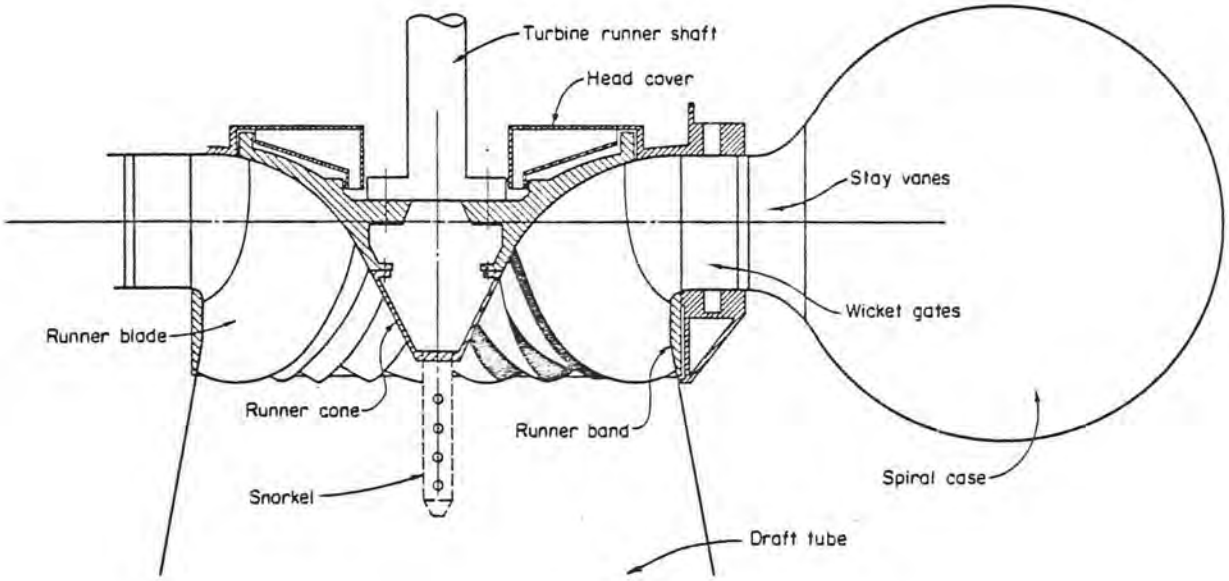

Figure 4. Definition sketch of turbine nomenclature.

Air admission may not always lead to decreased surge amplitudes. The reduction in surge amplitude has been found to be dependent on sigma (or tailwater level) (Ulith). In fact, for sigma values larger than about 0.3 to 0.4, air admission may increase the surge amplitude. An upper limit for the quantity of air which could be admitted advantageously was also noted (Isaev). For instance, during part load operation with a Kaplan turbine, the maximum reduction in surge amplitude was observed with 0.5 percent air. Increasing the airflow quantity to 3 or 4 percent increased the surges at the inlet to the elbow. Under motoring conditions 2 percent air resulted in the largest surge reduction. Increasing air quantities above 2 percent led to larger surges.

The necessity of providing for compressed air with high tailwater levels may or may not be a disadvantage. Frequently air is available at the plant in sufficient quantities and at adequate pressure to provide the required air admission. If air is admitted at the runner cone, the maximum pressure required is about equal to the submergence of the runner below the tailwater. With high-speed runners, air injection at the periphery of the head cover requires an air pressure of about 40 to 50 percent of the head. Admission in the spiral case would require a pressure approximately equal to the head on the unit. One side benefit of air admission upstream from the runner is protection of the runner from cavitation damage. It should be stressed, however, that compressed air, while it may be available for surge suppression, requires energy and equipment for its production.

Fins and Flow Splitters

Since the instability or surging is caused by the rotation of the flow in the draft tube, a logical way to eliminate the pulsations would be to eliminate or reduce the swirl. One means to reduce the swirl is to place fins parallel with the axis of the runner either on the walls on the draft tube or on the runner cone. The fins are usually a half a throat diameter long and extend about 0.1 to 0.2 throat diameters into the flow. Between two and eight fins are used.

If the fins extend far enough into the flow to touch each other, they are known as flow splitters, Figure 5. Normally, the flow splitters consist of three fins or vanes, although a greater number have been used.

The orientation, number of fins or elements of a flow splitter, and height of the fins or flow splitter are significant parameters in obtaining a maximum

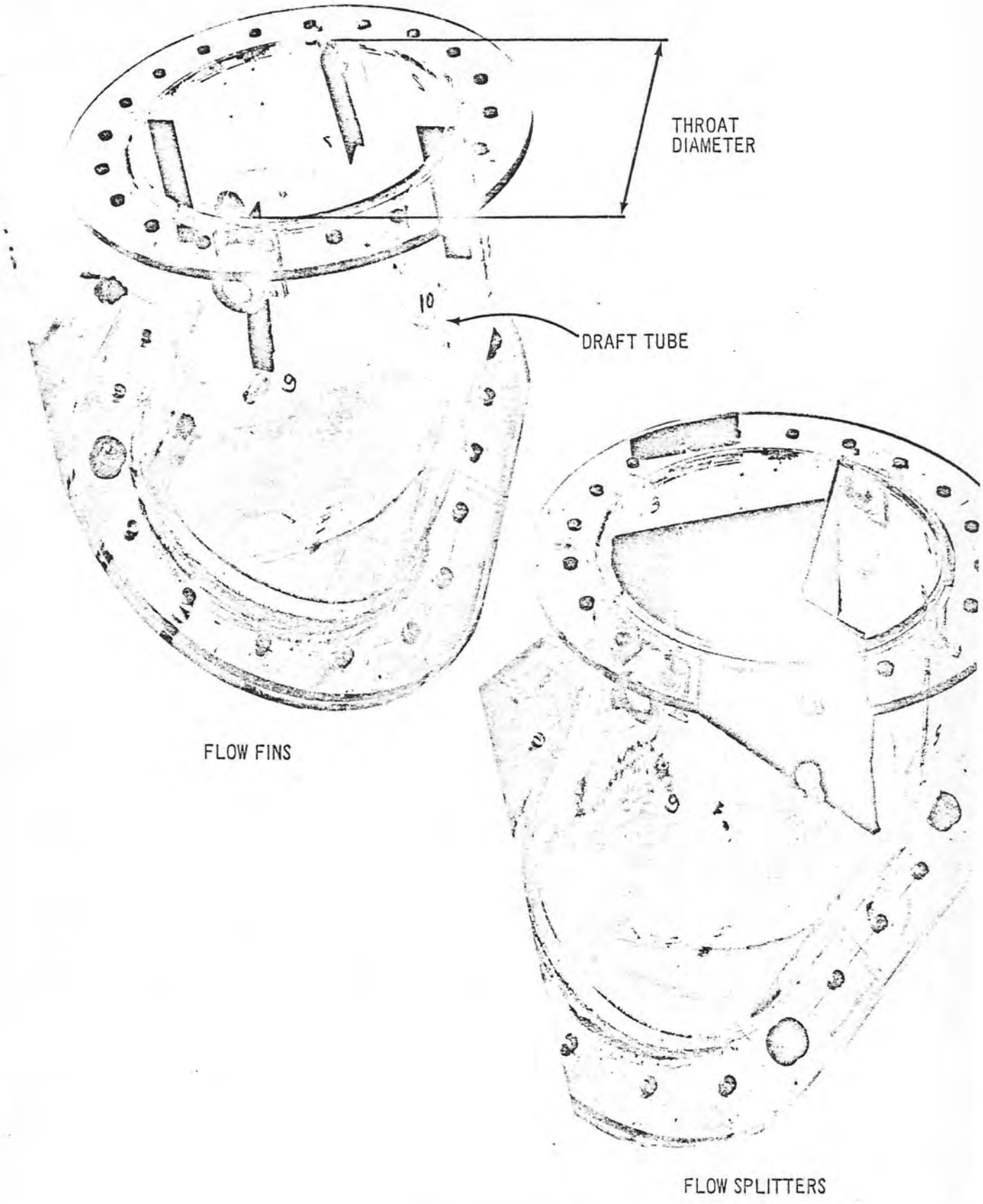

Figure 5. Fins and flow splitters.

reduction in the swirl. No specific guidelines can be given as to height or orientation of the fins since these parameters depend upon the height of the diffusor cone in the draft tube. However, tests indicate that the flow splitter should be place as high as possible in the draft tube cone for maximum effectiveness (Falvey).

The disadvantages of fins and flow splitters are a loss in efficiency, a necessity to guard the appurtenances from cavitation damage, high-frequency noise, and structural problems involved in installing them. Because of these disadvantages the use of fins is normally restricted to small units.

Extensions to Runner Cone

Another approach used in reducing the draft tube surges is to fill the reverse flow region on the axis of the draft tube with a solid body of rotation. The body can either be fixed by attaching it to the draft tube wall, as in the Moody spreading cone, or rotating by attaching it to the runner cone (Scheidenhelm's discussion of Allen). Their earliest use was on the Merrimack River in Massachusetts around the years 1860 to 1910, Figure 6. The basis for this concept comes from observations with rectilinear flow where areas of reverse flow are prevented from forming. Elimination of the reverse flow areas reduces the unsteadiness by streamlining the overall flow. Indiscriminant use of this principle is not recommended. One unpublished report described a low specific speed runner which stopped surging when the Hydraucone broke off 4 feet below the runner.

There are at least two disadvantages to using extension of the runner cone (Dziallas, Kovalev). These are the large lateral forces on the extension and the unfavorable velocity head recovery in the draft tube. These disadvantages limit this type of surge suppressor to relatively low specific speed units. In addition to these disadvantages, the diameter of the extension would have to be adjustable for optimum results since the diameter of the reverse flow area varies between 0.2 to 0.8 of the draft tube diameter.

Coaxial Hollow Cylinder

Model tests indicate that a hollow cylinder, which resembles a barrel with the ends cut out, placed concentrically in the draft tube will reduce the amplitude of the pressure surges and slightly increase efficiency (Vuskovic, Lecher), Figure 7. Significantly higher frequencies were also observed. In the zone of maximum surges, the frequencies corresponded roughly with the turbine's rotational speed. The design of these devices must be accomplished by model

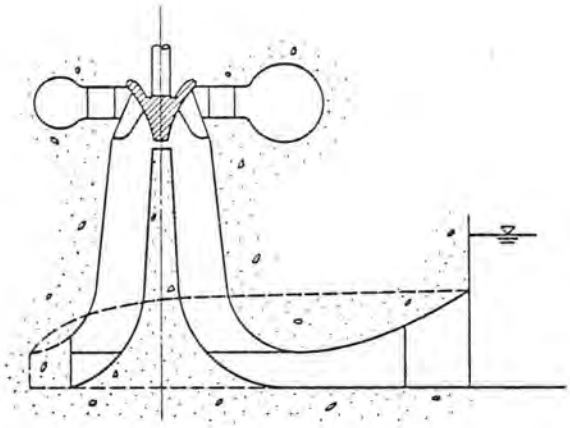

a. Moody spreading cone.

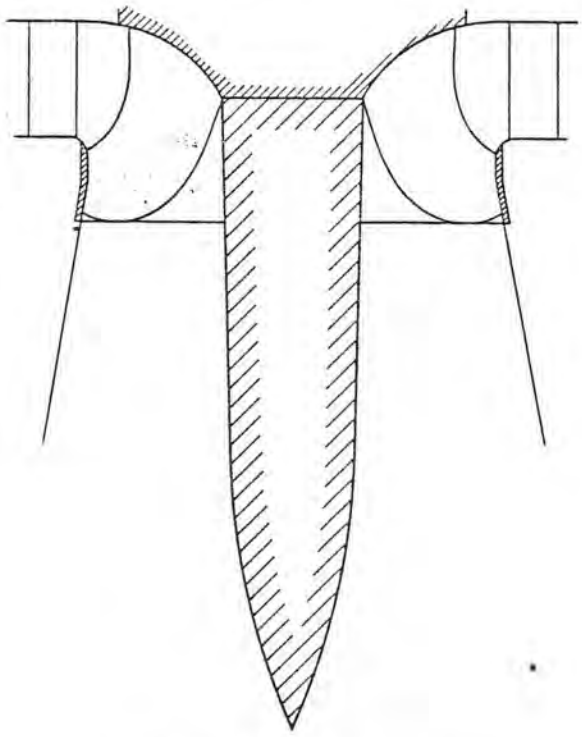

Configuration used at Washington Mills
Lawrence Risdon Wheel
1881 on Merrimack River

b. Rotating extension.

Figure 6. Extensions to runner cone.

testing since it was noted that small form changes alter the performance considerably. The largest reduction in the pressure pulsations amounted to 70 percent.

The major disadvantage of the coaxial hollow cylinder is providing enough strength in the supports to keep the cylinder centered. The cylinder must also be made rigid enough to keep it from deforming. To minimize losses in efficiency, the supports should be designed so they thet do not cause a significant restriction to the flow.

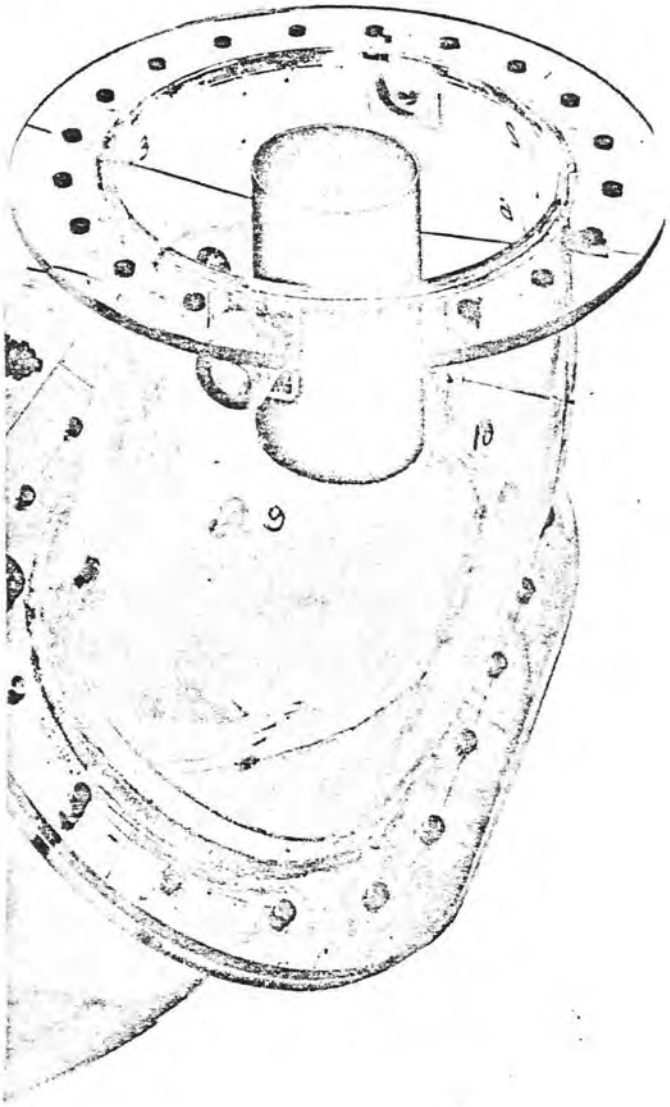

Figure 7. Coaxial hollow cylinder.

SYMBOLS USED IN THE TEXT

f	frequency, hz
g	acceleration of gravity
n	rotational speed of runner, rpm
p	pressure
r	radius from centerline of tube
r_a	radius of rotational vortex core
$A,B,$	constants
D	draft tube diameter
D_2	minimum clear diameter of runner
H	net available head across turbine
L	length of tube
N	number of wicket gates
N_s	specific speed
P	power generated by turbine, horsepower
Q	discharge
R	draft tube radius
S	minimum clear space between wicket gates
V_a	local axial velocity
V_s	sonic velocity
V_t	local tangential velocity
Δp	pressure fluctuation
α	angle between velocity vector and radial
ρ	density
ϕ	ratio of rotational speed of runner to maximum velocity for a given head (spouting velocity)
Ω	angular momentum = $\int_0^R 2\pi r^2 \rho V_a V_t \, dr$

Subscripts

1	upstream
2	downstream
m	model
p	prototype

CONVERSION FACTORS

In the English system of measurements, all turbine quantities are referred to unit dimensions which are:

length, 1 foot
discharge, 1 cubic foot per second
horsepower, 550 foot-pounds per second

In the metric system, the unit quantities are:

length, 1 meter
discharge, 1 cubic meter per second
horsepower, 75 kilogram-meters per second

Due to these differences, the unit characteristics of a turbine are not always the same in the metric and English systems. The following table gives the equivalents to aid the reader in referring the quantities mentioned in the articles to his own frame of reference.

Quantity	Definition	Multiply English units by these factors to obtain metric units
phi	$\phi = \frac{\pi D_2 n}{60\sqrt{2gH}}$	1.0
specific speed	$N_s = \frac{n P^{1/2}}{H^{5/4}}$	4.45
specific discharge	$Q_{11} = \frac{Q}{D_2^2 H^{1/2}}$	0.552
specific power	$P_{11} = \frac{P}{D_2^2 H^{3/2}}$	64.9
unit speed	$n_{11} = \frac{nD}{H^{1/2}}$	0.552

ALPHABETICAL LISTING OF AUTHORS

BIBLIOGRAPHY OF VORTEX ACTION IN CLOSED CONDUITS AND DRAFT TUBE SURGING

I. Bibliographies

1. Dobratz, B. M., 1964, Vortex Tubes, A Bibliography, University of California, Lawrence Radiation Laboratory, Livermore, California, UCRL-7829

A 101-item bibliography concerning energy, thermodynamic, and flow characteristics in tubes which contain a vortex. A large number of these references are concerned with the Ranque-Hilsch Tube.

2. Solomon, L., 1965, Fluid Motion and Sound, U.S. Department of Commerce, Clearinghouse for Federal Scientific and Technical Information, AD-625087

An annotated bibliography which summarizes the work done by the Department of Engineering, University of California, Los Angeles, in the field of sound generated by air jets. The only reference of direct interest was one concerning vortex sound. The other references are concerned with sound generation by other methods.

3. Kuchemann, D., 1965, Report on the IUTAM (International Union for Theoretical and Applied Mechanics) Symposium on Concentrated Vortex Motion in Fluids, Journal of Fluid Mechanics, Vol. 21, Part 1, pp 1-20

A state-of-the-art summary as defined at a symposium organized by the International Union for Theoretical and Applied Mechanics which met in July 1964. The summary included the following topics:

The Formation of Coherent Vortex Sheets
The Structure of Smooth Vortex Cores
Various Deviations from Smooth Core Flows
The Occurrence of Columnar Vortices in Rotating Fluid Systems
The Appearance and Structure of Vortex Wakes

Included are 95 references, many of which are discussed in the summary.

II. Mathematical Description of Flow

A. Theories Neglecting Viscosity and Turbulence

4. Kelvin (Sir William Thomson), 1910, Mathematical and Physical Papers, Cambridge University Press, Vol. IV, Chapter 15, Vibrations of a Columnar Vortex, pp 152-165

Originally published in 1880. Develops basic three-dimensional, unsteady, irrotational flow equations and investigated the effect of small sinusoidal disturbances on these equations of motion and continuity. The basic equations are solved with various boundary conditions which result in descriptions of the periodic disturbance in the motion of:

a. A rotating liquid in a space between two concentric circular boundaries which have infinitely small, simple harmonic motion.

b. A rotating fluid as above, except that the radius of the inner cylinder is zero.

c. A hollow irrotational vortex in a fixed tube.

d. A hollow irrotational vortex in a fluid of infinite expanse.

e. A combined Rankine vortex of infinite length located between two parallel plates.

The amplitude of the periodic disturbances as well as the radial and axial velocities is assumed infinitely small as compared with the tangential velocity.

5. Michelson, I., 1955, Theory of Vortex Whistle, The Journal of the Acoustical Society of America, Vol. 27, No. 5, pp 930-931

Develops a relationship for frequency based on two-dimensional, unsteady, isentropic flow. The tone produced is associated with the perturbation of a steady flow of speed U and density ρ_0. Under these conditions, the frequency, in hertz, is given by:

$$F = \frac{C}{\pi D}\left[\frac{2}{\gamma}\right]^{1/2}\left[\frac{P_1 - P_2}{P_1}\right]^{1/2}$$

where C = speed of sound
γ = 5/3 for monatomic gasses
γ = 7/5 for diatomic gasses
D = diameter of tube
P = reservoir and exit pressures

6. Squire, H. B., 1960, Analysis of Vortex Breakdown Phenomenon, Part 1, Aero Department, Imperial College, Report No. 102

The theory of standing waves on a cylindrical vortex is developed and applied to three cases of swirl. These cases are:

(1) forced and free vortex

$$V_t = V_o r \qquad \text{for } r \leqslant 1$$

$$V_t = V_o/r \qquad \text{for } r \geqslant 1$$

(2) a viscous vortex

$$V_t = V_o/r\,[1 - \exp(-r^2)]$$

(3) a specially constructed distribution

$$V_t^2 = \frac{V_o^2}{t} \int_o^t y^2 \operatorname{sech}^2 y\, dy$$

In every case, a uniform axial velocity distribution is assumed. The solutions predict a vortex breakdown when

$$1.0 \leqslant V_t/V_a \leqslant 1.20$$

7. Benjamin, T. B., 1962, Theory of the Vortex Breakdown Phenomenon, Journal of Fluid Mechanics, Vol. 14, pp 493-629

Development of a theory which predicts two states of flow in a vortex. The theory is based on a stationary axisymmetric perturbation of the stream function. The form of the perturbation is a standing wave, $\psi = \phi\,(Y) \sin(X + \nu)$. The two states of flow correspond to conditions before and after the perturbation. In the derivations, radial components of velocity are not considered. This theory was developed to explain the abrupt change in structure which sometimes occurs in swirling flow, especially in the leading-edge vortex formed above sweptback lifting surfaces.

8. Chanaud, R. C., 1963, Experiments Concerning the Vortex Whistle, Journal of the Acoustical Society of America, Vol. 35, No. 7, pp 953-960

Two-dimensional equations of rotation in a plane perpendicular to the tube axis were used to describe the flow. To these equations, nonaxisymmetric disturbances were applied to obtain a set of perturbed differential equations. The complete solution of these equations was not determined.

9. Gore, R. W. and Ranz, W. E., 1964, Backflows in Rotating Fluids Moving Axially through Expanding Crop Sections, American Institute of Chemical Engin...s Journal, Vol. 10, No. 1, pp 84-88

The axially symmetric equations for rotational flows were simplified through dimensional analysis. An axial inlet velocity distribution was assumed and substituted into the equations. Through an iterative procedure, a flow field is obtained which has some of the important features of the observed flow.

10. Kulonen, G. A. and Kulonen, L. A., 1966, On the Calculation of Axisymmetric Vortex Flow of an Ideal Incompressible Fluid in Curvilinear Channels, Leningrad Universitet, Vestnik, Seriya Matematiki, Mekhaniki i Astronomii, No. 1, pp 145-153

The equations of continuity and momentum are reduced to a single nonlinear partial differential equation which is solved for a 90° bend through successive approximations.

11. Benjamin, T. B., 1967, Some Developments in the Theory of Vortex Breakdown, Journal of Fluid Mechanics, Vol. 28, Part 1, pp 65-84

A further development of Reference 7. The requirement of infinitesimal perturbations is relaxed and the theory is expanded to include a change from cylindrical flow to one in which a finite standing wave exists.

12. Fraenkel, L. E., 1967, On Benjamin's Theory of Conjugate Vortex Flows, Journal of Fluid Mechanics, Vol. 28, Part 1, pp 85-96

A substantiation of Benjamin's theory (References 7 and 11) from a mathematicians point of view. The conclusions of Benjamin are found through a method which does not require the calculus of variations.

B. Theories Including Viscosity but Neglecting Turbulence

13. Talbot, L., 1954, Annular Swirling Pipe Flow, Journal of Applied Mechanics, Vol. 21, pp 1-7

The problem of rotationally symmetric steady swirl superimposed on Poiseuille flow in a round pipe was solved through numerical analysis. The solution was obtained through consideration of the momentum-integral method which is analogous to that used in boundary layer analysis. The results are not exact but are in the correct order of magnitude.

14. Howard, L. N., 1963, Fundamentals of the Theory of Rotating Fluids, Journal of Applied Mechanics, Transactions of the ASME, December, pp 481-485

An expository survey of some of the mathematical models which have been used in the theory of rotating fluids. The examples are restricted to geophysical fluid dynamics.

15. Turner, J. S., 1966, The Constraints Imposed on Tornadolike Vortices by the Top and Bottom Boundary Conditions, Journal of Fluid Mechanics, Vol. 25, Part 2, pp 377-400

Steady, incompressible, axisymmetric flow in a region remote from solid boundaries was assumed. The equations are solved by assuming an expression for the stream function. Boundary layer conditions which are responsible for the up and down flows in the vortex are examined. The results are in good agreement with experimental measurements.

16. Granger, R., 1966, Steady Three-dimensional Vortex Flow, Journal of Fluid Mechanics, Vol. 25, Part 3, pp 557-576

Exact differential equations of motion are developed in terms of the circulation and the stream function for steady axisymmetric flow. The equations are solved through the use of a power series provided the vorticity distribution along the axis of rotation is known. Solutions are restricted to small perturbations.

17. Cassidy, J. J. and Falvey, H. T., 1970, Observations of Unsteady Flow Arising After Vortex Breakdown, Journal of Fluid Mechanics, Vol. 41, Part 4, pp 727-736

In rotating flow moving axially through a straight tube, a helical vortex will be generated if the angular momentum flux is sufficiently large relative to the flux of linear momentum. This paper describes an experimental study of the occurrence, frequency and peak-to-peak amplitude of the wall pressure generated by this vortex. The experimental results are displayed in dimensionless form in terms of a Reynolds number, a momentum parameter and tube geometry.

C. Theories Including Viscosity and Turbulence

18. Hoffman, E. R. and Joubert, P. N., 1963, Turbulent Line Vortices, Journal of Fluid Mechanics, Vol. 16, Part 3, pp 395-411

Axisymmetric, steady-state flow is assumed. Various phenomenalistic considerations of the turbulent shear stresses are used to develop velocity profiles. This, in conjunction with dimensional analysis, leads to an empirical description of the flow which is substantiated with experiments.

19. Kreith, F. and Sonju, O. K., 1965, The Decay of a Turbulent Swirl in a Pipe, Journal of Fluid Mechanics, Vol. 22, Part 2, pp 257-271

Steady, incompressible, axisymmetric flow in a pipe was considered. The resulting equations were solved through the use of perturbation theory. The theoretical swirl velocity agreed well with experimental measurements at distances of less than 20 diameters but deviated further downstream.

D. Miscellaneous Mathematical Considerations

20. Betchov, R., 1965, On the Curvature and Torsion of an Isolated Vortex Filament, Journal of Fluid Mechanics, Vol. 22, Part 3, pp 471-479

The flow equations for a very thin, curved vortex filament in an inviscid fluid are considered. The elementary solution of a helical vortex filament is shown to be unstable.

21. Streeter, V. L. and Wylie, E. B., 1967, Hydraulic Transients, McGraw-Hill

A textbook describing various analytical methods to compute water-hammer waves in conduits and surge tanks. An impedance computational procedure for conduits is described which

permits a rapid examination of the system for resonance.

III. Experimental Observations with Elementary Models

22. Talbot, see Reference 13

Tests were made in a 1.25-inch inside-diameter plastic pipe with Reynolds numbers between 135 and 3,240. Swirl was induced by a rotating section 25 diameters long. The transition between stable swirl and unstable swirl was presented on a graph. For Reynolds numbers less than 1,800, a nonperiodic sinuous motion was the instability observed at the breakdown between stable and unstable flow. For Reynolds numbers in excess of 2,500, a spatially periodic disturbance was observed. Measurements of the swirl decay rate are presented.

23. Vonnegut, B., 1954, A Vortex Whistle, Journal of the Acoustical Society of America, Vol. 26, No. 1, pp 18-20

Tests were conducted with both air and water. In both cases, an audible sound was obtained as the spiraling flow left the cylindrical tube. From the experimental results, the following equation was derived to predict the frequency of the outlet sound:

$$F = \frac{V}{\alpha \pi D} \left[\frac{P_1 - P_2}{P_1} \right]^{1/2}$$

where F = frequency, in hz
α = a constant less than 1 which accounts for frictional losses in the cylinder
v = velocity of sound in ft/sec
D = diameter of the tube, in ft
P_1 = inlet pressure, in psi
P_2 = exit pressure, in psi

Results indicate that the frequency varies inversely as the length of the cylinder. In addition, the sound intensity dropped significantly with a conically diverging tube.

24. Murakami, M., 1961, Vibration of Water-Turbine Draft Tubes, Transactions ASME, Vol. 83, No. 1, pp 36-42

Experiments were performed on straight, conically diverging, conically converging, and elbow-type draft tubes. The inlet swirl was imparted by a set of stationary guide vanes placed at the turbine location. A theory is presented which essentially duplicates the classical development describing the motion of a line vortex within an irrotional flow field. A method is presented to estimate the size of the vortex core at the top of the draft tube. The deviations between the idealized mathematical description of flow and the true flow are reconciled through empirically determined values. The author concludes that through the use of his equations one can compute the frequency and force of the draft tube surges given the draft tube dimensions, the turbine runner dimensions, and the load conditions on the turbine.

25. Harvey, J. K., 1962, Some Observations of the Vortex Breakdown Phenomenon, Journal of Fluid Mechanics, Vol. 14, pp 585-594

Experiments were made with spiraling flow in a cylindrical tube. Tests indicated that a change in the flow state was observed when the ratio of the tangential velocity to the axial velocity was 1.21 at a point within the flow stream. The length to diameter ratio of the tube was 13.71 and the Reynolds number was about 9.7×10^3. The rotation of the fluid was induced through 18 swirl vanes located in a plenum chamber at the pipe entrance.

26. Chanaud, see Reference 8

Experiments were performed with both air and water in cylindrical and flared tubes. The rotation was imparted through a single nozzle which discharged tangentially into a large cylinder that was connected to a smaller diameter test section. The range of Reynolds numbers tested was 5×10^3 to 1.7×10^4 with water and 7×10^3 to 8.6×10^4 with air. Length to diameter ratios of 1.35, 2.70, 5.40, 10.8, and 21.6 were investigated. Investigations of the sound field in a plane passing through the axis of the tube reveal a dipole-type pressure level distribution. The pressure levels of signals measured at diametrically opposite locations near the tube exist were 180^o out of phase.

27. Hoffman, see Reference 18

Tests were made with air in which the vortex was generated by a wing which spanned a wind tunnel vertically. The lower half of the wing was mounted at an angle of incidence equal and

opposite to that of the upper half. It was found that for a turbulent line vortex rotating in the absence of constraining walls that the circulation of the vortex is proportional to the logarithm of the radius.

28. Gore, see Reference 9

Swirl was generated by passing air through a rotating perforated plate which was mounted perpendicular to the axis of the supply pipe. A critical value of the swirl ratio WR/V was noted for which the flow oscillated between forward flow and backflow. The critical swirl ratio was found to be independent of Reynolds numbers for $20<Re<60{,}000$ but that it depended on the geometry of the apparatus. With the plate flush with the end of the tube, the critical swirl ratio was 1.36. With the plate recessed 1 foot into a 0.4-foot-diameter tube the critical swirl ratio was 1.15.

29. White, A., 1964, Flow of a Fluid in an Axially Rotating Pipe, The Journal of Mechanical Engineering Science, the Institution of Mechanical Engineers, England, Vol. 6, No. 1, pp 47-54

The investigation studied the effect of rotation on turbulent and laminar flows by observing the pressure loss in a pipe. The pipe was 3/8-inch-diameter bore. Swirl was imparted through three different lengths of rotating pipe which were 69, 109, and 232 pipe diameters long. The range of Reynolds numbers varied between 1,000 and 30,000. The results indicate that the pressure drop decreases with rotation of the fluid when the flow is laminar. For Reynolds numbers greater than 8,000, the reduction in the friction factor was found to be primarily a function of a modified Rossby number (WD/V).

30. Chanaud, R. C., 1965, Observations of Oscillatory Motion in Certain Swirling Flows, Journal of Fluid Mechanics, Vol. 21, Part 1, pp 111-127

Experiments were conducted with both air and water with a cylindrical tube 0.5 inch in diameter and lengths which gave an L/D range of 1.35 to 21.6. In addition, tubes with conical expansions and contractions were investigated. The range of Reynolds numbers was from 130 to 7,000. Swirl was produced with a single tangential inlet, four tangential inlets, a set of stationary swirl blades, and a rotating section 30 pipe diameters long. The author notes that the terms in the equations of motion are all of such magnitude that it appears no important simplifications can be made to solve the problem analytically.

31. Kreith, see Reference 9

Swirl was generated with one of two twisted tapes having dimensionless pitch ratios of 9 and 15. The test section was constructed from 1-inch inside-diameter plastic pipe 100 inches long. Data were obtained in the range of axial Reynolds numbers from 18,000 to 61,000. The swirl decay rate as determined experimentally agrees rather well with that predicted theoretically.

32. Turner, see Reference 15

The experiments were performed in a 15- and a 22-cm-diameter cylinder. The water depth was 30 cm. Swirl was generated by rotating the cylinder and a "convection" region was established within the fluid by bubbling air up through the center of the vortex. The end of the air supply tube was placed 10 cm below the surface. This was provided with a hole to allow the air to escape. With the rigid lid, large oscillations in the vertical velocity were noted and the "waves passed up the center much as they would along a loose helical spring stretched from top to bottom of the tank."

33. Granger, see Reference 16

The experiments were conducted in a tank 4 feet high and 23 inches in diameter. Swirl was induced through a series of tangential inlets distributed over the entire surface of the cylindrical tank. The flow was recirculated and left the tank through a hole in the bottom surface of the tank. A free water surface condition existed at the top of the tank. Tests were made at circulation rates ($\Gamma = 2\pi r^2 W$) between 5.5 $in.^2/sec$ and 17 $in.^2/sec$. Large amplitude precessional oscillations were observed at the lower rate and air entered the vortex core at the upper rate. Dimensionless curves are presented which give the variation of vorticity and axial velocity along the vortex axis, the radial variation of vorticity and axial velocity, and the axial variations of the core radius.

34. So, K. S., 1967, Vortex Phenomena in a Conical Diffuser, American Institute of Aeronautics and Astronautics Journal, Vol. 5, No. 6, June, pp 1072-1078

The study resulted in defining five flow regimes representing three types of vortex flow and two types of transitional phenomena. The vortex flow types were (1) laminar, one cell; (2) turbulent, one cell; and (3) turbulent, two cell. For one-cell flow, the fluid spirals inward toward the axis of rotation at points near a solid boundary which is perpendicular to the axis. At points far from the boundary, the flow is away from the boundary outward along the axis. With two-cell flow, the fluid moves toward the boundary at small distances from the axis and away from the boundary at large distances from the axis. The two transitional flow types are: (1) a laminar vortex breakdown phenomena and (2) the occurrence of a two-celled vortex within the diffuser and a one-celled vortex downstream. The experiments were made with air in a 6^{o} diffuser having a throat diameter of 3.5 inches and a length of about 24 inches.

IV. Model and Prototype Tests with Draft Tubes and Turbines

35. Allen, C. M. and Winter, I. A., 1924, Comparative Tests on Experimental Draft-tubes, Trans ASCE, Vol. 87, pp 893-970

Model tests were conducted with a variety of draft tube shapes. Surging was observed to be the least severe with the most efficient draft tube. No quantitative results of surging amplitude or frequency were given.

36. Gibson, A. H. and Labrow, S., 1926, The Efficiency of Regain in Straight and Bent Draught-Tubes, the Institution of Civil Engineers, Selected Engineering Papers, No. 34

A theory is presented which indicated that the efficiency with curved draft tubes may be less than with straight draft tubes when swirl is present.

37. Heim, R., 1929, An Investigation of the Thoma Counterflow Brake, Mitteilungen des Hydraulischen Institut der Technischen Hochschule Munchen, Heft 3. Translated in 1935 by the American Society of Mechanical Engineers and entitled Transactions of the Munich Hydraulic Institute, Bulletin 3, pp 13-28

The brake consisted of a spiral vortex chamber connected to a long pipe or "draft tube." The resistance to flow through the chamber was greatest when flow entered the chamber through the long pipe. With flow leaving through the long pipe, a spiral vortex was observed for certain flow rates. This vortex was not eliminated when the pipe was arranged so that it discharged vertically upwards. Periodic oscillations were also observed for certain pressure ranges.

38. Hornsby, G. J., 1935, Hydraulic Model Studies for the Design of Draft Tubes for the Wheeler Dam, TVA, U.S. Bureau of Reclamation, Hydraulic Laboratory Report No. Hyd-35, Denver, Colorado

Swirl was induced in a model draft tube by 20 vanes set at angles of 0^{o}, 15^{o}, 30^{o}, and 45^{o} to the radial. An attempt was made to prevent air from being admitted to the draft tube. Ten draft tube configurations were tested (including alterations). All configurations had either one or two dividing piers. The performance of the draft tubes was evaluated on the basis of discharge coefficients. The results included pressure measurements along the top of the elbow and each draft tube conduit or barrel, as well as pressure measurements along the bottom of the elbow. Water profiles in the tailrace were also included. A poor velocity distribution at the exit of the draft tube was noted for large angles of swirl. Under some conditions all of the flow was concerned in one barrel.

39. Mockmore, C. A., 1938, Flow Characteristics in Elbow Draft-tubes, Trans ASCE, Vol. 103, pp 402-464, 39 Item bibliography

Swirl at the draft tube inlet caused pulsations with all models tested. However, one particular bend had the most severe pulsations when the angle of whirl at the entrance was about 45^{o}. The frequency was about 4.0 hz. A region of backflow was noted in the draft tube cone, but in none of the experiments did the backflow region extend halfway around the bend. The whirl was induced by a series of vanes and the flow made visible by the admission of air.

40. Rheingans, W. J., 1940, Power Swings in Hydroelectric Power Plants, Trans ASME, Vol. 62, pp 171-184

A classic in the field of draft tube surging. The paper deals with the characteristics of the surges, their relation to power swings, the elimination of surges in the field, and design considerations which will prevent draft tube surges from

producing excessive power swings. Some of the important facts determined by the author are as follows:

a. Power swings always occur over a narrow range of gate openings.

b. The frequency of the draft tube surge is given by

$$f = \frac{w}{216}$$

where w = rotational speed of the turbine in rpm
f = frequency of the draft tube surge or power swing in hertz.

c. In some cases, the addition of fins to the draft tube walls or the admission of air on the axis of the draft tube has reduced surging. However, these methods frequently result in reduced efficiencies.

41. Wigle, D. A., et al, 1946, Hydraulic Model Studies for Turbines at Grand Coulee Powerplant, U.S. Bureau of Reclamation, Hydraulic Laboratory Report No. Hyd-198, Denver, Colorado

Tests were made with a model turbine runner and with three draft tube designs. The draft tube studies included measurement of flow distribution at the draft tube exit in the 6 and 1/2-inch-diameter draft tube throat with the optimum gate opening; observations of draft tube surging under various operating conditions; and the effect of splitter vanes in the draft tube throat and on the runner cone. The velocity tranverses in the throat of the draft tube indicated zero velocity on the axis. In addition, velocity concentrations were found in the right and left draft tube barrels at the optimum gate opening. The draft tube surging phenomenon was recorded on movie film. No quantitative measurements were indicated. Five equally spaced radial fins 2 inches long were placed in the draft tube throat. These were not effective in straightening the vortex filaments. Fins placed on the runner fairwater cone were not effective in straightening the vortex filaments and they also reduced the efficiency and peak horsepower. A set of three equally spaced radial vanes in the draft tube throat which had a hub connecting them to the fairwater was effective in straightening the vortex filaments. The most effective orientation of the fins to reduce surging was one in which one fin pointed downstream in the direction of flow from the draft tube. These splitters were about 1 and 1/2 to 2 inches long.

42. Yamazaki, T. and Tajiri, S., 1954, Experimental Research on Cavitation of Francis Turbine and Flow Conditions below the Runner, Hitachi Review, Vol. 5, pp 17-26

Measurements of whirl velocity, axial velocity, efficiency, and cavitation potential of two model Francis runners were performed. The velocity measurements, which were potentially the most valuable part of the paper, are either in error or the whirl velocity was not accurately defined. The authors indicate a finite value of the whirl velocity on the axis of symmetry, when in fact it must be zero at that location.

43. Kito, F., 1959, The Vibration of Penstocks, Water Power, Vol. 11, pp 379-385, 392

A description of resonance in penstocks in which the vibrations are due to deformations of the penstock out of a circular shape. A method for computing the response of a penstock is presented. Prototype tests illustrate the method when the cause of the vibrations is surging in the draft tube. Methods to eliminate this type of resonance through stiffener rings are indicated.

44. Deriaz, P., 1960, A contribution to the Understanding of Flow in Draft Tubes of Francis Turbines, International Association for Hydraulic Research, Hydraulic Machinery and Equipment Symposium, Nice, France

The author classifies and explains the types of flow observed in draft tubes under various operating conditions. Pulsations of the flowing water were observed even when no water vapor core was present. If the ratio of pressure pulses per minute to revolutions per minute is in the range 3 to 6, the presence of a single rope vortex can be assumed. Specific speed apparently does not have an important influence on this ratio. The author concludes that the only way to truly remedy draft tube instabilities is by using variable pitch blades.

45. Isaev, I. M., 1961, Nluanie sposoba vpuska vozdukha na pulsatziiu davleniia b otsasivaiushchei trube modeli osevoi gidroturbing (Influence of a Method of Air Admission on

Pressure Surges in Draft Tube Models of Axial Hydro-Turbines), Gidroma shino stroenie Trudy LPI, No. 215, Moscow and Leningrad, pp 58-68, USBR Working Translation No. 756

This paper describes hydraulic model tests of the effects of air admission on pressure surges in axial hydraulic turbines. The reduction or growth in surge amplitude and the change in unit efficiency were investigated for several locations of air admission and varying quantities of air. The particular study described was for a Kaplan turbine. It was concluded that the most effective method was introduction of air through the flow deflecting part of the cone. Surge amplitudes were reduced by up to 45 percent and efficiency of the unit increased 0.5 to 1.0 percent. (Author's summary.)

46. Kovalev, N. N., 1961, Gidroturbiny. Konstruktsii i voprosy proektirovaniya (Hydroturbines, Design and Construction), Mashgiz Gosudarstvennoe Nauchno-Teknischeskoe Izdatel stvo Mashinostroitel'noi Literatury, Moskva-Leningrad, Translated from Russian and published for U.S. Department of the Interior by the Israel Program for Scientific Translations

An excellent summary of all facets of turbine design and construction. Indicates that extensions to runner hub decrease pressure fluctuations and increase efficiency. However, the danger of damaging the runner by hydraulic forces increases as the hub is made longer.

47. Kliuikov, N. T., 1963, Nekotoyre resultaty isnytanii modelei radial' no-osevykh gidroturbin (Some results of model tests on Francis Hydraulic Turbines), Energomashinostroenie, No. 4, pp 35-37

Surging was observed in four model turbines for operating speeds outside of the range 1.06 Nopt to 0.78 Nopt, where Nopt is the speed at maximum efficiency. The author indicates that the water entering the draft tube can obtain a rotation motion due to unequal flow distributions in the spiral case.

48. Struna, A. and Solc, L., 1963, L'Introduction de l'Air dans le Diffuseur (Admission of Air into the Draft Tube), IAHR 10th Congress, London, Vol. 4, pp 179-185, USBR Translation No. 736

The paper describes flow conditions in the runner and the formation of a vortex core at part loads. Methods, both of minimizing the effects of part load pulsations and of eliminating them, are given. The authors suggest a method of air admission which involves separate systems for admitting air to the draft tube center and to the periphery. An empirical formula is given which has been proved by experience. Further suggestions are given based on operating experience at hydroelectric power stations.

49. Ruud, F. O., 1964, Hydraulic Turbine Setting Criteria, ASME Paper No. 64-WA/FE-10

Presents a number of case histories taken from Bureau of Reclamation experience where cavitation damage and surging have occurred.

50. Dziallas, R. R., 1964, Francisturbinen bei Teil-und Uberlast (Francis Turbines with Partial- and Over Loads), VDI Berichte, No. 75, pp 53-64

A report of model tests in which the velocity distribution efficiency curves and pressure fluctuations are given. The figures present conditions which could be expected to occur in a typical unit. Various schemes to dampen the oscillations caused by the vortex are presented and their disadvantages discussed.

51. Anon., 1964, Wheeler Project Vibration Studies, Units 9-11, Tennessee Valley Authority, Report No. 3-494, Norris, Tennessee

A report of prototype vibration and pressure measurements on a fixed blade, axial flow turbine generator unit. Initial measurements on the unmodified unit revealed shaft vibrations whose energy was concentrated in the 9- to 10-cycle per revolution range. This corresponded approximately to the calculated natural frequency of the rotating mass. The cause of these vibrations was apparently a 0.4-cycle per revolution excitation by the draft tube vortex. The runner was modified by adding five guide vanes to the inner head cover and by slightly altering the shape of the leading edges of the blades. These modifications introduced a 4-cycle per revolution pressure variation ahead of the runner with only a minor change in the draft tube vortex motion.

52. Danilov, A. E., 1965, Pul'satsii davleniia v protochnoi chasti bloka agragatov Bratskoi GES

npinonizhennykh (puskovykh) naporakh i sviazannye cnimi nestatsionapnye iavleniia (Surges in the Water Passage of the Unit Blocks of Bratsk Powerplant at Low Heads and the Transient Phenomena Connected with Them), Tr. Koordinats., Soveschanii po gidrotekhn, No. 22, pp 201-209

A report of surging in the Bratsk turbines when operated at a head of 55 to 57 m. The design head is 96 m. The surging was practically eliminated by the addition of air through the turbine shaft. However, with air the efficiency of the units was lowered around 1.5 percent.

53. Hosoi, Y., 1965, Experimental Investigations of Pressure Surge in Draft Tubes of Francis Water Turbines, Hitachi Review, Vol. 14, No. 12

Experimental investigations were made with model turbines and the results analyzed with a simplified mathematical model of the flow conditions. Under these conditions the draft tube surge frequency was shown to be a function of the discharge, speed, and unit head. The surge amplitude was roughly proportional to the product of the angular velocity and the discharge with a constant head. Through manipulation of the simplified mathematical model, the author shows that the surge frequency at which the maximum surge amplitude is present can be given by

$$F = \frac{1}{2}(r_a/R)^2 \frac{N_1}{60}$$

or

$$f \approx \left(\frac{1}{3} \text{ to } \frac{1}{4}\right) \frac{N_1}{60}$$

for typical installations. This agrees with the empirically determined equation of Rheingans.

54. Shramkov, K. A., 1965, Periodicheskaia pul'satsiia davleniia v radial' no-osevykh gidroturbinakh (Periodic Pressure Surges in Francis Hydraulic Turbines), Gidrotekhnicheskoe Stroitel' stvo, No. 7, pp 34-37, U.S. Bureau of Reclamation Translation No. 629, Denver, Colorado

The author identifies two types of pressure surges, one in the spiral case and one in the draft tube. The spiral case surge is that one which has a frequency nearly the same as the rotational speed of the unit. This surge is associated with flow between the head cover and the runner. The second type of surge is caused by rotational flow in the draft tube. For loads between 40 to 85 percent, the surge in the draft tube is transmitted from the pier to the spiral case and penstock. The frequency was found to be a function of rotational speed of the unit (Rheingans formula) and independent of head and tailrace elevation. The draft tube pressure variations were 180° out of phase with the penstock fluctuations.

55. Giraud, H., 1966, Etude detaillee de la comparaison entre essais industriels et modele daus quelques cas bien definis (Detailed Study of Prototype and Model Test Comparisons for a Few Specific Cases), La Houille Blanche, No. 3, pp 299-311

Close agreement was found between model and prototype observations of the size of the vortex underneath the runners. The size of vortex was determined with a probe in the prototype and photographically in the model. The model predicted the prototype output to within plus and minus 1 percent of the maximum output. The author shows the usefulness of models in cavitation studies.

56. Kolychev, V. A. and Lasenko, V. E., 1966, Issledovanie potoka v radial' no-osevoi gidroturbine (Investigation of Flow in Francis Hydraulic Turbines), Izvestiya Vysshikh Vchebnykh Zavedenii (Moskeva) Energetika, No. 2, pp 89-96

The position of the wicket gates relative to the draft tube throat was found to have a significant effect on the velocity distribution in the draft tube. The nonuniformity of the distribution of both the axial and the circumferential components increases as the ratio Do/Di is changed from 1.8 to 1.16. Do is the distance from the centerline of the unit to the axis of the guide vanes and Di is the smallest radius to the inside of the lower wearing ring of the runner.

57. Vuskovic', I. and Velensek, B., 1966, Runner Outlet Vortex Core and Its Influence on

Pulsations in Francis and Propeller Turbine Draft Tube, Symposium on Vibrations in Hydraulic Pumps and Turbines, Institution of Mechanical Engineers, Manchester, England

The authors identify two states of flow in the vortex core. If the pressure within the core is higher than the vapor pressure of water, the core contains only water and is called "hard." Conversely, a "soft" core contains water vapor and exists when the core pressure is less than the vapor pressure of water. The most intense pressure pulsations occur with a hard core. The model tests allege to completely confirm the tests of Dziallas. Ribs mounted in the conical diffuser section of the draft tube and guide vanes below the runner were both found to reduce the efficiency of the unit. A coaxial cylindrical diffuser was found to reduce the pressure surges without an adverse effect on the efficiency. In addition, a significant increase in the frequency of the surges was noted. The diffuser diameter was one-half the draft tube throat diameter.

58. Falvey, H., 1967, Hydraulic Model Studies of the Fontenelle Powerplant Draft Tube and Tailrace, USBR Report No. Hyd-571, Denver, Colorado

Hydraulic model studies of the draft tube at Fontenelle Powerplant show that erosive flow concentrations in the tailrace can be reduced through the use of either a tri-vane flow splitter in the draft tube throat or baffle walls in the draft tube flow passages when water is passed through the facility with the turbine runner removed. The effect of flow splitter length, orientation, and vertical position in reducing flow concentrations is indicated. Baffle dimensions and distances above draft tube invert, as well as forces on the baffles are given.

59. Jansen, W., 1967, Flow Analysis in Francis Water Turbines, Trans ASME, Engr for Power, Vol. 89, Ser A, No. 3

A method is given to compute the velocity distribution in the flow passage between turbine blades through the use of analytical methods. By using certain simplifying assumptions, the velocity distribution on the pressure side and suction side of the blades is obtained. The method includes three-dimensional effects and also allows computation at off-design performance of the runner.

60. Konig, H. B. and Whippen, W. G., 1967, Vibration Problems at Conowingo, Water Power, July, pp 259-260

This report is a description of a severe vibration problem in a turbine unit. The vibrations cracked welds in the draft tube liner and caused extremely noisy operation. The pulsations were eliminated for all gate openings less than best gate (72 percent) by admitting air to the inlet side of the runner blade. Above 73 percent opening another kind of roughness was present which could not be alleviated by air admission to the inlet side of the blades. The specific speed of this unit was higher than that of any other fixed blade turbine installed by the bidder.

61. Shramkov, K. A., 1967, Gidravlicheskii rezonaus v vodovodakh GES (Hydraulic Resonance in the Conduits of Hydroelectric Powerplants), Gidrotekhnicheskoe Stroitel'stvo, No. 2, pp 12-16, U.S. Bureau of Reclamation Translation No. 689, Denver, Colorado

A discussion of investigations made in field units. The frequencies observed in the field were in the range predicted by resonance computations of the penstock based on a simplified theory. The amplitude of the pressure pulsations was found to increase as the submergence of the unit increased.

62. Barkov, N. K., 1968, Vpusk vozdukha i aeratsiia potoka v gidroturbinakh (Air Admission and Flow Aeration in Hydroturbines), Electricheskie Stantsii No. 8, pp 26-29, USBR Working Translation No. 635

Various methods of atmospheric and compressed air admission in hydraulic turbines are briefly described. Presently, atmospheric air is used successfully in hydraulic turbines for (1) filling in the breaks in flow continuity, (2) preventing erratic conditions and dangerous vibration during periods of abnormal flow whirling in the draft tube, and (3) stabilizing flow for partial loading and off-design head operation. Compressed air injection is accomplished by several techniques and practical devices. Compressed air is used to reduce erosive wear in hydraulic turbines due to cavitation. Research shows that air in flow cavities significantly lowers the rate of cavitation damage. It also appears to be highly effective in controlling pressure surging beyond the turbine runner. Further study of air injection is required

to improve the reliability and operation of contemporary hydromachines.

63. Lecher, W. and Baumann, K., 1968, Francis Turbines at Part-Load with High Back Pressure, Paper B4, IAHR Symposium, Lausanne, Switzerland

All Francis turbines show at part-load operation a rotating instability. Thereby, large pressure pulsations in the tailrace system can arise especially with high back pressure and a long tailrace tunnel without surge tank. This phenomenon was observed to a pronounced extent on the Francis turbines of a large pumped storage plant. The influence of different parameters, runner cap forms and of air supply at different places and in different quantities was investigated. With model tests, the conditions of the full-size plant were well reproduced. The investigation of many alternatives led to a solution by which, besides the great reduction of the pulsations, a considerable efficiency increase was obtained. These results were also proved by measurements taken on the prototype. (Author's summary.)

64. Ulith, P., 1968, A Contribution to Influencing the Part-Load Behavior of Francis Turbines by Aeration and σ-Value, Paper No. B1, IAHR Symposium, Lausanne, Switzerland

The amplitude of the pressure fluctuation measured at the draft tube wall is used as a characteristic mangitude to assess turbine draft tube flow. This magnitude depends on the variation of the pressure distribution in the draft tube cross section and, as a result, on the discharge, the σ-value and the airflow. The method of aeration above the vaneless space between guide wheel [wicket gate, sic] and runner is described. The test results obtained on a n_s = 308 [metric, sic] model turbine are indicated. (Author's summary.)

65. Cassidy, J. J., 1969, Experimental Study and Analysis of Draft-Tube Surging, Report No. REC-OCE-69-5, U.S. Bureau of Reclamation, Denver, Colorado

Draft tube surge experiments were conducted with models of draft tubes, using air as the fluid. The occurrence, frequency, and amplitude of surges were correlated with flow and draft tube geometry variables. Studies show that surges arise when angular momentum reaches a critical value relative to linear momentum. Surge frequency and peak-to-peak pressures are independent of viscous effects for Reynolds numbers above 80,000 and are correlated with a dimensionless momentum parameter for a particular draft tube shape. A criterion is given for predicting the surging threshold. Results of the study are applied to analysis of draft tube surging in the Fontenelle and the model of the Hoover replacement runners.

66. Falvey, H. T. and Cassidy, J. J., 1970, Frequency and Amplitude of Pressure Surges Generated by Swirling Flow, IAHR Symposium, Stockholm, Sweden, Transactions, Part 1, Paper E1

Reports on the investigation of swirling flow through straight tubes, conical diffusors, and elbow draft tubes. Frequencies and amplitudes of pressure surges produced by the swirling flow were measured and found to be essentially independent of viscous effects for Reynolds numbers larger than 1×10^5. Dimensionless frequency and pressure parameters as well as the onset of surging were correlated with the parameter $\Omega D/\rho Q^2$ where Ω and Q are, respectively, the fluxes of angular momentum and volume through the tube, D is the tube diameter and ρ is the fluid density. Relative length and shape of the tube were also found to be important.

The results of the study were used to analyze a particular draft tube for potential surging. Using performance data obtained from the model of the turbine and draft tube, a region of surge-free operation was outlined on the efficiency hill for the unit. Comparison was made between measured power swings and the predicted pressure fluctuations in the draft tube.

67. Mollenkopf, G. and Raabe, J., 1970, Measurements of Velocity and Pressure in the Draft Tube of a Francis Turbine, IAHR Symposium, Stockholm, Sweden, Transactions, Part 1, Paper B3

Measurements were made in a draft tube with a hot film probe which defined the instantaneous velocity vector. A Francis model turbine was used whose metric specific speed was 295 rpm. The measurements were made in the presence of a strong spiral vortex at two part-load conditions. The results also indicated that surge frequency

and amplitude could be predicted from scaling laws for a model head range of 2 to 9 meters.

68. Zolotov, L. A., Klabukov, V. M., and Ivanova, G. A., 1970, Flow Dynamic Characteristics Downstream of Hydraulic Turbine Runner and Their Influence on Conditions of Turbine Units Regulation, IAHR Symposium, Stockholm, Sweden, Transaction, Part 1, Paper B2

Discharge and pressure fluctuations in the draft tube were observed. At partial loads the discharge fluctuations reach plus and minus 10 percent of the rated discharge capacity. Whereas, at optimum capacity, the fluctuations are only plus and minus 1 percent. The influence of the discharge fluctuations on pressure fluctuations in the penstock were studied by water-hammer equations. The shape of the pressure wave in the penstock was found to be strongly dependent upon the time at which the draft tube disturbance occurred in the wicket gate closing cycle.

7-1750 (3-71)
Bureau of Reclamation

CONVERSION FACTORS—BRITISH TO METRIC UNITS OF MEASUREMENT

The following conversion factors adopted by the Bureau of Reclamation are those published by the American Society for Testing and Materials (ASTM Metric Practice Guide, E 380-68) except that additional factors (*) commonly used in the Bureau have been added. Further discussion of definitions of quantities and units is given in the ASTM Metric Practice Guide.

The metric units and conversion factors adopted by the ASTM are based on the "International System of Units" (designated SI for Systeme International d'Unites), fixed by the International Committee for Weights and Measures; this system is also known as the Giorgi or MKSA (meter-kilogram (mass)-second-ampere) system. This system has been adopted by the International Organization for Standardization in ISO Recommendation R-31.

The metric technical unit of force is the kilogram-force; this is the force which, when applied to a body having a mass of 1 kg, gives it an acceleration of 9.80665 m/sec/sec, the standard acceleration of free fall toward the earth's center for sea level at 45 deg latitude. The metric unit of force in SI units is the newton (N), which is defined as that force which, when applied to a body having a mass of 1 kg, gives it an acceleration of 1 m/sec/sec. These units must be distinguished from the (inconstant) local weight of a body having a mass of 1 kg, that is, the weight of a body is that force with which a body is attracted to the earth and is equal to the mass of a body multiplied by the acceleration due to gravity. However, because it is general practice to use "pound" rather than the technically correct term "pound-force," the term "kilogram" (or derived mass unit) has been used in this guide instead of "kilogram-force" in expressing the conversion factors for forces. The newton unit of force will find increasing use, and is essential in SI units.

Where approximate or nominal English units are used to express a value or range of values, the converted metric units in parentheses are also approximate or nominal. Where precise English units are used, the converted metric units are expressed as equally significant values.

Table I

QUANTITIES AND UNITS OF SPACE

Multiply	By	To obtain
	LENGTH	
Mil	25.4 (exactly)	Micron
Inches	25.4 (exactly)	Millimeters
Inches	2.54 (exactly)*	Centimeters
Feet	30.48 (exactly)	Centimeters
Feet	0.3048 (exactly)*	Meters
Feet	0.0003048 (exactly)*	Kilometers
Yards	0.9144 (exactly)	Meters
Miles (statute)	1,609.344 (exactly)*	Meters
Miles	1.609344 (exactly)	Kilometers
	AREA	
Square inches	6.4516 (exactly)	Square centimeters
Square feet	*929.03	Square centimeters
Square feet	0.092903	Square meters
Square yards	0.836127	Square meters
Acres	*0.40469	Hectares
Acres	*4,046.9	Square meters
Acres	*0.0040469	Square kilometers
Square miles	2.58999	Square kilometers
	VOLUME	
Cubic inches	16.3871	Cubic centimeters
Cubic feet	0.0283168	Cubic meters
Cubic yards	0.764555	Cubic meters
	CAPACITY	
Fluid ounces (U.S.)	29.5737	Cubic centimeters
Fluid ounces (U.S.)	29.5729	Milliliters
Liquid pints (U.S.)	0.473179	Cubic decimeters
Liquid pints (U.S.)	0.473166	Liters
Quarts (U.S.)	*946.358	Cubic centimeters
Quarts (U.S.)	*0.946331	Liters
Gallons (U.S.)	*3,785.43	Cubic centimeters
Gallons (U.S.)	3.78543	Cubic decimeters
Gallons (U.S.)	3.78533	Liters
Gallons (U.S.)	*0.00378543	Cubic meters
Gallons (U.K.)	4.54609	Cubic decimeters
Gallons (U.K.)	4.54596	Liters
Cubic feet	28.3160	Liters
Cubic yards	*764.55	Liters
Acre-feet	*1,233.5	Cubic meters
Acre-feet	*1,233,500	Liters

Table II

QUANTITIES AND UNITS OF MECHANICS

Multiply	By	To obtain
MASS		
Grains (1/7,000 lb)	64.79891 (exactly)	Milligrams
Troy ounces (480 grains)	31.1035	Grams
Ounces (avdp)	28.3495	Grams
Pounds (avdp)	0.45359237 (exactly)	Kilograms
Short tons (2,000 lb)	907.185	Kilograms
Short tons (2,000 lb)	0.907185	Metric tons
Long tons (2,240 lb)	1,016.05	Kilograms
FORCE/AREA		
Pounds per square inch	0.070307	Kilograms per square centimeter
Pounds per square inch	0.689476	Newtons per square centimeter
Pounds per square foot	4.88243	Kilograms per square meter
Pounds per square foot	47.8803	Newtons per square meter
MASS/VOLUME (DENSITY)		
Ounces per cubic inch	1.72999	Grams per cubic centimeter
Pounds per cubic foot	16.0185	Kilograms per cubic meter
Pounds per cubic foot	0.0160185	Grams per cubic centimeter
Tons (long) per cubic yard	1.32894	Grams per cubic centimeter
MASS/CAPACITY		
Ounces per gallon (U.S.)	7.4893	Grams per liter
Ounces per gallon (U.K.)	6.2362	Grams per liter
Pounds per gallon (U.S.)	119.829	Grams per liter
Pounds per gallon (U.K.)	99.779	Grams per liter
BENDING MOMENT OR TORQUE		
Inch-pounds	0.011521	Meter-kilograms
Inch-pounds	1.12985×10^6	Centimeter-dynes
Foot-pounds	0.138255	Meter-kilograms
Foot-pounds	1.35582×10^7	Centimeter-dynes
Foot-pounds per inch	5.4431	Centimeter-kilograms per centimeter
Ounce-inches	72.008	Gram-centimeters
VELOCITY		
Feet per second	30.48 (exactly)	Centimeters per second
Feet per second	0.3048 (exactly)*	Meters per second
Feet per year	$*0.965873 \times 10^{-6}$	Centimeters per second
Miles per hour	1.609344 (exactly)	Kilometers per hour
Miles per hour	0.44704 (exactly)	Meters per second
ACCELERATION*		
Feet per second^2	*0.3048	Meters per second^2
FLOW		
Cubic feet per second (second-feet)	*0.028317	Cubic meters per second
Cubic feet per minute	0.4719	Liters per second
Gallons (U.S.) per minute	0.06309	Liters per second
FORCE*		
Pounds	*0.453592	Kilograms
Pounds	*4.4482	Newtons
Pounds	$*4.4482 \times 10^5$	Dynes

Table II—Continued

Multiply	By	To obtain
WORK AND ENERGY*		
British thermal units (Btu)	*0.252	Kilogram calories
British thermal units (Btu)	1,055.06	Joules
Btu per pound	2.326 (exactly)	Joules per gram
Foot-pounds	*1.35582	Joules
POWER		
Horsepower	745.700	Watts
Btu per hour	0.293071	Watts
Foot-pounds per second	1.35582	Watts
HEAT TRANSFER		
Btu in./hr ft^2 degree F (k, thermal conductivity)	1.442	Milliwatts/cm degree C
Btu in./hr ft^2 degree F (k, thermal conductivity)	0.1240	Kg cal/hr m degree C
Btu ft/hr ft^2 degree F	*1.4880	Kg cal m/hr m^2 degree C
Btu/hr ft^2 degree F (C, thermal conductance)	0.568	Milliwatts/cm^2 degree C
Btu/hr ft^2 degree F (C, thermal conductance)	4.882	Kg cal/hr m^2 degree C
Degree F hr ft^2/Btu (R, thermal resistance)	1.761	Degree C cm^2/milliwatt
Btu/lb degree F (c, heat capacity)	4.1868	J/g degree C
Btu/lb degree F	*1.000	Cal/gram degree C
Ft^2/hr (thermal diffusivity)	0.2581	Cm^2/sec
Ft^2/hr (thermal diffusivity)	*0.09290	M^2/hr
WATER VAPOR TRANSMISSION		
Grains/hr ft^2 (water vapor) transmission)	16.7	Grams/24 hr m^2
Perms (permeance)	0.659	Metric perms
Perm-inches (permeability)	1.67	Metric perm-centimeters

Table III

OTHER QUANTITIES AND UNITS

Multiply	By	To obtain
Cubic feet per square foot per day (seepage)	*304.8	Liters per square meter per day
Pound-seconds per square foot (viscosity)	*4.8824	Kilogram second per square meter
Square feet per second (viscosity)	*0.092903	Square meters per second
Fahrenheit degrees (change)*	5/9 exactly	Celsius or Kelvin degrees (change)*
Volts per mil	0.03937	Kilovolts per millimeter
Lumens per square foot (foot-candles)	10.764	Lumens per square meter
Ohm-circular mils per foot	0.001662	Ohm-square millimeters per meter
Millicuries per cubic foot	*35.3147	Millicuries per cubic meter
Milliamps per square foot	*10.7639	Milliamps per square meter
Gallons per square yard	*4.527219	Liters per square meter
Pounds per inch	*0.17858	Kilograms per centimeter

GPO 839-626

ABSTRACT

A literature survey and a review of material related to draft tube surges is presented. The literature survey consists of an annotated bibliography of 68 articles published between 1910 and 1970. The review is restricted to three major areas: experiments with elementary models, experiments with model and prototype turbines, and field expedients to reduce surging. Velocity distributions and surge frequencies are given special attention in the first two areas. Present knowledge is sufficient for predicting the order of magnitude of draft tube surge frequencies and relative surge amplitudes. Additional studies are needed to refine prediction methods and to extend their scope to include pumps and pump-turbines. Model testing at full prototype heads is apparently not required to investigate draft tube surging. Has 68 references.

ABSTRACT

A literature survey and a review of material related to draft tube surges is presented. The literature survey consists of an annotated bibliography of 68 articles published between 1910 and 1970. The review is restricted to three major areas: experiments with elementary models, experiments with model and prototype turbines, and field expedients to reduce surging. Velocity distributions and surge frequencies are given special attention in the first two areas. Present knowledge is sufficient for predicting the order of magnitude of draft tube surge frequencies and relative surge amplitudes. Additional studies are needed to refine prediction methods and to extend their scope to include pumps and pump-turbines. Model testing at full prototype heads is apparently not required to investigate draft tube surging. Has 68 references.

ABSTRACT

A literature survey and a review of material related to draft tube surges is presented. The literature survey consists of an annotated bibliography of 68 articles published between 1910 and 1970. The review is restricted to three major areas: experiments with elementary models, experiments with model and prototype turbines, and field expedients to reduce surging. Velocity distributions and surge frequencies are given special attention in the first two areas. Present knowledge is sufficient for predicting the order of magnitude of draft tube surge frequencies and relative surge amplitudes. Additional studies are needed to refine prediction methods and to extend their scope to include pumps and pump-turbines. Model testing at full prototype heads is apparently not required to investigate draft tube surging. Has 68 references.

ABSTRACT

A literature survey and a review of material related to draft tube surges is presented. The literature survey consists of an annotated bibliography of 68 articles published between 1910 and 1970. The review is restricted to three major areas: experiments with elementary models, experiments with model and prototype turbines, and field expedients to reduce surging. Velocity distributions and surge frequencies are given special attention in the first two areas. Present knowledge is sufficient for predicting the order of magnitude of draft tube surge frequencies and relative surge amplitudes. Additional studies are needed to refine prediction methods and to extend their scope to include pumps and pump-turbines. Model testing at full prototype heads is apparently not required to investigate draft tube surging. Has 68 references.

REC-ERC-71-42
Falvey, H T
DRAFT TUBE SURGES–A REVIEW OF PRESENT KNOWLEDGE AND AN ANNOTATED BIBLIOGRAPHY
Bur Reclam Rep REC-ERC-71-42, Div Gen Res, Dec 1971. Bureau of Reclamation, Denver, 25 p, 7 fig, 68 ref

DESCRIPTORS–/ *draft tubes/ *turbines/ *surges/ *hydroelectric powerplants/ hydraulic machinery/ fluid mechanics/ unsteady flow/ laboratory tests/ model tests/ fluid flow/ non-uniform flow/ vortices/ bibliographies/ annotations/ velocity distribution/ amplitude/ air admission/ frequency
IDENTIFIERS–/ hydrodynamic stability

REC-ERC-71-42
Falvey, H T
DRAFT TUBE SURGES–A REVIEW OF PRESENT KNOWLEDGE AND AN ANNOTATED BIBLIOGRAPHY
Bur Reclam Rep REC-ERC-71-42, Div Gen Res, Dec 1971. Bureau of Reclamation, Denver, 25 p, 7 fig, 68 ref

DESCRIPTORS–/ *draft tubes/ *turbines/ *surges/ *hydroelectric powerplants/ hydraulic machinery/ fluid mechanics/ unsteady flow/ laboratory tests/ model tests/ fluid flow/ non-uniform flow/ vortices/ bibliographies/ annotations/ velocity distribution/ amplitude/ air admission/ frequency
IDENTIFIERS–/ hydrodynamic stability

REC-ERC-71-42
Falvey, H T
DRAFT TUBE SURGES–A REVIEW OF PRESENT KNOWLEDGE AND AN ANNOTATED BIBLIOGRAPHY
Bur Reclam Rep REC-ERC-71-42, Div Gen Res, Dec 1971. Bureau of Reclamation, Denver, 25 p, 7 fig, 68 ref

DESCRIPTORS–/ *draft tubes/ *turbines/ *surges/ *hydroelectric powerplants/ hydraulic machinery/ fluid mechanics/ unsteady flow/ laboratory tests/ model tests/ fluid flow/ non-uniform flow/ vortices/ bibliographies/ annotations/ velocity distribution/ amplitude/ air admission/ frequency
IDENTIFIERS–/ hydrodynamic stability

REC-ERC-71-42
Falvey, H T
DRAFT TUBE SURGES–A REVIEW OF PRESENT KNOWLEDGE AND AN ANNOTATED BIBLIOGRAPHY
Bur Reclam Rep REC-ERC-71-42, Div Gen Res, Dec 1971. Bureau of Reclamation, Denver, 25 p, 7 fig, 68 ref

DESCRIPTORS–/ *draft tubes/ *turbines/ *surges/ *hydroelectric powerplants/ hydraulic machinery/ fluid mechanics/ unsteady flow/ laboratory tests/ model tests/ fluid flow/ non-uniform flow/ vortices/ bibliographies/ annotations/ velocity distribution/ amplitude/ air admission/ frequency
IDENTIFIERS–/ hydrodynamic stability

REC-ERC-72-24

INFLUENCE OF DRAFT TUBE SHAPE ON SURGING CHARACTERISTICS OF REACTION TURBINES

Uldis J. Palde
Engineering and Research Center
Bureau of Reclamation

July 1972

MS-230 (8-70)
Bureau of Reclamation

TECHNICAL REPORT STANDARD TITLE PAGE

1. REPORT NO.	2. GOVERNMENT ACCESSION NO.	3. RECIPIENT'S CATALOG NO.
REC-ERC-72-24		

4. TITLE AND SUBTITLE	5. REPORT DATE
Influence of Draft Tube Shape on Surging Characteristics of Reaction Turbines	Jul 72
	6. PERFORMING ORGANIZATION CODE
7. AUTHOR(S)	8. PERFORMING ORGANIZATION REPORT NO.
Uldis J. Palde	REC-ERC-72-24
9. PERFORMING ORGANIZATION NAME AND ADDRESS	10. WORK UNIT NO.
Engineering and Research Center Bureau of Reclamation Denver, Colorado 80225	11. CONTRACT OR GRANT NO.
	13. TYPE OF REPORT AND PERIOD COVERED
12. SPONSORING AGENCY NAME AND ADDRESS	
	14. SPONSORING AGENCY CODE

15. SUPPLEMENTARY NOTES

16. ABSTRACT

Laboratory experiments, using a simplified air model, were conducted to obtain the correlation between draft tube shape and the draft tube surge characteristics—the range of occurrence, frequencies, and pressure amplitudes of the surges. Dimensionless parameters were used to compare results. The draft tube shape was found to have significant influence on the surging characteristics. Surge measurements obtained from two hydraulic turbine model studies are also compared using the dimensionless parameters. Hydraulic and air model studies of the same draft tube produced satisfactory correlation. The information presented can be used to predict the surge characteristics of prototype and model turbines, or as an aid in draft tube design where surge reduction or resonance minimization are considered as design criteria. Examples are included to illustrate application of the laboratory results.

17. KEY WORDS AND DOCUMENT ANALYSIS

a. *DESCRIPTORS*-- / *draft tubes/ turbines/ *surges/ *hydroelectric powerplants/ hydraulic machinery/ fluid mechanics/ dimensional analysis/ model tests/ fluid flow/ pressure/ frequency/ *shape/ resonance/ test results/ hydraulic design/ *reaction turbines/ hydraulic turbines/ noise (sound)/ hydraulic models/ vibration/ wicket gates/ hydraulic similitude

b. *IDENTIFIERS*-- / hydraulic pressure tests/ Fontenelle Dam, Wyo/ Grand Coulee Powerplant, Wash/ water pressure tests

c. *COSATI Field/Group* 13G

18. DISTRIBUTION STATEMENT	19. SECURITY CLASS (THIS REPORT)	21. NO. OF PAGES
Available from the National Technical Information Service, Operations Division, Springfield, Virginia 22151.	UNCLASSIFIED	29
	20. SECURITY CLASS (THIS PAGE)	22. PRICE
	UNCLASSIFIED	

REC-ERC-72-24

INFLUENCE OF DRAFT TUBE SHAPE ON SURGING CHARACTERISTICS OF REACTION TURBINES

by
Uldis J. Palde

July 1972

Hydraulics Branch
Division of General Research
Engineering and Research Center
Denver, Colorado

UNITED STATES DEPARTMENT OF THE INTERIOR
Rogers C. B. Morton
Secretary

*

BUREAU OF RECLAMATION
Ellis L. Armstrong
Commissioner

ACKNOWLEDGMENT

The study was conducted under the supervision of Dr. Henry T. Falvey, Head, Hydraulics Research Section, whose advice, encouragement, and patience is greatly appreciated. Appreciation is also expressed to Dr. Jack C. Cassidy (presently Head of the Civil Engineering Department, University of Missouri at Columbia) who patiently introduced the author to the draft tube surge phenomenon and its measurement in the laboratory. The help of Robert H. Kuemmich in resolving instrumentation problems is also appreciated. The entire research project was under the direction of William E. Wagner, Hydraulics Branch Chief, Engineering and Research Center, Denver.

CONTENTS

NOTATION

B	=	height of wicket gates
D_2	=	runner diameter at minimum opening
D_3, D	=	diameter of draft tube throat
f	=	frequency (hz)
g	=	acceleration due to gravity
H	=	net head across turbine
L	=	length of draft tube
N	=	number of wicket gates
n	=	rotational speed (rev/min)
n_{11}	=	unit speed
P	=	power
P_{11}	=	specific power
p'	=	pressure surge amplitude fluctuation from mean
Q	=	discharge
Q_{11}	=	specific discharge
R	=	radial distance to center of flow through wicket gates
S	=	width of opening between wicket gates
T	=	torque
V	=	axial velocity
α	=	radial inclination of flow through wicket gates
ϕ	=	ratio of maximum runner rotational velocity to the spouting velocity
ν	=	kinematic viscosity
π	=	3.1416
ρ	=	fluid density
δ	=	turbine cavitation number
Ω	=	flux of moment of momentum
ω	=	angular velocity (rad/sec)
$\phi_1, \phi_2, \phi_3, \phi_4$	=	functions
R	=	Reynolds number

Subscripts

m	=	model
p	=	prototype

CONCLUSIONS

1. An air model of the type described in this report can successfully be used to determine the surging characteristics of hydraulic turbine draft tubes. The equipment need have no more mechanical components than the minimum required to precisely introduce, control, and measure swirling flow at the draft tube inlet.

2. The shape of the draft tube has a significant influence on the surging characteristics—the range of surging, the frequency band of the surges, and the amplitude of the resulting pressure pulsations.

3. The throat geometry generally has more influence on the surging characteristics than the shape of the remaining downstream portion of the draft tube.

4. The degree of divergence of a draft tube is the most significant geometric feature affecting surging characteristics. Bends and relative length have lesser influence.

5. Surging can be minimized by using an equivalent draft tube expansion angle of about 15° through the whole length of the draft tube, and possibly eliminated entirely with greater angles.

6. The use of straight cylinder sections (any L/D) or constant diameter elbows in or near the draft tube throat will increase the range of surging and generally increase the frequency and amplitude of the surges.

7. The possibility of resonance with known natural frequencies of other features of the hydroelectric plant can be checked with fair accuracy using the results presented, if the turbine performance characteristics and wicket gate geometry are known. Resonance can be avoided by proper choice of geometric components in the draft tube design.

APPLICATIONS

The results presented in this report can be used to predict with fair accuracy the range of occurrence, frequencies, and pressure amplitudes of draft tube surges in prototype or model turbines. The draft tube shape and performance characteristics of the turbine must be known. The results can be used in draft tube design to help minimize the inevitable surging that will occur over some portion of the operating range of the turbine. Examples of dimensionless parameter evaluation are included to encourage the generalized comparison of surge measurement data obtained from prototype and model turbines.

INTRODUCTION

Draft tube surges have created problems in hydroelectric powerplants using reaction turbines for several decades.[1]*

Draft tube surges generally occur over a range of gate positions above or below best efficiency. The most common adverse effects of the surges are noticeable vibration and pounding noise in the powerplant. More serious manifestations, such as periodic variations in power output (power swings), vertical movement of the runner and shaft, and penstock pressure pulsations and vibration have often been attributed to draft tube surges.

For many years, there was considerable speculation and disagreement about the cause of draft tube surges. It is now generally accepted that the draft tube surge is a hydrodynamic instability which occurs in the draft tube as the result of rotation remaining in the fluid as it leaves the turbine runner and enters the draft tube throat. The hydrodynamic instability produces spiralling vortex flow in the draft tube, which has been referred to in the literature as "vortex breakdown."

Bureau of Reclamation powerplants have not been an exception to the draft tube surge problem. As a first step in finding a solution to the problem, a concentrated research effort was directed toward determining the basic nature and cause of draft tube surges. A bibliography of literature pertaining to draft tube surges and swirling flow in tubes was collected. An analysis and experimental investigation was conducted to gain an understanding of draft tube surging and to correlate occurrence, frequency, and amplitude of the surges with flow and geometric variables related to the flow through the turbine and draft tube. The experimental investigation was reported in a USBR report by Cassidy[2] while the review of existing knowledge and an annotated bibliography was compiled in another USBR report by Falvey.[1] Specific aspects of the studies were also presented in two papers by Cassidy and Falvey.[3,4]

Cassidy[2] noted that the dimensionless parameters used to correlate the occurrence, frequency, and amplitude of the surges were also functions of the draft tube shape. The results indicated that a thorough

*Numbers indicate references at end of report.

investigation of this aspect would be of great value in understanding the surge phenomenon, in predicting frequencies, and in applying measures to reduce or eliminate the surges. The experimental work presented in this report is a continuation and expansion of Cassidy's studies. The same experimental equipment and analysis were used. However, all results are from original data obtained subsequent to Cassidy's studies.

This report contains sufficient analysis and description of experimental equipment and procedure to provide an ample background for the analysis and application of experimental results. For a more thorough discussion of the analysis and description of the experimental equipment, the reader should refer to reference,[2] while background information on problems arising from draft tube surges and attempts to solve them can be obtained from reference.[1]

ANALYSIS

Dimensionless parameters were derived by Falvey and Cassidy[4] to help generalize experimental results of surging flow in a draft tube. It was assumed that for a particular draft tube shape, the frequency f and root-mean-square (rms) amplitude

$$\sqrt{\overline{(p')^2}}$$

of the surge are both functions of the density ρ and the viscosity ν of the fluid, the diameter D_3 and length L of the draft tube, the discharge Q, and the flux of the moment of momentum (angular momentum)Ω. Dimensional analysis yielded the following functional relationships:

pressure parameter

$$\frac{D_3^4\sqrt{\overline{(p')^2}}}{\rho Q^2} = \phi_1\left(\frac{\Omega D_3}{\rho Q^2}, \frac{L}{D_3}, R\right)$$

and frequency parameter

$$\frac{fD_3^3}{Q} = \phi_2\left(\frac{\Omega D_3}{\rho Q^2}, \frac{L}{D_3}, R\right)$$

Where R is the Reynolds number $4Q/\pi D_3\nu$. The ratio $\Omega D_3/\rho Q^2$ is referred to as the momentum parameter and is a ratio of angular momentum flux to linear momentum flux. The momentum parameter is, in effect, a useful measure of the amount of swirl in the flow. In applying it to the experimental study, the assumption was made that regardless of the manner in which angular momentum is introduced into the flow, the resulting surging characteristics will be the same for a particular value of $\Omega D_3/\rho Q^2$. The frequency parameter is a form on the Strouhal number fD_3/V (V is the axial velocity), written in terms of discharge.

Based on his initial experimentation with a simplified model using air as the fluid, Cassidy[2] concluded that:

1. For a given draft tube shape there is a critical value of $\Omega D_3/\rho Q^2$ above which surging flow exists.

2. The frequency and pressure parameters can be correlated with the momentum parameter for a given draft tube shape.

3. Frequency and rms pressure values of the surging flow are independent of viscous effects for Reynolds numbers above approximately 80,000 (prototype Reynolds numbers greatly exceed 80,000).

The momentum parameter $\Omega D_3/\rho Q^2$ can be computed for a turbine if the runner diameter, wicket gate geometry, and the performance characteristics are known. If we start with the basic expression for power,

$$P = \omega T \qquad (1)$$

where ω is the angular velocity and T is torque, and substitute

$$T = \Omega_1 - \Omega_2 \qquad (2)$$

where $\Omega_1 - \Omega_2$ is the rate of change of moment of momentum of the flow as it passes through the runner, we obtain

$$\frac{P}{\omega} = \Omega_1 - \Omega_2 \qquad (3)$$

Multiplying Equation (3) by $D_3/\rho Q^2$ and rearranging terms,

$$\frac{\Omega_2 D_3}{\rho Q^2} = \frac{\Omega_1 D_3}{\rho Q^2} - \frac{PD_3}{\rho\omega Q^2} \qquad (4)$$

The left side of Equation (4) is the momentum parameter associated with the flow at the draft tube throat. The first term on the right of the same equation is the momentum parameter of the flow leaving the wicket gates and entering the turbine runner and can be computed by

$$\frac{\Omega_1 D_3}{\rho Q^2} = \frac{D_3 R \sin\alpha}{BNS} \quad (5)$$

Equation (5) shows that $\Omega_1 D_3/\rho Q^2$ is entirely a function of wicket gate geometric variables (defined in Figure 1), and the draft tube throat diameter.

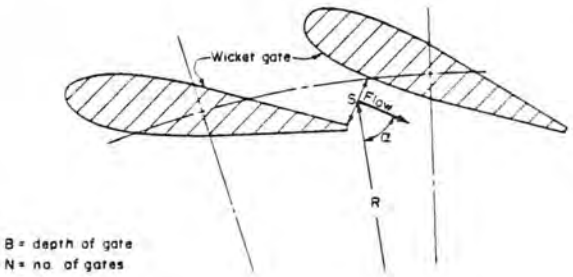

Figure 1. Definition sketch of flow leaving wicket gates and entering turbine runner.

The second term of Equation (4) can be computed from performance characteristics of the turbine, using the equation

$$\frac{PD_3}{\rho\omega Q^2} = \frac{550 \quad P_{11} \quad D_3}{2\sqrt{2g}\,\rho\, Q_{11}^2\, \phi\, D_2} \quad (6)$$

Where ϕ is the ratio of maximum runner rotational velocity to the spouting velocity (the computed velocity obtained from a velocity head equal to the net head), or

$$\phi = \frac{\pi D_3 n}{60\sqrt{2gH}} \quad (7)$$

P_{11} is the specific power, or

$$P_{11} = \frac{P}{D_2^2\, H^{3/2}} \quad (8)$$

and Q_{11} is specific discharge, or

$$Q_{11} = \frac{Q}{D_2^2\, H^{1/2}} \quad (9)$$

Combining Equations (4), (5), and (6), we obtain

$$\frac{\Omega_2 D_3}{\rho Q^2} = \frac{D_3 R \sin\alpha}{BNS} - \frac{550 \quad P_{11} \quad D_3}{2\sqrt{2g}\,\rho\, Q_{11}^2\, \phi\, D_2} \quad (10)$$

which can be evaluated for prototype or model turbines from data (in English units) normally obtained during performance tests.

LABORATORY MODEL

Laboratory experiments were conducted with air as the fluid and a model (Figure 2) utilizing some of the components of a model turbine which had been used in a prior hydraulic model study. The spiral case, stay vanes, and runner were removed. The wicket gates remained and served to produce swirl in the flow as it passed from a symmetrical pressure chamber into the draft tube (Figure 3). Radial inclination of the gates could be set at any angle between 0^o (radial) and 82^o (closed) to introduce varying amount of swirl in the flow.

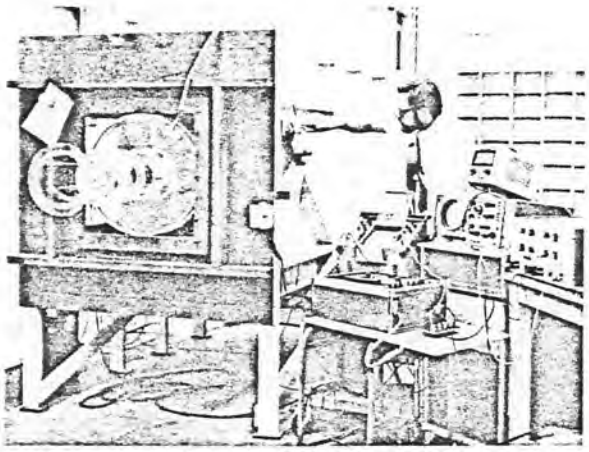

Figure 2. Laboratory air model and instruments. Photo PX-D-67575

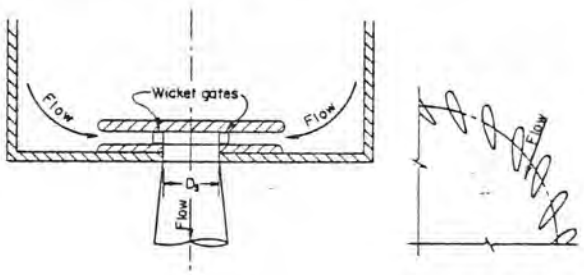

Figure 3. Schematic of laboratory air model.

The momentum parameter of the flow entering the draft tube could be determined in the simplified laboratory model with far less effort than would be required in a complete turbine model. Without the turbine runner, the momentum parameter at the draft tube throat is equal to that existing in the flow leaving the wicket gates. Equation (5) could therefore be used to compute the momentum parameter of the flow entering the draft tube:

$$\frac{\Omega_2 D_3}{\rho Q^2} = \frac{\Omega_1 D_3}{\rho Q^2} = \frac{D_3 R \sin\alpha}{BNS}$$

The computation of the pressure and frequency parameters required the measurement of discharge and the frequency and rms pressure of the draft tube surges. The rate of discharge was controlled at the wicket gate openings and varied along with the gate opening area with changes in the gate setting. The discharge was measured by a differential orifice located in the inlet pipe to the pressure box. Pressure differential across the orifice was measured with a pressure cell and conditioned by and recorded on one channel of a dual channel recorder-amplifier.

The plastic draft tubes being tested had piezometer taps at several locations along the walls. A pressure cell with a short piece of flexible tubing could be attached to the piezometers for dynamic pressure pickup. The signal was conditioned by the second channel of the recorder-amplifier and fed through a band-pass filter to an oscilloscope and rms meter. Frequencies of the periodic pressure pulsations were determined on the retentive screen of the oscilloscope. The instrumentation is shown in Figure 2.

LABORATORY PROCEDURE

The values of R, S, and α, defined in Figure 1, vary with the gate position. These quantities were carefully measured or graphically determined for numerous gate angle settings, and tables for use in computations were prepared from smoothed curves of R, S, and α versus gate angle. The value of the momentum parameter for a particular gate setting could then be readily computed using Equation (5).

For a particular draft tube, the range of gate settings for which surging flow could be detected was first noted, as well as the approximate maximum and minimum frequencies in that range. If the frequency band was not too great, the high- and low-pass circuits on the band-pass filter were set somewhat outside this band. Occasionally the frequencies varied greatly and the band pass was set to include most of the frequencies encountered, and later adjusted as required.

For a particular gate setting, a given draft tube surges at the same frequency throughout the entire tube (with a few notable exceptions). The amplitude, however, varies with location along the tube wall. Data were generally taken at a location where amplitude was maximum, since the frequency was best defined at that location.

For some tubes, data were obtained at several locations to determine the variation of amplitude with respect to location. For one draft tube, data were also obtained at several locations without feeding the signal through the band-pass filter, for comparison of rms pressures with the filtered signal results.

A run consisted of frequency and rms pressure measurements (along with discharge orifice pressure differential) taken at the same piezometer at numerous gate settings in the range of surging. The data, along with amplifier attenuation factors, air density, and descriptive information were recorded on data sheets suitable for ADP card keypunch use. The dimensionless parameters and other flow variables were then determined by computer. During the computer run, frequency and pressure parameter versus momentum parameter curves could be plotted on an online cathode-ray tube (CRT) and photographed on 35mm microfilm for later copying and convenient storage. The CRT plotting routine was designed so that any six frequency or pressure parameter curves, each with a different symbol, could be plotted on the same figure (microfilm frame) by simply specifying the desired run numbers for each figure. The graphs used in Figures 4 through 18 (following Results section) are computer generated.

DRAFT TUBE SHAPES STUDIED

Cassidy[2] determined that the draft tube shape definitely has an effect on the range of surging and on the frequency and rms pressure on the pulsations. His testing was limited to one model draft tube, an irregularly expanding cone, and several cylinders of varying diameter and length. From the results, it was not possible to extrapolate what shapes could eliminate or at least reduce the surging.

A systematic study to correlate the geometric shape components found in typical draft tubes with the surging characteristics was undertaken. A few of the shapes tested were actual models of draft tubes with

nor modifications. The greater majority, however, were simple geometrical shapes or combinations thereof, consisting of straight circular cylinders, truncated diverging cones, and circular cross-section elbows. The diameter, length, and angle of divergence were varied. Tests were repeated on all of the tubes which had already been tested by Cassidy[2] to provide a reliable base of comparison, since measurement instrument calibration discrepancies were discovered later.

Data were eventually obtained for about 75 distinct draft tube shapes (see Figure 1 in the Appendix). Only a fraction are included in the comparison of results which follow. The results that have been included generally reflect how different shapes or minor modifications have significant influence on the surging characteristics; they also show that some significant features, changes, or modifications have very minor, if any, influence. Many of these results were contrary to what might be expected or is presently assumed in draft tube design.

A minor limitation on the shapes that could be tested was imposed by the model itself. The downstream face of the pressure chamber had a thickness of 1.93 inches (4.9 centimeter (cm)) (see Figure 3), in which a rmanent circular opening of 6.13 inches (15.6 cm) in iameter was provided for the outflow. Although the size of this opening could not be increased, it could be decreased. Or the shape could be changed (with the inevitable reduction of inlet diameter) by positioning a machined plastic insert of the required dimensions in the opening. Many of the tubes tested had inlet diameters of approximately 6 inches (15 cm).

The results presented by Cassidy[2] and much of the data obtained initially in this study were taken on 6-inch-diameter draft tubes, attached to the outer face of the pressure box. Consideration was not given to the short circular cylinder as a geometrical component upstream of the shape being tested. Subsequently, it was discovered that the upstream cylindrical section had significant influence on the surging characteristics. Much of the data for this condition was thus obtained unintentionally. But the data proved to be of value, as reflected in some of the included comparisons of results.

RESULTS

The presented results should be considered largely for their qualitative comparisons. The onset of surging was only seldom discernable as a well-defined break in the ow regime, and was therefore usually subject to the investigator's interpretation. Rms pressure values were repeatable from day to day only within about a 10 percent variation. The values were also influenced by the frequency band pass used and somewhat by the presence of the short length of flexible tubing between the piezometer and pressure cell (producing a fairly constant amplification of about 13 percent). Pressure parameter curves should therefore be used primarily to indicate trends and the order of magnitude of the surges.

Frequencies in most cases could be precisely determined and were closely repeatable from day to day for the same draft tube and gate setting. The values of the resulting frequency parameter can therefore be used in a quantitative sense.

The results are presented as plots of the dimensionless parameters in Figures 4 through 18 (starting with page 8). In most cases, the surging characteristics of several shapes are compared in the same figure. Scaled schematic drawings (with only significant dimensions shown) of the shapes being compared are included in each figure. The symbol used for a tube in the parameter plots has been indicated on each draft tube at the location where the surges were measured. The run number has also been indicated adjacent to the symbol. Approximate distances along the tubes can be scaled. The range of surging is defined by the range of the momentum over which data points are plotted.

Figure 4 shows the surging characteristics of three draft tubes. The throats of both variations of the Fontenelle draft tube were modified from the actual prototype geometry. The Grand Coulee pump-turbine draft tube is geometrically similar to the prototype. Its cross section is circular for the entire length.

For all three draft tubes the frequency and pressure parameters initially increase with an increase of the momentum parameter. This was typical of all tubes tested. For some tubes, the pressure parameter continues increasing monotonously, while for others one or more peaks occur.

Most tubes surge over a finite range of momentum parameter, as is the case with the two variations of the Fontenelle draft tube. Others, like the Grand Coulee pump-turbine draft tube, surge continuously up to the point of complete wicket gate closure, where the momentum parameter approaches infinity. In the Grand Coulee pump-turbine draft tube, the maximum amplitudes occur near the end of the elbow, on the right side, where the amplitudes are much higher than at the start of the elbow (compare Runs 188 and 175, Figure 4). Although the pressure parameter generally attains the highest value at large values of momentum parameter (>2), the maximum value of the pressure pulsation amplitude itself usually occurs at a

momentum parameter value near 1, at the first peak of the pressure parameter.

A slight variation of the Fontenelle throat geometry produces significant changes in the surge parameter values but does not change the range of surging. Removal of the piers and progressively sections of the downstream end of the draft tube has little effect on the surge parameters. A short tube including only the first 30° of the elbow has only slightly different characteristics than the entire draft tube (see Figure 5).

Simple sections of truncated 15° cones surge over a smaller range of momentum parameter and display lower frequencies and amplitudes than the draft tubes (see Figure 6). The frequencies measured from the cones were far less well defined than those from any other shape. Different inlet diameters and L/D ratios have only slight effect on the dimensionless surge parameters. Figure 6 also verifies the validity of the dimensional analysis as related to geometric similarity.

Somewhat varying surging characteristics are displayed by 7.5° cones with variation of cone L/D (Figure 7). The longest and shortest tubes display surging ranges and frequency and pressure parameter curves quite similar to those of the Fontenelle draft tube. The surging range of the cone with L/D = 2.32, however, is far greater than the ranges of the other cones. The pressure parameter also increases continuously to higher values than for the other cones. It should be noted that a 7.5° cone with L/D $\approx$ 2.0 is used downstream of the constant-diameter elbow in the Grand Coulee pump-turbine draft tube.

Straight cylindrical tubes display surging characteristics quite different from those of expanding cones (see Figure 8). Short sections (L/D <1) produce high-frequency curves, while longer sections have two distinct frequencies—the higher being exactly double the lower. In a tube having an L/D of 0.96 the lower frequency predominates up to a momentum parameter value of about 2.0, while beyond this point only the higher frequency is apparent (Runs 109 and 110). Several other intermediate lengths between L/D = 0.96 and L/D = 3.58 were tested. The tubes all had surge characteristics similar to the tube with L/D = 3.58. It should be noted that both high- and low-frequency parameter curves of all cylinders show considerably higher values than those of draft tubes with expanding sections.

Adding a bellmouth entrance section to a long, straight cylinder does not alter the surging characteristics up to a momentum parameter value of about 2.0 (see Figure 9). The Reynolds number falls below 80,000 at momentum parameter values above about 1.8, and only results below this value should be considered. The bellmouth entrance possibly affects the distribution of the angular momentum at the entrance to the cylindrical section, but apparently does not change the total flux. The results tend to support the assumption that the manner of introduction of angular momentum is not significant.

Figure 10 illustrates the effect of adding short circular cylinders to the upstream end of a long 7.5° cone. The frequency and the range of surging are increased significantly as the length of cylinder is increased. Similar results were noted with the shorter 7.5° cones.

Adding circular cylinder sections upstream of a 15° cone has an even more pronounced effect on the surge characteristics (see Figure 11). A long cylinder has only slightly more influence than a short cylinder. Adding a cylinder to the downstream end of a long cone has no effect on the frequency, but does decrease the surge amplitude at higher momentum parameter values (Figure 11, Run 123).

The surge amplitude decreases with respect to distance from the inlet in an expanding cone, but generally increases in a long cylinder (Figure 12).

A 100° elbow produces lower frequencies than a cylinder of the same length (Figure 13). The range of surging is also reduced. In elbows of different lengths the highest pressure fluctuations were measured near the outlet. The fluctuations were always higher at the inside of the bend than at the outside, both in constant-diameter elbows and expanding cross-section elbows of draft tubes.

Substitution of a straight cylinder of equal length for the elbow in the Grand Coulee pump-turbine draft tube does not alter the frequency parameter values to a great extent (see Figure 14). An interesting phenomenon in the straight tube is the presence of a second frequency equal to about two-thirds of the predominant one. The predominant frequency parameter curve varies only slightly from the frequency parameter curve of the elbow draft tube. The maximum amplitude is typically higher in the elbow tube.

In addition to the frequency and pressure parameter curves for the above two draft tubes, parameter plots of their geometric components have been included in Figure 15 for comparison. The frequency parameter curve of the 7.5° cone is almost identical to those of the draft tubes. The frequencies of all the other

vidual components, however, are higher than the two complete draft tubes. While generally the most upstream components have the most influence, in this case just the opposite is true. A similar comparison is presented in Figure 16, where the influence of straight cylinder sections inserted between cone sections is illustrated.

Two lengths of 30° expanding cones were also tested. No periodic pressure fluctuations could be detected with the instruments and measuring techniques used in the other tests.

It was pointed out earlier that the amplitude of the surge varies with location along the tube wall. In simple symmetrical shapes the variance occurs in a fairly regular fashion (Figure 12). In an elbow of constant diameter the generalization can be made that pressure pulsation amplitude is highest near the outlet and higher at the inside than at the outside of the bend. In a more complex shape such as the Grand Coulee pump-turbine draft tube the amplitude variation is not as easily predictable throughout the total range of surging.

Rms values of pressure pulsation were obtained for the entire range of surging at about 30 locations in the and Coulee pump-turbine. The resulting pressure parameter curves at five cross sections (four curves at section quarter points for each section) are shown in Figure 17. The results provide sufficient information to obtain directly or interpolate the pressure parameter value at any location on the draft tube walls. The maximum value of the pressure pulsation amplitude itself in most cases occurs at the first peak of the pressure parameter curve, near a momentum parameter value of 1. Pressure parameter plots for the downstream portions of the exit cone have not been shown because the pressure pulsations vary in a fashion typical of expanding cones, i.e., decreasing downstream.

All recorded pressure amplitudes were influenced by the frequency filter band through which the amplified pressure transducer signal was passed before it reached the rms meter. The filtered rms value was always lower than what would have been measured without a band-pass filter. Some comparative data for four different locations in the Grand Coulee pump-turbine draft tube are shown in Figure 18. The unfiltered pressure parameter in most cases is not more than 20 percent higher than the filtered value.

SURGE MEASUREMENTS ON TURBINE MODELS

Recently the contracts for two different turbines for Bureau of Reclamation projects included requirements for pressure pulsation measurements during model tests. The manufacturers furnished the Bureau complete operating data and draft tube pressure pulsation oscillograms and magnetic recording tapes. From these data, it was possible to compute the dimensionless parameters. The frequency parameter results for these turbines, the Grand Coulee Third Powerplant turbine model, and the Grand Coulee Pumping Plant pump-turbine model are shown in Figure 19.

A shorter range of surging is produced by the turbine draft tube and its frequency parameter curve is lower. The difference in the surging characteristics can be attributed to the different shapes of the two draft tubes. The turbine draft tube area expands throughout the elbow for a distance of about 2.5 L/D, with an equivalent area cone expansion angle between 11° and 13°. Then there is a slight gradual decrease in area in the vicinity of the piers. The long, initial expanding section is sufficient, however, to produce surging characteristics typical of an equivalent area expanding cone. The frequency parameter curve is very similar to the one produced by the Fontenelle draft tube with conical throat (see Figure 4). The pump-turbine draft tube has a short, expanding initial section followed by a 100° constant-diameter elbow (centerline L/D = 2). The constant-diameter elbow near the entrance tends to extend the range of surging and produces higher frequencies, as was demonstrated by the air model tests (Figure 4).

AIR MODEL AND HYDRAULIC TURBINE MODEL COMPARISON

The Grand Coulee pump-turbine draft tube surge characteristics were determined both from the manufacturer's hydraulic scale model (1:9.5 scale) data and the laboratory air model (1:17.8 scale) data. The two tests were performed completely independently of each other. Coordination during the tests was not possible since the manufacturer's tests had been completed and reported when the air model tests were performed. The air model testing on this draft tube was part of the regular testing program, and therefore established procedures were used to obtain the data.

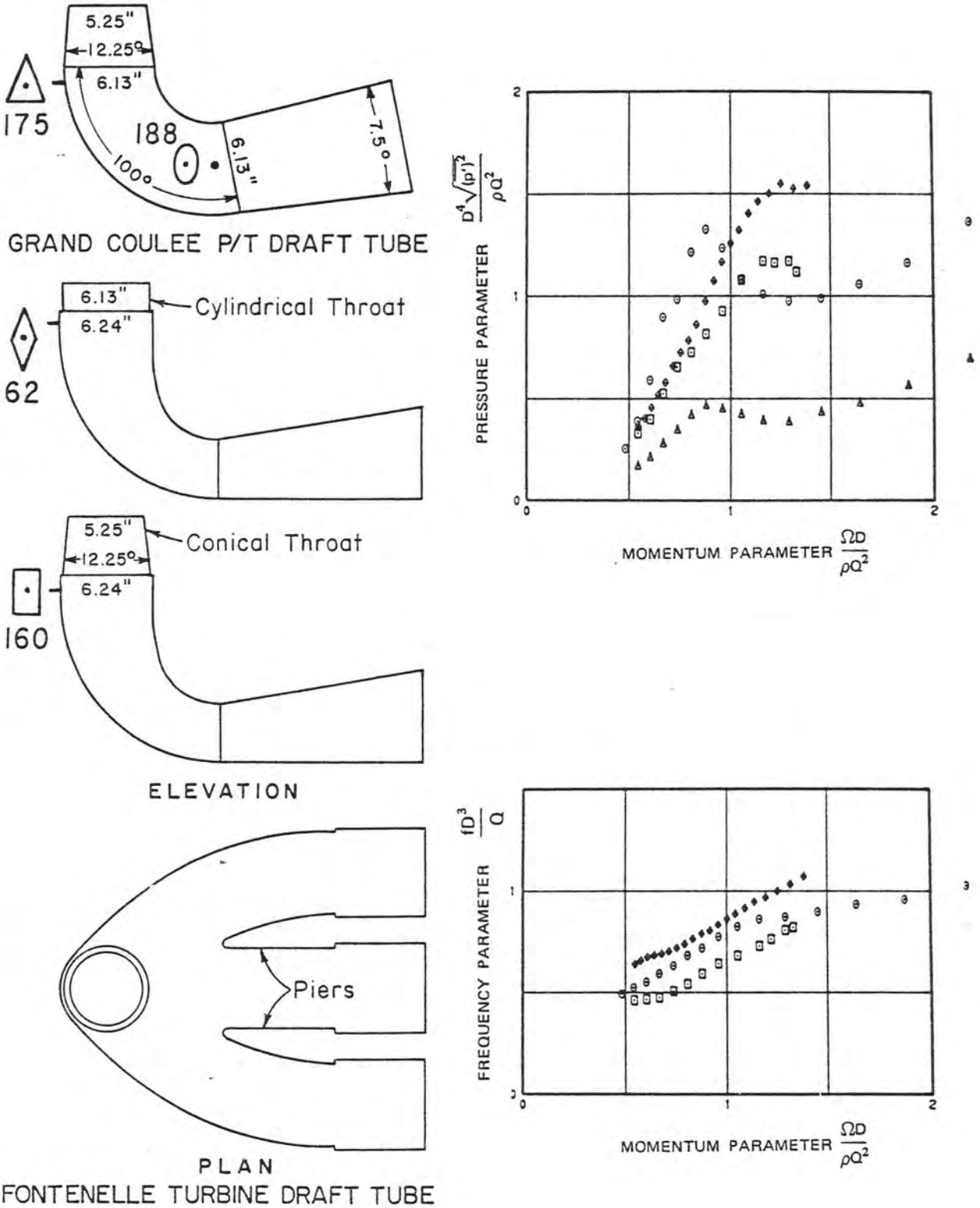

Figure 4. Surging characteristics of three model draft tubes.

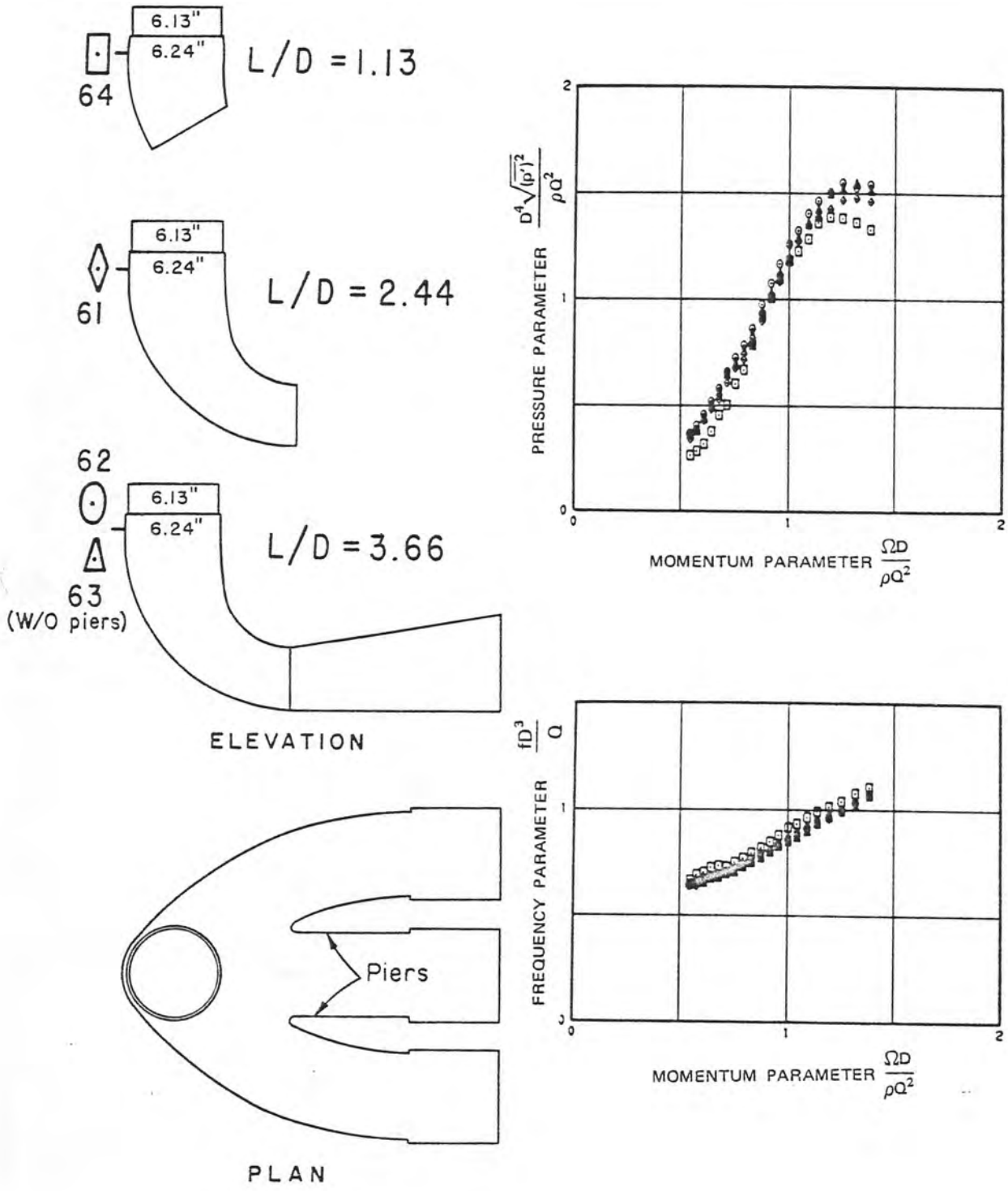

Figure 5. Effect of pier elimination and draft tube shortening on surging characteristics of Fontenelle draft tube.

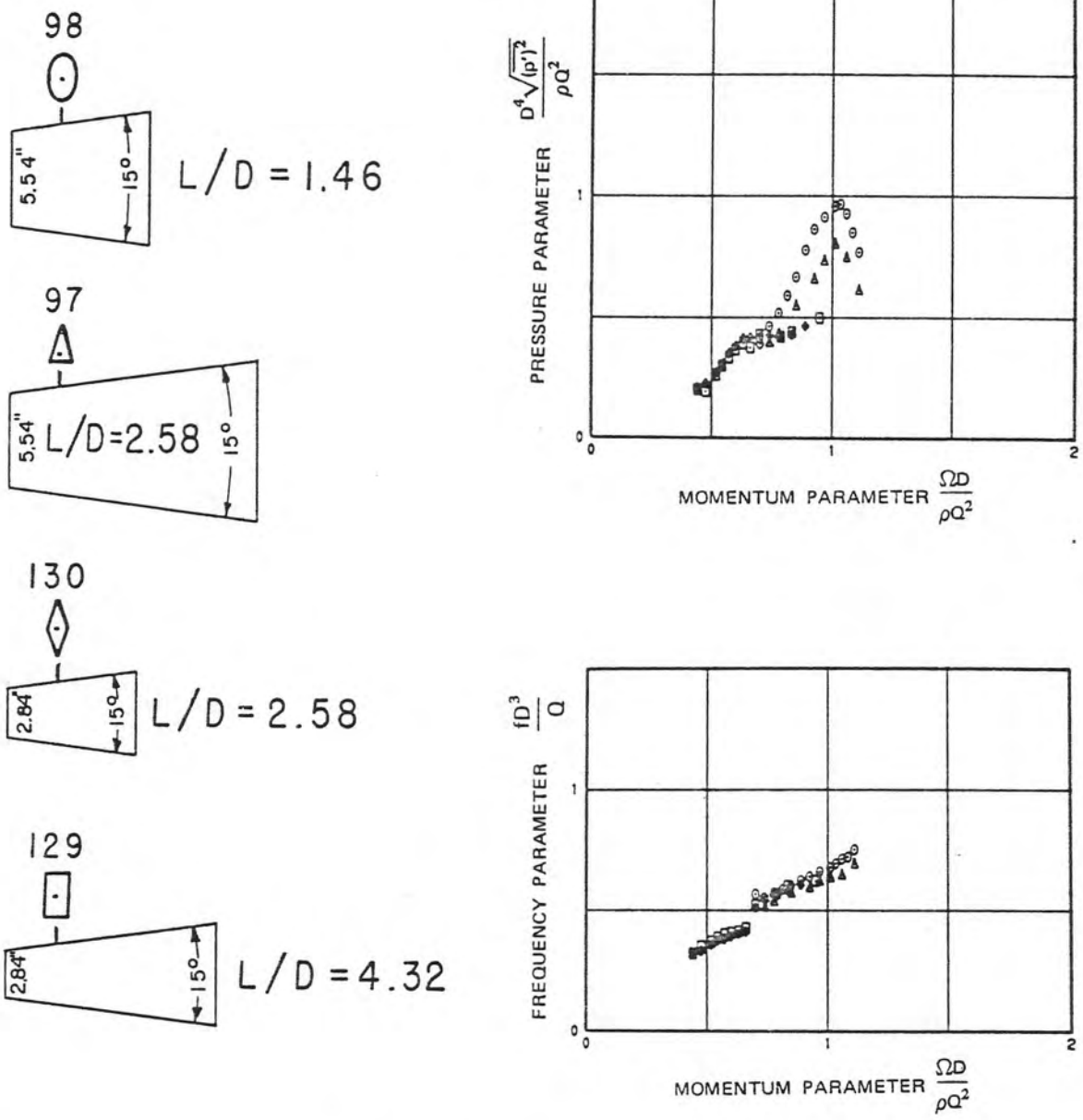

Figure 6. Surging characteristics of 15° truncated cones.

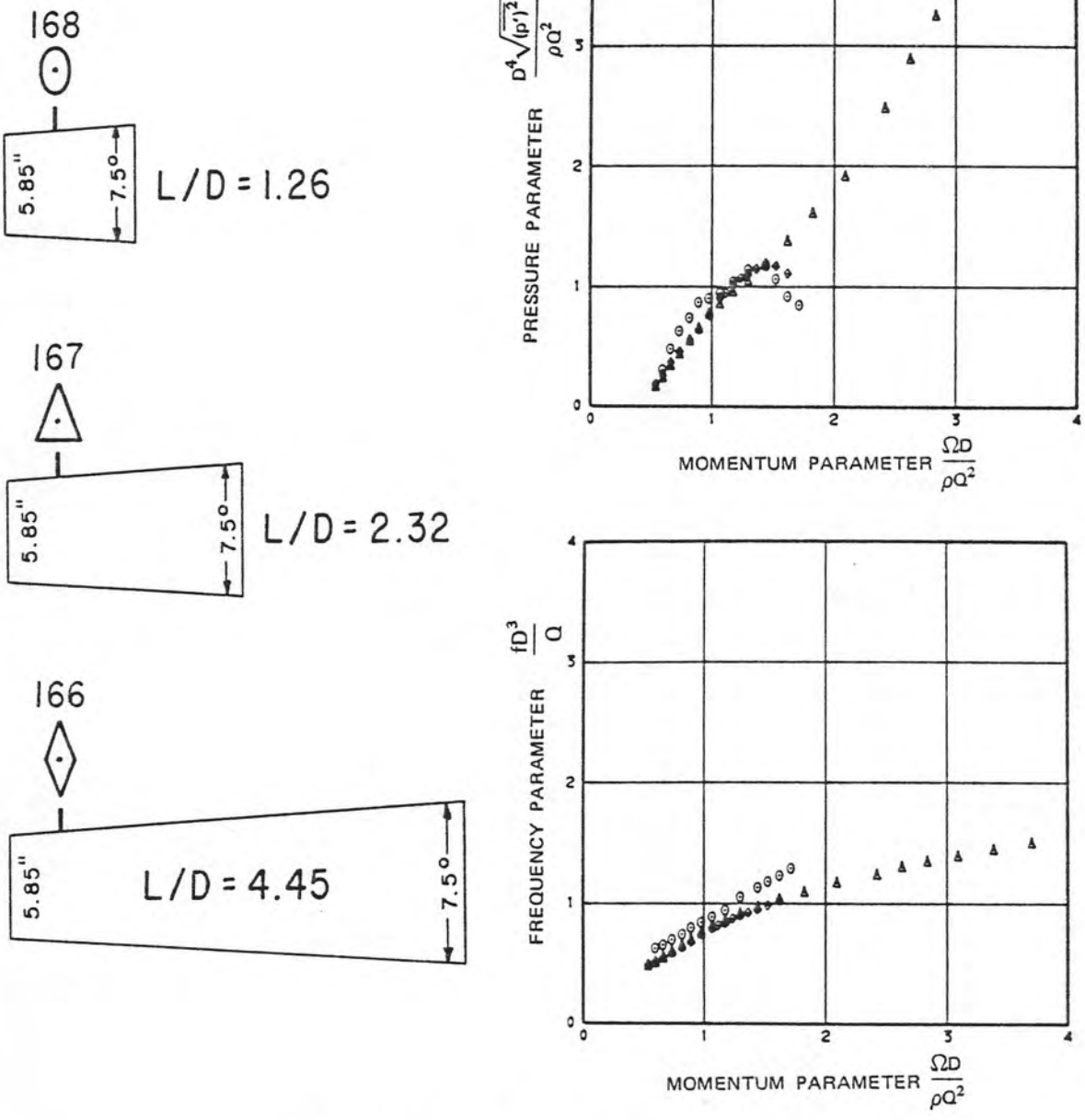

Figure 7. Surging characteristics of 7.5° cones.

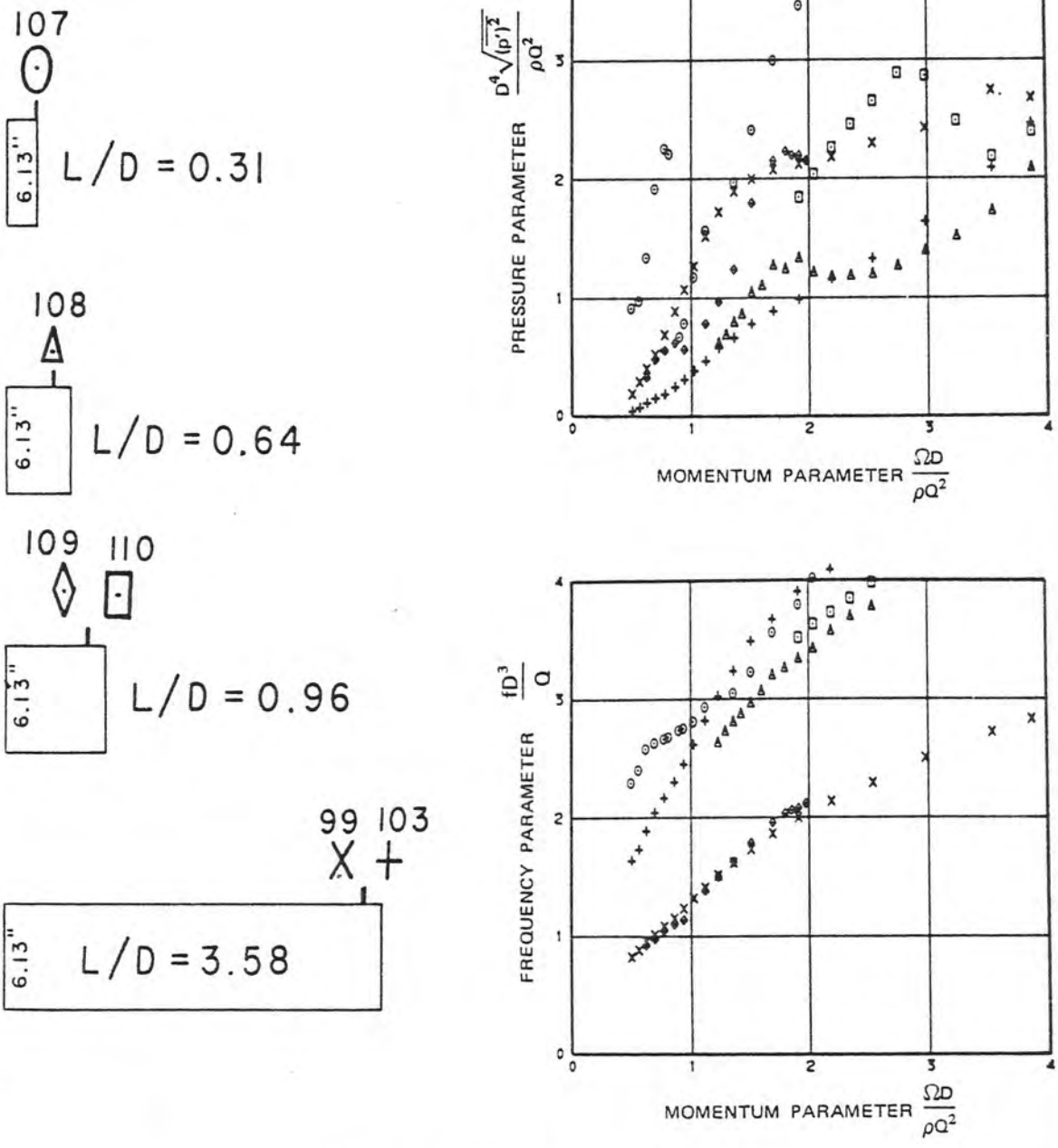

Figure 8. Surging characteristics of circular cylinders.

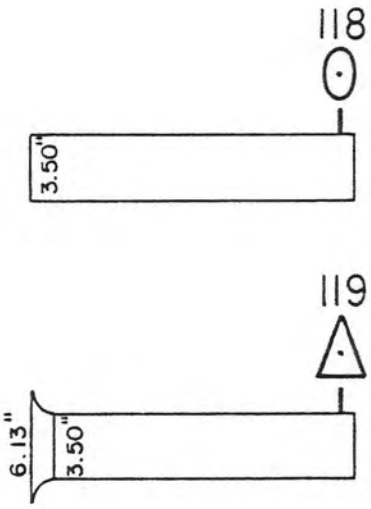

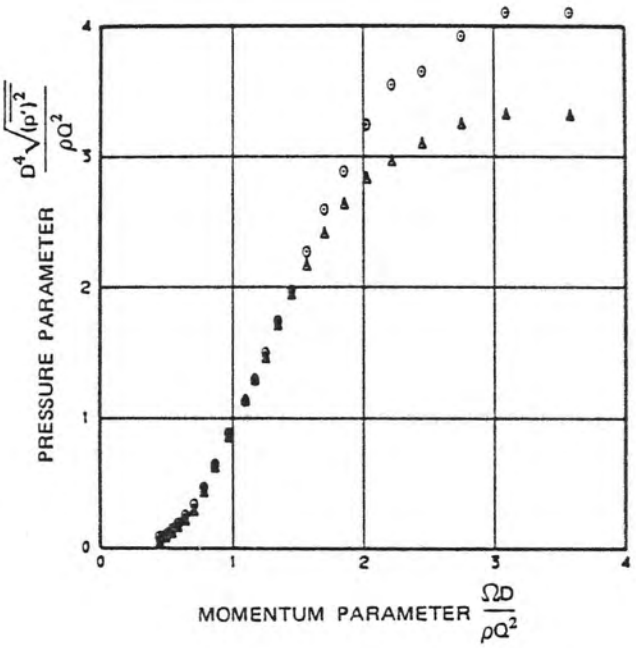

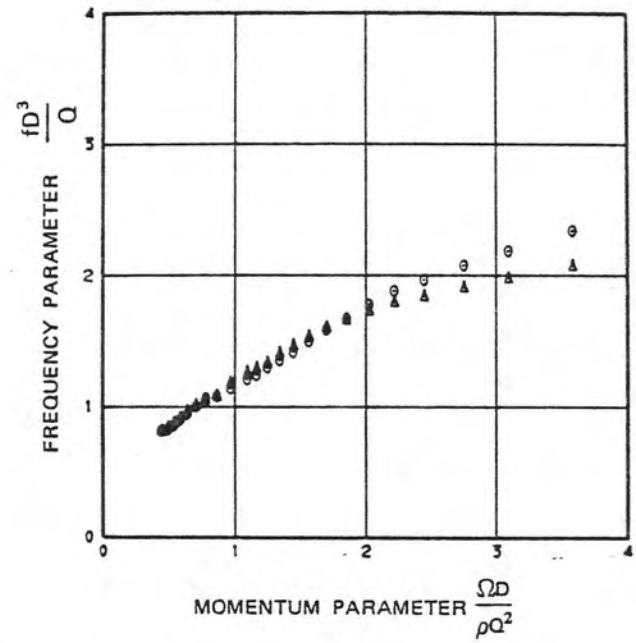

Figure 9. Influence of a bellmouth entrance on the surging characteristics of long, straight cylinders.

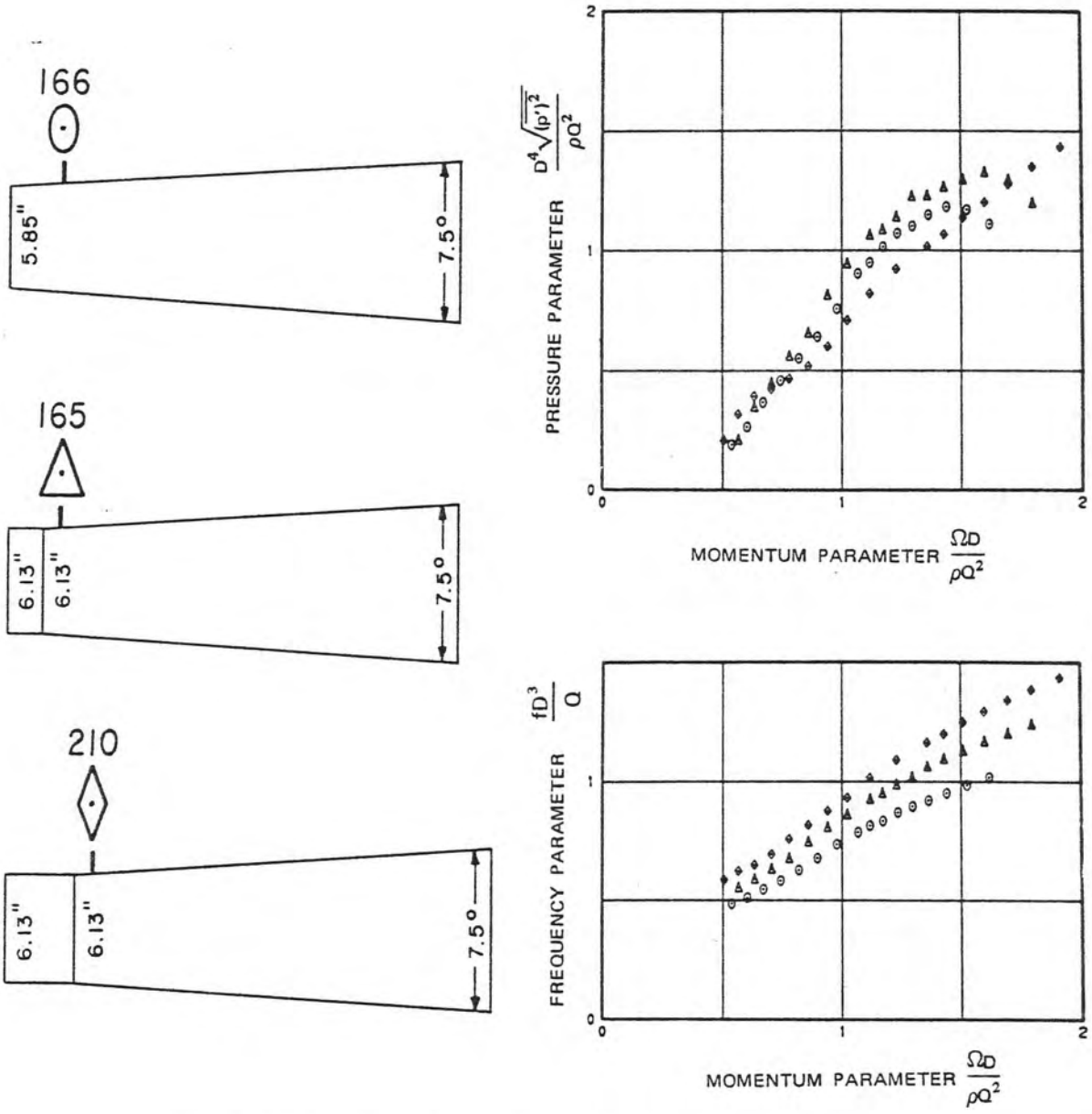

Figure 10. Influence of short, circular cylinders at the throat of a long 7.5° cone.

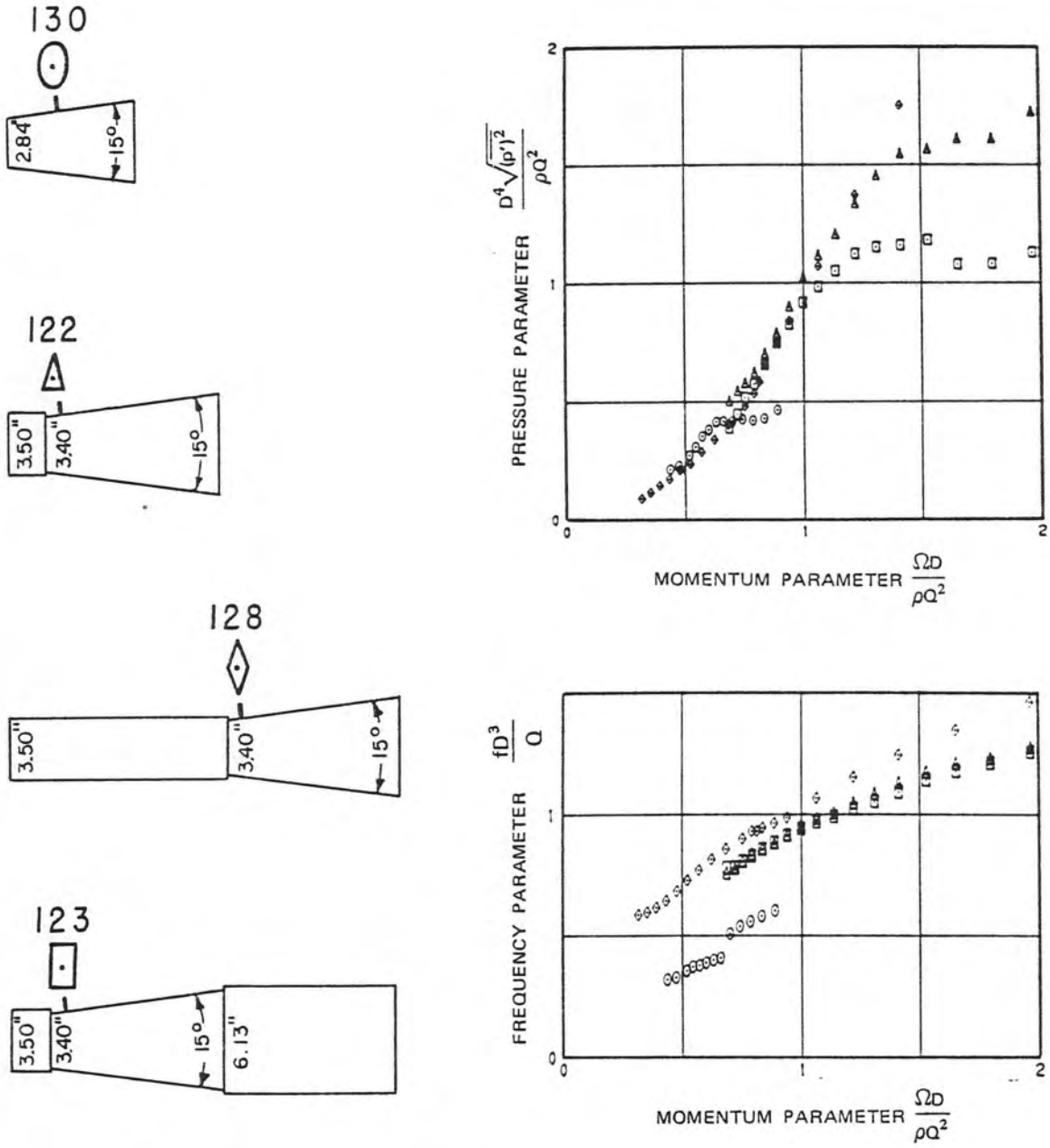

Figure 11. Surging characteristics of 15° cones in combination with circular cylinders.

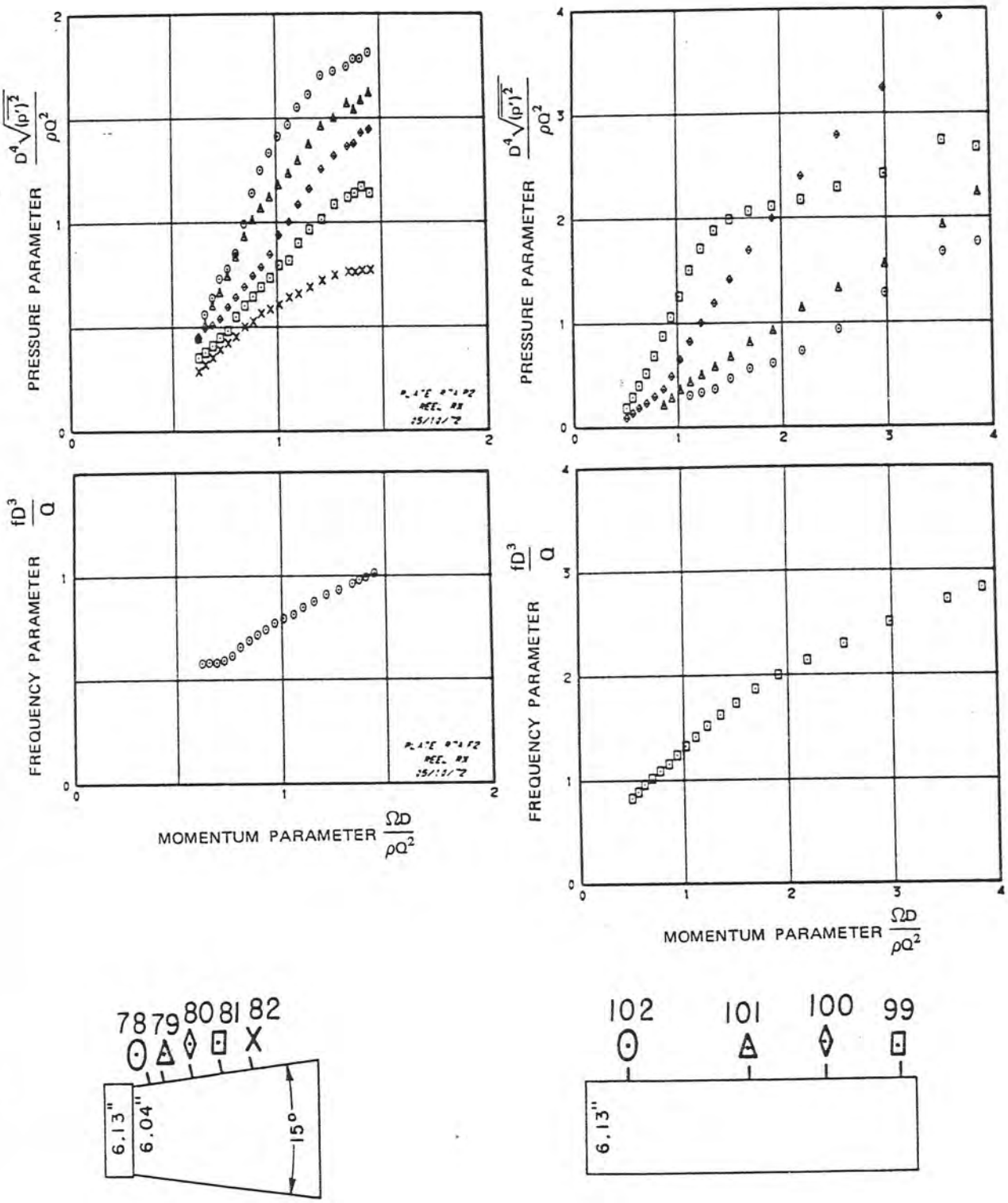

Figure 12. Variation of surge amplitude with respect to distance from inlet.

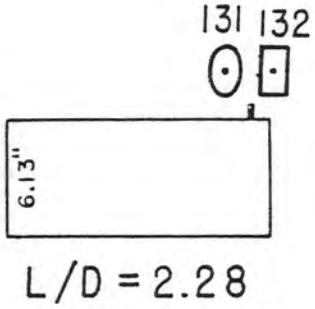

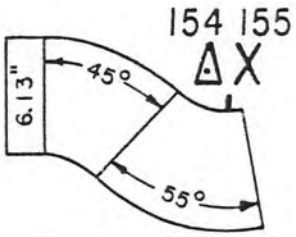

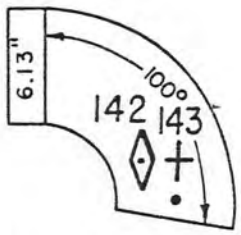

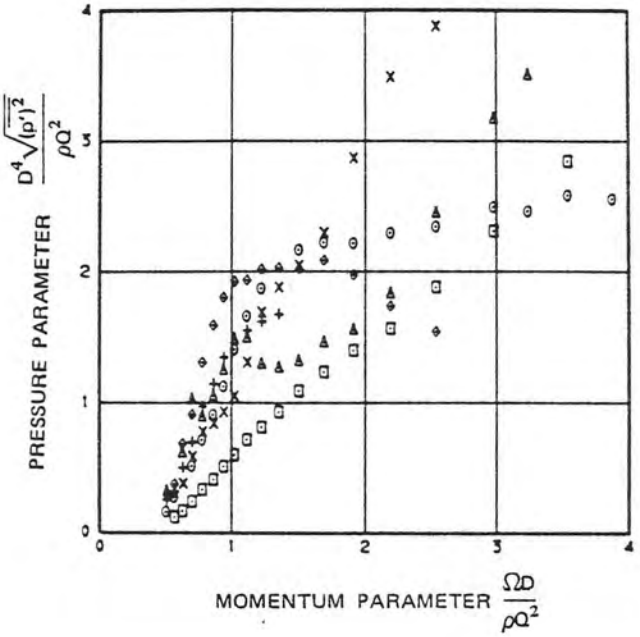

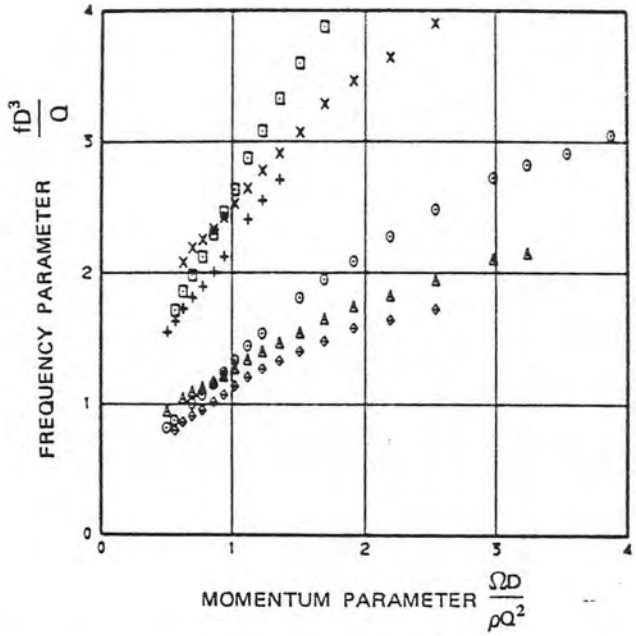

Figure 13. Effect of bends on surging characteristics.

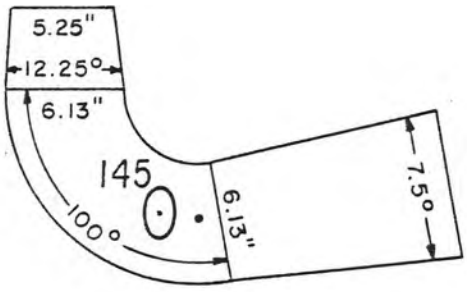

L/D = 5.30

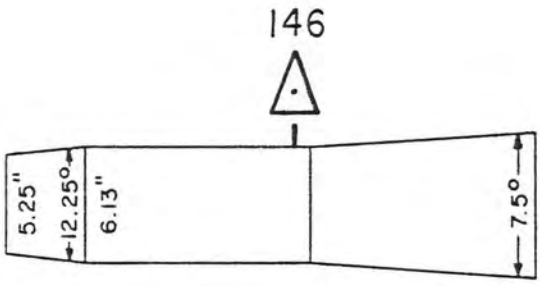

L/D = 5.30

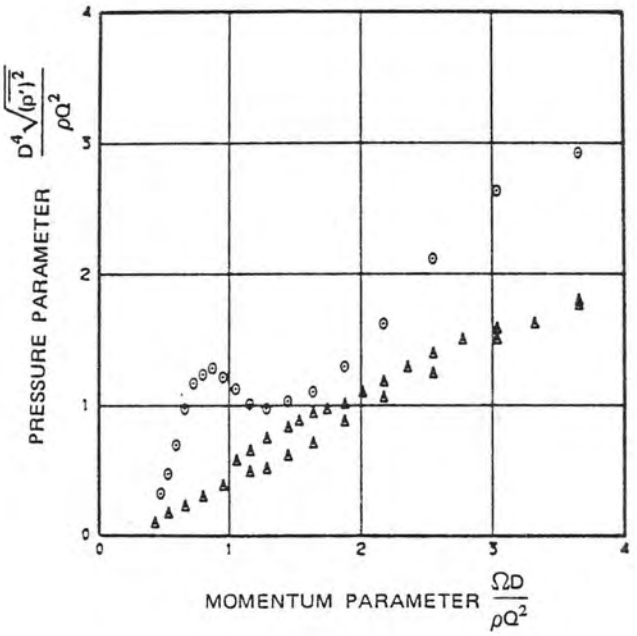

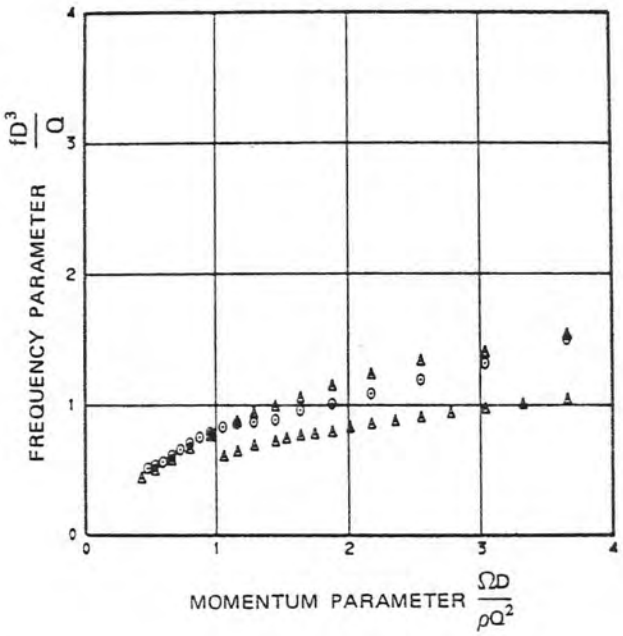

Figure 14. Effect on surging characteristics of replacement of Grand Coulee pump-turbine draft tube elbow with a straight cylinder of equal length.

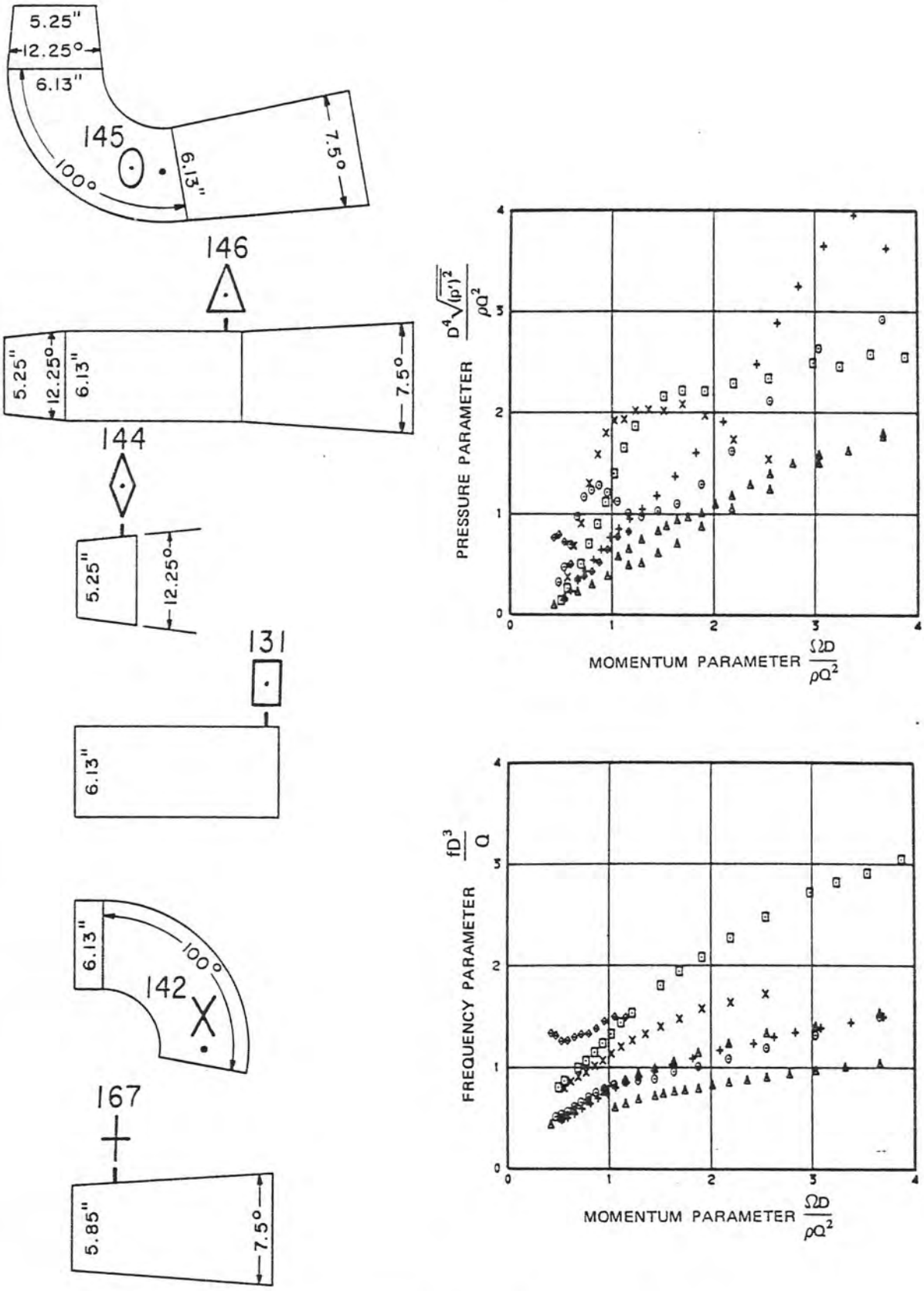

Figure 15. Comparison of surging characteristics of two draft tubes and their geometric components.

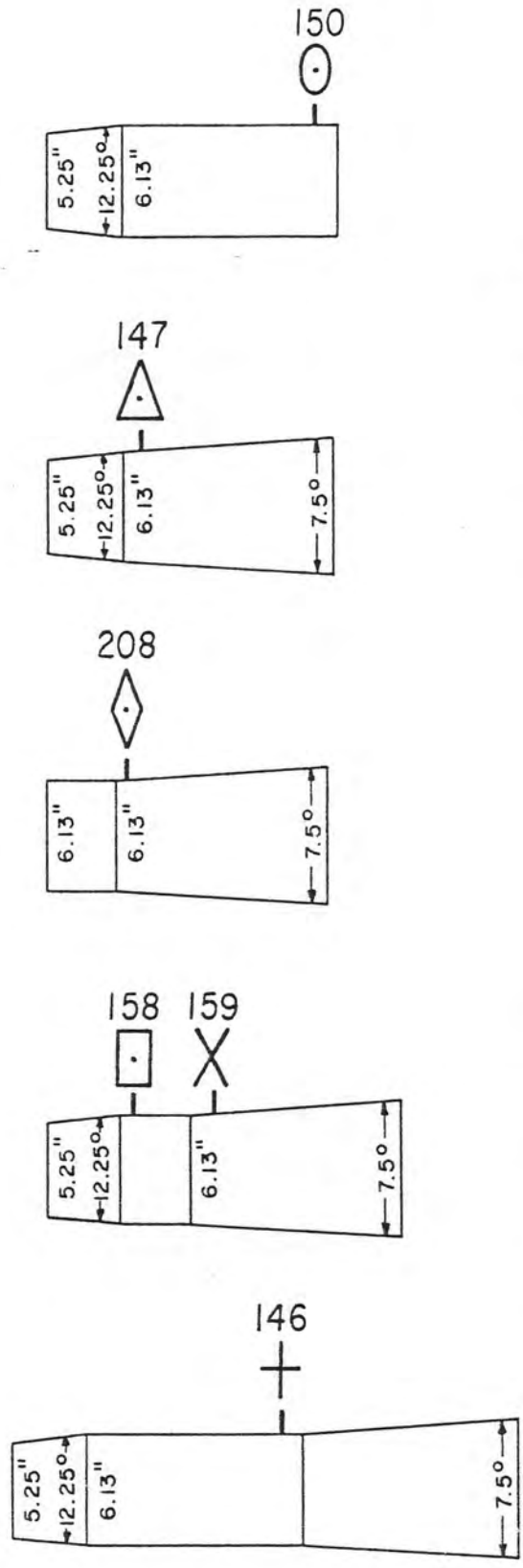

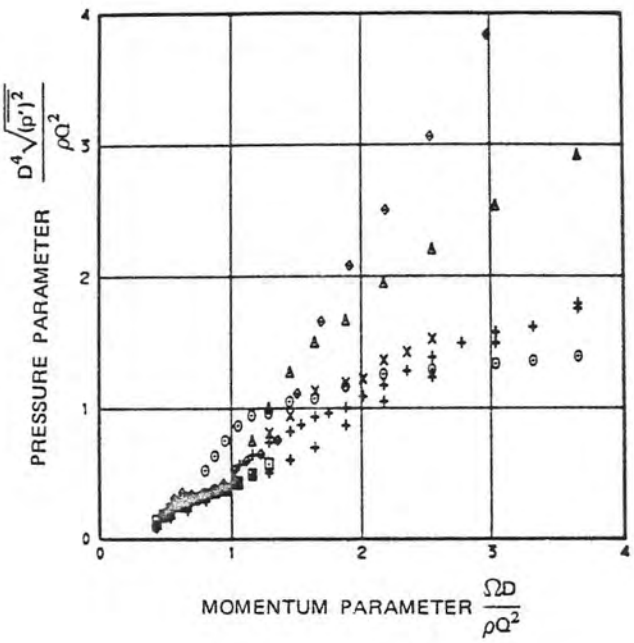

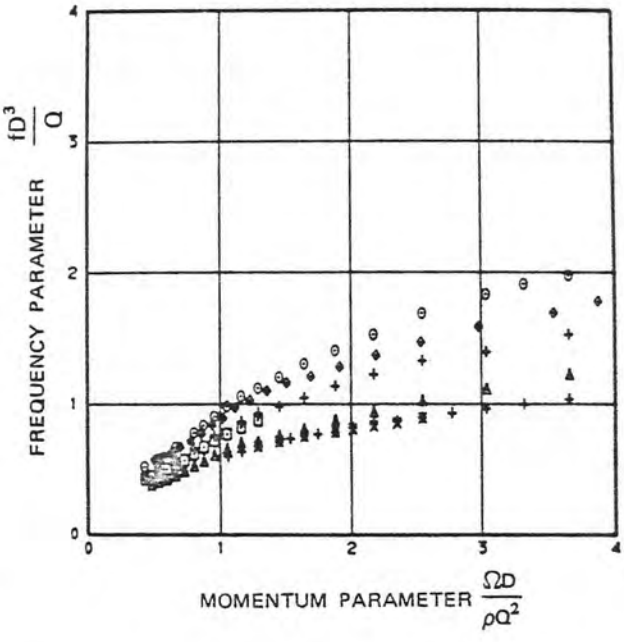

Figure 16. Comparison of surging characteristics of cone and cylinder combinations.

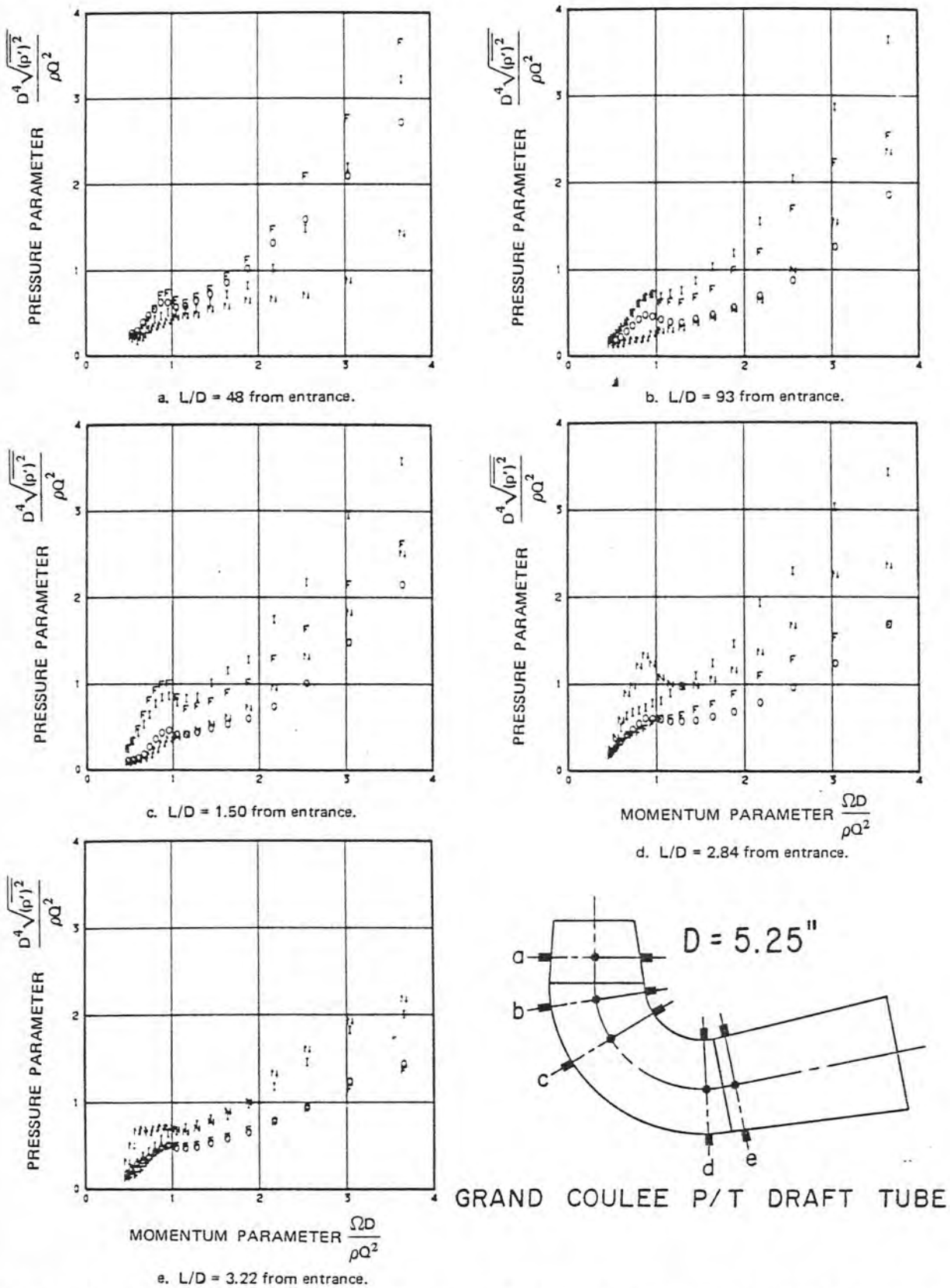

Figure 17. Pressure parameter variation with respect to location in the Grand Coulee pump-turbine draft tube. Plotted letter symbols used to define location: O = outside of bend; I = inside of bend; N = near side; F = far side. Coordinates are defined by center of symbol. Indicated distance from entrance is along centerline.

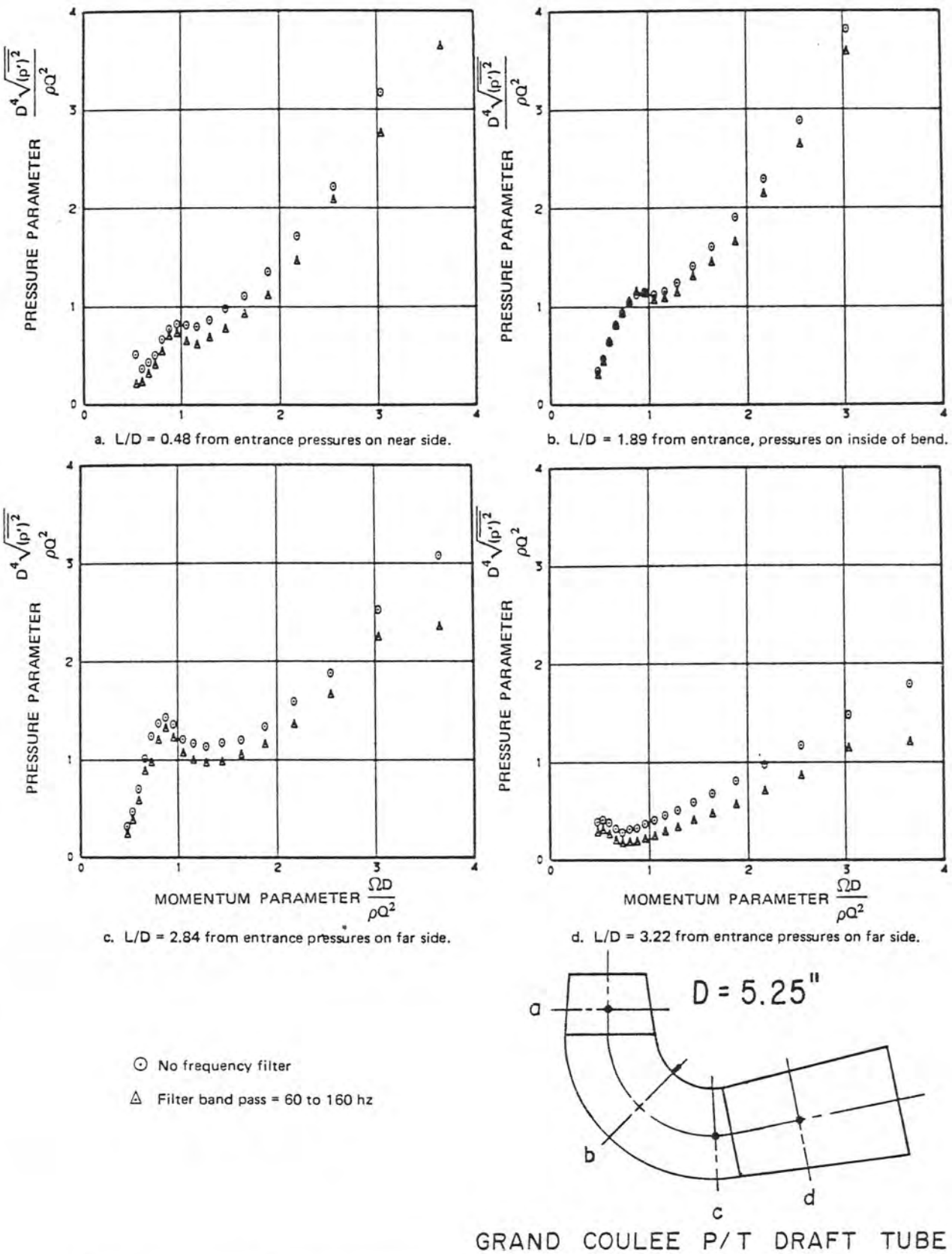

Figure 18. Comparison of filtered and unfiltered pressure parameter values for the Grand Coulee pump-turbine draft tube.

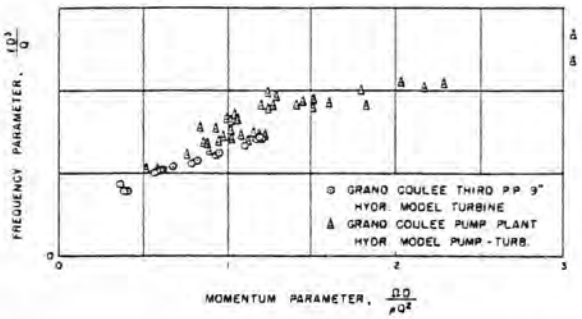

Figure 19. Comparison of frequency parameter for Grand Coulee Third Powerplant turbine and Grand Coulee Pumping Plant pump-turbine hydraulic models.

Pressure pulsation data were obtained at approximately the same location, near the draft tube inlet, in both tests. Results of the two tests are shown in Figure 20. The frequency parameter comparison is quite satisfactory. Pressure parameter values do not compare nearly as well. Since powerplant cavitation factor, δ, is a function of the vapor pressure of water, the air model could not be used to explore the effects of δ on pressure amplitude. The best comparison is obtained (as it should) from the hydraulic model tests with the highest value of δ (δ = 0.43). Taking into account the varying test equipment and techniques used in the two tests, the overall comparison of results is quite encouraging.

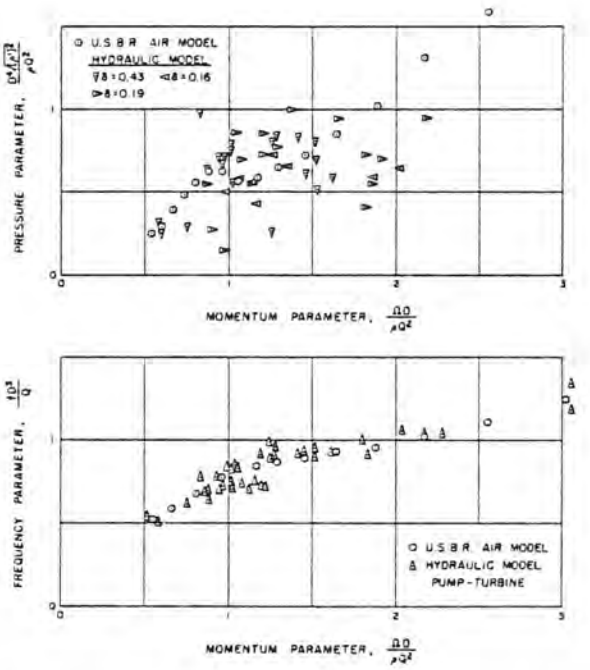

Figure 20. Comparison of frequency and pressure parameters for Grand Coulee pump-turbine draft tube computed from air model and hydraulic scale model pump-turbine.

The favorable comparison of results of the air model with the turbine model verifies a major assumption made in applying the results of the dimensional analysis to experimental studies. That is, that regardless of the manner in which angular momentum is introduced into the flow, the resulting dimensionless surging characteristics in geometrically similar draft tubes will be the same for a particular value of $\Omega D_3/\rho Q^2$. This says nothing about the accuracy of determining the correct value of $\Omega D_3/\rho Q^2$. Computing the momentum parameter for a complex flow such as that passing through the runner is subject to many uncertainties, and simplifying assumptions obviously must be made. The methods used to determine the value of the momentum parameter in the two studies are not as exact as could be desired, and possibly can be improved in future experiments and analyses.

The greatest improvement in increasing the accuracy of computing the momentum parameter would be a more accurate determination of the angular momentum of the flow through the wicket gates. Presently this is done by means of a graphical analysis of the flow direction. Measurements of wicket gate flow performed on hydraulic models would furnish valuable information. Conceivably the flow through two adjacent gates also varies with respect to location, caused by unsymmetrical flow from the spiral case. To obtain accurate values of the momentum parameter of the flow leaving the wicket gates, a complete circumferential integration may have to be performed at several gate settings.

Accurate measurement of discharge is also important in computing the momentum parameter of turbines. A discharge measurement error of 2 percent can cause errors of about plus or minus 0.06 to plus or minus 0.11 in the computed value of the momentum parameter. The corresponding relative error can approach 20 percent at the lower end of the momentum parameter surging range.

APPLICATION TO TURBINES

The air model tests and the two hydraulic turbine model tests conclusively demonstrate that for a given draft tube shape and at sufficiently high Reynolds numbers, there is correlation between the momentum parameter and the frequency and pressure parameters:

$$\frac{fD_3^3}{Q} = \phi_3 \left(\frac{\Omega D_3}{\rho Q^2}\right)$$

$$\frac{D_3^4 \sqrt{\overline{(p')^2}}}{\rho Q^2} = \phi_4 \left(\frac{\Omega D_3}{\rho Q^2}\right)$$

The momentum parameter for a turbine can be computed from Equation (10):

$$\frac{\Omega_2 D_3}{\rho Q^2} = \frac{D_3 R \sin\alpha}{BNS} - \frac{550 \quad P_{11} \quad D_3}{2\sqrt{2g}\,\rho\, Q_{11}^2\, \phi\, D_2} \qquad (10)$$

which requires a knowledge of the wicket gate geometry and turbine performance characteristics.

An example follows for the evaluation of Equation (10) for the Grand Coulee Pumping Plant pump-turbine Units 7 and 8.

To determine the values of the wicket gate geometric variables, two adjacent wicket gates are laid out (using a scale template) on a drawing at several gate positions from closed to full open, as in Figure 1. At each gate setting, the values of R and S are obtained by scaling. The flow direction is assumed to be normal to the smallest opening between the gates, S. The angle α is then measured between the flow direction and a radial line through the center of the opening. Values of R, S, and α can then be plotted as functions of gate angle (or some other defined base, such as percent of full gate) and a smooth curve constructed for each variable (Figure 21). Since the number of wicket gates N, their height B, and the draft tube diameter D_3 are constant and known, the quantity $D_3 R \sin\alpha/BNS$ can easily be computed for any gate setting. The result is the value of momentum parameter of the flow as it enters the turbine runner.

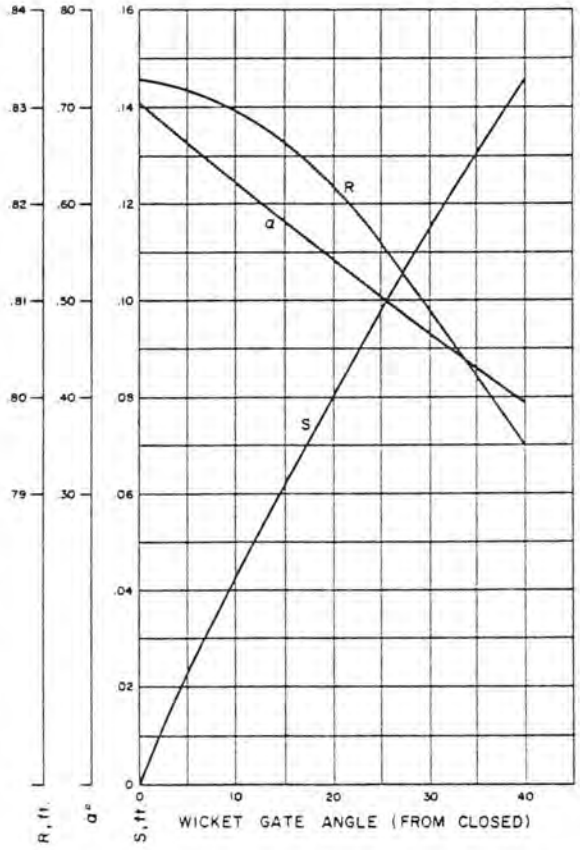

Figure 21. Wicket gate geometric characteristics for Grand Coulee Pumping Plant pump-turbine (Units P/G-7 and P/G-8) 1:9.5 scale hydraulic model studies.

The second term of Equation (10) evaluates the amount the momentum parameter is changed as the flow passes through the runner. Performance data obtained on the model (or prototype) turbine are sufficient to compute this term. All the necessary data required to compute the momentum parameter are tabulated in Table 1 for two test points.

Table 1

Run No.	Gate position from closed	Gate characteristics			Turbine performance data			
		R	S	α	H	Q	P	n
	o	ft	ft	o	ft	cfs	hp	rpm
30	30.0	0.809	0.1148	46.6	112.8	16.48	147.1	775
69	11.8	0.828	0.0492	60.2	134.5	9.48	103.1	1,285

Constants

D_2 ft	D_3 ft	B ft	N	g ft/sec^2	ρ lb-sec^2/ft^4
0.984	0.984	0.1967	20	32.2	1.94

or Run 30, using Equations (8), (9), and (7)

$$P_{11} = \frac{P}{D_2^2\, H^{3/2}} = \frac{147.1}{(.984)^2\,(112.8)^{3/2}} = 0.127$$

$$Q_{11} = \frac{Q}{D_2^2\, H^{1/2}} = \frac{16.48}{(.984)^2\,(112.8)^{1/2}} = 1.603$$

$$\phi = \frac{\pi D_3 n}{60\sqrt{2gH}} = \frac{3.14(.984)(775)}{60\sqrt{2(32.2)(112.8)}} = 0.468$$

The first term of Equation (10)

$$\frac{D_3 R \sin\alpha}{BNS} = \frac{(.984)(.809)(\sin 46.6)}{(.1967)(20)(.1148)} = 1.28$$

and the second term of Equation (10)

$$\frac{550\ P_{11}\ D_3}{2\sqrt{2g}\,\rho\, Q_{11}^2\,\phi\, D_2}$$

$$= \frac{550(.127)(.984)}{2(8.025)(1.94)(1.603)^2(.469)(.984)} = 1.86$$

or

$$\frac{\Omega D_3}{\rho Q^2} = 1.28 - 1.86 = -0.58$$

The minus sign indicates that the swirl direction of the flow entering the draft tube is opposite the rotation of the runner.

Similarly, for Run 69

$$\frac{\Omega D_3}{\rho Q^2} = 1.27$$

Here the swirl of the draft tube flow is in the same direction as the runner rotation.

Figure 22 shows the oscillograms of the pressure pulsations. The frequency of the draft tube surge is indicated on each recording. Corresponding values of the frequency parameter are tabulated in Table 2.

The pressure pulsation rms amplitude was obtained from isolines of pressure fluctuation expressed as percent of total head, drawn on a Q_{11} versus n_{11} ($n_{11} = nD_2/H^{1/2}$) plot. The values, as well as the resulting values of the pressure parameter, are given in Table 2.

The frequency and pressure parameter values determined above can be used to predict the surge frequency and pressure amplitude for the homologous prototype turbine having a geometrically similar draft tube. For the same value of the momentum parameter in model and prototype, i.e., when

$$\left(\frac{\Omega D_3}{\rho Q^2}\right)_m = \left(\frac{\Omega D_3}{\rho Q^2}\right)_p$$

Table 2

Run No.	f hz	D_3 ft	Q cfs	fD_3^3/Q	$\sqrt{(\overline{P'})^2}$ psf	$D_3^4\sqrt{(\overline{p'})^2}/\rho Q^2$
30	8.8	0.984	16.48	0.51	176	0.31
69	9.4	0.984	9.48	0.94	142	0.77

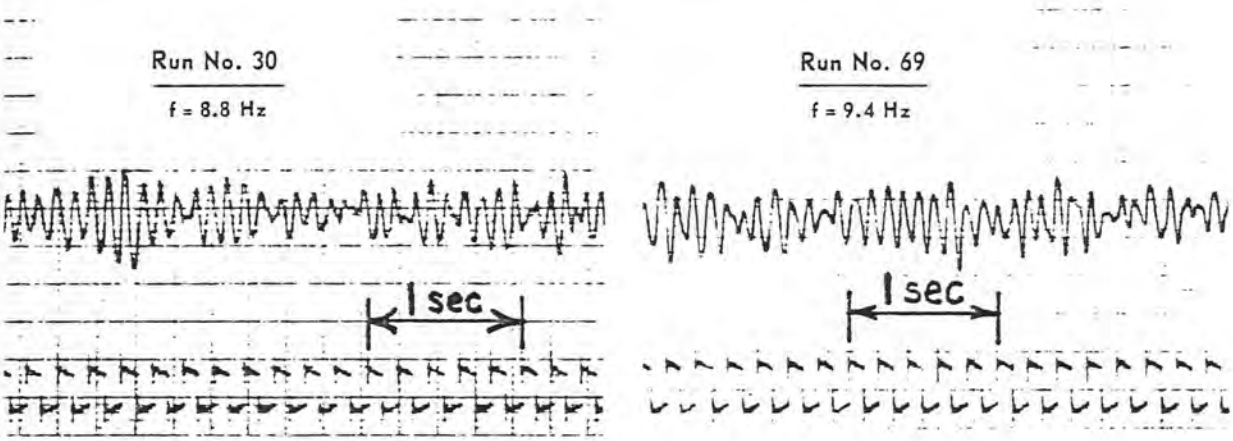

Figure 22. Oscillograms of pressure pulsations in Grand Coulee pump-turbine hydraulic model draft tube throat.

(where the subscripts m and p represent model and prototype, respectively) it follows that

$$\left(\frac{fD_3^3}{Q}\right)_m = \left(\frac{fD_3^3}{Q}\right)_p$$

and

$$\left(\frac{D_3^4\sqrt{\overline{(p')^2}}}{\rho Q^2}\right)_m = \left(\frac{D_3^4\sqrt{\overline{(p')^2}}}{\rho Q^2}\right)_p$$

The prototype frequency then can be determined from

$$f_p = \left(\frac{fD_3^3}{Q}\right)_m \left(\frac{Q}{D_3^3}\right)_p \quad (11)$$

and the prototype pressure pulsation rms amplitude from

$$\left(\sqrt{\overline{(p')^2}}\right)_p = \left(\frac{D_3^4\sqrt{\overline{(p')^2}}}{\rho Q^2}\right)_m \left(\frac{\rho Q^2}{D_3^4}\right)_p \quad (12)$$

The frequency and pressure amplitude of the prototype surge for Run 69 (δ = 0.19) are computed below. The prototype draft tube diameter, D_3 is given as 9.35 feet. Prototype discharge can be computed by using Equation (9), where D_2 in this case equals D_3. Prototype net head can be computed from the definition $n_{11} = nD_2/H^{1/2}$. The value of n_{11} for Run 69 is given as 109.1 in the model test results. The prototype unit will be operated at 200 rpm, and therefore the corresponding H for Run 69 is 294 feet. Then from Equation (9)

$$Q_p = Q_{11} D_2 H^{1/2}$$

$$Q_p = (.844)(9.35)^2(293)^{1/2}$$

$$Q_p = 1263 \text{ cfs}$$

Using Equation (11)

$$f_p = (.94)\frac{(1,263)}{(9.35)^3}$$

$$f_p = 1.45 \text{ hz}$$

Using Equation (12)

$$\left(\sqrt{\overline{(p')^2}}\right)_p = (.77)\frac{1.94\,(1,263)^2}{(9.35)^4} = 312 \text{ lb/ft}^2$$

$$\left(\sqrt{\overline{(p')^2}}\right)_p = 5.0 \text{ ft water}$$

The above values appear reasonable, but can be verified only after the units are installed, and prototype performance and draft tube surge data obtained.

It is not necessary to use specific model test points to compute prototype frequencies and pressure amplitudes. The characteristic frequency and pressure parameter curves for a particular draft tube can be established using a simplified model or any turbine–prototype or model. For the specific unit in question, sufficient data must be available to compute the momentum parameter (using Equation (10)) for the particular operating point where frequency and amplitude are to be computed. The corresponding values of the frequency and pressure parameters are obtained from the surge characteristic curves. The frequency and pressure amplitude are then computed as in the above example. Some other method of determining prototype discharge may be used.

REFERENCES

1. Falvey, H. T., "Draft Tube Surges–A Review of Present Knowledge and an Annotated Bibliography," Report No. REC-ERC-71-42, U.S. Bureau of Reclamation, Denver, Colorado, December 1971

2. Cassidy, J. J., "Experimental Study and Analysis of Draft-Tube Surging," Report No. REC-OCE-69-5, U.S. Bureau of Reclamation, Denver, Colorado, October 1969

3. Cassidy, J. J., and Falvey, H. T., "Observations of Unsteady Flow Arising After Vortex Breakdown," *Journal of Fluid Mechanics*, Vol. 41, Part 4, pp 727-736, 1970

4. Falvey, H. T. and Cassidy, J. J., "Frequency and Amplitude of Pressure Surges Generated by Swirling Flow," *Transactions of Symposium Stockholm 1970*, International Association for Hydraulic Research, Part 1, Paper E1, Stockholm, Sweden, 1970

5. Rheingans, W. J., "Power Swings in Hydroelectric Power Plants," *Transactions*, American Society of Mechanical Engineers, Vol. 62, pp 171-184, 1940

APPENDIX

DRAFT TUBE SHAPES TESTED WITH THE AIR MODEL

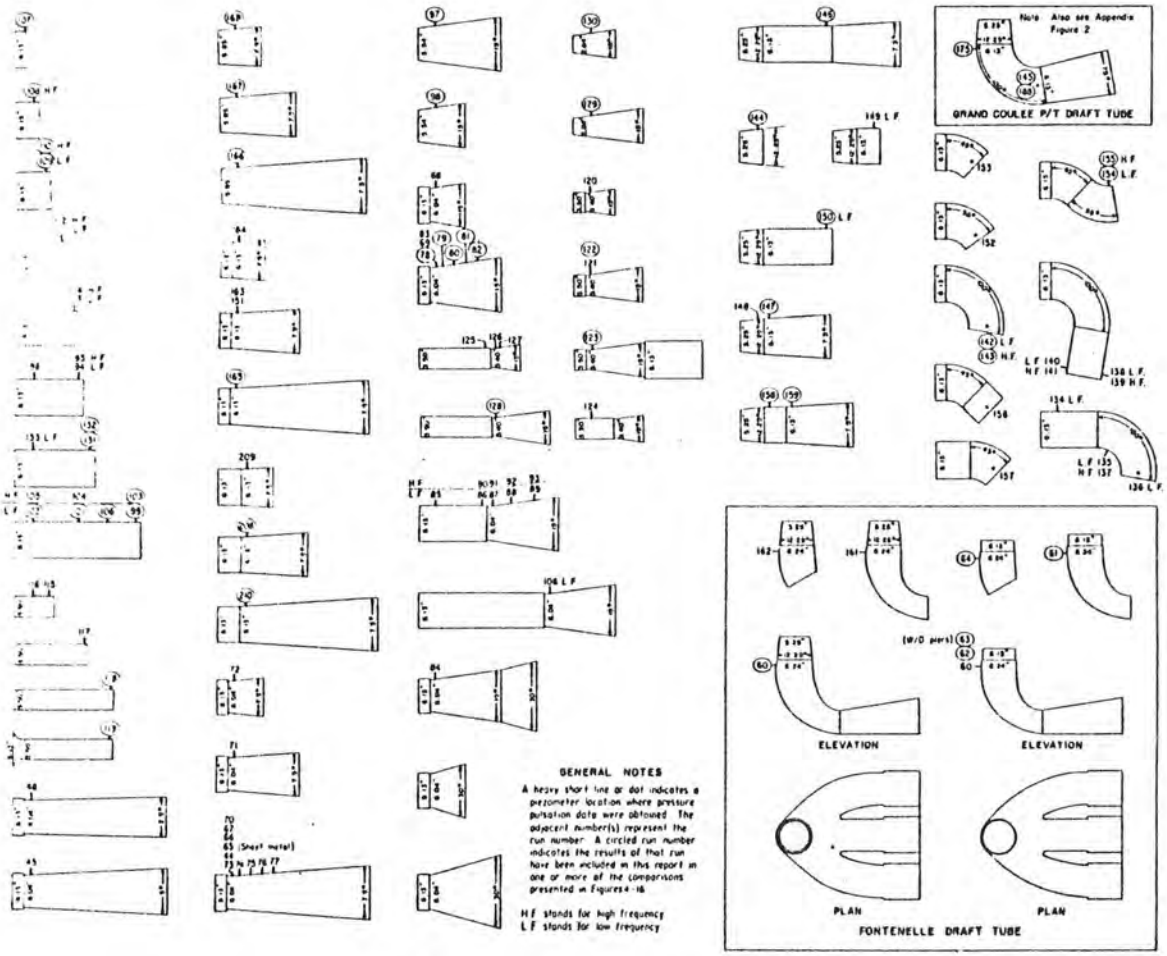

Figure 1. Draft tube shapes for which surge data were obtained with the air model.

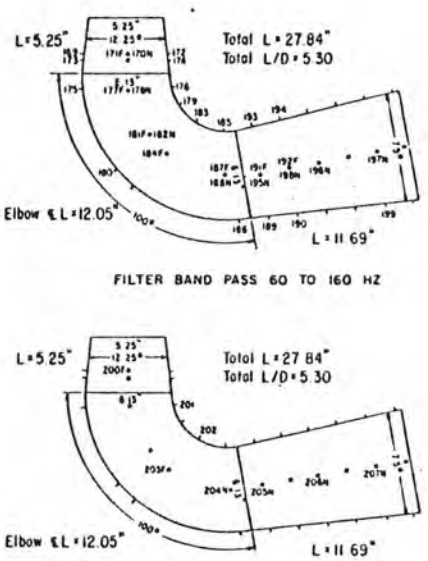

Figure 2. Locations on the Grand Coulee Pumping Plant pump-turbine draft tube where surge data were obtained with the air model.

7-1750 (3-71)
Bureau of Reclamation

CONVERSION FACTORS–BRITISH TO METRIC UNITS OF MEASUREMENT

The following conversion factors adopted by the Bureau of Reclamation are those published by the American Society for Testing and Materials (ASTM Metric Practice Guide, E 380-68) except that additional factors (*) commonly used in the Bureau have been added. Further discussion of definitions of quantities and units is given in the ASTM Metric Practice Guide.

The metric units and conversion factors adopted by the ASTM are based on the "International System of Units" (designated SI for Systeme International d'Unites), fixed by the International Committee for Weights and Measures; this system is also known as the Giorgi or MKSA (meter-kilogram (mass)-second-ampere) system. This system has been adopted by the International Organization for Standardization in ISO Recommendation R-31.

The metric technical unit of force is the kilogram-force; this is the force which, when applied to a body having a mass of 1 kg, gives it an acceleration of 9.80665 m/sec/sec, the standard acceleration of free fall toward the earth's center for sea level at 45 deg latitude. The metric unit of force in SI units is the newton (N), which is defined as that force which, when applied to a body having a mass of 1 kg, gives it an acceleration of 1 m/sec/sec. These units must be distinguished from the (inconstant) local weight of a body having a mass of 1 kg, that is, the weight of a body is that force with which a body is attracted to the earth and is equal to the mass of a body multiplied by the acceleration due to gravity. However, because it is general practice to use "pound" rather than the technically correct term "pound-force," the term "kilogram" (or derived mass unit) has been used in this guide instead of "kilogram-force" in expressing the conversion factors for forces. The newton unit of force will find increasing use, and is essential in SI units.

Where approximate or nominal English units are used to express a value or range of values, the converted metric units in parentheses are also approximate or nominal. Where precise English units are used, the converted metric units are expressed as equally significant values.

Table I

QUANTITIES AND UNITS OF SPACE

Multiply	By	To obtain
LENGTH		
Mil	25.4 (exactly)	Micron
Inches	25.4 (exactly)	Millimeters
Inches	2.54 (exactly)*	Centimeters
Feet	30.48 (exactly)	Centimeters
Feet	0.3048 (exactly)*	Meters
Feet	0.0003048 (exactly)*	Kilometers
Yards	0.9144 (exactly)	Meters
Miles (statute)	1,609.344 (exactly)*	Meters
Miles	1.609344 (exactly)	Kilometers
AREA		
Square inches	6.4516 (exactly)	Square centimeters
Square feet	*929.03	Square centimeters
Square feet	0.092903	Square meters
Square yards	0.836127	Square meters
Acres	*0.40469	Hectares
Acres	*4,046.9	Square meters
Acres	*0.0040469	Square kilometers
Square miles	2.58999	Square kilometers
VOLUME		
Cubic inches	16.3871	Cubic centimeters
Cubic feet	0.0283168	Cubic meters
Cubic yards	0.764555	Cubic meters
CAPACITY		
Fluid ounces (U.S.)	29.5737	Cubic centimeters
Fluid ounces (U.S.)	29.5729	Milliliters
Liquid pints (U.S.)	0.473179	Cubic decimeters
Liquid pints (U.S.)	0.473166	Liters
Quarts (U.S.)	*946.358	Cubic centimeters
Quarts (U.S.)	*0.946331	Liters
Gallons (U.S.)	*3,785.43	Cubic centimeters
Gallons (U.S.)	3.78543	Cubic decimeters
Gallons (U.S.)	3.78533	Liters
Gallons (U.S.)	*0.00378543	Cubic meters
Gallons (U.K.)	4.54609	Cubic decimeters
Gallons (U.K.)	4.54596	Liters
Cubic feet	28.3160	Liters
Cubic yards	*764.55	Liters
Acre-feet	*1,233.5	Cubic meters
Acre-feet	*1,233,500	Liters

Table II

QUANTITIES AND UNITS OF MECHANICS

Multiply	By	To obtain
MASS		
Grains (1/7,000 lb)	64.79891 (exactly)	Milligrams
Troy ounces (480 grains)	31.1035	Grams
Ounces (avdp)	28.3495	Grams
Pounds (avdp)	0.45359237 (exactly)	Kilograms
Short tons (2,000 lb)	907.185	Kilograms
Short tons (2,000 lb)	0.907185	Metric tons
Long tons (2,240 lb)	1,016.05	Kilograms
FORCE/AREA		
Pounds per square inch	0.070307	Kilograms per square centimeter
Pounds per square inch	0.689476	Newtons per square centimeter
Pounds per square foot	4.88243	Kilograms per square meter
Pounds per square foot	47.8803	Newtons per square meter
MASS/VOLUME (DENSITY)		
Ounces per cubic inch	1.72999	Grams per cubic centimeter
Pounds per cubic foot	16.0185	Kilograms per cubic meter
Pounds per cubic foot	0.0160185	Grams per cubic centimeter
Tons (long) per cubic yard	1.32894	Grams per cubic centimeter
MASS/CAPACITY		
Ounces per gallon (U.S.)	7.4893	Grams per liter
Ounces per gallon (U.K.)	6.2362	Grams per liter
Pounds per gallon (U.S.)	119.829	Grams per liter
Pounds per gallon (U.K.)	99.779	Grams per liter
BENDING MOMENT OR TORQUE		
Inch-pounds	0.011521	Meter-kilograms
Inch-pounds	1.12985×10^6	Centimeter-dynes
Foot-pounds	0.138255	Meter-kilograms
Foot-pounds	1.35582×10^7	Centimeter-dynes
Foot-pounds per inch	5.4431	Centimeter-kilograms per centimeter
Ounce-inches	72.008	Gram-centimeters
VELOCITY		
Feet per second	30.48 (exactly)	Centimeters per second
Feet per second	0.3048 (exactly)*	Meters per second
Feet per year	$*0.965873 \times 10^{-6}$	Centimeters per second
Miles per hour	1.609344 (exactly)	Kilometers per hour
Miles per hour	0.44704 (exactly)	Meters per second
ACCELERATION*		
Feet per second^2	*0.3048	Meters per second^2
FLOW		
Cubic feet per second (second-feet)	*0.028317	Cubic meters per second
Cubic feet per minute	0.4719	Liters per second
Gallons (U.S.) per minute	0.06309	Liters per second
FORCE*		
Pounds	*0.453592	Kilograms
Pounds	*4.4482	Newtons
Pounds	$*4.4482 \times 10^5$	Dynes

Table II—Continued

Multiply	By	To obtain
WORK AND ENERGY*		
British thermal units (Btu)	*0.252	Kilogram calories
British thermal units (Btu)	1,055.06	Joules
Btu per pound	2.326 (exactly)	Joules per gram
Foot-pounds	*1.35582	Joules
POWER		
Horsepower	745.700	Watts
Btu per hour	0.293071	Watts
Foot-pounds per second	1.35582	Watts
HEAT TRANSFER		
Btu in./hr ft^2 degree F (k, thermal conductivity)	1.442	Milliwatts/cm degree C
Btu in./hr ft^2 degree F (k, thermal conductivity)	0.1240	Kg cal/hr m degree C
Btu ft/hr ft^2 degree F	*1.4880	Kg cal m/hr m^2 degree C
Btu/hr ft^2 degree F (C, thermal conductance)	0.568	Milliwatts/cm^2 degree C
Btu/hr ft^2 degree F (C, thermal conductance)	4.882	Kg cal/hr m^2 degree C
Degree F hr ft^2/Btu (R, thermal resistance)	1.761	Degree C cm^2/milliwatt
Btu/lb degree F (c, heat capacity)	4.1868	J/g degree C
Btu/lb degree F	*1.000	Cal/gram degree C
Ft^2/hr (thermal diffusivity)	0.2581	Cm^2/sec
Ft^2/hr (thermal diffusivity)	*0.09290	M^2/hr
WATER VAPOR TRANSMISSION		
Grains/hr ft^2 (water vapor transmission)	16.7	Grams/24 hr m^2
Perms (permeance)	0.659	Metric perms
Perm-inches (permeability)	1.67	Metric perm-centimeters

Table III

OTHER QUANTITIES AND UNITS

Multiply	By	To obtain
Cubic feet per square foot per day (seepage)	*304.8	Liters per square meter per day
Pound-seconds per square foot (viscosity)	*4.8824	Kilogram second per square meter
Square feet per second (viscosity)	*0.092903	Square meters per second
Fahrenheit degrees (change)*	5/9 exactly	Celsius or Kelvin degrees (change)*
Volts per mil	0.03937	Kilovolts per millimeter
Lumens per square foot (foot-candles)	10.764	Lumens per square meter
Ohm-circular mils per foot	0.001662	Ohm-square millimeters per meter
Millicuries per cubic foot	*35.3147	Millicuries per cubic meter
Milliamps per square foot	*10.7639	Milliamps per square meter
Gallons per square yard	*4.527219	Liters per square meter
Pounds per inch	*0.17858	Kilograms per centimeter

GPO 835 - 188

ABSTRACT

Laboratory experiments, using a simplified air model, were conducted to obtain the correlation between draft tube shape and the draft tube surge characteristics—the range of occurrence, frequencies, and pressure amplitudes of the surges. Dimensionless parameters were used to compare results. The draft tube shape was found to have significant influence on the surging characteristics. Surge measurements obtained from two hydraulic turbine model studies are also compared using the dimensionless parameters. Hydraulic and air model studies of the same draft tube produced satisfactory correlation. The information presented can be used to predict the surge characteristics of prototype and model turbines, or as an aid in draft tube design where surge reduction or resonance minimization are considered as design criteria. Examples are included to illustrate application of the laboratory results.

ABSTRACT

Laboratory experiments, using a simplified air model, were conducted to obtain the correlation between draft tube shape and the draft tube surge characteristics—the range of occurrence, frequencies, and pressure amplitudes of the surges. Dimensionless parameters were used to compare results. The draft tube shape was found to have significant influence on the surging characteristics. Surge measurements obtained from two hydraulic turbine model studies are also compared using the dimensionless parameters. Hydraulic and air model studies of the same draft tube produced satisfactory correlation. The information presented can be used to predict the surge characteristics of prototype and model turbines, or as an aid in draft tube design where surge reduction or resonance minimization are considered as design criteria. Examples are included to illustrate application of the laboratory results.

ABSTRACT

Laboratory experiments, using a simplified air model, were conducted to obtain the correlation between draft tube shape and the draft tube surge characteristics—the range of occurrence, frequencies, and pressure amplitudes of the surges. Dimensionless parameters were used to compare results. The draft tube shape was found to have significant influence on the surging characteristics. Surge measurements obtained from two hydraulic turbine model studies are also compared using the dimensionless parameters. Hydraulic and air model studies of the same draft tube produced satisfactory correlation. The information presented can be used to predict the surge characteristics of prototype and model turbines, or as an aid in draft tube design where surge reduction or resonance minimization are considered as design criteria. Examples are included to illustrate application of the laboratory results.

ABSTRACT

Laboratory experiments, using a simplified air model, were conducted to obtain the correlation between draft tube shape and the draft tube surge characteristics—the range of occurrence, frequencies, and pressure amplitudes of the surges. Dimensionless parameters were used to compare results. The draft tube shape was found to have significant influence on the surging characteristics. Surge measurements obtained from two hydraulic turbine model studies are also compared using the dimensionless parameters. Hydraulic and air model studies of the same draft tube produced satisfactory correlation. The information presented can be used to predict the surge characteristics of prototype and model turbines, or as an aid in draft tube design where surge reduction or resonance minimization are considered as design criteria. Examples are included to illustrate application of the laboratory results.

REC-ERC-72-24
Palde, U J
INFLUENCE OF DRAFT TUBE SHAPE ON SURGING CHARACTERISTICS OF REACTION TURBINES
Bur Reclam Rep REC-ERC-72-24, Div Gen Res, September 1972. Bureau of Reclamation, Denver, 29 p, 22 fig, 2 tab, 5 ref, append

DESCRIPTORS--/ *draft tubes/ turbines/ *surges/ *hydroelectric powerplants/ hydraulic machinery/ fluid mechanics/ dimensional analysis/ model tests/ fluid flow/ pressure/ frequency/ *shape/ resonance/ test results/ hydraulic design/ *reaction turbines/ hydraulic turbines/ noise (sound)/ hydraulic models/ vibration/ wicket gates/ hydraulic similitude
IDENTIFIERS--/ hydraulic pressure tests/ Fontenelle Dam, Wyo/ Grand Coulee Powerplant, Wash/ water pressure tests

REC-ERC-72-24
Palde, U J
INFLUENCE OF DRAFT TUBE SHAPE ON SURGING CHARACTERISTICS OF REACTION TURBINES
Bur Reclam Rep REC-ERC-72-24, Div Gen Res, September 1972. Bureau of Reclamation, Denver, 29 p, 22 fig, 2 tab, 5 ref, append

DESCRIPTORS--/ *draft tubes/ turbines/ *surges/ *hydroelectric powerplants/ hydraulic machinery/ fluid mechanics/ dimensional analysis/ model tests/ fluid flow/ pressure/ frequency/ *shape/ resonance/ test results/ hydraulic design/ *reaction turbines/ hydraulic turbines/ noise (sound)/ hydraulic models/ vibration/ wicket gates/ hydraulic similitude
IDENTIFIERS--/ hydraulic pressure tests/ Fontenelle Dam, Wyo/ Grand Coulee Powerplant, Wash/ water pressure tests

REC-ERC-72-24
Palde, U J
INFLUENCE OF DRAFT TUBE SHAPE ON SURGING CHARACTERISTICS OF REACTION TURBINES
Bur Reclam Rep REC-ERC-72-24, Div Gen Res, September 1972. Bureau of Reclamation, Denver, 29 p, 22 fig, 2 tab, 5 ref, append

DESCRIPTORS--/ *draft tubes/ turbines/ *surges/ *hydroelectric powerplants/ hydraulic machinery/ fluid mechanics/ dimensional analysis/ model tests/ fluid flow/ pressure/ frequency/ *shape/ resonance/ test results/ hydraulic design/ *reaction turbines/ hydraulic turbines/ noise (sound)/ hydraulic models/ vibration/ wicket gates/ hydraulic similitude
IDENTIFIERS--/ hydraulic pressure tests/ Fontenelle Dam, Wyo/ Grand Coulee Powerplant, Wash/ water pressure tests

REC-ERC-72-24
Palde, U J
INFLUENCE OF DRAFT TUBE SHAPE ON SURGING CHARACTERISTICS OF REACTION TURBINES
Bur Reclam Rep REC-ERC-72-24, Div Gen Res, September 1972. Bureau of Reclamation, Denver, 29 p, 22 fig, 2 tab, 5 ref, append

DESCRIPTORS--/ *draft tubes/ turbines/ *surges/ *hydroelectric powerplants/ hydraulic machinery/ fluid mechanics/ dimensional analysis/ model tests/ fluid flow/ pressure/ frequency/ *shape/ resonance/ test results/ hydraulic design/ *reaction turbines/ hydraulic turbines/ noise (sound)/ hydraulic models/ vibration/ wicket gates/ hydraulic similitude
IDENTIFIERS--/ hydraulic pressure tests/ Fontenelle Dam, Wyo/ Grand Coulee Powerplant, Wash/ water pressure tests

IAHR AIRH

SYMPOSIUM 1974

MODEL AND PROTOTYPE TURBINE DRAFT TUBE SURGE ANALYSIS BY THE SWIRL MOMENTUM METHOD

Uldis J. Palde — United States — Denver, Colorado
Hydraulic Engineer — Bureau of Reclamation — USA

SYNOPSIS

Turbine draft tube surges result from excessive swirl in the flow entering the draft tube. A quantitative measure of the swirl is obtained by computing the dimensionless "momentum parameter" of the swirl, $\Omega D_3/\rho Q^2$ (where Ω is the flux of angular momentum, D_3 is the draft tube inlet diameter, ρ is the fluid density, and Q is the discharge). Turbine model study results show that surging occurs only at operating points where the momentum parameter is greater than a critical value for the particular draft tube. The method is used to identify surge-free and surging areas on model and prototype turbine performance diagrams. A prediction of the surging range and frequencies is compared to measurements subsequently obtained on the prototype.

Les ondes de surpression dans l'aspirateur de la turbine proviennent d'un tourbillonnement excessif du courant y pénétrant. Une mesure quantitative de ce tourbillon peut être obtenue en faisant intervenir le "paramêtre du moment" de ce dernier $\Omega D_3/\rho Q^2$ (où Ω est le flux du moment angulaire, D_3 - le diamètre à l'admission du conduit, ρ - la densité du fluide, et Q - la décharge). Les résultats de l'étude d'un modèle de turbine montrent que les ondes de surpression n'apparaissent qu'en certains points, là où le paramêtre du moment est plus grand qu'une certaine valeur critique pour ce genre de conduit. La méthode est utilisée pour déterminer les zônes avec et sans ondes de surpression d'après les diagrammes de fonctionnement d'un modèle et d'un prototype. L'estimation de l'importance et de la fréquence des ondes de surpression est alors comparée aux résultats obtenus ensuite sur le prototype.

INTRODUCTION

Turbine draft tube surges arise as a result of excessive swirl remaining in the flow leaving the runner and entering the draft tube. Cassidy and Falvey [1] proposed that a dimensionless "momentum parameter,"

$$Swirl = \frac{\Omega D_3}{\rho Q^2}$$

where Ω = angular momentum (moment of momentum per second)

D_3 = draft tube inlet diameter

ρ = fluid density

Q = discharge

could be used as a measure of the amount of swirl in the flow. The momentum parameter reflects the ratio of angular to linear momentum of the swirling flow. Thus, when there is no net angular momentum in the flow, the momentum parameter equals zero. Experiments indicated that for a particular draft tube shape, periodic pressure pulsations occur only above a critical $\Omega D_3/\rho Q^2$ value, and that frequencies and amplitudes, expressed in dimensionless form, were unique functions of the momentum parameter.

Cassidy and Falvey showed that the pressure pulsations are initiated simultaneously with the occurrence of the flow phenomenon known as "vortex breakdown." After vortex breakdown has taken place, the flow is characterized by a spiraling (helical) vortex and reverse flow along the axis. The spiraling vortex produces periodic, high-intensity pressure fluctuations in the tube. Evaluation of the momentum parameter for the swirl in the flow leaving a Francis turbine runner was first presented by Falvey and Cassidy [2] in 1970. The effect of the draft tube shape on surge frequencies and amplitudes was thoroughly investigated and reported by Palde [3]. All experimental work in connection with the above studies was performed at the Bureau of Reclamation laboratories on a special model where the swirl could be easily controlled and measured, using air as the fluid.

METHOD OF ANALYSIS AND COMPUTATION

The evaluation of the momentum parameter for the flow entering a turbine draft tube consists of computing the dimensionless momentum flux introduced by the wicket gates and subtracting the amount of momentum flux converted to torque by the runner,

$$\frac{\Omega D_3}{\rho Q^2} = \left(\frac{\Omega D_3}{\rho Q^2}\right)_{W.G.} - \left(\frac{\Omega D_3}{\rho Q^2}\right)_r \qquad (1)$$

$$\text{where } \left(\frac{\Omega D_3}{\rho Q^2}\right)_{W.G.} = \frac{D_3 R \sin\alpha}{BNS} \qquad (2)$$

$$\text{and } \left(\frac{\Omega D_3}{\rho Q^2}\right)_r = \frac{PD_3}{\rho\omega Q^2} \qquad (3)$$

The symbols used in Equation (2) are defined in Figure 1.

In Equation (3),

P = turbine power output

ρ = density of water

ω = angular velocity of the turbine

Q = discharge through the turbine

The direction of flow through the gates is defined to be perpendicular to the minimum space between the tail of a gate and the body of the adjacent downstream gate. R, α, and S are evaluated for several gate positions using a graphical gate layout, and the results can be used to construct the curves shown in Figure 2a. The entire term $D_3 R \sin\alpha / BNS$ can be evaluated for each gate opening, resulting in a single wicket gate momentum parameter curve shown in Figure 2b. The shape of the curve is a function of the particular wicket gate shape and layout.

Inspection of Equations (1), (2), and (3) reflects the advantage of employing the momentum parameter method to define the amount of swirl in the flow. The momentum parameter can be computed if the wicket gate layout and shape are known, and the performance characteristics of the turbine are available. The procedure is much simpler than direct measurement on a model of the entire velocity vector distribution in the flow entering the draft tube. The method, however, does not always yield accurate results. Much of the inaccuracy is thought to be due to the oversimplification inherent in the graphical method of determining the angular momentum of the flow through the wicket gates. Laboratory studies of flow through the wicket gates are being planned to determine how the accuracy of the momentum parameter method could be improved.

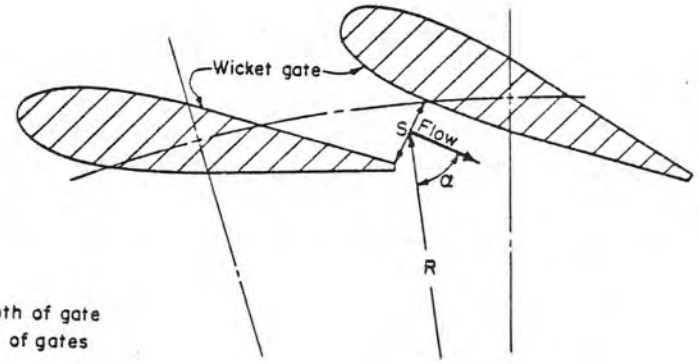

Figure 1. Definition sketch of flow leaving wicket gates and entering turbine runner.

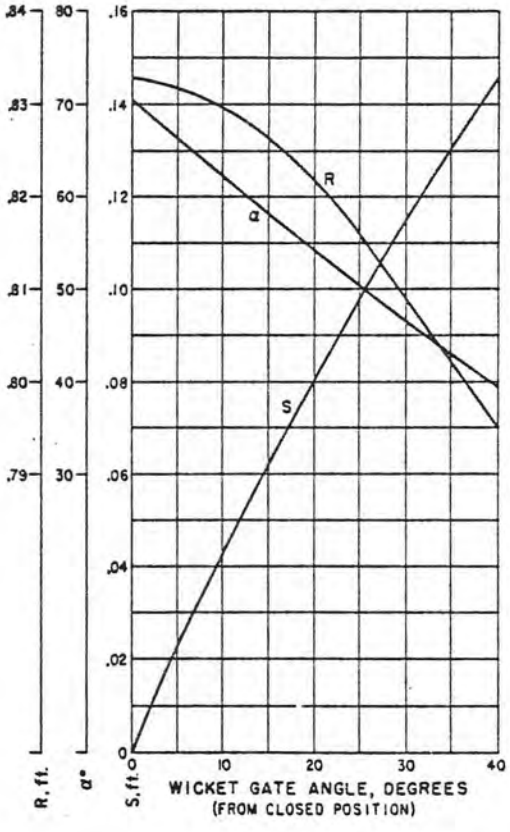

a. Variation of R, α, and S with wicket gate angle.

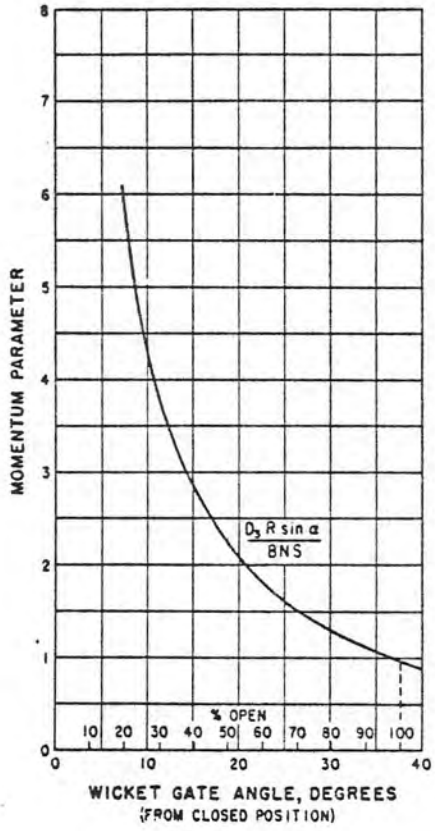

b. Wicket gate momentum parameter as function of gate angle.

Figure 2. Wicket gate geometric characteristics for Grand Coulee Pumping Plant pump turbines (Units 7 and 8).

TURBINE MODEL STUDIES

The Bureau of Reclamation recently installed a high head model turbine test stand at its Estes Powerplant in Colorado. A 1:3.333 scale model (9" throat diameter) of the Francis turbines for the first three 600 MW units of Grand Coulee Third Powerplant was initially installed in the stand. Dominion Engineering Works of Montreal designed the turbine and built the model. The primary emphasis during the initial tests performed during 1973 was on draft tube surge investigations.

Model Test Data

Data were obtained to evaluate performance characteristics using an automatic data acquisition and computation system. Draft tube pressures were measured at two locations in the throat by means of piezometers and pressure transducers. The pressure output signal was recorded by an oscillograph. The signal was also monitored on a retentive-screen oscilloscope, allowing for convenient determination of surge frequencies. Amplitude of pressure fluctuations was monitored on a root-mean-square meter.

For each model turbine test point the combination of Equations (1), (2), and (3) was used to compute the momentum parameter:

$$\frac{\Omega D_3}{\rho Q^2} = \frac{D_3 R \sin \alpha}{BNS} - \frac{PD_3}{\rho \omega Q^2} \qquad (4)$$

The dimensionless frequency parameter

$$\frac{fD_3^3}{Q}$$

and the dimensionless pressure parameter

$$\frac{D_3^4 \sqrt{(P')^2}}{\rho Q^2}$$

as well as the root-mean-square pressure $\sqrt{(P')^2}$ as percent of net test head, were also computed for each run.

Range of Surging in Model

Although the model could be tested under the prototype range of net heads of 67 meters to 108 meters, most of the tests were performed at lower than prototype heads. The speed coefficient

$$\phi_2 = \frac{\pi D_2 n}{60\sqrt{2gH}} \qquad (5)$$

where D_2 = runner throat diameter

n = rotational speed in RPM, and

H = net head across turbine

was used as the independent test point variable. From the test results it was verified that at a given opening and a particular value of ϕ_2 the same value of $\Omega D_3/\rho Q^2$ is computed by Equation (4) for any combination of rotational speed and head yielding the given ϕ_2 value. In other words, the momentum parameter is a function of the gate opening and ϕ_2. The characteristic momentum parameter contours (plotted, for instance, on a specific power, P_{11}, vs ϕ_2 diagram) can therefore be obtained from tests at any head. The range of surging is then defined by the $\Omega D_3/\rho Q^2$ contour above which surging occurs for the particular draft tube being used. Figure 3, plotted from the results of the Grand Coulee model draft tube surge tests, illustrates the above principle. The critical momentum parameter value in the model was observed to vary between about 0.31 and 0.34, depending on gate opening and the cavitation factor, sigma. A critical momentum parameter value of 0.33 has been used in Figure 3 to delineate the periodic surge area.

Range of Surging in Prototype

Equation (4) can be applied to the prototype in the same manner. The wicket gate momentum parameter curve derived from Equation (2) is the same for the model and the prototype, since it depends entirely on geometry. The first term on the right of Equation (4) is therefore already known for all gate openings. The second term is evaluated from prototype quantities stepped up from model data. Instead of presenting the predicted prototype draft tube surges for the Grand Coulee 600 MW turbines, a prediction (using the same method) for the Grand Coulee Pumping Plant Pump-Turbines, for which comparative data from actual prototype operation are available, is presented later in the paper.

Effect of Draft Tube Vortex Core on Surging

A visible vortex core below the turbine runner at certain gate openings and operating conditions is commonly accepted as somehow related to the occurrence of draft tube surging. The association is valid only in this respect: If a hollow vortex core is present, its instability and draft tube surging are one and the same occurrence. This fact offers no information, however, about the operating points at which surging will occur.

Observations of flow in the draft tube over a wide range of test conditions disclosed that a hollow vortex core in the flow below the runner was neither necessary now sufficient for draft tube surging to occur. Rather, the model studies indicated that the intensity of swirl (as measured by the value of the momentum

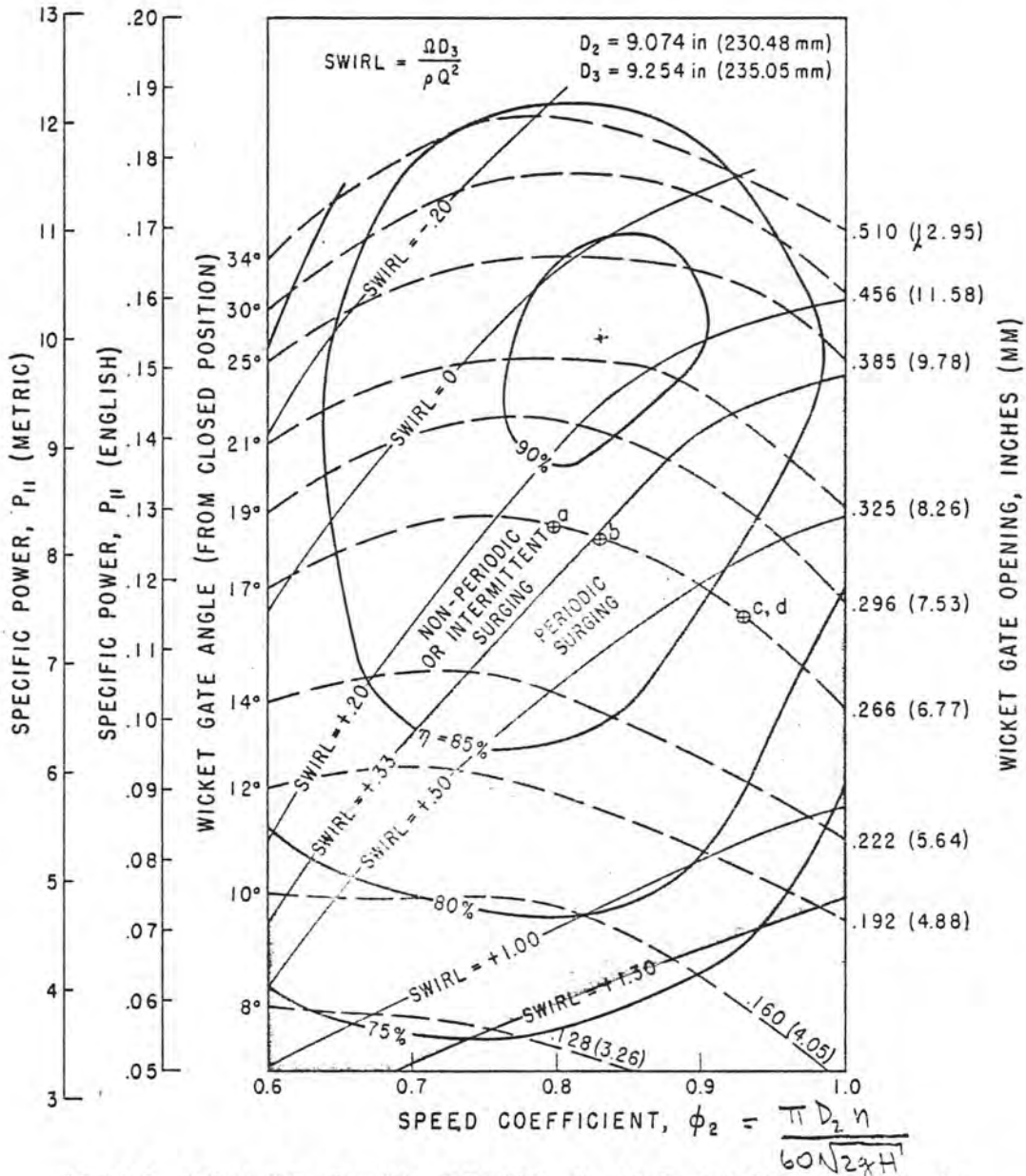

GRAND COULEE THIRD POWER PLANT UNITS 19, 20, 21
DEW 9" MODEL TURBINE

Figure 3. Range of surging as determined from model tests of the Grand Coulee Third Powerplant 600 MW turbines (model scale 1:40.333).

$f = ?, \sqrt{\overline{(P')^2}} = 0.8\%$ of H

a. Irregular pressure pulsations. $\Phi_2 = .80$, $\delta = .12$, $\frac{\Omega D}{\rho Q^2} = .27$, $\frac{fD^3}{Q} = ?$

$f = 7.8$ Hz, $\sqrt{\overline{(P')^2}} = 0.7\%$ of H

b. Surging at critical swirl. $\Phi_2 = .83$, $\delta = .12$, $\frac{\Omega D}{\rho Q^2} = .33$, $\frac{fD^3}{Q} = .34$

$f = 12.0$ Hz, $\sqrt{\overline{(P')^2}} = 2.1\%$ of H

c. Surging at high tailwater. $\Phi_2 = .93$, $\delta = .26$, $\frac{\Omega D}{\rho Q^2} = .58$, $\frac{fD^3}{Q} = .52$

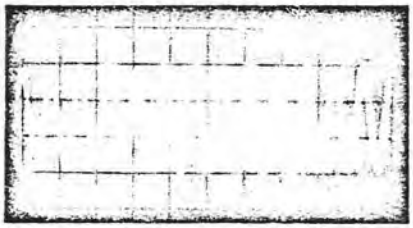

$f = 13.0$ Hz, $\sqrt{\overline{(P')^2}} = 2.5\%$ of H

d. Surging at low tailwater. $\Phi_2 = .93$, $\delta = .10$, $\frac{\Omega D}{\rho Q^2} = .59$, $\frac{fD^3}{Q} = .54$

Figure 4. Photos of draft tube wall pressure fluctuation traces displayed on a retentive oscilloscope screen, and corresponding flow conditions. Wicket gates at 17°, or approximately 45% of rated output gate.

parameter) was clearly the governing factor for the occurrence of surging. Figure 4 illustrates some relationships between the vortex core and surging. Figure 4b. shows a hollow vortex core which appears to be vertical. However, the vortex does in fact deflect toward the wall (thus becoming a spiraling vortex) farther downstream in the draft tube, producing low amplitude pressure pulsations throughout the tube. At lower momentum parameter values (between about 0.10 and 0.20) a vertical hollow core exists at some gate openings and sufficiently low tailwater values. The overall swirl is not high enough, however, to deflect the vortex core, and thus surging does not occur. The condition shown in Figure 4c., with higher swirl, produces high amplitude surging without the presence of a hollow vortex core. Figure 4d. shows flow conditions with the same amount of swirl as in 4c., but with lower tailwater producing a highly visible, spiraling hollow vortex core. The above operating points have been marked on the model hill curves, Figure 3, with letters on the plot corresponding to letters designating the photos in Figure 4.

PROTOTYPE SURGE ANALYSIS

The swirl momentum method was used to predict the surging characteristics of the Grand Coulee Pumping Plant Pump-Turbines, Units 7 and 8. Performance and draft tube surge test data from a homologous model were available from the model test report of the manufacturer, NOHAB of Trollhättan, Sweden. Additional surging characteristic data for the particular draft tube shape were obtained with the Bureau of Reclamation simplified air model. The relationships between the

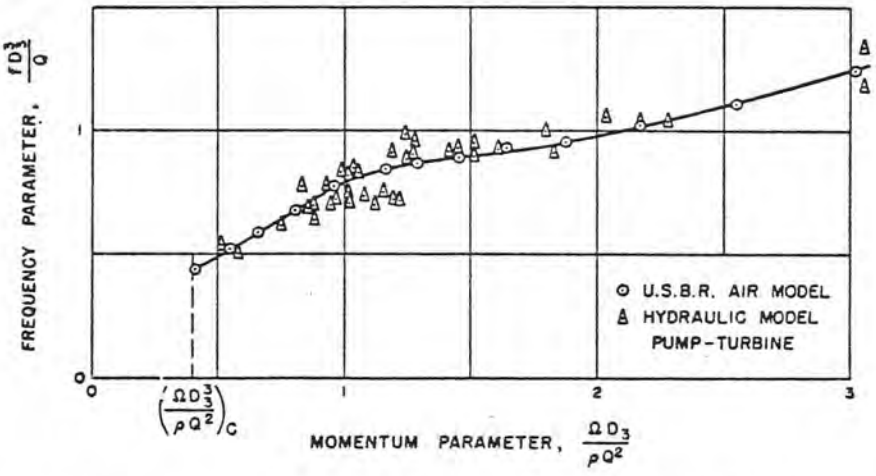

Figure 5. Frequency parameter curve for the Grand Coulee Pump-Turbine draft tube computed from two independent model tests.

mementum and frequency parameters determined from the two tests are shown in Figure 5. The critical momentum parameter value was found to be between about 0.4 and 0.5, but a value of 0.40 has been used in this application.

Method of Computation from Model Data

The value of the momentum parameter for each point of computation was determined from Figure 2b. In the second term P and Q were obtained from expected prototype quantities given in the NOHAB model test report. The computed value of the momentum parameter for each point was entered in Figure 5 to obtain the value of the frequency parameter, fD_3^3/Q, from which the frequency was determined. Figure 6 shows the results of the surging prediction. Surging is expected to occur over the dark shaded areas, where the value of the momentum parameter is greater than 0.40 (absolute value). Intermittent periodic and/or irregular high amplitude pressure pulsations can be expected to occur between contours of about 0.25 and 0.40 (absolute value), the light shaded areas in the figure.

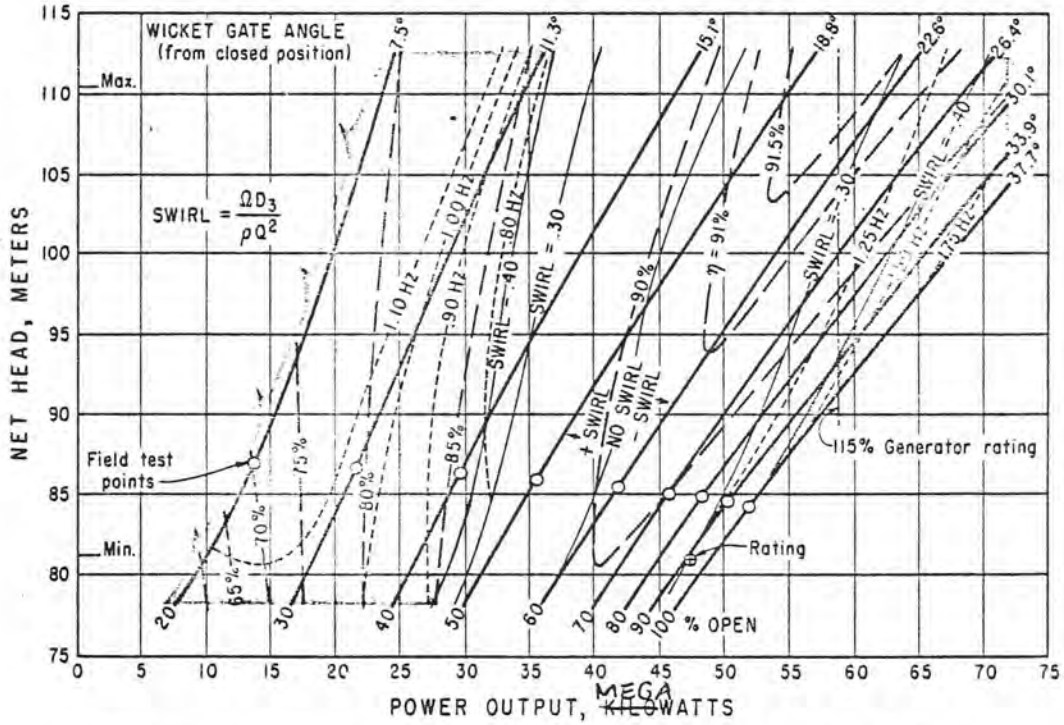

GRAND COULEE PUMPING PLANT UNITS P/T-7 AND P/T-8

Figure 6. Expected turbine performance and predicted draft tube surge range and frequencies for the Grand Coulee Pump-Turbines.

Prototype Field Tests

Draft tube surge test data were obtained at several gate settings over the entire operating range, at a gross head of about 87 meters (286 feet). The test points are shown as circles on the plot of Figure 6. The predictions and results of the field tests are compared in the table below.

RUN NO	GATES		PREDICTED		MEASURED	
	%	DEGREES	SURGE	FREQ. (Hz)	SURGE	FREQ. (Hz)
1	14	5.2	YES	?	NO	—
2	20	7.4	YES	1.10	YES	.70
3	30	11.3	YES	1.07	YES	1.30
4	40	15.1	YES	.85	YES	1.47
5	50	18.8	NO	—	YES	1.14
6	60	22.6	NO	—	NO	—
7	70	26.4	NO	—	NO	—
8	80	30.1	NO	—	NO	—
9	90	33.9	INTERM.	1.25	NO	—
10	100	37.7	INTERM.	1.50	NO	—

The measured range of surging at about 87 meters net head extends to slightly higher gate openings than the predicted range. Measured frequencies are higher than those predicted (by as much as 75 percent at 40 percent gate) over most of the surging range. It should be noted that for this turbine (n = 200 rpm) the well-known Rheingans [4] formula, $f = n/(60 \times 3.6)$, predicts a surge frequency of 0.93 Hz. The above comparison may therefore be considered good in relation to the available knowledge of surge frequency prediction.

IMPROVEMENTS NEEDED IN THE METHOD

The above example is the first known instance where predicted surge computations using the swirl momentum method were checked in the field. The comparison indicates that the method needs improvement. This has been confirmed by recent computations for model turbines also, where the surging range predicted by application of Equation (4) did not agree with observations in the model.

The most likely cause for the disagreement can be attributed to the evaluation of Equation (2), i.e., the curve in Figure 2b. On examining the definition sketch in Figure 1 it is evident that the effective values of R and α (and possibly S) could be considerably different than those obtained from the simplified graphical analysis, which does not take into account the influence of upstream conditions.

Stay vanes could certainly influence the flow direction. Circulation arising from flow through the spiral case could also influence the angular momentum of the flow.

A correct evaluation of the wicket gate momentum parameter curve is absolutely necessary for usefulness of the momentum parameter method. Experimental or improved analytical methods could be employed to achieve the desired accuracy. A study to better define the flow through the wicket gates is presently in progress at the Bureau of Reclamation.

The effect of an improved momentum parameter curve can be applied qualitatively to the surge prediction for the case of the Grand Coulee Pump-Turbines. A momentum parameter curve (Figure 2b) giving values only about 0.25 to 0.30 higher in the vicinity of 50-percent gate would have produced a prediction agreeing much more closely with the field measurements. The range of surging would cover the field test point at 50-percent gate, as it should. The predicted frequencies would be about 20 percent higher. Also, the computed zero swirl line shown in Figure 6 would fall to the right of the efficiency contour peaks, as it probably should.

FUTURE APPLICATIONS

The swirl momentum method can be improved to produce better predictions of prototype surging. Even with present limitations, the method can be used to evaluate proposed changes in turbine design directed toward increasing the surge-free operating range of Francis turbines. Equation (4) relates turbine dimensions or quantities affecting the value of the momentum parameter, i.e., the amount of swirl. Continued investigations may disclose how flow passages may be shaped to reduce the swirl in common turbine operating areas, thus increasing the surge-free operating range.

CONCLUSION

The swirl momentum method is a useful tool for the analysis and prediction of surging characteristics of prototype Francis turbines. The accuracy of the method must be improved, however, before it can be applied with full confidence for prototype predictions.

ACKNOWLEDGMENT

Appreciation is expressed to Fred Ruud, Bureau of Reclamation, for his special effort in obtaining the field data needed for the comparison of the Grand Coulee Pump-Turbine surging characteristics. The data were obtained on Unit 7 during acceptance tests in November 1973.

REFERENCES

1. Cassidy, J. J. and Falvey, H. T., "Observations of Unsteady Flow Arising after Vortex Breakdown," Journal of Fluid Mechanics, Vol. 41, Part 4, pp 727-736, 1970

2. Falvey, H. T. and Cassidy, J. J., "Frequency and Amplitude of Pressure Surges Generated by Swirling Flow," Transactions of Symposium, Stockholm, 1970, IAHR, Part 1, Paper E1, Stockholm, Sweden, 1970

3. Palde, J. J., "Influence of Draft Tube Shape on Surging Characteristics of Reaction Turbines," Report REC-ERC-72-24, U.S. Bureau of Reclamation, Denver, Colorado, USA, 1972

4. Rheingans, W. J., "Power Swings in Hydroelectric Power Plants," Transactions, American Society of Mechanical Engineers, Vol. 62, pp 171-184, 1940.

IAHR

HENRY T. FALVEY

8TH SYMPOSIUM 8E

SECTION FOR HYDRAULIC MACHINERY EQUIPMENT AND CAVITATION

6-9 SEPTEMBER 1976
LENINGRAD, USSR

INITIAL OPERATION OF 600-MW TURBINES AT GRAND COULEE THIRD POWERPLANT

by

Frederick O. Ruud*

SUMMARY

The first 600-MW hydroelectric generator at Grand Coulee Third Powerplant was started on August 25, 1975. Initial operation and testing of the unit is described. Load rejection tests were made up to and including 690 MW. Sustained load tests indicated draft tube surges at loads of 300 to 400 MW.

Oscillograph records were taken of vertical thrust, lateral shaft motion, pressure changes, gate opening, and speed. Records of the initial start, the load rejections, and draft tube surges versus power swings for the full range of operation are presented and discussed.

Le première générateur hydro-électrique de puissance de 600 MW dans l'usine génératrice troisième à Grand Coulee a commencé d'opérer le 25 août 1975. Le fonctionnement préliminaire et essayage de l'unité se decrivent. Essais de déclenchement de charge ont été fait jusqu'à génération de 690 MW. Essais à charge soutenue ont indiqué ondes dan le tuyau d'échappement à charges de 300 à 400 MW.

On a enregistré par oscillographe pousée verticale, mouvement latéral de l'arbe, changements de pression, ouverture de la vanne et vitesse angulaire de la roue. Enregistrements de la début, des essais de déclenchement de charge et des ondes dams le tuyau d'echappement en fonction de variations de puissance par la gamme entiere de fonctionnement se donnent et se discutent.

*Head, Special Studies and Testing Section
Bureau of Reclamation, Denver, Colorado, USA

INTRODUCTION

The 600-MW hydroelec
largest hydraulic tu
Pacific Northwest po
transmitted over int
units are under cons
plant to 3,900 MW.
capacity at Grand Co

INSTRUMENTATION

The large size of th
operation led to the
shows the general ou

An eight-channel dir
deflection near the
ing and rotating spe
the load rejections,

In addition, a recor
the full range of op
in the paper, and ar

INTRODUCTION

The 600-MW hydroelectric units at Grand Coulee Third Powerplant are presently the largest hydraulic turbines in existence. These units provide peaking power to the Pacific Northwest power grid. Energy surplus to local needs in the Northwest is transmitted over intertie lines to the Southwest during summer months. Additional units are under construction to bring the installed capacity of the Third Powerplant to 3,900 MW. More units are presently planned to bring the total installed capacity at Grand Coulee to approximately 10,000 MW.

INSTRUMENTATION

The large size of these units and the need for information regarding their initial operation led to the decision to measure certain important parameters. Figure 1 shows the general outline of the shaft and the shaft deflection gage locations.

An eight-channel direct-writing oscillograph was used to record thrust, shaft deflection near the guide bearings, penstock and draft tube pressures, gate opening and rotating speed. These records were taken during the initial start and the load rejections, as well as during normal operations.

In addition, a record of draft tube surges versus power output was obtained for the full range of operation. Photographs of these original records are included in the paper, and are marked with appropriate information.

Third Powerplant was
g of the unit is
uding 690 MW. Sus-
300 to 400 MW.

al shaft motion, pres-
itial start, the load
the full range of

600 MW s l'usine
le 25 août 1975. Le
crivent. Essais de
de 690 MW. Essais à
ment à charges de

ement latéral de l'arbe,
e angulaire de la roue.
de charge et des ondes
puissance par la gamme

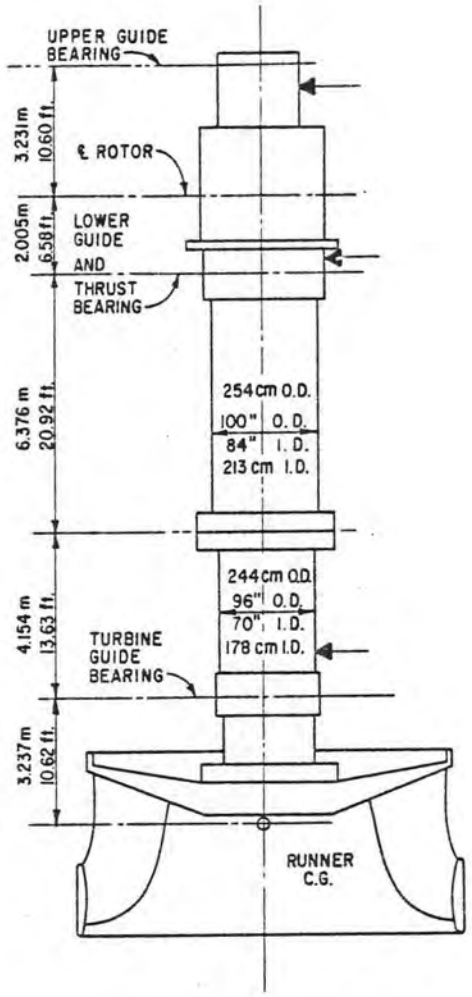

FIGURE 1. LOCATION OF SHAFT DEFLECTION GAGES.

INITIAL STARTUP

The first operatio
oscillograph recor
are typical of the

Upon starting, the
sure. As the gate
to vibrate in the
ment of the shaft
bearing.

The vertical thrust
The apparent natura
seen to be about 7
A timing trace mark

The lateral shaft m
mately 0.012 inch (
0.004 inch (0.1 mm)
guide bearing. The
an apparent 0.005-in
main shaft.

On September 4, 1975
load rejection tests

INITIAL STARTUP

The first operation of the 600-MW unit was on August 25, 1975. Figure 2 shows the oscillograph record of the initial start. Certain phenomena shown on this record are typical of the transient operation of hydroelectric units.

Upon starting, the gates were opened rapidly to about 12 percent followed by reclosure. As the gates open to admit substantial flow to the turbine, the shaft begins to vibrate in the horizontal and vertical directions. The maximum horizontal movement of the shaft was about 0.046 inch (1.2 mm) at the lower generator guide bearing.

The vertical thrust varies from 2,500 tons (22.24 MN) to 4,500 tons (40.03 MN). The apparent natural frequency of vertical oscillation of the rotating parts is seen to be about 7 Hz. Downsurge in the penstock was about 25 psi (0.172 MPa). A timing trace marking 1-second intervals is at the bottom of each record.

The lateral shaft movements on this and subsequent runs ultimately became approximately 0.012 inch (0.3 mm) peak-to-peak at the upper generator guide bearing, 0.004 inch (0.1 mm) at the lower guide, and 0.004 inch (0.1 mm) at the turbine guide bearing. The larger runout at the upper guide was considered to be due to an apparent 0.005-inch (0.13-mm) misalinement of the auxiliary shaft above the main shaft.

On September 4, 1975, following preliminary tests and equipment adjustments, the load rejection tests began. The 150-MW test was conducted without incident. The

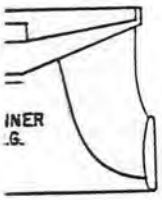

DEFLECTION GAGES.

FIGURE 2. INITIAL START, UNIT 19, GC III.

5,000 T = 44.5 MN, 0.050 inch = 1.27 mm
200 psi = 1.38 MPa, 35 psi = 0.24 MPa

penstock pressure
cent and the thrus
runouts were essen

Upon building up lo
surges at a gate op
dicted by model stu
mately 337 ft (103
(55.2 kPa) commence
increased severely.
except for the ecce
outs increased an a
ing, 0.010 inch (0.
(0.35 mm) at the tu
500 tons (4.45 MN)

Figure 3 shows the c

Various systems of a
the draft tube surge
partially effective
of the shaft were un

One may note that th
the unit to oscillat
lated for some time.

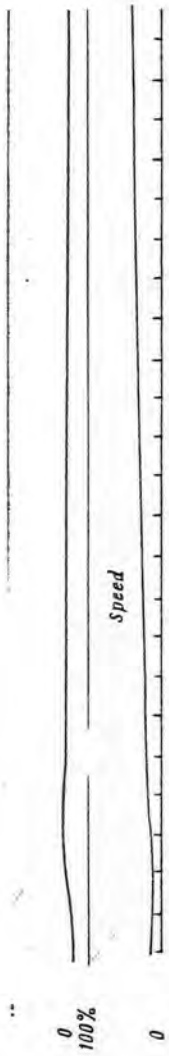

FIGURE 2. INITIAL START, UNIT 19, GC III.

5,000 T = 44.5 MN, 0.050 inch = 1.27 mm
200 psi = 1.38 MPa, 35 psi = 0.24 MPa

penstock pressure rise was 18 psi (0.124 MPa), the speed increase was about 5 percent and the thrust load was momentarily reduced by 500 tons (4.45 MN). Bearing runouts were essentially unchanged.

Upon building up load for the 300-MW rejection, the unit began to show draft tube surges at a gate opening of 34 percent. Reference 1 describes the surging predicted by model studies of this unit. The gross head at this time was approximately 337 ft (103 m). The output was about 310 MW when surges of about 8 psi (55.2 kPa) commenced in the draft tube. Simultaneously, the shaft runouts increased severely. Prior to surging, the runouts were about 0.003 inch (0.08 mm) except for the eccentricity of the stub shaft. During surging, the shaft runouts increased an additional 0.010 inch (0.25 mm) at the upper guide bearing, 0.010 inch (0.25 mm) at the lower generator guide bearing and 0.014 inch (0.35 mm) at the turbine guide bearing. Vertical thrust variations of up to 500 tons (4.45 MN) were noted in synchronism with the draft tube surges.

Figure 3 shows the onset of surging, and the record of the events discussed.

Various systems of admitting compressed air were used in an attempt to reduce the draft tube surges. Adding compressed air to the center of the runner was partially effective in reducing the pressure surges. However, the movements of the shaft were unchanged.

One may note that the periodic draft tube pressure surges caused the shaft of the unit to oscillate at the same frequency. This phenomenon had been postulated for some time. These tests were the first instance where we have obtained

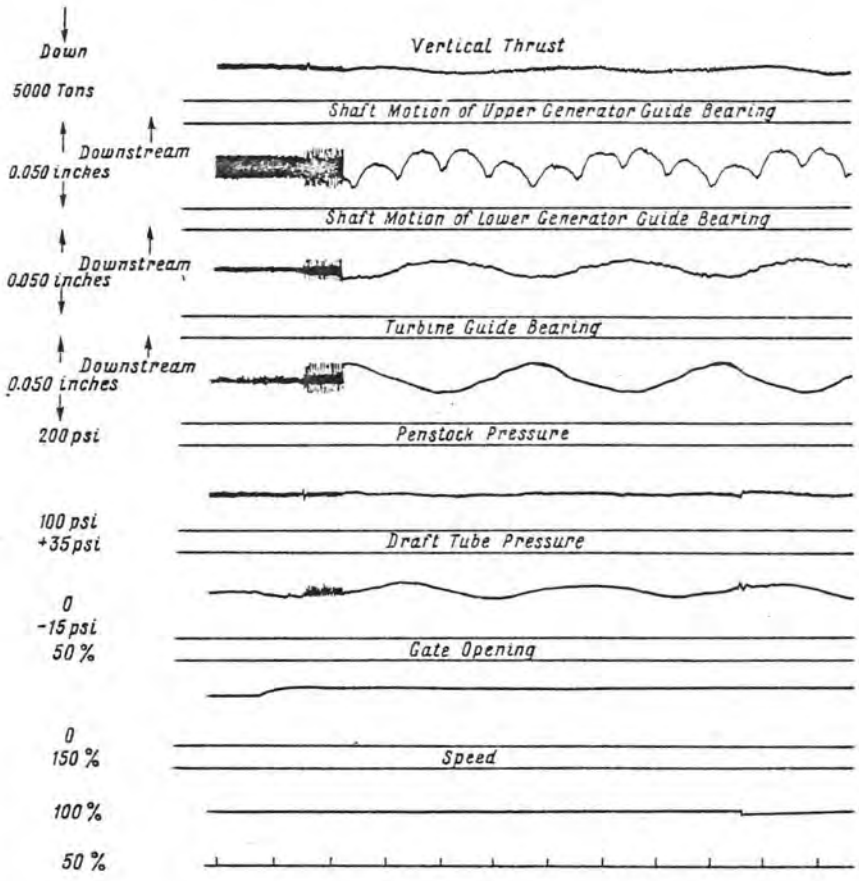

FIGURE 3. ONSET OF SURGING AT 300 MW, UNIT 19, GC III.

5,000 T = 44.5 MN, 0.050 inch = 1.27 mm
200 psi = 1.38 MPa, 35 psi = 0.24 MPa

prototype records of
is believed the shaft
turbine runner. This
units at Grand Coulee
occurrence on all uni

Because the shaft mot
might increase as hig
would increase at 400
amount of surging in
air being periodicall
Pressure variations i
runouts were less tha
without special preca

Since the unit was su
However, it was decid
erating speed and red
of the unit. Upon 30
and the speed rise was
slight increase in thr
2,500 tons (22.2 MN)
static amount of 2,800
normal values of less

Figure 4 shows the osc

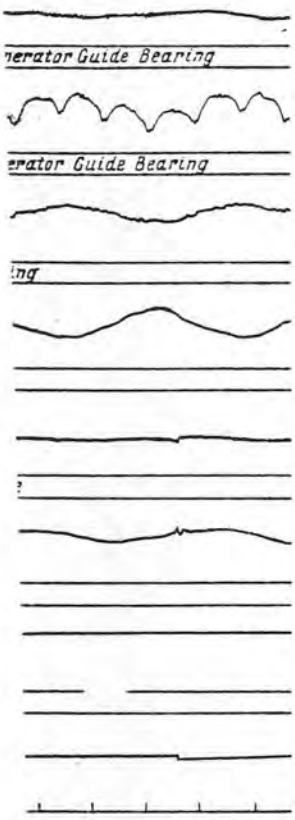

UNIT 19, GC III.

= 1.27 mm
.24 MPa

prototype records of shaft movements directly caused by draft tube surges. It is believed the shaft deflection was caused by pressure unbalance beneath the turbine runner. This effect has been subsequently verified on the other smaller units at Grand Coulee. However, the phenomenon is believed to be a general occurrence on all units having draft tube surges.

Because the shaft motion was substantial, concern was expressed that the motion might increase as higher loads were attained. Model data had indicated the surging would increase at 400 MW. However, as the generator output reached 400 MW, the amount of surging in the draft tube was reduced. This was due to atmospheric air being periodically drawn into the draft tube through the center of the runner. Pressure variations in the draft tube decreased to about 5 psi (34.5 kPa) and shaft runouts were less than 0.005 inch (0.13 mm). The unit was subsequently operated without special precautions in the draft tube surge range of gate openings.

Since the unit was surging at 300 MW, load rejection could have caused concern. However, it was decided to proceed with the 300-MW load rejection since accelerating speed and reduced wicket gate opening would lead to improved stability of the unit. Upon 300-MW rejection, the pressure rise was 18 psi (0.124 MPa) and the speed rise was 11 percent. As the gates began to close, there was a slight increase in thrust to 3,500 tons (31.1 MN) followed by a decrease to 2,500 tons (22.2 MN) thrust. Subsequently, the thrust returned to the steady static amount of 2,800 tons (24.9 MN). The shaft runouts returned to previous normal values of less than 0.005 inch (0.13 mm) without abnormal incident.

Figure 4 shows the oscillographic record of the 300-MW load rejection.

FIGURE 4. 300-MW LOAD REJECTION, UNIT 19, GC III.

5,000 T = 44.5 MN, 0.050 inch = 1.27 mm
200 psi = 1.38 MPa, 35 psi = 0.24 MPa

On September 7, load r
anomalies of operation
were extremely satisfa
(0.13 mm) for steady-s
sient operation.

Figures 5 and 6 show t
load rejections. One
indicate the quality o
required no balancing

The transient vibratio
acceptable levels for
for shaft vibration du

POWER SWINGS

Much concern has been
variations in power ou
versus power output.
rejecting 600 MW.

The surging starts in
power output until a l
relatively rapidly and

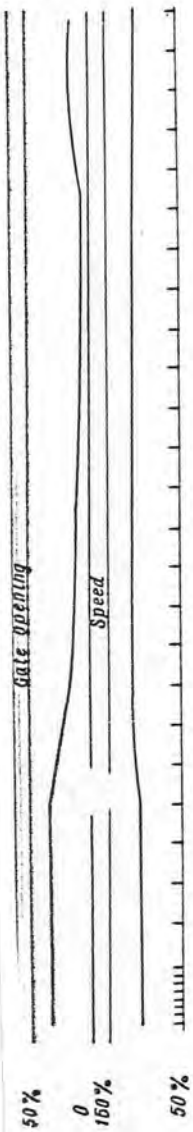

FIGURE 4. 300-MW LOAD REJECTION, UNIT 19, GC III.

5,000 T = 44.5 NN, 0.050 inch = 1.27 mm
200 psi = 1.38 MPa, 35 psi = 0.24 MPa

On September 7, load rejections of 450, 600, and 690 MW were made. No serious anomalies of operation were observed in these load rejections. Shaft runouts were extremely satisfactory during this operation, being less than 0.005 inch (0.13 mm) for steady-state operation and well within a normal range for transient operation.

Figures 5 and 6 show the original oscillograph records of the 600-MW and 690-MW load rejections. One may note that the shaft runouts prior to load rejection indicate the quality of operation of the unit under constant load. The unit required no balancing weights, and operated very well at all loaded conditions.

The transient vibrations during startup and load rejections were well within acceptable levels for units of this size and speed. Reference 2 gives criteria for shaft vibration during transient operations.

POWER SWINGS

Much concern has been expressed over the relation of draft tube pressure surges to variations in power output. Figure 7 shows a record of the draft tube pressures versus power output. This was taken during the period of load buildup prior to rejecting 600 MW.

The surging starts in the vicinity of 300 MW, but does not apparently affect power output until a load of 350 MW is reached. However, the load changes relatively rapidly and the surges take a few seconds to build up.

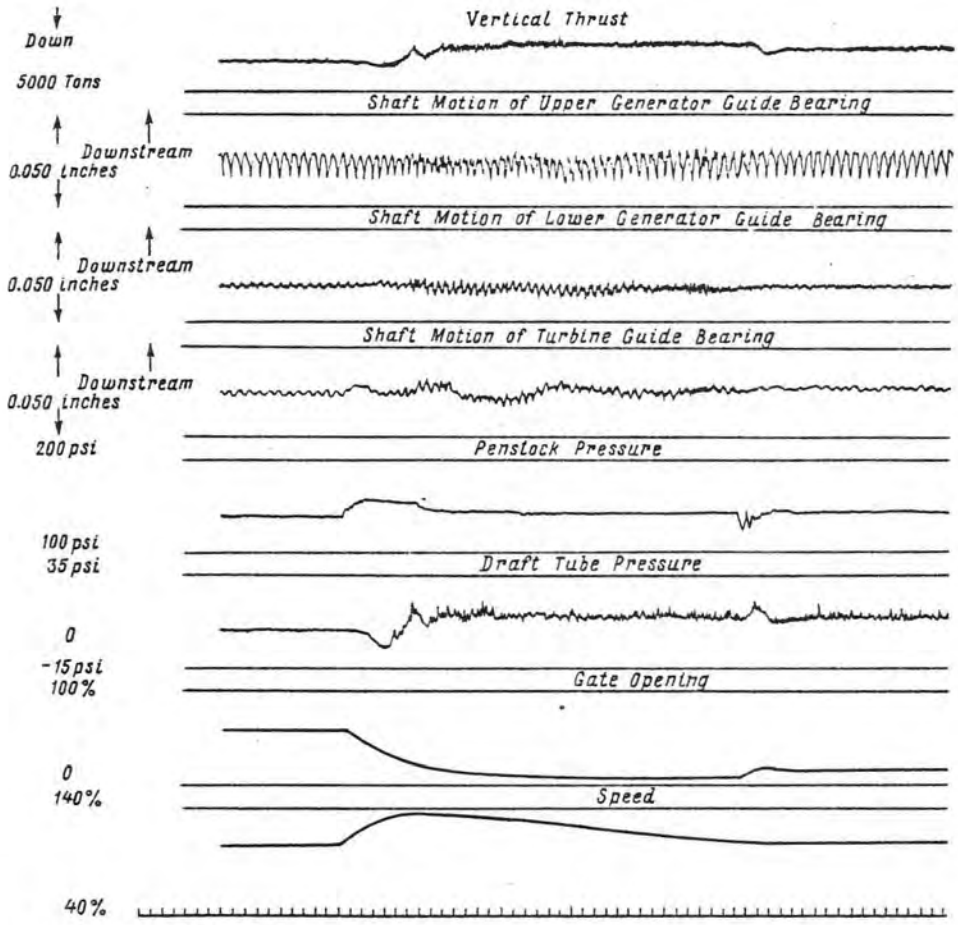

FIGURE 5. 600-MW LOAD REJECTION, UNIT 19, GC III.

5,000 T = 44.5 MN, 0.050 inch = 1.27 mm
200 psi = 1.38 MPa, 35 psi = 0.24 MPa

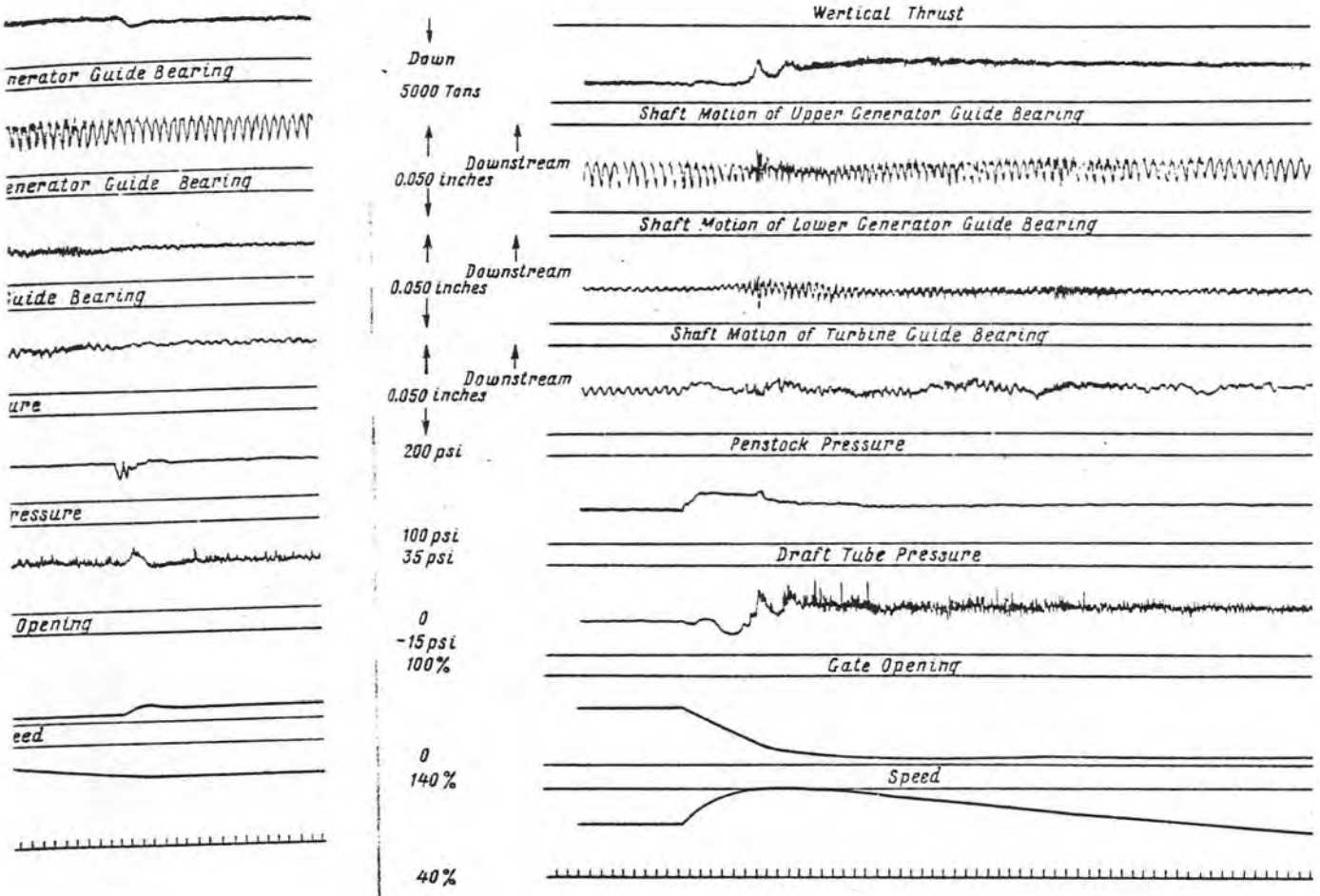

FIGURE 6. 690-MW LOAD REJECTION, UNIT 19, GC III.

5,000 T = 44.5 MN, 0.050 inch = 1.27 mm
200 psi = 1.38 MPa, 35 psi = 0.24 MPa

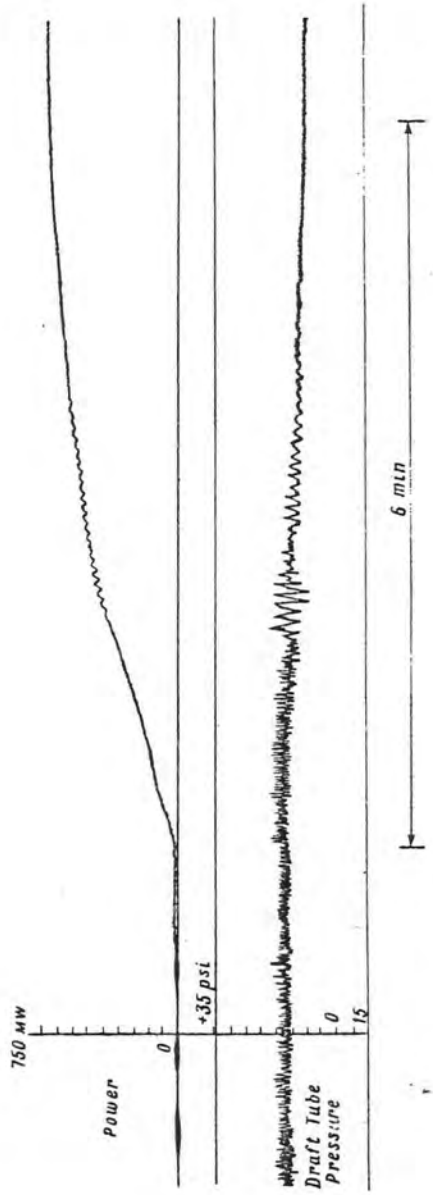

FIGURE 7. POWER SWINGS VS. DRAFT TUBE SURGES, 0 to 615 MW.

5,000 T = 44.5 MN, 0.050 inch = 1.27 mm
200 psi = 1.38 MPa, 35 psi = 0.24 MPa

While the surges r
persist as long as
550 MW load. Thes
the unit.

CONCLUSIONS

The 600-MW hydroele
very well. The sha
within acceptable l
speed rise on load

The occurrence of d
predicted values fo
the surges were pre
were found to occur
vent normal operati

ACKNOWLEGEMENTS

Westinghouse Electr
generators. Bingha
this project.

Many persons of bot
tions to the initia
were in charge of t

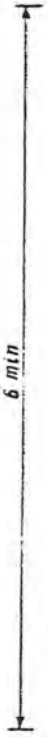

FIGURE 7. POWER SWINGS VS. DRAFT TUBE SURGES, 0 to 615 MW.
5,000 T = 44.5 MN, 0.050 inch = 1.27 mm
200 psi = 1.38 MPa, 35 psi = 0.24 MPa

While the surges reduce to about 5 psi (34.5 kPa) near 400 MW, power swings persist as long as any surge is present. Figure 7 shows some power variation at 550 MW load. These are relatively small and cause no concern during operation of the unit.

CONCLUSIONS

The 600-MW hydroelectric units at the Grand Coulee Third Powerplant operate very well. The shaft vibration levels during startup and operation are well within acceptable limits for units of this size and speed. The head rise and speed rise on load rejection are quite acceptable.

The occurrence of draft tube surges was expected, and generally agrees with predicted values for this unit. Synchronous shaft oscillations resulting from the surges were previously observed on the model tests of this unit. These were found to occur in the prototype in the predicted range, but do not prevent normal operation of the unit.

ACKNOWLEGEMENTS

Westinghouse Electric Company, Pittsburgh, Pennsylvania, furnished the electric generators. Bingham-Willamette of Portland, Oregon, supplied the turbines for this project.

Many persons of both companies and their subcontractors made important contributions to the initial startup of these units. Bureau of Reclamation engineers were in charge of the initial testing and operation of the units.

REFERENCES

1. Palde, Uldis J., "Model and Prototype Turbine Draft Tube Surge Analysis by the Swirl Momentum Method", 7th IAHR Symposium on Hydraulic Machinery, Vienna Austria, October 1974

2. Ruud, Frederick O., "Proposed Vibration Criteria for Transient Operation of Hydroelectric Units", 2nd International JSME Symposium on Fluid Machinery and Fluidics, Tokyo, September 1972

Subject I.

I-1. A.S.Abel
O.G.Vin
L.L.Dol
I.S.She

I-2. K.Petril

I-3. J.Klein
F.Stroh
D.Enzen

I-4. W.V.Nes

I-5. E.Krame
R.Nordm

I-6. L.Arosi
M.Rosna

I-7. J.Seyde

I-8. R.Angeh
K.Hölle
B.Barp,

ASCE — IAHR/AIHR — ASME

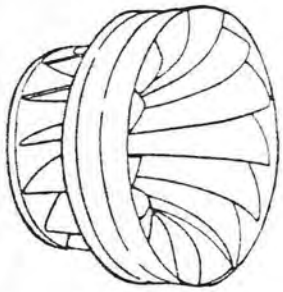

JOINT SYMPOSIUM on design and operation of FLUID MACHINERY

PROCEEDINGS

VOLUME I

POLYPHASE FLOW TRANSIENTS
PRESSURE RECOVERY DEVICES
INTAKE STRUCTURES
COOLING WATER SYSTEMS

June
12 - 14,
1978

Colorado
State
University
Fort Collins,
Colorado, USA

ectric

Charles, K. E.,
antially
y Life Stages
nt and Impinge-

rst, T. J.,
ems for
oposed Power
ional Workshop
bruary 1976.

d Fish Protec-
ournal of EE6,

PENSTOCK INTAKE VORTEX AND RELATED TURBINE OPERATION MODEL STUDIES

R. B. Dexter, Research Hydraulic Engineer (Retired)
E. R. Zeigler, Hydraulic Engineer

Bureau of Reclamation, E&R Center
Post Office Box 25007, Denver, Colorado 80225 USA

ABSTRACT

A literature search indicated Froude number modeling of intake vortices with a large model scale may produce inadequate results. Therefore larger than Froude number model discharges were used to intensify vortex action in a 1:120 scale model. The model study showed the intake trashracks inhibited vortex action, and air-entraining vortices could be suppressed by rafts. The literature search did not yield information to define intake vortex conditions that would be unacceptable for turbine operation. General information indicated that air-entraining vortices are to be avoided. A reaction-type model turbine was operated at prototype head to investigate the effect of vortex entrained air upon draft tube pressure surges and turbine runner deflections. Airflow in the model turbine for short periods did not result in untenable pressure surges or runner deflections. However, the airflow did create operational conditions comparable to rough operation in the periodic draft tube pressure surge range and this operation can be tolerated for only a limited time.

Une quête de la littérature a indiquée la possibilité d'obtenir les résultats insuffisants quand on fait un modèle des tourbillons á une prise d'eau avec une grande échelle de nombre Froude. Donc, debits plus grand que le debit par le Froude échelle étaiént utilisé d'intensifier l'action du tourbillon dans un 1:125 modèle. L'essais du modèle a indiqué que le grille de la prise d'eau a inhibé l'action du tourbillon et les tourbillons qu' aspirent l'air pourraient supprimé par les radeaux. La quête de la litterature ne rend pas les renseignements concernant les conditions mauvaises pour l'operation de la turbine avec un tourbillon á la prise d'eau. Donc, en générale les tourbillons qu' aspirent l'air doivent être évité. Une turbine de la réaction était opéré sur une charge qui a correspondu avec la charge en nature d'étuder l'effet d'un tourbillon avec l'air sur les fluctuations dans l'aspirateur et sur les déviations de la roue de la turbine. L'écoulement d'air dans la turbine pour une court durée ne produit pas les grandes variations ou in la pression ou en la déviation de la roue. Donc, l'écoulement a produit les conditions de l'operation comparable de la zone de l'operation mauvaise qu' est causé par le tourbillon dan l'aspirateur et on peut toléré cette opération pour une durée très limitée.

INTRODUCTION

During the active design stages of the Grand Coulee Third Powerplant, two hydraulic model studies were made: [1]* a study of the powerplant forebay channel and tailrace and [2] a study of the entrance, transition, and penstock bends. Vortices of an intermittent nature were noted in the forebay during both studies. Thus, a more intensive vortex study [3] was made with the existing 1:120 scale model.

A literature search was made concerning vortex effect upon turbines and vortex modeling. No information was found defining at what point vortex conditions were unacceptable; but air-entraining vortices were reported detrimental to hydraulic machinery operation. Thus tests were made with an air-entraining vortex at the penstock intake of a 1:40.33 model of the Grand Coulee Third Powerplant turbines with the model operating at prototype head.

MODELING INTAKE VORTICES

Hydraulic modeling of vortices is a problem because of the lack of similitude between model and prototype. The Froude, Weber, and Reynolds numbers should be used in dealing with the question of similitude [4]. However, an accurate relationship among these three numbers when applied to vortex modeling is not known. If using only Froude scaling, a vortex may be scarcely detectable in the model, but a very awesome occurrence in the prototype [5]. In another study [6], a prototype had air-entraining vortices which the Froude scaled model did not have, and a vortex modeling technique was developed which somewhat overcame the deficiency of Froude number modeling. This technique was designated the Equal Velocity Method because for some tests the model penstock velocity was equal to that of the prototype.

The Equal Velocity Method involves many model tests with different water depths and penstock velocities. For each test condition, vortex observations are made, and data points plotted on a graph similar to that of figure 1. A boundary line or envelope curve is drawn between the air-entraining and non-air-entraining data points. At water surface elevations below the curve, there is a danger of air-entraining vortices forming in the prototype. In study [7], effects of corrective measures were shown on the graph, figure 2.

Study [6] commented about a shape characteristic of the boundary curves:

> "The shape of the boundary curve varies with the circumstances, but in general the curves have one limb tending to become asymptotic to a constant velocity and another limb tending to become asymptotic to a constant depth."

---

* Numbers in brackets designate references listed at the end of this paper.

Also, "The transition between the two regions is more abrupt in some cases than in others."

Thus, the vertical (constant velocity) and horizontal (constant depth) limbs of the boundary curve were important indicators for vortex action in the model. For lower model velocities, the vertical limb shows velocity as a very critical and sensitive factor. Air-entraining vortices will form in the model only after attaining some minimum threshold velocity. Thereafter, the vortex becomes insensitive to velocity and the water depth is the critical and sensitive factor. Relatively small increases in water depth prevented formation of air-entraining vortices.

Therefore, it appears that a model penstock velocity which is greater than the Froude scale velocity, but considerably less than the prototype penstock velocity, may be sufficient for vortex model testing. In model study [7] of intake vortices at a hydroelectrical powerplant, the model scale was 1:200, and the horizontal limb of the boundary curve was attained before reaching the one-third prototype velocity. Both studies [6] and [7] suggest that an unknown measure of safety occurs by using the Equal Velocity Method for vortex modeling since the model vortex conditions may be more intense than those occurring in the prototype. Therefore, if the vortex is prevented in the model, the solution is believed to provide an unknown degree of safety in the prototype.

THE INTAKE MODEL STUDY

Location and flow geometry concerning the Grand Coulee Third Powerplant intakes is shown in figure 3 and the model in figure 4. Insomuch as possible, the Equal Velocity Method was used for the vortex studies. However, because of model head difference between the forebay and tailrace water surface elevations, the model penstock velocities were limited to about one-third of the prototype penstock velocity. Tests were made with multiple Froude number discharges for one prototype unit. Thus, a model discharge of 0.0057 m^3/s corresponded to an 878-m^3/s prototype unit discharge. In this paper the designation 1Q refers to one Froude number discharge passing through each operating unit, 2Q for two Froude number discharges, and 3Q for three Froude number discharges.

Initial tests were made without model trashracks, and air-entraining vortices occurred intermittently, figure 5. The vortices could not be submerged by the maximum reservoir water surface elevation, and thus the boundary curves had no horizontal limbs. Vortex severity increased with the number of operating units. The predominant vortex action was at the first operating unit downstream from the juncture of the Grand Coulee and Forebay Dams. For three unit operation, there was diminished vortex action at the last downstream unit and infrequent vortex action at the middle unit. A vortex would form 12 to 30 m in front of an intake, intensify while traveling toward the intake, then move along the forebay dam, and dissipate, figure 6. Vortex severity was the greatest in the region immediately in front of the intake. This vortex-prone region was very susceptible to vortex formation and

continuation of a developed vortex. Also, in some cases model discharge influenced whether or not the vortex moved upstream or downstream along the forebay dam, figure 7. Thus, the equal velocity method of vortex modeling may distort location of vortex action.

Model trashracks were constructed which simulated the prototype trashrack shape and calculated head loss. The trashracks were 41 m high, a 14-m radius semicircular shape, and at the furthest point extended 7 m out from the headwall. There were no air-entraining vortices and the vortex severity was considerably reduced by the trashracks, figure 8. Previously, without trashracks, a vortex with a continuous air core entered the intake. The trashrack occupied and restrained a portion of the vortex-prone region from contributing to vortex action. Also, the front of the trashrack provided resistance to the rotating water as the vortex approached, and the vortex dissipated upon reaching the trashrack, figure 9.

The juncture of Grand Coulee Dam and Forebay Dam forms a sharp corner where a flow separation occurred, producing eddies that traveled to the intakes. Corner modifications were made and a guidewall aligned the flow with the forebay channel, figure 10. The surface currents approached the intakes less directly, reducing vortex action, especially for the no trashrack test condition. Vortices occurred slightly downstream from the first unit and, being closer to the dam, more readily dissipated, figure 11. Thus, it was concluded that flow separation from the dam corner contributed to vortex formation, but was not the sole cause of the problem. Also, it was believed that the model produced proportionally larger flow separation than the prototype. More waterflow tended to enter the forebay channel at a right angle because of area limitation of the model reservoir (arrow, fig. 4).

Vortex suppression rafts were tested. Various rafts were tried - floating, submerged, different total areas, depth, and grid spacing - and all were successful. The raft was effective in preventing objectionable vortices when positioned near the center of the vortex formation area. Also, the raft was effective when positioned where the traveling vortices had their most severe development. Vortices would form beyond the raft and dissipate when passing beneath the raft.

Although the rafts were effective, there was some question because of the uncertainty that the intermittent vortices could be on the verge of dissipating. Therefore, a strong and steady vortex was generated in the model. With the stable and persistent vortex, the uncertainty was removed, the rafts definitely suppressed the vortex. However, swirl still remained beneath the raft and entered the intake, figure 12. In the event the hydraulic model did not simulate severe enough vortices, dissipation of the more severe generated vortex was believed to provide a measure of safety in the raft tests.

Figure 8.
and 20 o

Figure 9.
20, and

n some cases model
ex moved upstream or
Thus, the equal
rt location of vortex

simulated the proto-
. The trashracks
ape, and at the fur-
1. There were no
ty was considerably
sly, without trash-
tered the intake.
on of the vortex-
on. Also, the front
otating water as the
pon reaching the

bay Dam forms a
producing eddies
tions were made and
channel, figure 10.
ss directly, reduc-
rack test condition.
first unit and,
d, figure 11. Thus,
dam corner contri-
cause of the
produced propor-
ype. e water-
ight angle because
, fig. 4).

ious rafts were
as, depth, and
t was effective
oned near the cen-
t was effective
their most severe
t and dissipate

some question
vortices could
ong and steady
le and persistent
finitely sup-
d beneath the
vent the hydrau-
dissipation of
provide a measure

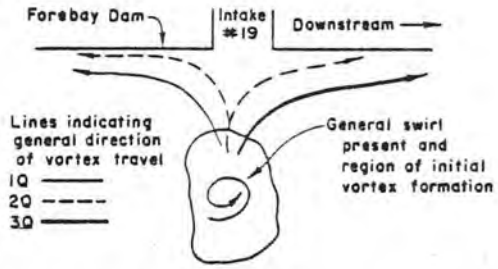

Figure 7. - Varying location of vortex action with respect to discharge.

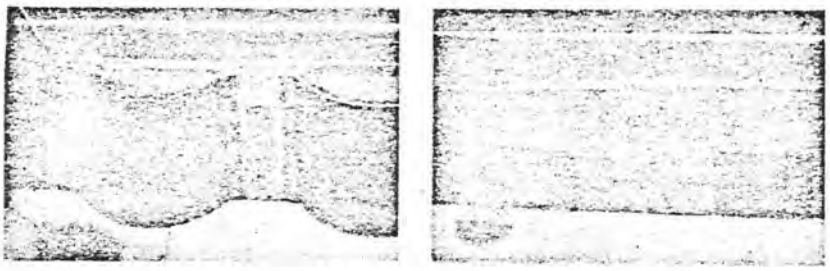

Figure 8. - Vortex action with and without trashracks. Units 19 and 20 operating 3Q each, reservoir elevation 393 m.

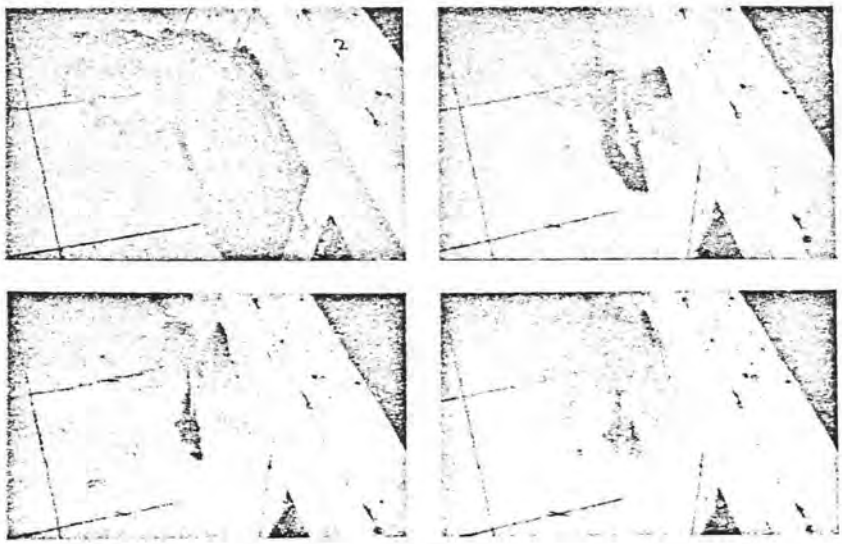

Figure 9. - Dissipation of vortex on the trashracks. Units 19, 20, and 21 operating 3-1/2Q each, and reservoir elevation 393 m.

Figure 10. - Flow conditions of the corner with and without the guidewall.

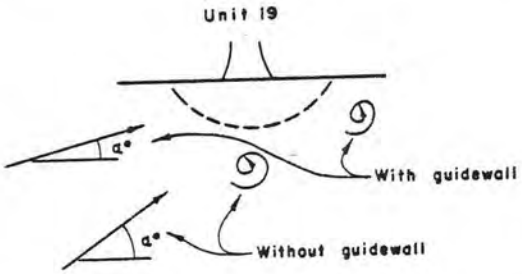

Figure 11. - Corner effect upon vortex action.

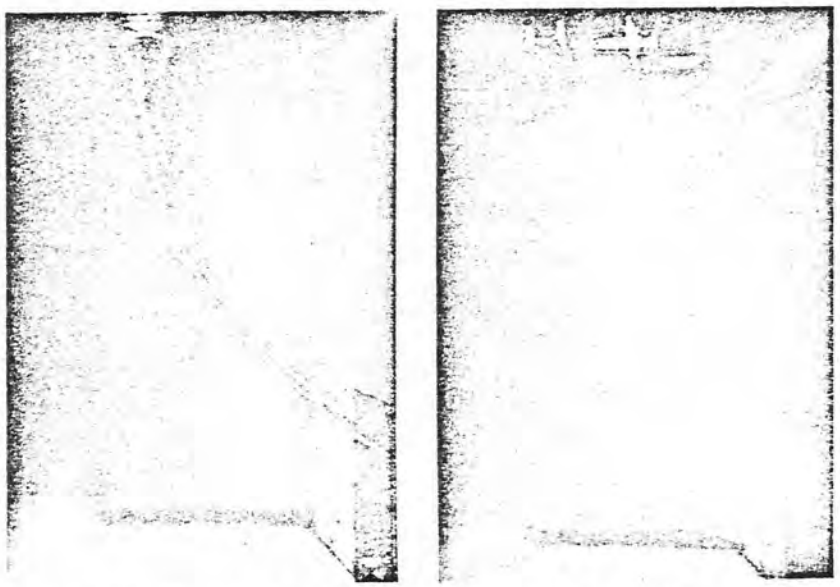

Figure 12. - The generated vortex without and with a raft.

ner with and without the

With guidewall

swall

ı vort action.

hout and with a raft.

Results of the model vortex tests were not considered conclusive for recommending modifications to the design. These tests were interpreted as indicating a danger of vortex formation, and in this event, the model tests showed rafts would suppress objectionable vortex action. The designers requested information for making a preliminary raft design. Model tests were reviewed, rough measurements made of rotational velocities; and design guideline information given for raft dimensions, forebay area of appreciable vortex occurrence, and flow velocities. Also, the precaution was taken of alerting project forces about a possible vortex problem. Prototype observations were to be made at the initial operation of each unit. If vortices of questionable strength formed, then the unit could immediately be shut down.

THE INTAKE MODEL VORTEX REPRESENTATION

The lack of vortex similitude with the 1:120 scale model was recognized and the Equal Velocity Method used to protect against inadequacy of Froude number vortex modeling. However, there was the predicament of not obtaining the full range of model penstock velocities required by the Equal Velocity Method. Thus, at the time it was unknown whether a degree of safety was provided by the model tests. Although with trashracks there were no air-entraining vortices, there was some concern whether vortex conditions might be more severe in the prototype. To date, three units of the Grand Coulee Third Powerplant have been installed, have operated, and no reports have been received of vortices in the forebay channel above the intakes. Evidently, model penstock velocities, considerably less than required by the Equal Velocity Method, produced vortex action more severe than that which occurs at the prototype.

PASSAGE OF AIR THROUGH A MODEL TURBINE

The possibility of air-entraining vortices occurring at the Grand Coulee Third Powerplant Penstock Intake, along with the uncertainty of their effect upon the turbines, resulted in studies using a model turbine. A 1:40.33 scale model of the 600-megawatt turbines was furnished as part of the contract for the first three prototype turbines of the Grand Coulee Powerplant installation. A test facility was in operation in which the waterway, including the turbine, was modeled from the penstock intake structure to the draft tube outlet. Pressure transducers were installed in the draft tube throat and proximity sensors (electronic micrometers) were installed to face the lower band of the turbine runner for measurement of runner deflections. Compressed air could be supplied above the water surface in the headwater tank to maintain an intentionally created vortex. Rate of airflow into the headwater tank to maintain the vortex was metered. The test facility was installed at Estes Powerplant, Estes Park, Colorado, where the model turbine could be operated at or near the prototype rated head of 87 meters.

A series of tests was made to investigate the effect of air-entraining vortices upon draft tube throat pressure surges and runner deflection. Compressed air was fed into the headwater tank and an air-entraining vortex existed over the penstock intake, until the supply of a limited volume air compressor receiver was exhausted. Control tests were made without an air-entraining vortex. Photographic recordings of transducer output images of draft tube pressure surges and runner deflections were made for a range of turbine operational parameters.

Figure 13 shows comparisons of draft tube surge pressure and runner deflection amplitudes and frequencies without and with entrained air. When the turbine was operating near peak efficiency and at minimum draft tube pressure surge amplitudes, figure 13A, vortex entrained air increased pressure surge and runner deflection amplitudes, as shown by figure 13B. Note that the sensitivity of the draft tube throat pressure surge trace of figure 13B is one-fifth the sensitivity of the corresponding trace of figure 13A.

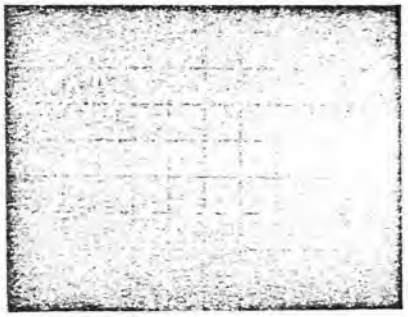

13A. No airflow, smooth operation, near peak efficiency.
Top: Draft tube throat pressure.
Vert scale, 1 div = 0.12 m
Horiz scale, 1 div = 0.1 sec
Bottom: Runner deflection.
Vert scale, 1 div = 6×10^{-3} mm

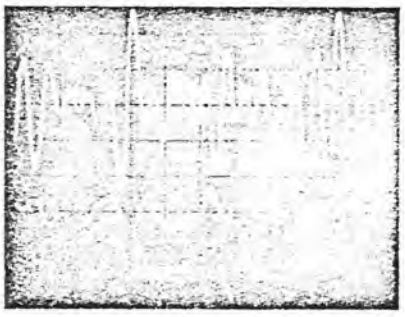

13B. Same operation as above with airflow.
Top: Draft tube throat pressure.
Vert scale, 1 div = 0.60 m
Horiz scale, 1 div = 0.1 sec
Bottom: Runner deflection.
Vert scale, 1 div = 6×10^{-3} mm

Figure 13. - Comparison of model turbine draft tube throat pressure surges and runner deflections without and with vortex entrained airflow.

A test was performed with the turbine operating near peak efficiency but in the intermittent draft tube pressure surge range. A third and final test was made with the turbine operating at reduced efficiency in the periodic draft tube pressure surge range. Changes of draft tube pressure surge and runner deflection amplitudes due to vortex entrained air are summarized in table 1.

Table 1. - *Changes of draft tube surge pressure and runner deflection amplitudes due to vortex entrained air*

Efficiency (percent)	Airflow to waterflow (percent)	Draft tube surge amp. (m water)	Runner deflect. (mm)	Remarks
91.05	0.	0.3	0.	No vortex, fig. 13A[1]
	2.8	3.0	.008	Constant vortex, fig. 13B
90.67	0.	0.5	0.	No vortex[2]
	3.1	0.9	0.	Constant vortex
86.62	0.	4.6	.006	No vortex[3]
	3.3±.3	4.6	.006	Variable vortex
	2.4±.4	7.6	.006	Intermittent vortex

[1] Near peak efficiency, negligible draft tube pressure surges before vortex.
[2] Off peak efficiency, intermittent draft tube pressure surges before vortex.
[3] Reduced efficiency, periodic draft tube pressure surges before vortex.

Comparison of draft tube pressure surge amplitudes and runner deflection values in the first and second lines of table 1 reveal that vortex entrained air created significant pressure surges and runner deflection when the turbine was operating near peak efficiency. The largest runner deflection occurred for this situation. When the machine was operating in the intermittent draft tube pressure surge range the passage of air created a relatively small increase in pressure surge amplitude without increase of runner deflection.

The last three lines of table 1 show that draft tube pressure surges reached maximum amplitudes and runner deflection values were near maximum when the machine was operating in the periodic draft tube surge range. Air supplied by an intermittent vortex significantly increased pressure surge amplitudes.

A significant conclusion may be made from the model investigation about passage of vortex entrained air through a reaction-type turbine. The conclusion is that the passage of air is equivalent to operation of the machine in the periodic draft tube

pressure surge range. If a reaction-type turbine was operating in the periodic pressure surge range, when an intermittent vortex entrained air, then the pressure surges would be amplified and operation of the machine would be very rough. A turbine would normally be operated at or near peak efficiency and should vortex entrained air pass through, the resultant pressure surges and unbalanced transverse load acting on the runner would be comparable to operation in the periodic draft tube pressure surge range. This phenomenon would not create immediate serious consequences but action should be taken immediately to eliminate the air-entraining vortex at the penstock intake. This action would require a decrease of turbine discharge. If this decrease resulted in turbine operation in an untenable draft tube surge range then the unit would have to be shut down.

REFERENCES

[1] King, D. L., "Hydraulic Model Studies for Grand Coulee Third Powerplant Forebay and Tailrace Channels," Bureau of Reclamation Report REC-ERC-73-2, February 1973.

[2] Rhone, T. J., "Hydraulic Model Studies for the Penstocks for Grand Coulee Third Powerplant," Bureau of Reclamation Report REC-ERC-74-12, August 1974.

[3] Zeigler, E. R., "Hydraulic Model Vortex Study - Grand Coulee Third Powerplant," Bureau of Reclamation Report REC-ERC-76-2.

[4] Berge, J. P., "Study of Vortex Formation and Other Types of Abnormal Flow in an Enclosure With or Without Open Surface," La Houille Blanche, Vol. 21, No. 1, pp. 13-40, 1966, Bureau of Reclamation Translation No. 665, October 1967.

[5] Angelin, S. and Larsen, P., Discussion - "Factors Influencing Flow in Large Conduits," Journal of the Hydraulic Division, ASCE, Vol. 92, No. HY4, pp. 201-202, July 1966.

[6] Denny, D. F., and Young, G. A., The Prevention of Vortices and Swirl at Intakes, Transactions, 7th Meeting of International Association for Hydraulic Research, Seventh Congress of IAHR, Publication C.1, Lisbon, 1975.

[7] Linford, A., "Application of Models to Hydraulic Engineering," Water and Water Engineering, Vol. 69, No. 829, pp. 105-110, March 1965.

Re
Eng. Mgr.
Managing
Asst. Chi
Mgr. Nucl

ABSTRACT

The occur
pump sump
due to vil
ing the pe
Unit 1 Em
perfecting
tection fr
der emerge
A hydrauli
180°F and
permitted
able dimen
ducted usi
screen blo
No vortex
trapped un
entraining
in a horiz
developmen
eliminated

RESUME

La présence
ables dans
quer des pe
son des vib
évaluer le
Farley (Ref
teurs) et p
protège non
admission d
Un modèle h
pouvant att
nal a permi
nombres ill
été pratiqu
pour différ
diverses pr
tourbillon
que la masse
tend à provo
aient obstru
eur de la ca
d'une cage
permis de s

ASCE — IAHR/AIHR — ASME

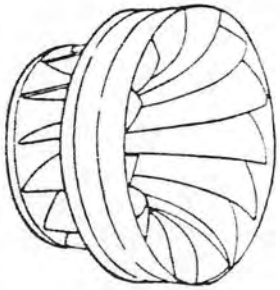

JOINT SYMPOSIUM on design and operation of FLUID MACHINERY

PROCEEDINGS

VOLUME I

POLYPHASE FLOW TRANSIENTS
PRESSURE RECOVERY DEVICES
INTAKE STRUCTURES
COOLING WATER SYSTEMS

June
12 - 14,
1978

Colorado
State
University
Fort Collins,
Colorado, USA

STUDIES OF A METHOD TO PREVENT DRAFT TUBE SURGE IN PUMP-TURBINES

Thomas A. Seybert*

Walter S. Gearhart*

Henry T. Falvey**

*APPLIED RESEARCH LABORATORY
The Pennsylvania State University
Post Office Box 30
State College, PA 16801

**Bureau of Reclamation
Post Office Box 25007
Denver, Colorado 80225

ABSTRACT

This paper describes a method of preventing draft tube surge in pump-turbines by injecting some high energy fluid from the spiral casing into the draft tube counter to the direction of the swirl. An air flow facility was used to simulate the flow in the draft tube. The study investigated the effectiveness of various nozzle geometries in reducing draft tube surge over a range of swirl parameters. The results of these tests provide design criteria for selecting injection nozzle configuration. The minimum ratio of bypass flow to draft tube flow to prevent draft tube surge for various swirl parameters was determined. The loss in efficiency associated with bypassing fluid into the draft tubes is evaluated for the Grand Coulee Third turbines.

Cet essai décrit une méthode d'empêcher les ondes de pression dans des tubes d'aspiration des pompes-turbines par l'injection d'une partie du fluid de la bâche spirale dans l'aspirateur contre la direction de la rotation. Un modèle experimental, que utiliser l'air pour le fluid, était employé de simuler l'écoulement dans l'aspirateur. L'étude a examiné l'efficacité des divers géomètries de la buse en réduisant les ondes de pression pour un rang des paramètres de la rotation. Les résultats des essais fournissent le dessin critère pour le choix de la configuration de la buse. Le rapport minimal entre l'écoulement diverti et l'écoulement dans l'aspirateur etait déterminé enfin d'éliminer les ondes de pression pour les divers paramètres de la rotation. La perte du rendement á cause de la diversion du fluid dans l'aspirateur est evalué pour les Grand Coulee Third turbines.

NOMENCLATURE

S	momentum parameter
Ω	flux of moment of momentum
D	diameter of draft tube
D'	diameter of injection nozzle
ρ	mass density
Q	flowrate
r_i	radius of trailing edge of wicket gates
V_{θ_i}	circumferential velocity of wicket gate exit
$\overline{V_{\theta_T}}$	circumferential velocity in draft tube throat
$\overline{V_{A_T}}$	axial velocity in draft tube throat
Q_B	bypass discharge
Q_T	turbine discharge
η	efficiency
H	head
A_N	total area of injection nozzles
A_T	area of draft tube throat
γ	density
g	gravitational constant
P	power
α	fluid flow angle at trailing edge of wicket gates
f	frequency of surge condition
$\sqrt{\overline{P^2}}$	rms value of surge condition

Note: all dimensions are in SI units.

INTRODUCTION

The occurrence of draft tube surge in hydroelectric turbines has received considerable attention during the past decade as

evidenced by
bibliography

The gen
is related t
the discharg
an unstable
pulsations d
may cause se
and vertical

Realizi
with the amo
obvious solu

Straigh
been suggest
losses or st
has, in some
tions. Appe
cylinder to
the intensit
majority of
excessive er
induce exces

A METHOD TO

A meth
off design
machine whe
efficiency
the draft t
is operatin
negative sw

'The me
a series of
immediately
arrangement
fluid in th
discharge f
separate ro
of injectin
An arrangem
positive or
will be dir
spiral casi
activated c
the flow tc
discharging

evidenced by reference [1] which is a review and annotated bibliography on the subject.

The general consensus is that the origin of draft tube surge is related to the amount of angular momentum or swirl left in the discharge flow from the turbine. The swirl gives rise to an unstable flow pattern in the draft tube which causes pressure pulsations described as draft tube surge. The draft tube surge may cause severe noise and vibration, variation in power output and vertical movement of runner and shaft.

Realizing that the onset of draft tube surge is associated with the amount of swirl present in the discharge flow, the obvious solution would consist of eliminating the swirl.

Straightening vanes and fins located in the draft tube have been suggested and tried but have resulted in either efficiency losses or structural and cavitation damage. Injection of air has, in some cases, reduced the magnitude of the pressure pulsations. Appendages attached in the draft tube such as a hollow cylinder to contain the vortex core or solid fairings to reduce the intensity of the vortex have met with limited success. The majority of the methods that have been attempted cause either excessive energy losses, result in cavitation damage, or induce excessive structural vibrations.

A METHOD TO PREVENT DRAFT TUBE SURGE

A method that reduces the rotation in the draft tube flow at off design conditions and does not effect the efficiency of the machine when it is operating at or near its point of best efficiency is necessary. It must not consist of appendages in the draft tube or impair the performance of the machine when it is operating as a pump. The elimination of either positive or negative swirl should be provided.

The method that is considered in this paper consists of a series of flush mounted nozzles located in the draft tube immediately downstream of the turbine rotor. A schematic of the arrangement is shown in Figure (1). The nozzles will inject fluid in the draft tube counter to the peripheral motion of the discharge flow. Although not indicated in the figure, two separate rows of nozzles could be provided with one row capable of injecting fluid in a direction opposite to that of the other. An arrangement such as this would permit the reduction of either positive or negative swirl. It is envisioned that the nozzles will be directly connected to the high pressure fluid in the spiral casing or penstock. An appropriate system of valving, activated on the basis of wicket gate opening, would control the flow to the nozzles and could control the number of nozzles discharging.

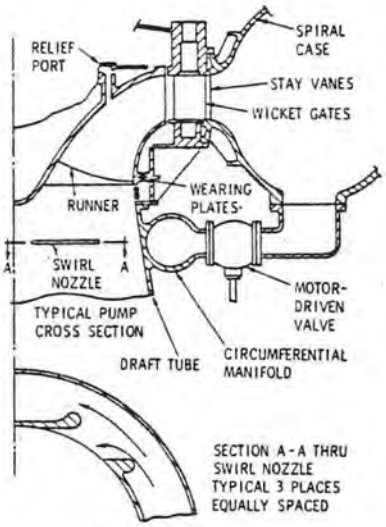

Figure 1 - Schematic of Proposed Means of Preventing Draft Tube Surge

An alternate arrangement to that shown in Figure (1) would consist of swirl nozzles individually connected to the spiral casing by separate piping and valving.

The nozzles shall be flush mounted on the wall of the draft tube and thereby provide a minimum flow disturbance when the swirl nozzles are inactive. Their presence should not cause any loss in efficiency or cavitation resistance of the machine when they are inactive. Of primary importance is an evaluation of the amount of fluid that must be drawn from the high pressure side of the turbine and discharged into the draft tube. The bypassing of such fluid represents an energy loss that for purposes of analysis, will be considered as totally unrecoverable. On this basis, the swirl in the draft tube must be reduced to some specified value with a minimum rate of injected fluid if the described technique is to be successful. An engineering estimate of the ratio of bypassed flow to flow through the turbine can be obtained on the basis of momentum consideration.

The momentum or swirl parameter describing the ratio of angular to axial momentum flux in the draft tube is defined in [2]. Figure (2) illustrates the nomenclature and stations considered where,

$$S = \frac{\Omega D}{\rho Q^2} = \frac{4\, r_i\, V_{\theta_i}\, D}{\pi\, \overline{V}_{A_T}\, D^2} \quad . \qquad (1)$$

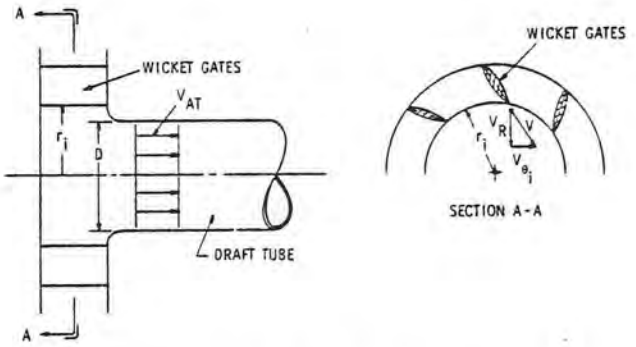

Figure 2 - Schematic of Flow Leaving Wicket Gates

The conservation of angular momentum is assumed constant between the wicket gate exit and the draft tube throat. The quantity $\overline{V_{A_T}}$ represents a mass averaged axial velocity in the draft tube. The assumption is made that the radial distribution of tangential velocity at a given section in the draft tube is represented by a potential vortex. On this basis the mass averaged quantity $\overline{V_{\theta_T}}$, at a given section of the draft tube, would occur at the diameter D associated with the mean area of the draft tube. This can be expressed algebraically as:

$$r_i V_{\theta_i} = \frac{\overline{D}}{2} (\overline{V_{\theta_T}}) = \frac{D}{2(1.414)} \overline{V_{\theta_T}} \quad , \qquad (2)$$

and substituted in (1) to give

$$S = \frac{1}{2.22} \overline{V_{\theta_T}} / \overline{V_{A_T}} \quad . \qquad (3)$$

It is proposed to reduce the ratio of angular to axial momentum flux that exists in the draft tube at any given gate opening to that level which exists prior to the occurrence of periodic draft tube surge. This level would be attained when the angular momentum of the draft tube flow and that of the injected fluid is summed to give a resultant swirl parameter, S, which is less than that at which periodic draft tube surge is predicted to occur, S^*.

If the critical swirl paramter S^* is not to be exceeded, in the draft tube, the amount of fluid that must be injected through the swirl nozzles can be evaluated. The quantities of flow and velocity associated with the critical swirl parameter

shall be noted by an asterisk. The quantity of bleed fluid required to obtain the critical swirl parameter S^* in the draft tube can be determined by equating the difference between the angular momentum from the turbine discharge $Q_T V_{\theta_T}$ and that of the bypass fluid $Q_B \sqrt{2gH}$ to the angular momentum at the critical condition $Q_T^* V_{\theta_T}^*$. Thus,

$$\frac{(Q_T V_{\theta_T})}{(Q_T^* V_{A_T}^*)} - \frac{Q_B \sqrt{2gH}}{(Q_T^* V_{A_T}^*)} = \left[\frac{Q_T^* V_{\theta_T}^*}{Q_T^* V_{A_T}^*}\right] = 2.22\, S^* \qquad (4)$$

and Equation (4) can be rearranged to provide a ratio of bypass flow to draft tube flow in terms of the swirl parameters (S) and (S^*) as

$$\frac{Q_B}{Q_T} = \frac{2.22\, V_{A_T}^* \left[S\left(\frac{V_{A_T}}{V_{A_T}^*}\right) - \left(\frac{V_{A_T}^*}{V_{A_T}}\right) S^*\right]}{\sqrt{2gH}} \quad . \qquad (5)$$

The decrease in efficiency ($\Delta\eta$) of the turbine due to bleeding bypass fluid to the swirl nozzles assuming that none of the bypass fluid energy is recovered is:

$$\Delta\eta = (100)\left(\frac{Q_B}{Q_T}\right) \quad . \qquad (6)$$

If Equation (5) is considered for a given (S), the numerator is essentially constant, independent of turbine head. This is based on the assumption, for cavitation purposes, that the velocity at the design condition in the draft tube throat for conventional turbine installations has some upper limit. The ratio of Q_B/Q_T specified by (5) decreases as some reciprocal function as head is increased. On this basis, Equation (6) indicates the decrease in efficiency, due to bleeding bypass fluid to the swirl nozzles, will be less in a high head turbine than in a low head turbine.

TEST APPARATUS

Investigations for this paper were conducted in an air flow facility as shown in Figure (3). Similar studies conducted in [2] and [3] have shown that the use of air as a working fluid has been quite successful in characterizing the swirl parameter in draft tube flow and predicting the occurrance of draft tube surge. The main air supply was provided by a variable speed

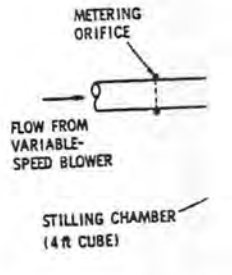

Fig

centrifugal blow
ment. The meter
chamber where sc
the stilling cha
draft tube radia
angle between t
angle between 0
It can be shown
reduces to K(t
and α is the av
data across the
probe were used
settings. This
parameter as a
by an auxiliary
arrangement ent
section locate
injection flui
flow) Q_T, coul
valve on the a
provided three
circumferentia
Nozzle geometr
pointed out th
sum of the thr
the nozzle tes
draft tube (L/
all along the
could be repla

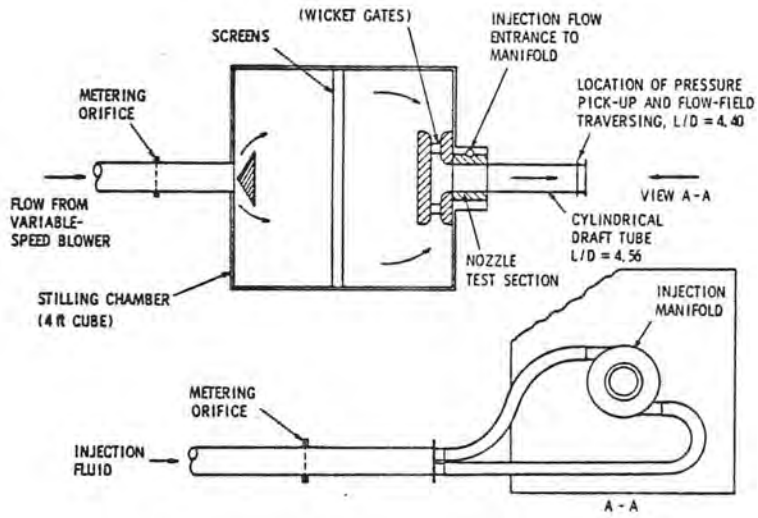

Figure 3 - Schematic of Air Flow Facility

centrifugal blower and was measured by an orifice meter arrangement. The metered air flow was diffused as it entered a stilling chamber where screens were used to reduce flow turbulence across the stilling chamber flow field. The air entered a cylindrical draft tube radially through wicket gate type swirl vanes. The angle between the vanes and a radial line could be set at any angle between 0° (radial position) and 82.5° (closed position). It can be shown that the dimensionless momentum parameter $\Omega D/\rho Q^2$ reduces to $K(\tan \alpha)$ for this test facility, where K = constant and α is the average flow angle leaving the wicket gates. Traverse data across the trailing edge of the wicket gates using a prism probe were used to determine flow angles for various wicket gate settings. This data was used to develop a relation for swirl parameter as a function of gate setting. Injection fluid provided by an auxiliary air supply and measured by an orifice meter arrangement entered the manifold of the injection nozzle test section located just below the wicket gates. Any ratio of injection fluid flow, Q_B to fluid flow through the gates (turbine flow) Q_T, could be provided by the proper setting of a butterfly valve on the auxiliary air supply blower. The nozzle test section provided three points of fluid injection equally spaced in a circumferential plane perpendicular to the draft tube centerline. Nozzle geometries tested are shown in Table I. It should be pointed out that in Table I, A_N, nozzle area, was defined as the sum of the three separate nozzle areas. After passing through the nozzle test section, the air flow entered the cylindrical draft tube (L/D=4.56). Pressure taps and probe holes were located all along the length of the tube. The cylindrical draft tube could be replaced with an elbow type (Fontenelle) draft tube.

Table I

NOZZLE SHAPES TESTED

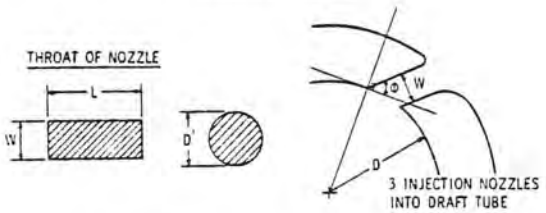

Nozzle Number	Injection Angle, Φ (deg)	Nozzle Area, A_N (sq in.)	A_N/A_T (%)	L/W
1	30	1.500	5.09	8.0
2	↓	0.750	2.54	4.0
3		0.375	1.27	0.5
4	↓	1.125	3.84	1.5
5	0	0.750	2.54	1.0
	15	↓	↓	↓
	30			
	45	↓	↓	↓
6	30	0.188	0.64	4.0
7	↓	0.750	2.54	0.25
8		0.610	2.04	circle, D' = 0.5 in.
9		1.325	4.48	circle, D' = 0.75 in.
10		0.375	1.27	1.0
11		↓	↓	4.0
12				0.25
13		1.50	5.04	1.0
14	↓	↓	↓	4.0
15				0.25

The unsteady pressure produced by the swirling flow in the draft tube was monitored at the last pressure tap (L/D=4.40) on the draft tube by a dynamically calibrated differential pressure transducer. The pressure signal was sent to a Spectral-Dynamics real time analyzer in conjunction with an ensemble averager from which the frequency, f, of the surging condition could be established.

Figure (4) shows typical data received from the analyzer. The root mean square value, $\sqrt{\overline{p}^2}$, of the surging condition was read from an RMS meter after the signal was passed through a line filter with a characteristic 48 dB per octave roll-off. The band pass of the filter was set at 20 Hz to 120 Hz for all tests. The frequency of all observed pressure surges was between 35 and 70 Hz. Directly across from the pressure pickup tap used on the draft tube was a probe hole used for flow field measurements. A prism probe was used to obtain total pressure, static pressure and fluid flow angle as a function of radial distance across the draft tube for various flow conditions. The basic parameters used in this study to describe the surging condition were the dimensionless groups suggested by [5], namely pressure parameter ($D^4\sqrt{\overline{p}^2}/\rho Q^2$) and frequency parameter (fD^3/Q).

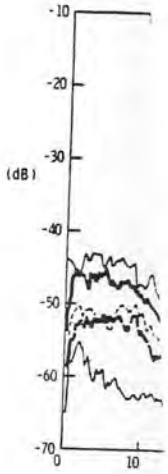

DISCUSSION OF

The effec
geometries were
in reducing the
draft tube. Al
as recommended
compressible ef
the reduction i
is shown by Fig
and the frequenc
is increased. T
at a Q_B/Q_T of 16
this condition o

The angle o
studied with res
swirl in the drai
gated, these beir
The nozzle geomet
Table I, and the
parameter of 0.8
that, up to the 4
amplitude is inde
of the curves in
to completely elim
of Q_B/Q_T required,

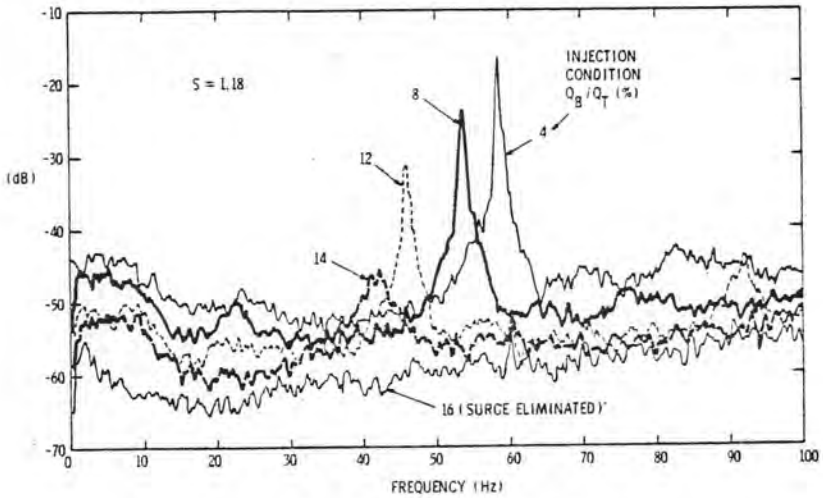

Figure 4 - Spectral Analysis of Surge

DISCUSSION OF EXPERIMENTAL RESULTS

The effect of various fluid injection angles and nozzle geometries were investigated on the basis of their effectiveness in reducing the unsteady pressure amplitude measured in the draft tube. All tests were at a Reynolds Numbers above 80,000 as recommended in [3] and at velocities low enough to prevent compressible effects. A typical spectral analysis indicating the reduction in the amplitude of the unsteady surge pressure is shown by Figure (4). It is apparent that both the amplitude and the frequency of the surge are reduced as the ratio of Q_B/Q_T is increased. The spectral analysis indicates no pressure peaks at a Q_B/Q_T of 16% indicating that surge has been eliminated at this condition of fluid injection.

The angle of fluid injection as defined in Table I was studied with respect to its effect on reducing surge for a given swirl in the draft tube. Four angles of injection were investigated, these being 0°, 15°, 30° and 45° as defined by Table I. The nozzle geometry used in these tests was #5, described in Table I, and the results are shown in Figure (5) for a swirl parameter of 0.8 and 1.18. The most significant result being that, up to the 45° angle tested, the reduction of surge pressure amplitude is independent of injection angle. The lower end points of the curves in Figure (5) represent that ratio of Q_B/Q_T required to completely eliminate surge and it is evident that the quantity of Q_B/Q_T required, is equal for the four injection angles tested.

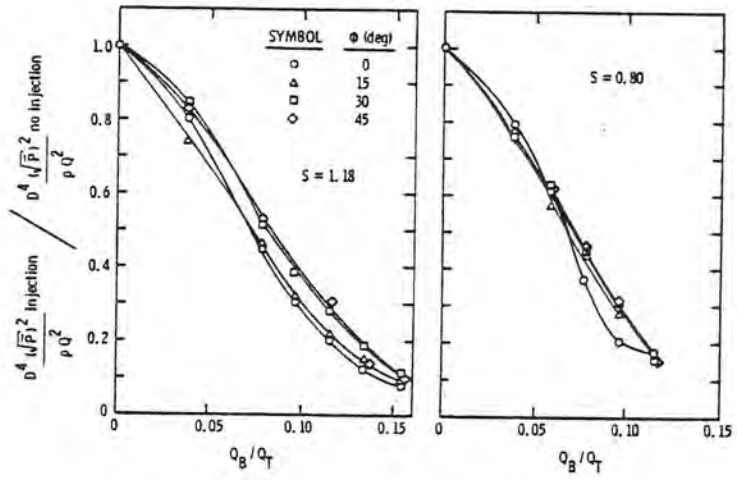

Figure 5 - Comparison of Nozzle Angle of Injection

An injection angle of 30° was selected for the tests to investigate the effect of the length to width ratio of the injection nozzle as well as the ratio of the area of the injection nozzles to the draft tube throat area. The ratio Q_B/Q_T is plotted against the surge pressure parameter for a series of nozzle geometries at the swirl parameters in Figure (6). The lower extremity of each curve represents a condition where surge is eliminated and thereby indicates the ratio of Q_B/Q_T required to eliminate surge for a given A_N/A_T ratio. Figure (6) illustrates that for a given ratio of Q_B/Q_T, the reduction in the surge pressure amplitude is greater as A_N/A_T decreases. This results directly from the fact that to inject a given ratio of Q_B/Q_T into the draft tube the head and hence the velocity must increase as A_N/A_T decreases. Since the momentum of the injected fluid increases as the square of the spouting velocity from the nozzles, smaller ratios of Q_B/Q_T are required to eliminate surge as the head on the turbine increases.

Table I lists the various nozzle geometries tested and defines their characteristic dimensions. The rather surprising result being that for the various L/W nozzles tested, no measurable difference was observed in the ratio of Q_B/Q_T required to eliminate surge at a given A_N/A_T. This result suggests that the choice of a nozzle geometry to obtain a given A_N/A_T would consist of selecting that geometry which would give the least hydraulic losses and permit the easiest fabrication. On this basis, a cylindrical nozzle which would be elliptical at its intersection with the barrel of the draft tube would seem appropriate.

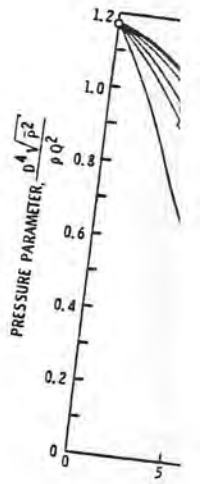

Figur

The tangentia
the draft tube were
by means of a prism
of the local static
velocity distributi
meters of 0.24, 0.4
figures represents s
at a setting corresp

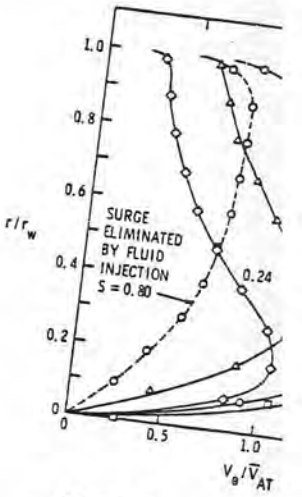

Figure 7 - Axial a

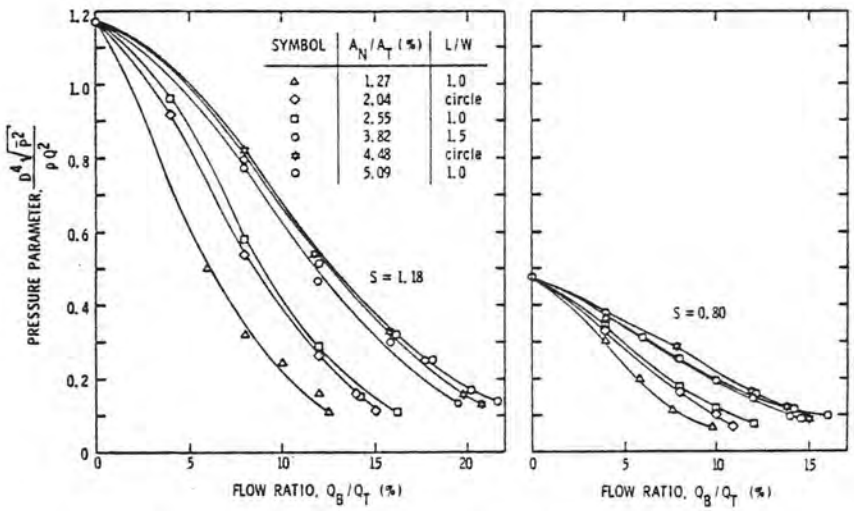

Figure 6 - Comparison of Nozzle Geometries

The tangential and axial velocity components of the flow in the draft tube were measured at a station indicated on Figure (3) by means of a prism probe which provided a time averaged reading of the local static, total pressure and flow angularity. The velocity distributions are shown by Figure (7) for swirl parameters of 0.24, 0.41, 0.80 and 1.18. The dashed line in these figures represents similar traverse data having the wicket gates at a setting corresponding to a swirl of 0.8 but with fluid

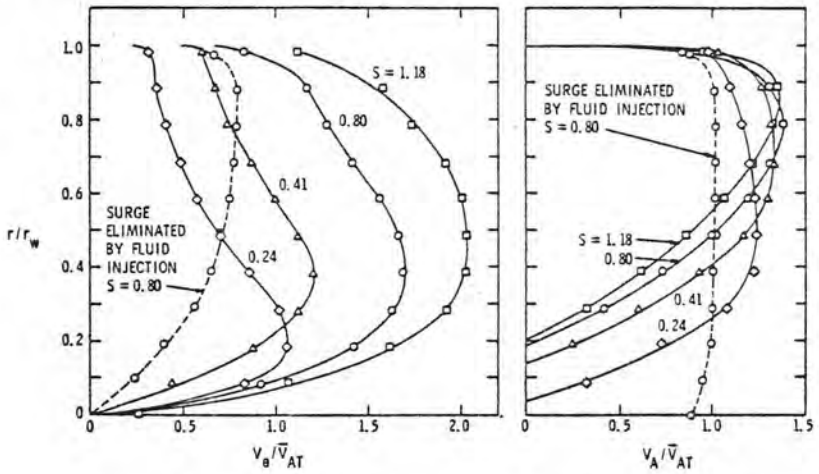

Figure 7 - Axial and Tangential Velocity Distribution

injected to eliminate surge. It is evident that the reversal of axial flow at the axis of rotation is eliminated and considerable swirl has been removed from the flow when fluid is injected.

Without injection, the outer portion of the flow approaches a free vortex or constant angular momentum distribution with solid body rotation near the center. The peripheral velocity distribution downstream of a turbine runner may deviate from that indicated in Figure (7). The effect of such variation has not been investigated in the present studies but deserves future consideration.

COMPARISON OF TEST RESULTS WITH PREDICTIONS

The ratio of bleed flow to turbine flow was previously derived in Equation (5), assuming ideal momentum transfer between the injected and draft tube flow. On the basis of the preceding experimental data, it is possible to derive an empirical relation that applies to pump-turbines. The bypass flow can be expressed as

$$Q_B = K_1 (2g\ H)^{1/2}\ A_N \quad , \tag{6}$$

where K_1 is a nozzle coefficient and assumed equal to 0.9. The flow through the turbine can be written as

$$Q_T = \frac{1}{\eta} \frac{P}{H\gamma} \quad . \tag{7}$$

The ratio of bypass flow to turbine flow is then

$$Q_B/Q_T = 39{,}100\ \eta \frac{A_T}{P} \frac{A_N}{A_T} H^{3/2} \quad . \tag{8}$$

The results of experimental data indicating, for a given A_N/A_T, that ratio of Q_B/Q_T required to eliminate surge at two swirl parameters are shown in Figure (8). A curve fitting of this data indicates a relation

$$Q_B/Q_T = 0.719\ (A_N/A_T)^{0.401} \tag{9}$$

reversal of
considerable
jected.

approaches
on with
velocity
te from that
n has not
future

riously derived
ween the
eceding
cal relation
e expressed

(6)

0.9. The

(7)

(8)

ven A_N/A_T,
o swirl
of this

(9)

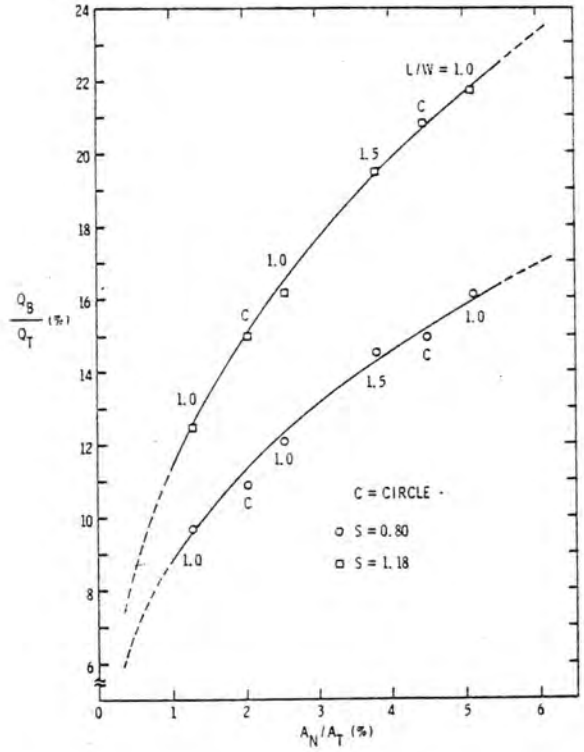

Figure 8 - Injected Flow Required to Eliminate Surge for Cylindrical Draft Tube

for S=1.18 and,

$$Q_B/Q_T = 0.473\ (A_N/A_T)^{0.366} \qquad (10)$$

for S=0.80.

Considering a swirl parameter of 1.18, it is possible by substituting (9) in (8) to obtain a relation for Q_B/Q_T of,

$$Q_B/Q_T = \frac{1}{2054\ [(n)\ \frac{A_T}{P}]^{0.67}\ H} \qquad (11)$$

In similar fashion, the substitution of (10) in (8) provides a relation of Q_B/Q_T for a swirl parameter of 0.8,

$$Q_B/Q_T = \frac{1}{1460\ (\frac{\eta\ A_T}{P})^{0.578}\ H^{0.867}} \quad . \qquad (12)$$

An elbow-type draft tube was also evaluated to indicate the influence of draft tube shape. The draft tube tested was similar to the Fontenelle configuration described in [3]. The data and equations relating A_N/A_T to Q_B/Q_T required to eliminate surge for this draft tube is shown in Figure (9). By applying the same analysis as indicated for the cylindrical draft tube, the ratio of bypass flow to turbine flow for the elbow-type draft tube

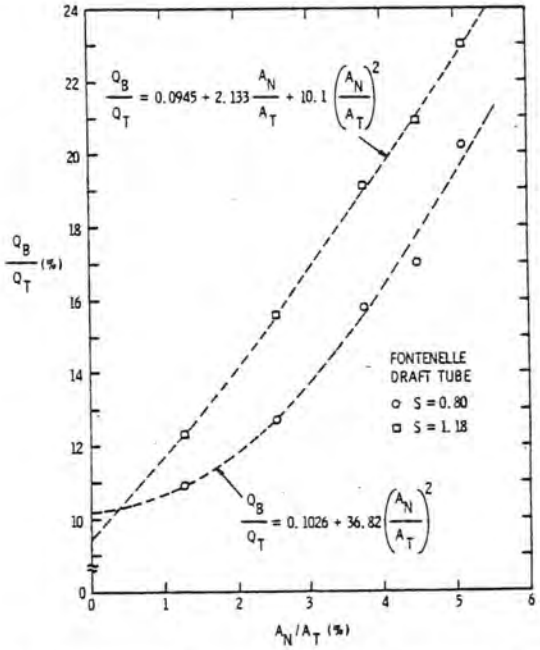

Figure 9 - Injected Flow Required to Eliminate Surge for Elbow Draft Tube

was calculated. Using performance, geometrical data and a speed coefficient of ϕ=0.8 for the model of the Grand Coulee Third Power Plant Units given in [4], the bypass flow rates were determined for a cylindrical, and an elbow-type draft tube, Table II.

(8) provides a

(12)

:o indicate the
:ted was similar
The data and
inate surge
:lying the same
)e, the ratio
draft tube

for

a speed
ird
e
e,

Table II

GRAND COULEE THIRD POWER PLANT BYPASS RATES

	S=0.8	S=1.18
Predicted Ideal (Eq. (5))	Q_B/Q_T=6.35%	Q_B/Q_T=5.62%
Predicted Empirically	Q_B/Q_T=10.3%	Q_B/Q_T=13.9% (cylindrical)
	Q_B/Q_T=11.5%	Q_B/Q_T=13.0% (elbow)

The comparison indicates that the empirically derived quantity of Q_B/Q_T required to eliminate surge at a swirl parameter of 1.18 is about 2.5 times greater than that predicted assuming an ideal momentum transfer. At the lower swirl parameter, the difference between the estimated values of Q_B/Q_T is not as great. The availability of performance characteristics and geometries of other existing or new turbine installations would permit making similar estimates of the required Q_B/Q_T to eliminate surge at the specified values of swirl parameter.

It should be emphasized that solution of Equation (11) and (12) in conjunction with Figure (9) also specifies the A_N/A_T required, for a given turbine, to eliminate surge at a swirl of 0.8 or 1.18.

SUMMARY AND RECOMMENDATIONS

Experimental studies with respect to eliminating draft tube surge by injecting fluid into the draft tube counter to the existing swirl resulted in the following observations.

As the ratio of injected fluid Q_B/Q_T is increased, both the surge frequency and the amplitude of the surge pressure decreases in magnitude.

The use of various nozzles geometries with a fixed A_N/A_T indicates no measurable change in the effectiveness of the nozzle in reducing or eliminating the surge. Similarly, nozzle injection angles up to 45° show no difference in their effectiveness in reducing surge. On this basis the nozzle geometry would be selected primarily on the basis of hydraulic efficiency and ease of fabrication.

Empirical data is presented which permits estimating the area of the injection nozzles and the quantity of bleed fluid required for turbines of specified performance characteristics.

At a given swirl parameter, the quantity, Q_B/Q_T required to eliminate surge decreases as higher head turbines or lower specific speed machines are considered.

Further investigations are required to gather data indicating the influence of draft tube shape on the effectiveness of fluid injection in reducing draft tube surge.

The hydrodynamic effects such as cavitation arising from the interaction of the draft tube flow with the high velocity injection jets should be experimentally investigated.

ACKNOWLEDGMENT

This work was performed at The Applied Research Laboratory of The Pennsylvania State University and sponsored by the United States Department of the Interior, Bureau of Reclamation of Denver, Colorado as part of the Bureau's Pumped Storage Research Activities under their Energy Research and Development Program.

REFERENCES

[1] Falvey, H. T., "Draft Tube Surges--A Review of Present Knowledge and an Annotated Bibliography," Report No. REC-ERC-71-42, U. S. Bureau of Reclamation, Denver, Colorado, December 1971.

[2] Cassidy, J. J., "Experimental Study and Analysis of Draft-Tube Surging," Report No. REC-OCE-69-5, U. S. Bureau of Reclamation, Denver, Colorado, October 1969.

[3] Palde, U. J., "Influence of Draft Tube Shape on Surging Characteristics of Reaction Turbines," Report REC-ERC-72-24, U. S. Bureau of Reclamation, Denver, Colorado, USA, 1972.

[4] Palde, U. J., "Model and Prototype Turbine Draft Tube Surge Analysis by the Swirl Momentum Method," IAHR and AIRH Symposium, 1974.

[5] Falvey, H. T. and Cassidy, J. J., "Frequency and Amplitude of Pressure Surges Generated by Swirling Flow," Transactions of Symposium Stockholm 1970, International Association for Hydraulic Research, Part 1, Paper E1, Stockholm, Sweden, 1970.